UNIVERSITAT POLITÈCNICA DE CATALUNYA

DOCTORAL THESIS

Quantum Brownian motion revisited: extensions and applications

Author:
Aniello LAMPO

Supervisor:
Prof. Dr. Maciej LEWENSTEIN

Miguel Ángel GARCÍA MARCH

July 16, 2018

Declaration of Authorship

The thesis relies on the material published in the following papers:

- P. Massignan, A. Lampo, J. Wehr, M. Lewenstein, *Quantum Brownian motion with inhomogeneous damping and diffusion* - Physical Review A, 91 (3), 033627 (2015).
- A. Lampo, S.H. Lim, J. Wehr, P. Massignan, M. Lewenstein, *Lindblad model for quantum Brownian motion* - Physical Review A, 94 (4), 042123 (2016).
- A. Lampo, S.H. Lim, M.A. García March, M. Lewenstein, *Bose Polaron as an instance of quantum Brownian motion* - Quantum 1, 30 (2017).
- A. Lampo, C. Charalombous, M.A. García March, M. Lewenstein, *Open quantum system theory for Bose polarons in a trapped Bose-Einstein condensate* - arXiv:1803.08946 (2018).

Further papers

- L. Fratino, A. Lampo, H.T. Elze, *Entanglement dynamics in a quantum–classical hybrid of two q-bits and one oscillator* - Physica Scripta 2014 (T163), 014005 (2014).
- A. Lampo, L. Fratino, H.T. Elze, *Mirror-induced decoherence in hybrid quantum-classical theory* - Physical Review A, 90 (4), 042120 (2014).
- A. Lampo, J. Tuziemski, M. Lewenstein, J.K Korbicz, *Objectivity in the non-Markovian spin-boson model* - Physical Review A 96 (1), 012120 (2017).
- S.H. Lim, J. Wehr, A. Lampo, M.A. García-March, M. Lewenstein, *On the Small Mass Limit of Quantum Brownian Motion with Inhomogeneous Damping and Diffusion* - Journal of Statistical Physics, 1-27 (2017).

- C. Charalombous, M.A. García March, A. Lampo, M. Mehboudi, M. Lewenstein, *Two distinguishable impurities in BEC: squeezing and entanglement of two Bose polarons* - arXiv:1805.00709v1 (2018).
- M. Mehboudi, A. Lampo, , C. Charalombous, L.A. Correa, M.A. García March, M. Lewenstein, *Using polarons for sub-nK quantum non-demolition thermometry in a Bose-Einstein condensate* - arXiv:1806.07198 (2018).
- J. Tuziemski, A. Lampo, M. Lewenstein, J.K Korbicz, *Objectivity in a spin-register* - In preparation

0.1 Abstract - English Version

Quantum Brownian motion represents a paradigmatic model of open quantum system, namely a system which cannot be treated as an isolated one, because of the unavoidable interaction with the surrounding environment. In this case the central system is constituted by a quantum particle, while the bath is made up by a large set of uncoupled harmonic oscillators. In the original model, the interaction between the system and the environment shows a linear dependence on the particle position. Such a particular form corresponds to a homogeneous environment, inducing a damping and diffusion which depends on the state. This is not the most general situation: often the environment shows an inhomogeneous character given by a space-dependent density, involving a non-linearity in the coupling with the central system. One of the main motivations of the thesis is the study of quantum Brownian motion in presence of this non-linear coupling. In particular we focus on the case in which the bath-particle interaction depends quadratically on the position of the latter. There exist several techniques aimed to treat the physics of the model. For instance one could consider the master equation, namely an equation ruling the temporal evolution of the state of the Brownian particle, here represented by its reduced density matrix. We derive such an equation in the Born-Markov regime and look into its stationary solution, studying its configuration in the phase space. For a non-linear quadratic coupling the stationary state may be approximated by means of a Gaussian Wigner function, that experiences genuine position squeezing (i.e. the position variance of the particle takes a value smaller than that associated to the Heisenberg principle, although this is

fulfilled) at low temperature and as the coupling with the bath grows. However, the Born-Markov master equation is not the most appropriate tool to investigate the regime in which squeezing occurs, since the underlying hypothesis in general fail at strong coupling and low temperature, leading to violations of the Heisenberg principle. To overcome this problem we recall alternative methods, such as a Lindblad equation, namely a master equation constructed to preserve the positivity of the state at any time, and Heisenberg equations. In particular we employ the Heisenberg equation formalism to explore the behavior of the Bose polaron, i.e. an impurity embedded in a Bose-Einstein condensate. This experimentally feasible system attracted a lot of attention in the last years. We derive the equation of motion of the impurity position showing that it shows the same form of the famous equation derived by Langevin in 1909 in the context of classical Brownian motion. The main difference lies in the fact that the impurity Langevin-like equation for the impurity carries a certain amount of memory effects, while the original one was purely Markovian. An important part of the work is devoted to the solution of the motion equation for the impurity, in order to calculate the position variance that can be measured in experiments. For this goal we distinguish the case in which the impurity is trapped in a harmonic potential and that where it is free of any trap. In the latter case the impurity the position variance exhibits a quadratic dependence on time (i.e. ballistic diffusion), as a consequence of memory effects. When the impurity is trapped in a harmonic potential it approaches an equilibrium state localized in average in the middle of the trap. Here, at low temperature and for certain values of the coupling strength we detect genuine position squeezing. When we consider a gas with a Thomas-Fermi profile we find that such an effect is improved if we make the gas trap tighter. Genuine squeezing plays an important role in the context of quantum metrology and opens a wide range of possibility to design new protocols, such as the quantum thermometer.

0.2 Abstract - Spanish Version

El movimiento Browniano cuántico es uno de los principales modelos de sistema abierto, es decir un sistema cuyo comportamiento no se puede tratar de manera separada de su entorno. Este modelo describe la física de una partícula acoplada a un entorno de osciladores. En la versión

original del modelo la interacción entre la partícula y el entorno manifiesta una dependencia lineal de la posición de ambos los sistemas. Esta forma analítica del acoplamiento corresponde a un entorno homogeneo, asociado a una fricción y una difusión que dependen del estado del sistema. En todo caso, esta no es la situación más general: a menudo el enorno es inhomogeneo, ya que la densidad no es constante, y esto produce una interacción cuya dependencia de la posición de la partícula no es lineal. Una de las motivaciones principales de esta tesis es el estudio del movimiento Browniano cuántico en presencia de acoplamiento nonlineal. En particular, estudiamos el caso de dependencia cuadrática en la posición de la partícula. Existen muchas técnicas para abordar el modelo. Por ejemplo, se puede emplear la master equation, o sea un ecuación que gobierna la evolución en el tiempo del estado de la partícula, representado por el operador densidad reducido. Derivamos esta ecuación en el régimen de Born-Markov, y estudiamos la forma del estado estacionario en el espacio de las fases. Cuando el acoplamiento es cuadrático, este estado se puede aproximar por medio de una función de Wigner de forma Gausiana, cuya peculiaridad es la emergencia de genuine position squeezing (la varianza de la posición adquiere un valor más bajo de el asociado a la cota de Heisenberg) a temperaturas bajas y cuando el acoplamiento crece. Sin embargo, la ecuación de Born-Markov no es la herramienta más adecuada para tratar el régimen en el que detectamos squeezing, porque las hipótesis subyacentes en general no valen a temperaturas bajas e interacción fuerte, llevando a violaciones del principio de Heisenberg. Para superar este obstáculo es posible emplear métodos alternativos, por ejemplo la ecuación de Lindblad, es decir una ecuación cuya forma sirve para preservar la positividad del estado en cualquier instante, y las ecuaciones de Heisenberg. En particular, aplicamos el formalismo de las ecuaciones de Heisenberg para investigar el comportamiento del Bose polaron, o sea una impureza en un condensado de Bose-Einstein. Es un sistema realista experimentalmente que ha atraido mucha atención recientemente. Derivamos la ecuación del movimiento de la impureza y mostramos que su forma analítica es la misma que la de la ecuación de Langevin para el movimiento Browniano clásico. La diferencia principal es que en este caso la dinámica acarrea efectos de memoria. Una parte importante del trabajo consiste en solucionar esta ecuación del movimiento para evaluar la varianza de la posición, que se puede medir en experimentos. Aquí diferenciamos dos casos: cuando la impureza está atrapada en un potencial armónico, y cuando no hay

trampa armónica. En el segundo caso la varianza es proporcional al cuadrado del tiempo (difusión balística), como consecuencia de los efectos de memoria. Cuando la impureza está atrapada alcanza un estado de equilibrio localizado en el medio de la trampa. En este estado, bajando la temperatura y considerando valores del coupling más fuertes detectamos otra vez squeezing. Si consideramos un gas con un densidad de Thomas-Fermi se puede comprobar que este efecto se puede optimizar aprietando la trampa del gas. El estudio del squeezing es muy importante en el marco de la metrología cuántica porque permite el desarrollo de nuevo protocolos como el termometro cuántico.

Acknowledgements

This PhD thesis would not have been possible without the assistance of a large number of people.

First of all, I would like to thank Maciej Lewenstein for the great scientific support, especially in the complicated moments of my PhD, but also to give me the freedom to "personalize" my scientific activity and to self-manage my working hours.

Then, I would like to thank Miguel Ángel García March for trusting my project and pushing it towards new and interesting directions, highlighting the usefulness of my results.

I also want to thank my family, my girlfriend Lucía, and the members of the QOT ICFO group (from 2014 to 2018), including visiting scientists such as Jan Wehr, Jarek Korbicz and Jan Tuziemski.

Contents

Chapter 1

Introduction

Brownian motion: from classical to quantum

Brownian motion refers to random dynamics of heavy particles suspended in a liquid or a gas, generated by their collisions with the constituents of the fluid around. This transport phenomenon is named after the botanist Robert Brown. In 1827, while he was looking through a microscope at pollen grains in water, he noted that the grains moved, but he was not able to determine the mechanisms that caused this motion. Atoms and molecules had long been theorized as the constituents of the matter, and many years later, Albert Einstein explained in precise detail how the motion observed by Brown was a result of the pollen being moved by individual water molecules. So, Brownian motion became an important model aimed to approach a large set of different contexts characterized by a non-deterministic behavior, or where dissipative processes occur, as result of the unavoidable interaction with the environment around (cf. Mazo, 2002; Gardiner and Zoller, 2004; Breuer and Petruccione, 2007; Weiss, 2008).

In his study of the Brownian motion, Albert Einstein considered both the pollen grains and the water molecules as classical objects, because a macroscopic particle in a viscous medium can be correctly described by the classical theory. We refer to such system as classical Brownian motion. However, in many situations of physical interest, we are not able to describe the dynamics of the system in a completely classical manner. For instance, as the temperature starts to achieve very low values,

we expect to encounter quantum effects. To address these issues, a theory of quantum Brownian motion (QBM) was developed. The QBM describes the behavior of a particle coupled with a thermal[1] bath made up of a large number of quantum harmonic oscillators, satisfying the Bose-Einstein statistics. It represents a paradigmatic example of open quantum system, *i.e.* a system whose dynamics is affected by the surrounding non-controllable degrees of freedom, and it has been studied for decades (Caldeira and Leggett, 1983a; Caldeira and Leggett, 1983b; Grabert, Schramm, and Ingold, 1988; Hu, Paz, and Zhang, 1992; Breuer and Petruccione, 2007; Schlosshauer, 2007; Waldenfels, 2014; Vega and Alonso, 2017).

First of all, QBM is often adopted to analyze some problems lying at the core of the foundations of quantum mechanics. Here, one of the main unsolved questions regards the so-called *quantum to classical transition*, *i.e.* how the classical features, we experience every day in the macroscopic world, arise from the underlying quantum domain. For instance, the *non-observability of interference*: why is it so difficult to detect quantum interference effects on mesoscopic and macroscopic scales? Moreover, there is the famous *problem of outcomes*, also known as the measurement problem: what, within a measurement process, selects a particular outcome among the different possibilities described by the quantum probability distribution? Almost all the attempts to deal with these issues are based on the idea that a quantum system cannot be considered as isolated from the degrees of freedom around. Conversely, it continuously interacts with these degrees of freedom, and the quantum effects are suppressed, just as a consequence of such an interaction (Schlosshauer, 2007; Zurek, 2009). In this framework, QBM is often employed to describe this interaction concretely and in detail, in order to approach quantitatively the problems mentioned above (Schlosshauer, 2007; Blume-Kohout and Zurek, 2008; Tuziemski and Korbicz, 2015; Galve, Zambrini, and Maniscalco, 2016).

In addition, QBM has been employed to investigate the origins of friction, *i.e.* the force resisting the relative motion of solid surfaces, fluid layers, and material elements sliding against each other. Friction is a macroscopic phenomenon, but its microscopic mechanisms are still only partially known and controversial. The theory of QBM has often been

[1] More generally, the bath can be initially in a non-necessarily thermal stationary state of some dynamics.

employed in this context, *i.e.* to construct a microscopic theory of the friction (Gardiner and Zoller, 2004; Caldeira and Leggett, 1983a; Caldeira and Leggett, 1983b). Analogous theories have been devised in quantum electrodynamics in order to explain the origins of radiation damping and Lamb shift (Rzazewski and Zakowicz, 1971; Zakowicz and Rzazewski, 1974; Rzazewski and Zakowicz, 1976; Wodkiewicz and Eberly, 1971; Rzazewski and Zakowicz, 1980; Lewenstein and Rzazewski, 1980).

Finally, QBM is also exploited for more practical purposes. For example, in many physical situations it constitutes the default choice for evaluating the decoherence and dissipation processes occurring in a system due to the interaction with the surrounding non-controllable degrees of freedom (Weiss, 2008). This task is particularly important in all experiments aimed to build and detect macroscopic coherent superpositions. In this context, it is very important to monitor decoherence, because it destroys the interference effects, and QBM permits to analyze these processes providing analytical expressions for the time scales ruling them (Marshall et al., 2003; Gröblacher et al., 2015). Obviously, the importance of decoherence and dissipation goes beyond this class of problems, and plays a very important role also in other fields, such as quantum biology: also in this case QBM provides a good scheme to describe the effects disturbing quantum features in many biological processes (Abbot, Davies, and Pati, 2008).

Quantum Brownian motion in an inhomogeneous environment

The vast majority of the literature on QBM is devoted to microscopic models in which the coupling of the Brownian particle to the bosonic bath is linear both in bath creation and annihilation operators, and in position (or momentum) of the particle. The case when such coupling is non-linear in either the bath or the system operators has been investigated, for instance, in the old papers of Landauer, 1957, who studied non-linearity in bath operators, and Dykman and Krivoglaz, 1975, Hu, Paz, and Zhang, 1993, Brun, 1993, and Banerjee and Ghosh, 2003, who considered both situations. Physically, the case of a coupling that deviates from linearity in the system coordinates, corresponds to a situation where damping and diffusion are spatially inhomogeneous. Obviously, this non-linearity might have both classical and quantum consequences, and as such deserves careful analysis.

The inhomogeneity mentioned above has been recently intensively studied in the context of classical Brownian motion and other classical diffusive systems. In particular, explicit formulas were derived for *noise-induced drifts* in the small-mass (Smoluchowski, 1916; Kramers, 1940) and other limits (Hottovy, Volpe, and Wehr, 2012a; Hottovy, Volpe, and Wehr, 2014; McDaniel et al., 2014). Noise-induced drifts have been shown to appear in a general class of diffusive systems, including systems with time delay and systems driven by colored noise. Applications include Brownian motion in diffusion gradient (Volpe et al., 2010; Brettschneider et al., 2011), noisy electrical circuits (Pesce et al., 2012) and thermophoresis (Hottovy, Volpe, and Wehr, 2012b). In the first two cases the theoretical predictions have been demonstrated to be in an excellent agreement with the experiments. Diffusion in inhomogeneous and disordered media is presently one of the fastest developing subjects in the theory of random walks and classical Brownian motion (Haus and Kehr, 1987; Havlin and Ben-Avraham, 1987; Bouchaud and Georges, 1990; Klafter and Sokolov, 2011), and finds important applications in various areas of science. There is a considerable interest in the studies of various forms of anomalous diffusion and non-ergodicity (Metzler and Klafter, 2004; Klafter and Sokolov, 2011; Höfling and Franosch, 2013; Metzler et al., 2014), based either on the theory of heavy-tailed continuous-time random walk (Montroll and Weiss, 1965; Scher and Montroll, 1975), or on models characterized by a diffusivity (*i.e.* a diffusion coefficient) that is inhomogeneous in time (Saxton, 1993) or space (Hottovy, Volpe, and Wehr, 2012a; Cherstvy and Metzler, 2013). Particularly impressive is the recent progress in single particle imaging, for instance in biophotonics (cf. Tolić-Nørrelykke et al., 2004; Golding and Cox, 2006; Jeon et al., 2011; Weigel et al., 2011; Kusumi et al., 2012; Bakker et al., 2012; Cisse et al., 2013 and references therein), where the single particle trajectories of a receptor on a cell membrane can be traced. It is presently intensively investigated how random walk and classical Brownian motion models with inhomogeneous diffusion may be employed in the description of such phenomena (Massignan et al., 2014; Manzo et al., 2014; Gil et al., 2017).

The examples mentioned above are strictly classical, but the recent unprecedented progress in control, detection and manipulation of ultracold atoms and ions (Lewenstein, Sanpera, and Ahufinger, 2012) are giving us the possibility to perform similar kind of experiments (e.g., single particle tracking to monitor the real time dynamics of given atoms) in

the quantum regime (Krinner et al., 2013). Note that such experiments were unthinkable 20 years ago (see the corresponding paragraphs about difficulties to observe QBM in Gardiner and Zoller, 2004). Note also that ultracold set-ups will naturally involve spatial inhomogeneities, due to the necessary presence of trapping potentials and eventual stray fields. This is in fact one of the motivation of this work: to formulate and study theory of the QBM in the presence of spatially inhomogeneous damping and diffusion.

Quantum Brownian motion in ultracold gases

An immediate application of our theory concerns ultracold quantum gases. Quantum gases have sparked off intense scientific interest in recent years, both from the theoretical and experimental point of view. They are an excellent testbed for manybody theory, and are particularly useful to investigate strongly coupled and correlated regimes, which remain hard to reach in the solid state field (Bloch, Dalibard, and Zwerger, 2008; Lewenstein, Sanpera, and Ahufinger, 2012).

In particular QBM may be useful to approach the polaron problem. The concept of *polaron* has been introduced by Landau and Pekar to describe the behavior of an electron in a dielectric crystal (Landau and Pekar, 1948). The motion of the electron distorts the spatial configuration of the surrounding ions, which let their equilibrium positions to screen its charge. The movement of the ions is associated to phonon excitations that dress the electron. The resulting system, which consists of the electron and its surrounding phonon cloud, is called polaron. The concept of polaron has been extended to describe a generic particle, the impurity, in a generic material, e.g. a conductor, a semiconductor or a gas (Fröhlich, 1954; Alexandrov and Devreese, 2009). One important example is that of an impurity embedded in an ultracold gas. This system has been widely studied both theoretically and experimentally, in the case of a ultracold Fermi (Schirotzek et al., 2009; Kohstall et al., 2012; Koschorreck et al., 2012; Massignan, Zaccanti, and Bruun, 2014; Lan and Lobo, 2014; Levinsen and Parish, 2014; Schmidt et al., 2012) or Bose gas (Côté, Kharchenko, and Lukin, 2002; Massignan, Pethick, and Smith, 2005; Cucchietti and Timmermans, 2006; Palzer et al., 2009; Catani et al., 2012; Spethmann et al., 2012; Rath and Schmidt, 2013; Fukuhara et al., 2013; Shashi et al., 2014; Benjamin and Demler, 2014; Grusdt et al., 2014a; Grusdt et al., 2014b; Christensen, Levinsen, and Bruun, 2015a; Levinsen, Parish, and Bruun,

2015; Ardila and Giorgini, 2015; Volosniev, Hammer, and Zinner, 2015; Grusdt and Demler, 2016; Grusdt and Fleischhauer, 2016; Shchadilova et al., 2016b; Shchadilova et al., 2016a; Castelnovo, Caux, and Simon, 2016; Ardila and Giorgini, 2016; Robinson, Caux, and Konik, 2016; Jørgensen et al., 2016; Hu et al., 2016; Rentrop et al., 2016).

In the QBM framework, the impurity plays the role of the Brownian particle, while the bath consists of the degrees of freedom related to the gas. The main reason to study this system from the open quantum systems point of view lies in the possibility to better describe the motion of the impurity, rather than its spectral quantities, such as ground state, energy levels and so on, like in the majority of the literature nowadays. The interest in the motion of the impurity is motivated by a recent class of experiments aimed to measure observable related to the impurity dynamics, for instance that of Catani et al., 2012. Here, the physics of an impurity in a gas in one dimension is considered, and its position variance is measured, evaluating in a quantitative manner important features of the motion, such as oscillations, damping and slope. To evaluate this kind of behavior a continuous-variable model such as QBM is appropriate. The application of QBM to the *Bose polaron* system (an impurity in a Bose gas) is another fundamental motivation of the present work.

Plan of the thesis

The thesis is organized as follows. In chapter 2 we resume the essentials of classical Brownian motion. This part of the thesis does not contain any original result and basically relies on the material presented in Mazo, 2002, but it is important to present the main results of the classical Brownian motion in order to make the manuscript self-consistent. We describe the experimental observation of Robert Brown and then we proceed by going through the theoretical study of Einstein, who wrote an equation for density probability of the pollen grains, termed Fokker-Planck equation. In this way he computed the mean square displacement of the pollen grains, predicting a linear dependence on time (diffusion effect). Actually Einstein was not the only one who tried to propose a theoretical explanation of Brownian motion. Other scientists, such as Marian Von Smoluchowski and then Paul Langevin, dealt with the same problem, although with different techniques. In particular, Langevin treated Brownian motion by means of a stochastic differential equation ruling the temporal evolution of the grains position. He also found diffusion effect

for the mean square displacement. This was detected in experiments in 1909 by Perrin, confirming theories of Brownian motion and providing a convincing evidence of the corpuscular essence of the matter.

In chapter 3 we start to study QBM. The physics of QBM may be explored by means of different formal tools. Among these, the most common is the master equation, *i.e.* an equation ruling the temporal evolution of the reduced density matrix of the central system, here represented by the quantum Brownian particle. The master equation is a fundamental object in the field of open quantum systems and permits to evaluate in a quantitative manner both decoherence and dissipation, as well as the average values of the observables. However, in many cases the structure of a master equation may result complicated and the procedure to solve it is often not so easy. Therefore, one usually looks into a particular class of approximated master equations, allowing to deal with a certain problem in a mathematical simple manner. An important example is provided by the Born-Markov master equation, based on the absence of self-correlations within the environment (Markov approximation) and the assumption that the global state of the system plus the bath remains separable at all times (Born approximation). In the majority of the situations this kind of equations can be solved analytically providing a description of the behavior of the central system. Comparisons with experiments suggested that the predictions of this model are reasonable in many cases (Moy, Hope, and Savage, 1999; Kirton et al., 2012). We derive the Born-Markov master equations for QBM, constituting the quantum analogue of the equation derived by Einstein. We solve this master equation and we focus on its stationary solution, which can be represented in the phase-space by means of a Gaussian Wigner function. We study how its geometrical configuration in the phase-space varies as the system parameters of the system, such as temperature and interaction strength, change: In particular, as the temperature decreases and the interaction strength grows, the quantum Brownian particle experiences cooling and genuine position squeezing. The latter is particularly important: it occurs when the position variance of the particle takes a values smaller than that associated by the Heisenberg principle, although this is fulfilled. Thus it corresponds to high spatial localization of the Brownian particle, namely to a good knowledge of the particle position, compared with the characteristic length scales of the systems.

In chapter 4 we translate the same analysis to the QBM with a nonlinear coupling. We exhibits the Born-Markov master equation for the

most general non-linear coupling, paying special attention to the situation where the dependence on the Brownian particle position is quadratic. Here, the Gaussian Wigner function just provides an approximation for the stationary state. Also in this case, it is possible to detect squeezing and cooling as the temperature approaches very low values and the bath-system coupling gets more and more strong. In this regime, anyway, both Born and Markov approximations are not fulfilled and the resulting master equation is not appropriate. In particular it yields to violations of the positivity of the density operator associated to the state of the central system, related to violations of the Heisenberg principle. There exist several methods to overcame this problem. For instance, one could recall a master equation in a Lindblad form. This class of equations was proposed in 1976 in parallel and independently by both Lindblad, 1976a and Gorini, Kossakowski, and Sudarshan, 1976[2]. Lindblad master equations arise from the requirement that the positivity of the reduced density matrix is ensured at all times. This type of equations are currently used, for instance to approach the dynamics of the spin-boson model (Leggett et al., 1987). In chapter 5 we aim to treat the QBM model by means of a Lindblad master equation, in both the case of a linear and non-linear coupling. We find that the Lindblad character of this equation induces a rotation in the phase space of its stationary solution, depending, of course, on the system parameters. Also in this case the stationary state exhibits genuine position squeezing and cooling as the interaction strength increases. When the coupling is non linear, anyway, we find that up a certain value of the system-bath coupling the quantum Brownian particle does not approach a Gaussian stationary state.

Nevertheless, the fundamental problem of a Lindblad model in QBM is that it cannot be derived from the microscopic model of quantum Brownian motion. Accordingly, we look into Heisenberg equations formalism in order to study QBM (chapter 6). We show that the temporal evolution of the position of the Brownian particle manifests the classical one derived by Langevin. The treatment of QBM model by means of Heisenberg equations belongs to standard textbook material, in both the linear (Ackerhalt and Rzazewski, 1975; Weiss, 2008; Breuer and Petruccione, 2007) and non-linear case (Barik and Ray, 2005). Our main contribution,

[2]Gorini, Kossakowski and Sudarshan submitted their paper on March 19th 1975, and Lindblad one on 7th April 1975, about three weeks later. The former was published in May 1976, while the latter in June 1976.

which is actually the most important part of the thesis, is the applications of Heisenberg equations to the polaron problem (chapter 7). In fact, the physical Hamiltonian associated to an impurity in a BEC may be expressed as that of the QBM model: the impurity plays the role of the quantum Brownian particle while the environment is represented by the Bogoliubov modes. Accordingly, the theory of QBM may be employed to investigate the polaron problem. Here, Heisenberg equations approach leads to a differential stochastic equation for the position impurity, representing the quantum analogue of that derived by Langevin. The only difference lies in the fact that it is non-local in time, *i.e.* the dynamics of the impurity carries a certain amount of the memory effects. The presence of memory effects affects the solution of the quantum Langevin equation for the impurity. In fact we employ it to evaluate the position variance, which has been measured by Catani et al., 2012. In the case in which the impurity is untrapped position variance depends on time (the impurity runs away) but not linearly, namely the impurity does not experience diffusion. Precisely it is proportional to the square of time. This super-diffusive behavior is a consequence of memory effects. The study of systems exhibiting a certain degree of memory effects attracted in the last years a lot of interest because of the possibility to exploit non-Markovianity as a resource for quantum technology Liu et al., 2011; Gröblacher et al., 2015; González-Tudela and Cirac, 2017. In particular the recent work of Guarnieri, Uchiyama, and Vacchini, 2016 shows the relation existing between non-Markovian character of a special dynamics and the backflow of energy. In this context, super-diffusion represents an important result because it constitutes a witness of memory effects on a measurable quantity.

When the impurity is embedded in a harmonic potential the impurity oscillates collapsing in the middle of the trap. Accordingly, the position variance approaches at long-times a stationary value. In this case, when temperature reaches very low values the position variance shows genuine position squeezing, representing high-spatial localization of the impurity. The detection of such an effect in a concrete measurable system represents an important results, especially for quantum metrology applications.

The results in chapter 7 concerns the situation in which the gas is homogeneous. In chapter 8 we extend this discussion to the more realistic case provided by a trapped gas. To consider a Bose-Einstein condensate in a trapping potential is crucial to study this system in experimental

realistic conditions. Precisely we consider a harmonic trap leading to a parabolic density profile, called Thomas-Fermi density profile. Also in this case the Hamiltonian of the system may be put in the form of that of the quantum Brownian motion model. The main difference with the homogeneous gas lies in the spectral density that exhibits a higher super-ohmic degree, suggesting that the amount of memory effects is bigger. We detail how, for the untrapped case, the diffusion coefficient, which is a measurable quantity, depends on the Bose-Einstein condensate trap frequency. Also, we show that, for the trapped case, the squeezing can be enhanced or inhibited by tuning the Bose-Einstein condensate trap frequency.

Chapter 2

Classical Brownian motion

Brownian motion is the random movement of a particle suspended in a fluid. This phenomenon played a very important role in the history of science because it leaded to the idea that matter is made up by atoms. In this chapter we briefly present the fundamental results concerning classical Brownian motion, focusing on a description of the original observations and of the main theoretical attempts to study it. This part does not contain any original result and it is basically based on the material published in Mazo, 2002. However, it is important to address this topic in detail because it yields a physical insight concerning the main features of the phenomenon, such as diffusion, arising also in its quantum counterpart. Moreover, a dissertation on the classical Brownian motion is fundamental in order to make self-consistent the discussion of its quantum extension, on which the thesis relies.

We start by going through the experiment of Robert Brown (Sec. 2.2), who first detected the motion of the pollen grain in a fluid. In addition to observe the movement, Brown recognized that it was not produced by the living origin particle, but it was a matter of dynamics. On this trail, a long time later, the first theoretical attempt to analyze in a quantitative manner Brown's experiment arrived. The author of this study was Albert Einstein, who in 1905 constructed a statistical theory showing that the random movement of pollen grains was due to fluctuations of particles constituting the fluid (Sec. 2.3). This was also argued by the polish Marian von Smoluchowski, who developed a kinetic model to explain Brownian motion in terms of the collisions of the constituents of the fluid embedding the pollen grains. Precisely, both Einstein and Smoluchovski computed the mean square displacement, predicting that it linearly depends on time. Such a behavior is termed diffusion and it has been derived also in another theory created a few years later by Langevin (1908),

who proposed to describe Brownian motion by means of a stochastic differential equation (Sec. 2.4). The diffusion behavior has been detected experimentally by Perrin in 1908 and represents a strong confirmation of the theories of Brownian motion (Sec. 2.5). Thanks to this result Perrin won the Nobe prize in 1909 providing a strong evidence for the atomist hyptohesis of the matter.

2.1 Historical background

In the year 1803, Napoleon sold France's North American colonies to the newborn United States, for the small sum of sixty million francs. In the American history books, such a deal is known as "the Luisiana Purchease". President Thomas Jefferson, wishing to find out exactly what he had bought, sent out an expedition of exploration under the leadership of Meriweather Lewis and William Clark, which left in 1804, reached the Pacific Ocean in November 1805, and returned in 1806. Among the contributions of this mission, one of the least significant would have the greatest impact, albeit indirectly, on science.

The story of the expedition, based on Lewis' and Clark's journal, constitutes a fascinating adventure story. In addition to geographical and ethnographical informations, the expedition also brought back botanical specimens. A genus of plants from among these specimens, a wild flower found in the Pacific Northwest of the United States, was named Clarkia Pulchella in honor of Captain William Clark (see Fig. 2.1). In 1826, specimens of Clarkia Pulchella where brought to England by the Scots botanists David Douglas.

By the year 1827, Robert Brown (1773-1858) was a renewed botanist. As a young man, Brown studied medicine at Edinburgh, but never finished his studies nor took a degree. He enlisted in a newly raised Scottish regiment and was posted to Ireland, where he was appointed Surgeon's Mate, although seems to have spent more time collecting botanical specimens than attending to patients.

Brown acquired some reputation as a botanist, and he had come to the attention of Sir Joseph Banks who was organizing an expedition to Australia, or, as it was then called, New Holland. Banks had need of a botanist for the expedition, and offered the position to Brown; Brown's

FIGURE 2.1: Clarkia Pulchella's picture from Wikipedia

medical experience no doubt weighed in his favor. Robert Brown accepted as soon as he could in spite of his connection with the army, and his formal career as a botanist begun.

Besides collecting and classifying, Brown made several important discoveries in botany. Perhaps, the one most celebrated by biologists is the achievement concerning the eukaryotic character of the plant cell, namely that they have nucleus. Among the physicians and mathematicians, anyway, he is known primarily for the eponymous motion associated with his name.

2.2 The Brown experiment

In 1827, Brown was investigating the way in which pollen acted during impregnation. He wanted to employ non-spherical grains, in order to be able to observe their orientation. The first plant he studied under the microscope was just Clarkia Pulchella, whose pollen contains granules varying from about five to six microns in linear dimension. It is these granules, not the whole pollen grains, upon which Brown made his observations. Precisely, he detected the motion of the particles immersed in water, and after frequently repeated observations he concluded that such

a motion arose neither from currents in the fluid, nor from its gradual evaporation, but belonged to the particle itself.

This inherent incessant motion of a small particles suspended in a fluid is nowadays called Brownian motion in honor of Robert Brown. Although similar observations had been made earlier by other scientists, Brown was the first to treat the phenomenon in a quantitative manner, showing that the motion was not due to the living origin of the particles: it is not a biological phenomenon, but a physical one. For instance, Brown had strongly illuminated the specimens under his microscope and hence had heated them. This caused evaporation of the ambient fluid, and Brown asked whether this evaporation might be causing the motion he observed. To answer this experimentally, he made a mixture of water containing particles with an immiscible oil and shook the mixture; small drops of water were formed in the oil, some containing only a single particle. These were stable and did not evaporate for some time. He realized that, in all the drops formed, the motion of the particles takes place with undiminished activity, although the principal causes assigned for the motion, namely, evaporation and their mutual attraction and repulsion are either materially reduced, or absolutely nil.

Brown had his results printed in a pamphplet, entitled "A brief account of microscopical observations made in the months of June, July, and August, 1827 on the particles contained in the pollen of plants; and on the general existence of active molecules in organic and inorganic bodies". This work was originally intended for private circulation but was reprinted in the archival literature shortly after its appearance (Brown, 1828). Brown used the word "molecule" in the title in a sense different from its current one. It referred to earlier teaching of the Comte de Buffon who introduced this word for the ultimate constituents of the bodies of living beings. This had nothing to do with the later development of Dalton's atomic theory in which the word molecule took on its modern meaning. Brown published a second paper on the motion in the 1829, where he reported the experiments on the oil-water emulsion mentioned above, and discussed previous observations which could have been interpreted as prior to his (Brown, 1829).

After Brown's experiment, thousand of similar systems, constituted by particles suspended in several kinds of environments, have been examined and the motion still manifested the typical character detected by Brown. An important feature of the Brownian motion is: The rapidity of the motions are greater, the smaller the size of the suspended particles

(note that the velocity of the Brownian particle does not represent a measurable quantity, this point will be clarified in the next sections). Another important property of the motion is its stability in time. The motion persists as long as the particle remains suspended in the fluid. This has been observed in preparations allowed to stand for over a year. Finally, a very characteristic property is the independence of most external influences. Electric fields, light (as long as it is not absorbed and does not heat the system), gravity (as long as the particles do not settle out) and similar disturbances from outside seem to have no effect. Moreover, the motion exhibits a dependence on the nature of the fluid medium, and especially on its viscosity. Temperature also has a marked effect, however. This could be expected because of the dependence on the viscosity, which is appreciably temperature dependent. Whether there is a residual temperature effect, above that due to the temperature dependence of viscosity, cannot be ascertained on experimental grounds alone. Without a theory to tell how to determine the effect due to viscosity it is not possible see if there is additional temperature dependence.

What is a mechanism showing these properties? The first answer that comes to mind is molecular collisions. The kinetic theory of matter asserts that the molecules of a fluid are constantly in motion with a mean kinetic energy proportional to the temperature. For systems at the equilibrium such a kinetic motion is stable in time, and is independent of external influences. Thus we conjecture that the observed irregular motions of a suspended impurity are due to irregular transfers of energy and momentum from the fluid molecules to the particle because of the irregularly occurring molecular collisions between the suspended particle and the medium constituents.

There is a nuance which deserves to be clarified. Collisions increasing the velocity of the heavy particle will, on average, be balanced by collisions decreasing that velocity. Thus, the net mean change in velocity due to many collisions will be much smaller than that due to an individual collision. How then can the observed motion be due to collisions? Although the average effect of the collisions will indeed be small, there will be fluctuations about that average. Fluctuations large enough to lead to observable effects, while relatively rare, are still common enough to explain the phenomenon. Precisely, as explained in Sec. 4.1 of the book of Mazo, 2002, the fluctuations in velocity due to fluctuations in collision numbers can therefore explain the observed Brownian motion qualitatively.

2.3 Einstein's theory

We now start to discuss the quantitative attempts to treat Brownian motion. Chronologically, the first relevant one was that of Albert Einstein[1], who published in 1905 a paper (Einstein, 1905) where he proposed an explanation of the behavior observed by Robert Brown[2]. The theory developed by Einstein may be defined as a statistical one, namely it does not relies on a microscopic kinetic model, but it refers to generic probability distributions. This is both its strength and weakness. The strength is that it is applicable to a wide range of circumstances and is easily generalizable. The weakness is that it does not carry so much insight on what is happening at the microscopic dynamical time scale.

In addition to its statistical character, we may define Einstein's theory as a mesoscopic one: it refers to timescales long enough to contain many elementary events, yet short enough to be effectively infinitesimal on an observational scale. Precisely, we introduce a characteristic time τ_{r}, short compared to macroscopically observable times, yet long with respect to the inverse collision frequency, such that the particle's motions in two consecutive time intervals of length τ_{r} are independent. Equivalently, we state that successive collisions of the Brownian particle with the surrounding degrees of freedom are independent events. Physically, it means that after a collision between the Brownian particle and a constituent of the environment, the latter interacts with a large number of other constituents, in order to make its dynamical state scarcely dependent on its state before the previous collision with the Brownian one. This happens, for instance, when the density of the medium is sufficiently low so that a collision between the Brownian particle and a given constituent of the medium will be followed by a high number of collisions between the former and other particles of the medium, before it scatters again with the original constituent. In conclusion we may say that during τ_{r} a large number of collisions occur, in order to destroy the suspended Brownian particle dependence on its initial conditions. In other words we say

[1] Several studies on Brownian motion have been performed already of Einstein's, but they do not lead to brilliant conclusions. These works are mentioned in section 1.2 of Mazo, 2002.

[2] Einstein also published a second paper (Einstein, 1906a). Apparently, in the period between the two publications he had apparently been convinced of the relevance of his considerations for the understanding of the phenomenon associated with the name of Brown. Einstein published two additional short papers on Brownian motion (Einstein, 1907; Einstein, 1908).

that the process described above is Markovian. Of course Einstein never used such a term, because the famous work of Markov (Markov, 1907) concerning Markov chains came two years later.

As we stated in the beginning of the section, Einstein's framework is not based on a kinetic model, but employs probability distributions. Let $p(x,t)$ be the probability density that the particle be at position x at time t. There is no external force so the system is homogeneous, *i.e.* $p(x,t) = p(-x,t)$. Let $\phi(\Delta, \delta_t)$ be the probability of the particle moving a distance Δ in time δt. The hypothesis of a Markov process permits to write a Chapman-Kolmogorov equation for it:

$$p(x, t+\delta_t) = \int p(x-\Delta, t)\phi(\Delta, \delta_t)d\Delta. \tag{2.1}$$

From the Chapman-Kolmogorov equation, we immediately derive the Fokker-Planck one:

$$\frac{\partial p(x,t)}{\partial t} = D\frac{\partial^2 p(x,t)}{\partial x^2}, \tag{2.2}$$

where

$$D = \lim_{t\to 0}\frac{1}{2\delta_t}\int \Delta^2\phi(\Delta, \delta_t)d\Delta. \tag{2.3}$$

Equation (2.2) is the well known diffusion equation, and D has the physical significance of the self-diffusion coefficient of the Brownian particle. The derivation of such an equation presented here follows Einstein's very close. Of course, he did not use the terms "Chapman-Kolmogorov" and "Fokker-Planck" in his derivation. These equations had not yet been derived by the authors from whom they are named.

Multiplying both sides of Eq. (2.2) by x^2 and integrate over all space, the left-hand side yields by definition

$$\int x^2\dot{p}(x,t)dx = \frac{\partial\langle x^2\rangle}{\partial t}, \tag{2.4}$$

while the right-hand side leads to $6D$, because of the Green theorem. In the end one finds

$$\frac{\partial\langle x^2\rangle}{\partial t} = 6D, \tag{2.5}$$

and consequently

$$\langle x^2\rangle = 6Dt. \tag{2.6}$$

The constant of integration must vanish because $\langle x^2 \rangle$ has to be equal to zero at $t = 0$. Since the starting time for observation (the time at which we took the particle position to be at the origin) was arbitrary, this result shows that the sample paths of the random motion are differentiable nowhere because $\Delta r \sim t^{1/2}$. This conclusion applies for all times, because the process has independent increments. Of course, the conclusion is absurd when considered as a microscopic description of the path. It is the result of extrapolating a mesoscopic description down to a microscopic level[3].

We aim now to express the diffusion coefficient D as a function of the system parameters, such as temperature, etc. Consider a suspension of particles in a fluid with a spatially constant external field, for example gravity, imposed upon it. We denote the external force by F, and choose the z axis of the coordinate system in the direction of F. The potential of the external field is $-Fz$. The suspended particle will move in the z direction and attain a terminal velocity, v, given by

$$v = F/\xi, \tag{2.7}$$

in which ξ is the friction constant. The suspension is supposed to be diluted enough so that the individual particles in it do not interact with each other, but only with the constituents of the surrounding medium. The system is bounded in the z direction; the container has a bottom, for instance. Accordingly, the motion will build up a concentration gradient in the z direction, that produces a diffusion current in the opposite direction to the current induced by the external force. Eventually, the concentration gradient will become large enough that two currents will cancel each other, and the system will reach equilibrium. If we denote the local concentration of suspended particles by $n(z)$, then the particle current induced by the external force is nv; that induced by the concentration gradient is $-D\frac{\partial n}{\partial z}$. This quantity is equal, because of the Fick's law, to the flux current. We have:

$$\frac{nF}{\xi} = -D\frac{\partial n}{\partial z}. \tag{2.8}$$

But at equilibrium $n(z)$ is given by the Boltzmann law

$$n(z) \sim \exp[-Fz/k_{\mathrm{B}}T], \tag{2.9}$$

[3]This topic was discussed in Einstein, 1906b.

which replaced in Eq. (2.8) leads to

$$D = k_{\mathrm{B}}T/\xi. \tag{2.10}$$

This is the Einstein relation between the friction coefficient and the diffusion one. Einstein actually did not write it down in this form, but immediately assumed that the friction constant was given by Stokes'law:

$$\xi = 6\pi\eta a, \tag{2.11}$$

where η and a are the viscosity and the radius of the suspended particles, respectively. Replacing Eq. (2.11) into Eq. (2.10) one obtains the Stokes-Einstein relationship:

$$D = \frac{k_{\mathrm{B}}T}{6\pi\eta a}. \tag{2.12}$$

Accordingly, Einstein's result for the mean square displacement takes the form

$$\langle x^2 \rangle = \frac{k_{\mathrm{B}}T}{\pi\eta a}t. \tag{2.13}$$

One year later, in 1906, Marian von Smoluchowski (1872-1917) proposed another theoretical model (Smoluchowski, 1906) to study Brownian motion[4]. His attempt was based on a kinetic microscopic model, providing a good insight of dynamical mechanisms underlying the phenomenon. Just by studying the collisions by means of the conservation of the momentum and energy, and assuming no memory effects, Marian Smoluchowski derived an expression for the mean square displacement. However, his result was larger than the Einstein's by a factor $\sqrt{\frac{32}{27}} \approx 1$. They are remarkably close considering of all the approximations that went into theory. Smoluchowski and many subsequent commentators claim that his result was, in fact, $\sqrt{\frac{64}{32}}$ larger, but this was because of the error of a factor of two in his formula for the friction constant of heavy particle in a dilute gas. His result was actually closer than he thought. It is now universally agreed, and was agreed even by Smoluchowski, that Einstein result is the correct one.

[4]Smoluchowski approached the study of Brownian motion around 1900, but he published his results only in 1906, under the impetus of Einstein's paper.

2.4 The Langevin theory

The Einstein and Smoluchowski theories look very different on the surface. One employs the dynamics of the particle motion, while the other is a purely statistical theory. A link between the two conceptions was provided in 1908 by P. Langevin (Langevin, 1908). A suspended particle in a fluid is acted upon by forces due to the molecules of the solvent. This force may be expressed as a sum of its average value and a fluctuation around such an average value. Langevin's idea was to treat the mean force dynamically and the residual fluctuating part of the force probabilistically.

We assume that the mean force on a particle moving slowly in a viscous medium is given by

$$F_{\text{av}} = -\xi v, \tag{2.14}$$

where v is the velocity of the particle relative to the resting fluid. The differences in sign between it and the relation in Eq. (2.7) is due to the fact that the former refers to the velocity induced by an external force, while the latter concerns the force caused by a given velocity. The two are equal in magnitude and opposite in sign.

We shall denote the residual fluctuating force by X. We know little about X in detail, so we shall make only a few statistically hypothesis about its properties. First of all, X is a fluctuation about a mean, so it must, itself, have zero mean

$$\langle X \rangle = 0. \tag{2.15}$$

Second, we assume that X is a stationary process with a very short correlation time:

$$\langle X(t)X(t+s)\rangle = \langle X^2\rangle \phi(s), \tag{2.16}$$

in which $\phi(s)$ is a function that is very sharply peaked about $s = 0$. The correlation time is also short compared to M/ξ (the only characteristic time of the system) that ϕ may be taken to be a Dirac delta function, *i.e.* $\phi(s) \sim \delta(s)$. In other word this is the way in which Langevin implemented in his approach Markov approximation. Moreover it is not correlated with the position of the particle at time t, nor with the velocity at any previous time:

$$\langle X(t)x(s)\rangle = 0, \quad \langle X(t)\dot{x}(s)\rangle = 0, \quad t > s. \tag{2.17}$$

Newton's second law of motion for this system reads

$$M\ddot{x} = -\xi\dot{x} + X(t). \tag{2.18}$$

This differential equation cannot be solved in the usual sense because we do not know enough about $X(t)$. Furthermore, in order that its correlation time as short as assumed X must be a fluctuating function. Precisely we require it is a Wigner measure.

We multiply both sides of Eq. (2.18) for $x(t)$ and then we take the mean value of the result. Recalling the average values in Eq. (2.18) we get

$$M\langle x\frac{\partial v}{\partial t}\rangle = -\xi\langle xv\rangle. \tag{2.19}$$

Since $v = \dot{x}$, such an equation may be put in the form

$$\frac{M}{2}\frac{\partial^2\langle x^2\rangle}{\partial t^2} + \frac{\xi}{2}\frac{\partial\langle x^2\rangle}{\partial t} = 2k_{\mathrm{B}}T, \tag{2.20}$$

where we have used the equipartition theorem $\langle v^2\rangle = 3k_{\mathrm{B}}T/M$. The solution of this equation is very easy to find. Imposing $\langle x^2(0)\rangle = 0$ we have

$$\langle x^2(t)\rangle = \frac{6k_{\mathrm{B}}T}{\xi}t + B\left[\exp(-\xi t/M) - 1\right], \tag{2.21}$$

where B is an integration constant specified by $\langle xv\rangle = 0$ at time zero. Although we do not need to know it, the value of B can be computed to be $6Mk_{\mathrm{B}}T/\xi^2$. Thus, after a time of the order of ξ/M, Einstein's result is valid. For typical situations, this time is indeed quite short, of the order of 10^{-7} seconds. Consequently, Einstein's result may be considered to be valid for practical purposes for all time.

Why is this result equal to Einstein's for practical purposes only, and not for all time? Einstein worked completely in the configuration space of the Brownian particle; he never introduced the velocity of the particle. Thus he completely neglected the inertia of the particle and the possibility of the persistence of velocity. In other words, the short time, τ, after which the displacements of the particle should be independent, should be longer than M/ξ. Langevin, on the other hand, worked in the particle's phase space and was able to treat the velocity relaxation. Langevin's description is on a finer scale than that of Einstein.

2.5 The Perrin experiment

The scientific achievements we presented in this chapter had a great impact on the vision of the nature in the beginning of the nineteenth century. How can one explain the incessant movement of the particle detected by Robert Brown, which seems to contradict the second law of thermodynamics? The key of the answer provided by the theoretical studies of Einstein, Smoluchowski and Langevin lies in fluctuations. Then, what is fluctuating? This may be only explained on the basis of particles.

The idea of a corpuscolar reality is the most significant contribution of the Brownian motion to the representation of the world in that period. Actually, since the time of John Dalton (1766-1844) the intuition that the matter was made up of elementary particles called atoms, and their unions, now called molecules, took strong hold in the scientific community. Such a hypothesis became particularly popular especially after the First International Chemistry Conference in Karlsruhe in 1860 where Stanislao Cannizarro showed how the ideas of Amadeo Avogadro could be used to construct a rational table of atomic weights. Even so, there were skeptics. The most prominent of these where Wilhelm Ostwald (1853-1932) and the physicist Ernest Mach (1838-1916), who argued that there was not any experimental proof of the existence of atoms. Exner (1900) and Svedberg (1906) already made quantitative analysis of Brownian motion (Exner, 1900; Svedberg, 1906), but they did not have Einstein of Smoluchowski results available; the experiments were not suitable for a detailed verification of the theory. This had to wait for the experiments of Jean Perrin (1870-1942), a convinced atomist.

Perrin aimed to study the dependence of the mean square displacement on the radius of the particle. This kind of experiment was not so easy: It was necessary to prepare a monodisperse suspension, not a trivial task. In 1908 Perrin (and his PhD students) prepared a suspension of particles of gamboge of mastic of uniform size and observed the particles with a camera lucida, a device that projects an image on a plane surface suitable for tracing. He made measurements of the displacements for as many as 200 distinct granules, confirming the predictions of Einstein and Langevin discussed above (Perrin, 1908a; Perrin, 1908b). Perrin published these results in a long paper (together with his student) in 1909 (Perrin, 1909), and became an energetic proselytizer for the reality of atoms. He received the Nobel Prize in 1926 for his work on the discontinuous structure of matter.

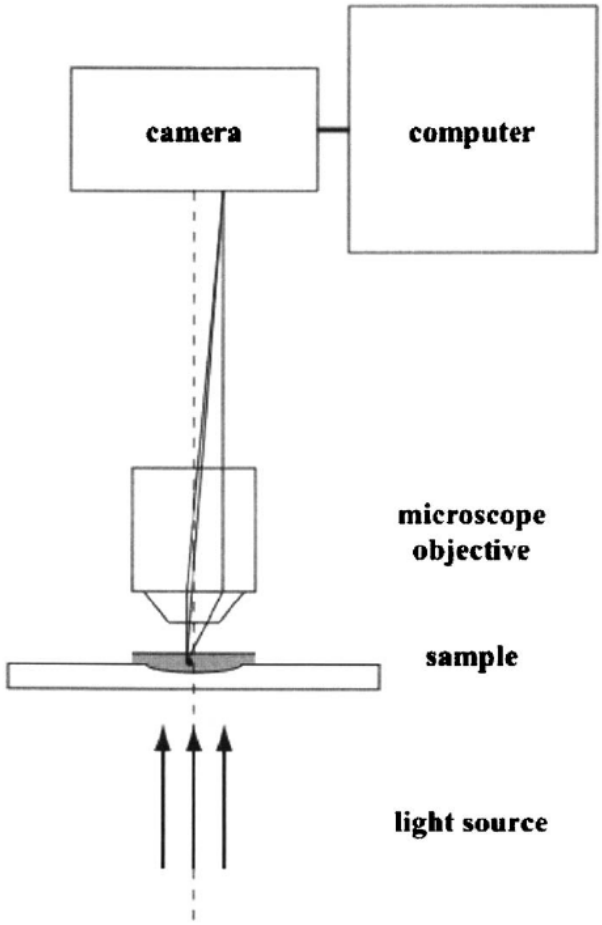

FIGURE 2.2: Set-up of the Perrin's experiment revisited by Newburgh, Peidle, and Rueckner, 2006.

Perrin was apparently also the first to realize that the path of a particle undergoing Brownian motion must have elements in common with a graph of a function which is not differentiable. Such functions had previously been studied by mathematicians and regarded as pathological cases, whose only importance was in illustrating what was really encompassed within the general concept of function. But now, according to Perrin, these so-called pathological functions can be seen to have a physical realization. This idea was taken up by mathematicians and forms the basis for a branch of the theory of stochastic, or random, processes, itself a subfield of the theory of probability.

Perrin's experimental verification of the Einstein-Smoluchowski theory, together with the work of J.J. Thompson on the electron, was rapidly, successful in persuading most of the anti-atomist that atoms really did exist. Ostwald, one of the most prominent skeptics, recanted in a new edition of his influential textbook. Only Mach was not convinced, and continued to consider the existence of atoms as only a hypothesis.

2.6 Summary

In this chapter we presented a brief dissertation on classical Brownian motion. We resume now the main contents of the chapter, according a chronological order.

- 1827: Robert Brown observes the motion of pollen grains immersed in water: Brownian motion was detected. After frequently repeated observations he concluded that such a motion arose neither from currents in the fluid, nor from its gradual evaporation, but belonged to the particle dynamics.

- 1905: Einstein proposes a statistical mesoscopic theory to treat Brownian motion, based on an equation for the density probability of the pollen grains (Eq. (2.2)). He employed this equation to calculate the mean square displacement in Eq. (2.13), finding a linear dependence on time. Such a particular dependence on time is termed diffusion effect.

- 1906: Marian von Smoluchowski treats Brownian motion by means of a kinetic microscopic model. He also evaluates the mean square

displacement recovering a diffusive behavior, although with a different coefficient in front of the time. He recognizes a few years later that Einstein's result was the correct one.

- 1908: Paul Langevin studies Brownian motion with a stochastic differential equation (Eq. 2.18), leading to the same result of Einstein for the mean square displacement, and extending it to generic instants.

- 1909 Perrin publishes a paper where he presents experimental results confirming the result for the mean square displacement. This was a strong proof for theories of Brownian motion, as well as for atomist reality.

Chapter 3

Quantum Brownian motion

In the previous chapter we described the main theoretical attempts to treat the grains motion detected by Robert Brown. These theories are purely classical and rely on *phenomenological* equations, *i.e.* equations that are not derived in a Hamiltonian framework, but are proposed starting from experimental results that one aims to interpret. In this chapter we move our analysis to the quantum domain. The standard procedures of quantization are based on the existence of Hamiltonians (or equivalently Lagrangians) for the system in which one is interested. So, the first step to approach the study of Brownian motion in the quantum regime is to look for a Hamiltonian description of the phenomenon observed by Robert Brown. Precisely, one has to write a Hamiltonian leading to the phenomenological equations, such as those of Einstein [Eq. (2.2)] and Langevin [Eq. (2.18)]. Then, by replacing functional variables with operator ones it is possible to obtain a quantum Hamiltonian for Brownian motion. This is the point of view adopted, for instance, by Caldeira and Leggett, 1983a.

In Sec. 3.1 we introduce the Hamiltonian of QBM. It describes a quantum particle, usually trapped in a harmonic potential, coupled to a set of non-interacting harmonic oscillators. The Hamiltonian encodes all the information to study the physics of QBM. There exist several tools to do this. In the current chapter we consider the master equation formalism, *i.e.* we use an equation for the reduced density operator of the central Brownian particle. Such a topic belongs to standard textbook material, but we present the re-examination published in the paper of Massignan et al., 2015. Here we focused on the evaluation of the stationary state of the system, and the analysis of its geometrical configuration in the phase-space as the system parameters, such as temperature and interaction strength, vary. This kind of analysis leads to the detection of special

effects for the impurity, such as squeezing and cooling. We discuss the regime of validity of the method adopted.

3.1 Hamiltonian

The QBM model describes the behavior of a quantum particle interacting with a thermal bath made up by a huge number of harmonics oscillators, satisfying the Bose-Einstein statistics. Despite its simplicity, QBM gained popularity in condensed matter physics due to its very general nature, and its convenience to describe dissipation in a quantum context. The model is defined by the Hamiltonian

$$H = H_{\mathrm{S}} + H_{\mathrm{B}} + H_{\mathrm{I}}, \tag{3.1}$$

where the system, bath and interaction terms are respectively

$$H_{\mathrm{S}} = H_{\mathrm{sys}} + V_c(x) = \frac{p^2}{2m} + U(x) + V_c(x), \tag{3.2}$$

$$H_{\mathrm{B}} = \sum_k \left(\frac{P_k^2}{2M_k} + \frac{M_k \omega_k^2 X_k^2}{2} \right) - E_0 = \sum_k \hbar \omega_k a_k^\dagger a_k, \tag{3.3}$$

$$H_{\mathrm{I}} = -\sum_k \kappa_k X_k x. \tag{3.4}$$

In the above expressions p is the particle momentum, m its mass, $U(x)$ the trapping potential depending on its position denoted by x. The expression

$$V_c(x) = \sum_k \frac{\kappa_k^2}{2 m_k \omega_k^2} x^2, \tag{3.5}$$

represents the so-called counter-term, needed in the following to remove unphysical divergent renormalizations of the trapping potential arising from the coupling to the bath, as showed in the book of Breuer and Petruccione, 2007. The bath bosons have masses M_k and frequencies ω_k, and their momenta and positions are denoted by P_k and X_k, respectively. Alternatively, we describe them with the help of annihilation and creation operators, a_k and $a_k^\dagger$. From the bath Hamiltonian, we have removed the constant zero-point energy E_0.

The parameters in Eq. (3.4) denoted by κ_k characterize the coupling of the bath modes to the system and refer to an interaction term depending linearly on the position of the Brownian particle, as well as on those of the bath constituents. This situation is the conventional one, and corresponds to a quantum system undergoing state-independent damping and diffusion, *i.e.* damping and diffusion independent on the position (or other observables).

We will restrict our discussion in the following to the one dimensional (1D) case, but generalizations to 2D or 3D are straightforward. Moreover, we shall consider the impurity trapped in a harmonic potential, *i.e.*

$$U(x) = m\Omega^2 x^2/2, \tag{3.6}$$

where Ω is the frequency of the trap.

3.2 Born-Markov master equation

The Hamiltonian introduced in the previous section embodies all the information one needs to describe the physics of QBM. The high number of constituents of the bath often makes impossible an exact study of the temporal evolution of the whole system. So, one usually proceeds by tracing away the environment degrees of freedom to focus only on the analysis of the quantum Brownian particle. In this framework, the particle represents a paradigmatic example of open quantum system, namely a system which is not closed, but continuously affected by the presence of the bath.

There exist several different techniques to handle with open quantum systems and in particular with QBM. In this chapter we shall look into the master equation formalism. A master equation is an equation for the reduced density matrix of the central system and can be considered as the analogue of the Schrödinger equation for open systems. We will study a very special kind of master equation: the Born-Markov master equation, allowing to treat many problems in a mathematically simple form. Comparisons between the predictions of models based on this equation and experiments have shown that the Born and Markov assumptions on which the master equation is based are reasonable in many cases. However we emphasize already at this stage that there are various important physical systems (for example, low-temperature solid-state system) which do not obey to Markovian dynamics and which therefore cannot

be appropriately modeled using the Born-Markov master equation. The goal of the present section is the introduction of the general structure of the Born-Markov master equation and the discussion of its regime of validity.

3.2.1 General structure of a master equation

In the ordinary formalism of open quantum systems, the reduced density operator $\rho_{\mathrm{S}}(t)$ is computed via

$$\rho_{\mathrm{S}}(t) = \mathrm{Tr}_{\mathrm{E}}\left[\tilde{U}(t)\rho_{\mathrm{SE}}(0)\tilde{U}^{\dagger}(t)\right], \tag{3.7}$$

where $\tilde{U}(t)$ denotes the time-evolution operator for the whole composite system SE. As is evident from Eq. (3.7), this approach requires that we first determine the state of the total system at a generic instant, before we can arrive at the reduced description through the trace operation. In general this task is not so easy (sometimes impossible) to carry out in practice for the majority of the systems.

In contrast, in the master equation formalism the reduced density matrix $\rho_{\mathrm{S}}(t)$ is calculated directly from an expression of the form

$$\rho_{\mathrm{S}}(t) = \mathcal{L}(t)\rho_{\mathrm{S}}(0), \tag{3.8}$$

where the operator $\mathcal{L}(t)$ is the so-called *dynamical map* ruling the temporal evolution of the central system[1]. Expression in Eq. (3.8) is called *master equation* for $\rho_{\mathrm{S}}(t)$, and it represents the most general structure that such an equation can take.

Obviously, if the master equation is exact, then Eq. (3.7) and (3.8) must be equivalent by definition, *i.e.* it ensues the identity

$$\mathcal{L}(t)\rho_{\mathrm{S}}(0) = \mathrm{Tr}_{\mathrm{E}}\left[\tilde{U}(t)\rho_{\mathrm{SE}}(0)\tilde{U}^{\dagger}(t)\right], \tag{3.9}$$

and the master equation would amount to nothing else but a trivial rewriting of Eq. (3.7). The master equation approach, thus, is convenient only if one imposes certain assumptions concerning the system-environment states and dynamics, in order to evaluate the approximate time evolution

[1] Since $\mathcal{L}(t)$ constitutes an operator that in turns acts on another operator, it is commonly named *superoperator*.

of $\rho_{\rm S}(t)$, even when it is not possible to compute the exact global dynamics. In fact, here we shall restrict our attention to master equations (valid under particular hypothesis) that may be written as first-order differential equations showing a *local in time* structure, namely which can be cast in the form

$$\dot{\rho}_{\rm S}(t) = \mathcal{L}[\rho_{\rm S}(t)] = -\frac{i}{\hbar}\,[H_{\rm S}, \rho_{\rm S}(t)] + \mathcal{D}[\rho_{\rm S}(t)]. \tag{3.10}$$

This equation is local in time in the sense that the change of the state of the central system at time t depends only on the form of such a state evaluated at t, but not at any other times $s \neq t$. The superoperator $\mathcal{L}$ appearing in Eq. (3.10) acts on $\rho_{\rm S}(t)$ and typically depends on the initial state of the environment and different terms in the Hamiltonian. To convey the physical intuition behind $\mathcal{L}$, it has been decomposed into two parts:

- A *unitary* part that is provided by the usual von Neumann commutator with the self-Hamiltonian $H_{\rm S}$. In general, as we also stated in Sec. 3.1, this term is not identical to the unperturbed free Hamiltonian we indicated by $H_{\rm sys}$, generating the evolution of the central system in absence of the interaction with the environment. This coupling often perturbs the free Hamiltonian, leading to a renormalization of its spectrum through the introduction of a counter-term, like that in Eq. (3.5). This effect (often termed *Lamb-shift*) has nothing to do with the non-unitary evolution induced by the environment but alters only the unitary part of the reduced dynamics.

- A *non-unitary* part $\mathcal{D}[\rho_{\rm S}(t)]$ that embodies the action of the environment (decoherence, dissipation and so on). Of course, if such a term is equal to zero, the central system follows an unitary evolution and the resulting master equation differs from the standard Von Neumann one for closed systems only because of the possible presence of a counter-term.

3.2.2 Structure of the Born-Markov master equation

The Born-Markov master equation is based on two core approximations that may be stated as below:

- *The Born approximation*, meaning that the coupling between the system and the environment is sufficiently weak and the latter is reasonably large such that changes of its state are negligible and that related to the composite system remains separable at all times, *i.e.*

$$\rho_{\mathrm{S}}(t) = \rho_{\mathrm{S}}(t) \otimes \rho_{\mathrm{E}}, \tag{3.11}$$

  with ρ_{E} approximately constant at all times.

- *The Markov approximation*, corresponding to a situation where *memory effects* of the environment are negligible, in the sense that any self-correlation within the environment induced by the interaction with the central system decay rapidly compared to the characteristic timescale over which the state varies noticeably.

Assume now these assumptions hold. Suppose further that the system-bath interaction is described by a Hamiltonian term of the form

$$H_{\mathrm{SE}} = \sum_k S_k \otimes E_k, \tag{3.12}$$

where S_k and E_k are self-adjoint operators acting on the Hilbert spaces of the central system and the environment, respectively. Then the evolution of $\rho_{\mathrm{S}}(t)$ is given by *the Born-Markov master equation*

$$\dot{\rho}_{\mathrm{S}}(t) = -\frac{i}{\hbar}\left[H_{\mathrm{S}}, \rho_{\mathrm{S}}(t)\right] - \frac{1}{\hbar^2}\sum_k \{[S_k, B_k\rho_{\mathrm{S}}(t)] + [\rho_{\mathrm{S}}(t)C_k, S_k]\}, \tag{3.13}$$

with

$$B_k \equiv \int_0^\infty \mathrm{d}\tau \sum_j C_{kj}(\tau) S_j^{(\mathrm{I})}(-\tau), \tag{3.14}$$

$$C_k \equiv \int_0^\infty \mathrm{d}\tau \sum_j C_{kj}(-\tau) S_j^{(\mathrm{I})}(-\tau). \tag{3.15}$$

Here $S_j^{(\mathrm{I})}(-\tau)$ denotes the system operator S_j in the interaction picture[2]. The quantity $C_{kj}(\tau)$ is given by

$$C_{kj}(\tau) \equiv \langle E_k^{(\mathrm{I})}(\tau) E_j \rangle_{\rho_{\mathrm{E}}}, \tag{3.16}$$

where the average is taken over the initial environmental state ρ_{E} (recall that the Born approximation demands that such a state remains approximately constant at all times). The quantity in Eq. (3.16) will be referred to as the *environment self-correlation functions* in the following. The reason for this terminology is easy to understand. The operators E_k can be thought of as observables "measured" on the environment by the interaction with the central system. Self-correlation functions then tell us to what extent the result of such a "measurement" of a particular E_k is correlated with the result of a "measurement" of the same observable carried out a time τ later. Broadly speaking, these functions quantify to what degree the environment retains information over time about its interaction with the system. In fact, the Markov approximation corresponds to the assumption of a rapid decay of these environment self-correlation functions with respect to the timescale set by the evolution of the system. Such a timescale is the relaxation one τ_{S}, namely that associated to dissipation process, *i.e.* the transfer of energy from the central system and the environment. Accordingly, we may state that the Markov approximation relies on the following inequality

$$\tau_{\mathrm{B}} \ll \tau_{\mathrm{S}}, \tag{3.17}$$

where the quantity in the left hand-side is the time according which environment self-correlation functions decay. The constraint in Eq. (3.17) is appropriate if the environment is only weakly coupled to the central system, and if the temperature of the bath is sufficiently high.

In conclusion the structure of the Born-Markov master equation of a given system remains fixed by its Hamiltonian and the two approximations discussed above. A clear derivation of equation (3.13) goes widely beyond the purpose of the present thesis. However it may be found in section 4.2 of the book of Schlosshauer, 2007 and in section 3.3 of the that of Breuer and Petruccione, 2007. Moreover, in section 9.1 of their book,

[2]The definition of interaction picture belongs to standard textbook material. A clear explanation may be found in the Appendix of Schlosshauer, 2007.

Breuer and Petruccione, 2007 show that the Born-Markov master equation may be derived even by the Nakajima-Zwanig equation. Precisely, it follows from an expansion in the bath-system coupling constant at the second order. This point of view will be useful to better understand the results we shall present in the chapter.

3.3 The Born-Markov master equation of quantum Brownian motion

In this section we present the Born-Markov master equation of the QBM model, namely we specialize the structure in Eq. (3.13) to the Hamiltonian (3.1). Such a Hamiltonian shows an interaction term in Eq. (3.4) that may be reduced to the decomposition in Eq. (3.12): x plays the role of S_k (with only one index), while $\kappa_k X_k$ is the equivalent of E_k. Thus we can start to evaluate the environment self-correlation function for QBM which in this case remains defined as

$$\mathcal{C}(\tau) = \sum_{ij} \kappa_i \kappa_j \langle X_i^{(\mathrm{I})}(\tau) X_j \rangle_{\rho_\mathrm{E}}. \tag{3.18}$$

The terms related to different indexes vanish because of the fact that the environmental oscillators do not interact among them and are therefore completely uncorrelated. Hence, for $i \neq j$,

$$\langle X_i^{(\mathrm{I})}(\tau) X_j \rangle_{\rho_\mathrm{E}} = \langle X_i^{(\mathrm{I})}(\tau) \rangle_{\rho_\mathrm{E}} \langle X_j \rangle_{\rho_\mathrm{E}} = 0, \tag{3.19}$$

since the expectation value of the position coordinate of a harmonic oscillator is equal to zero.

Our task of evaluating $\mathcal{C}(\tau)$ is now reduced to the computation of the averages values referred to equal indexes, *i.e.*

$$\mathcal{C}(\tau) = \sum_{i} \kappa_i^2 \langle X_i^{(\mathrm{I})}(\tau) X_i \rangle_{\rho_\mathrm{E}}. \tag{3.20}$$

This may be easily accomplished. Let us switch to the representation of the position operators of the bath in terms of the creation and annihilation ones:

$$X_i = \sqrt{\frac{\hbar}{2 m_i \omega_i}} \left(a_i + a_i^\dagger \right). \tag{3.21}$$

Then its time evolution in the interaction picture writes as

$$\begin{aligned} X_i(\tau) &= \exp[-\frac{i}{\hbar}H_{\rm E}\tau]X_i\exp[\frac{i}{\hbar}H_{\rm E}\tau] \\ &= \sqrt{\frac{\hbar}{2m_i\omega_i}}\left(a_i e^{-i\omega_i\tau}+a_i^\dagger e^{i\omega_i\tau}\right). \end{aligned} \tag{3.22}$$

Accordingly[3]

$$\langle X_i^{(\rm I)}(\tau)X_i\rangle_{\rho_{\rm E}} = \frac{\hbar}{2m_i\omega_i}\left[\langle a_i a_i^\dagger\rangle_{\rho_{\rm E}}e^{-i\omega_i\tau}+\langle a_i^\dagger a_i\rangle_{\rho_{\rm E}}e^{i\omega_i\tau}\right]. \tag{3.23}$$

But the quantity

$$N_i = \langle a_i^\dagger a_i\rangle_{\rho_{\rm E}} \tag{3.24}$$

is simply the mean occupation number of the $i^{\rm th}$ oscillator of the environment. By assumption, the environment is in thermal equilibration, which corresponds to assume that

$$N_i \equiv N_i(T) = \frac{1}{\exp[\hbar\omega_i/k_{\rm B}T]-1}. \tag{3.25}$$

Using this expression and the standard commutation relation for the creation and annihilation operators it turns

$$\begin{aligned} \langle X_i^{(\rm I)}(\tau)X_i\rangle_{\rho_{\rm E}} =& \frac{\hbar}{2m_i\omega_i}\{[1+N_i(T)]\,e^{-i\omega_i\tau}+N_i(T)e^{i\omega_i\tau}\} \\ =& \frac{\hbar}{2m_i\omega_i}\{[1+2N_i(T)]\cos(\omega_i\tau)-i\sin(\omega_i\tau)\} \\ =& \frac{\hbar}{2m_i\omega_i}\{\coth\left(\frac{\hbar\omega_i}{2k_{\rm B}T}\right)\cos(\omega_i\tau)-i\sin(\omega_i\tau)\}, \end{aligned} \tag{3.26}$$

where in the last step we employed the fact that

$$\begin{aligned} 1+2N_i(T) =& 1+\frac{2}{e^{\hbar\omega_i/k_{\rm B}T}-1} \\ =& \frac{e^{\hbar\omega_i/k_{\rm B}T}+1}{e^{\hbar\omega_i/k_{\rm B}T}-1} = \coth\left(\frac{\hbar\omega_i}{2k_{\rm B}T}\right). \end{aligned} \tag{3.27}$$

[3] Note that the average values of $a_i a_i$ and its adjoint are zero, as can be easily proved by hand.

hence the environment self-correlation function can now be written as

$$\begin{aligned}\mathcal{C}(\tau) =& \sum_i \frac{\hbar\kappa_k^2}{2m_i\omega_i}\left[\coth\left(\frac{\hbar\omega_i}{2k_{\mathrm{B}}T}\right)\cos(\omega_i\tau) - i\sin(\omega_i\tau)\right] \\ \equiv& \nu(\tau) - i\eta(\tau),\end{aligned} \tag{3.28}$$

Here, the functions

$$\begin{aligned}\nu(\tau) &= \frac{1}{2}\sum_i \kappa_i^2 \langle\{X_i(\tau), X_i\}\rangle_{\rho_{\mathrm{E}}} \\ &= \sum_i \frac{\hbar\kappa_i^2}{2m_i\omega_i}\coth\left(\frac{\hbar\omega_i}{2k_{\mathrm{B}}T}\right)\cos(\omega_i\tau) \\ &\equiv \hbar\int_0^\infty d\omega J(\omega)\coth\left(\frac{\hbar\omega}{2k_{\mathrm{B}}T}\right)\cos(\omega\tau),\end{aligned} \tag{3.29}$$

$$\begin{aligned}\eta(\tau) &= \frac{1}{2}\sum_i \kappa_i^2 \langle[X_i(\tau), X_i]\rangle_{\rho_{\mathrm{E}}} \\ &= \sum_i \frac{\hbar\kappa_i^2}{2m_i\omega_i}\sin(\omega_i\tau) \\ &\equiv \hbar\int_0^\infty d\omega J(\omega)\sin(\omega\tau),\end{aligned} \tag{3.30}$$

are commonly named in the literature as *noise kernel* and *dissipation kernel*, respectively.

The function $J(\omega)$, introduced in Eqs. (3.29) and (3.30), is defined as

$$J(\omega) = \sum_i \frac{k_i^2}{2m_i\omega_i}\delta(\omega - \omega_i), \tag{3.31}$$

and is called *spectral density* of the environment. Spectral densities play an immensely important role in the theoretical and experimental study of open quantum systems. They encapsulate the physical properties of the environment once one traces away its degrees of freedom. In modeling the environment, one often goes to a continuum limit in which the description in terms of individual oscillators with discrete frequencies ω_i and masses m_i is replaced by the density $J(\omega)$ corresponding to a continuous spectrum of environmental frequencies ω.

Having successfully determined the environment self-correlation function $\mathcal{C}(\tau)$, we have completed the main step in the derivation of the desired Born-Markov master equation for QBM. The rest of the derivation is now straightforward. The operators in Eqs. (3.14) and (3.15) are immediately written down as

$$B = \int_0^\infty d\tau \mathcal{C}(\tau) x^{(\mathrm{I})}(-\tau), \tag{3.32}$$

$$C = \int_0^\infty d\tau \mathcal{C}(-\tau) x^{(\mathrm{I})}(-\tau), \tag{3.33}$$

where

$$\begin{aligned} x^{(\mathrm{I})}(\tau) =& \exp[-\frac{i}{\hbar} H_{\mathrm{S}} \tau] x \exp[+\frac{i}{\hbar} H_{\mathrm{S}} \tau] \\ =& x \cos(\Omega\tau) + \frac{p}{m\Omega} \sin(\Omega\tau), \end{aligned} \tag{3.34}$$

is the position operator of the quantum Brownian particle in the interaction picture. Inserting Eqs. (3.32) and (3.33) into the general expression for the Born-Markov equation (3.13) we have

$$\begin{aligned} \dot{\rho}_{\mathrm{S}}(t) =& -\frac{i}{\hbar} [H_{\mathrm{S}}, \rho_{\mathrm{S}}(t)] \\ & - \frac{1}{\hbar^2} \int_0^\infty d\tau \{ \mathcal{C}(\tau) \left[x, x^{(\mathrm{I})}(-\tau) \rho_{\mathrm{S}}(t) \right] + \mathcal{C}(-\tau) \left[\rho_{\mathrm{S}}(t) x^{(\mathrm{I})}(-\tau), x \right] \}. \end{aligned} \tag{3.35}$$

Recalling the decomposition $\mathcal{C}(\tau) = \nu(\tau) - i\eta(\tau)$ involving the noise and the dissipation kernels and the expression of the position of the Brownian particle in Eq. (3.34), we obtain, rearranging terms properly,

$$\begin{aligned} \dot{\rho}(t) =& -\frac{i}{\hbar} \left[\hat{H}_S + C_x x^2, \rho(t) \right] - \frac{iC_p}{\hbar m\Omega} [x, \{p, \rho(t)\}] \\ & - \frac{D_x}{\hbar} [x, [x, \rho(t)]] - \frac{D_p}{\hbar m\Omega} [x, [p, \rho(t)]], \end{aligned} \tag{3.36}$$

with

$$C_x = -\int_0^\infty \mathrm{d}\tau\, \eta(\tau)\cos(\Omega\tau), \tag{3.37}$$

$$C_p = \int_0^\infty \mathrm{d}\tau\, \eta(\tau)\sin(\Omega\tau), \tag{3.38}$$

$$D_x = \int_0^\infty \mathrm{d}\tau\, \nu(\tau)\cos(\Omega\tau), \tag{3.39}$$

$$D_p = -\int_0^\infty \mathrm{d}\tau\, \nu(\tau)\sin(\Omega\tau). \tag{3.40}$$

The upper limit of the time integrals above is a consequence of the Markovian approximation underlying the derivation of Eq. (3.36). Beyond such an approximation, the upper limit of the integrals is t, rather than ∞, and the coefficients of the master equation get time-dependent. The master equation evaluated with these pre-Markovian coefficients is usually called *Redfield equation*, and constitutes a middle-ground between the equation (3.36) and the exact one, valid for arbitrary system-environment interaction strengths. The analytical structure of this time-dependent coefficients have been studied in detail in the literature, for instance by Hu, Paz, and Zhang, 1992. Of course, this time-dependent coefficients approach the form of the Markovian ones above at long-time.

Equation (3.36) is the master equation for QBM. It completely rules the dynamics of the central Brownian particle, as well as the decoherence and dissipation processes it undergoes because of the influence of the environment. Moreover, as we will see in the following, it permits to evaluate the observables of the system. Note that we indicated the reduced density matrix of the central Brownian particle by ρ, rather than ρ_{S} in order to make the notation lighter.

In this chapter we focus on the case where the spectral density is Ohmic (*i.e.* it is linear in ω at low frequencies) and has a Lorentz-Drude (LD) cut-off,

$$J(\omega) = \frac{m\gamma}{\pi}\omega\frac{\Lambda^2}{\omega^2+\Lambda^2}. \tag{3.41}$$

The specific choice of cut-off function yields minor quantitative changes

to the coefficients, but as physically expected, it does not alter their asymptotic behaviour. Exploiting the Matsubara representation

$$\coth\left(\frac{\hbar\omega}{2k_{\rm B}T}\right)=\frac{2k_{\rm B}T}{\hbar\omega}\sum_{n=-\infty}^{\infty}\frac{1}{1+(\nu_n/\omega)^2}, \tag{3.42}$$

with frequencies $\nu_n=2\pi nk_{\rm B}T/\hbar$, the noise and dissipation kernels may be evaluated analytically with the help of the Cauchy's residue theorem[4],

$$\nu(\tau)=\frac{mk_{\rm B}T\gamma\Lambda^2}{\hbar}\sum_{n=-\infty}^{\infty}\frac{\Lambda e^{-\Lambda|\tau|}-|\nu_n|e^{-|\nu_n\tau|}}{\Lambda^2-\nu_n^2}, \tag{3.43}$$

$$\eta(\tau)=\frac{m\gamma\Lambda^2}{2}{\rm sign}(\tau)e^{-\Lambda|\tau|}. \tag{3.44}$$

The explicit form of the dissipation and noise kernels permits to evaluate the analytical structure of the self-correlation function, and in particular its time dependence. We observe that it involves basically the timescales $1/\Lambda$ and $1/\nu_n=\hbar/2\pi nk_{\rm B}T$ for $n\neq 0$. The largest correlation time is thus equal to

$$\tau_{\rm B}={\rm Max}\{1/\Lambda,\hbar/2\pi k_{\rm B}T\}. \tag{3.45}$$

Accordingly the condition in Eq. (3.17) for the applicability of the Born-Markov approximation becomes

$$\hbar\gamma\ll{\rm Min}\{\hbar\Lambda,2\pi k_{\rm B}T\}, \tag{3.46}$$

where $1/\gamma$ represents the relaxation timescales.

The coefficients can be evaluated as follows:

$$\begin{aligned}C_x(\Omega)&=-\frac{m\gamma}{2\pi}\int_{-\infty}^{\infty}{\rm d}\omega\,\mathcal{P}\left(\frac{1}{\omega+\Omega}\frac{\omega\Lambda^2}{\omega^2+\Lambda^2}\right)\\&=-\frac{m\gamma\Lambda^3}{2(\Omega^2+\Lambda^2)},\end{aligned} \tag{3.47}$$

$$C_p(\Omega)=\frac{m\gamma\Omega\Lambda^2}{2(\Omega^2+\Lambda^2)}, \tag{3.48}$$

$$D_x(\Omega)=\frac{m\gamma\Omega\Lambda^2}{2(\Omega^2+\Lambda^2)}\coth\left(\frac{\hbar\Omega}{2k_{\rm B}T}\right). \tag{3.49}$$

[4] In particular, the integrals defining both kernels may be reduced to the Fourier transform of a Lorentzian function.

In the first equation above we have used the identity

$$2i\int_0^\infty \mathrm{d}\tau\ \sin(\omega\tau) = \int_{-\infty}^{\infty} \mathrm{d}\tau\, \mathrm{sign}(\tau) e^{i\omega\tau} = 2i\mathcal{P}\left(\frac{1}{\omega}\right), \tag{3.50}$$

where $\mathcal{P}$ denotes the principal value of the integral.

The derivation of the anomalous diffusion coefficient D_p is more involved[5]. One has

$$D_p(\Omega) = -\int_{-\infty}^{\infty} \frac{\mathrm{d}\omega}{2\pi}\mathcal{P}\left[\frac{m\gamma\Lambda^2}{\omega+\Omega}\frac{\omega}{\omega^2+\Lambda^2}\coth\left(\frac{\hbar\omega}{2k_\mathrm{B}T}\right)\right]. \tag{3.51}$$

To perform the principal part integration with the standard trick

$$\int \mathrm{d}\omega\, \mathcal{P}\left[\frac{f(\omega)}{\omega}\right] = \int \mathrm{d}\omega\ \left[\frac{f(\omega)-f(0)}{\omega}\right] \tag{3.52}$$

we need the numerator to be a polynomial in ω. Inserting the Matsubara representation of the hyperbolic cotangent in Eq. (3.51), one finds

$$\begin{aligned}\frac{\pi(\Omega^2+\Lambda^2)}{m\gamma\Omega\Lambda^2}D_p(\Omega) &= -\frac{\pi}{\hbar}\sum_{n=-\infty}^{\infty}\frac{k_\mathrm{B}T}{(\Omega^2+\nu_n^2)}\frac{(\Omega^2-\Lambda|\nu_n|)}{\Lambda+|\nu_n|}\\ &= \frac{\pi k_\mathrm{B}T}{\hbar\Lambda} + \mathrm{Di}\Gamma\left(\frac{\hbar\Lambda}{2\pi k_\mathrm{B}T}\right) - \mathrm{Re}\left[\mathrm{Di}\Gamma\left(\frac{i\hbar\Omega}{2\pi k_\mathrm{B}T}\right)\right].\end{aligned} \tag{3.53}$$

The function $\mathrm{Di}\Gamma(z) \equiv \Gamma'(z)/\Gamma(z)$ is the logarithmic derivative of the Gamma function, and it is plotted in Fig. 3.1 for both real and imaginary arguments.

The C_x term provides a term which strongly renormalizes the harmonic potential frequency. The role of the counterterm V_c introduced in the Hamiltonian is exactly to remove this spurious contribution, and from Eq. (3.36) we see explicitly that a perfect cancellation is obtained by choosing $V_c(x) = -C_x x^2$. Regarding the other coefficients, as we will see in the following, C_p provides momentum damping, D_x yields normal momentum diffusion, and D_p contributes to anomalous diffusion. The D_x term may also be seen as the one responsible for decoherence in the position basis, as widely discussed by Schlosshauer, 2007; Zurek, 2003; Schlosshauer, 2005. There, the density matrix may be represented

[5]The name of this coefficient will be explained later.

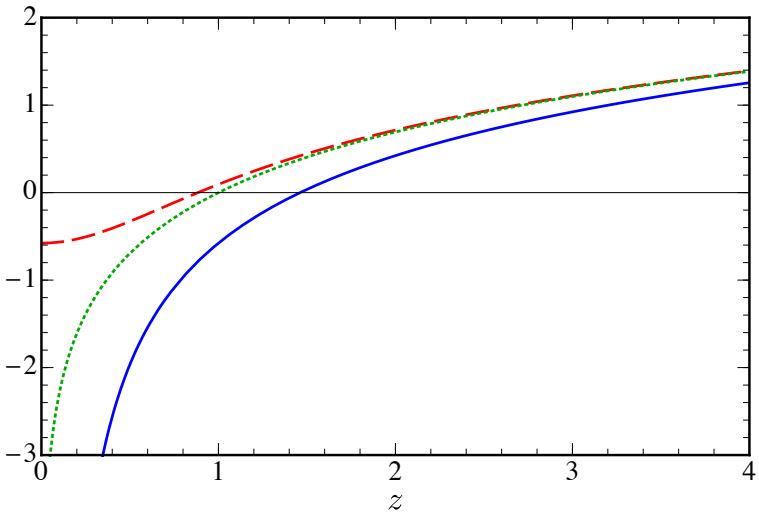

FIGURE 3.1: Plots of the adimensional functions $\mathrm{Di}\Gamma(z)$ (continuous) and $\mathrm{Re}[\mathrm{Di}\Gamma[(iz)]$ (dashed). At large z, both functions approach $\log(z)$ (dotted).

as $\rho(x_1, x_2, t) = \langle x_1|\rho(t)|x_2\rangle$, and one finds $\partial_t \rho(x_1, x_2, t) = -D_x(x_1 - x_2)^2\rho(x_1, x_2, t)/\hbar + \ldots$, so that the off-diagonal components of ρ decohere at a rate directly proportional to the square of the distance between them, $\gamma^{(1)}_{x_1,x_2} = D_x(x_1 - x_2)^2/\hbar$.

3.3.1 Caldeira-Leggett limit

We look now into the high-temperature and large cut-off limits

$$k_{\mathrm{B}}T/\hbar \gg \Lambda \gg \Omega. \tag{3.54}$$

Here we may use the series expansions

$$\mathrm{Di}\Gamma(z) = -z^{-1} - \tilde{\gamma} + \pi^2 z/6 + O(z^2) \tag{3.55}$$

$$\mathrm{Re}[\mathrm{Di}\Gamma(iz)] = -\tilde{\gamma} + O(z^2), \tag{3.56}$$

with $\tilde{\gamma}$ the Euler gamma, and real dimensionless argument z, to find

$$\frac{D_p}{\hbar m\Omega} = -\frac{k_{\rm B}T\gamma}{\hbar^2\Lambda} + O\left(\frac{\Lambda}{T}\right). \tag{3.57}$$

Replacing it into Eq. (3.36), at high-T one finds

$$\begin{aligned}\dot{\rho}(t) = &-\frac{i}{\hbar}\left[H_{\rm sys},\rho(t)\right] - \frac{i\gamma}{2\hbar}[x,\{p,\rho(t)\}] \\ &-\frac{m\gamma k_{\rm B}T}{\hbar^2}[x,[x,\rho(t)]] + \frac{\gamma k_{\rm B}T}{\hbar^2\Lambda}[x,[p,\rho(t)]].\end{aligned} \tag{3.58}$$

Since p is of order $m\Omega x$ in an harmonic potential, the last term may be neglected as it scales as Ω/Λ, and in this way we have the usual *Caldeira-Leggett master equation*:

$$\dot{\rho}(t) = -\frac{i}{\hbar}\left[H_{\rm sys},\rho(t)\right] - \frac{i\gamma}{2\hbar}[x,\{p,\rho(t)\}] - \frac{m\gamma k_{\rm B}T}{\hbar^2}[x,[x,\rho(t)]]. \tag{3.59}$$

Hereafter we will refer to the regime defined by the constraint in Eq. (3.54) as *the Caldeira-Leggett limit*. Note that in the case of a harmonic potential trapping the Brownian particle, or more generally upon neglecting quantum effects for the general non-harmonic potential, the corresponding time dependent equation for the Wigner function in this regime has a particularly simple interpretation (Gardiner and Zoller, 2004): it is a Fokker–Plank equation for the probability distribution in the phase space of a classical Brownian particle undergoing damped motion with a damping constant γ under the influence of a Langevin stochastic noise–force $F(t)$. The noise is Gaussian and white, but it fulfills the fluctuation–dissipation relation, *i.e.* the average of the noise correlation satisfies

$$\langle F(t+\tau)F(t)\rangle = 2\gamma k_{\rm B}T. \tag{3.60}$$

This relation assures that the stable stationary state of the dynamics is the classical Gibbs-Boltzmann state. In terms of the coefficients entering the master equation the fluctuation–dissipation relation implies that

$$D_x/C_p = 2k_{\rm B}T/\hbar\Omega. \tag{3.61}$$

3.3.2 Large cut-off limit

We want to look at the limit

$$\Lambda \gg \Omega, k_{\rm B}T/\hbar, \quad \Omega \sim k_{\rm B}T/\hbar. \tag{3.62}$$

This is motivated by the fact that, as we shall see in the chapters related to the applications of QBM to real systems, the cut-off frequency has a concrete physical meaning and it may be in general much larger than the temperature. In this case we find

$$\begin{aligned}\dot{\rho}(t) = &-\frac{i}{\hbar}\left[H_{\rm sys}, \rho(t)\right] - \frac{i\gamma}{2\hbar}[x, \{p, \rho(t)\}] \\ &- \frac{m\gamma\Omega}{2\hbar}\coth\left(\frac{\hbar\Omega}{2k_{\rm B}T}\right)[x, [x, \rho(t)]] - \frac{D_p}{\hbar m\Omega}[x, [p, \rho(t)]].\end{aligned} \tag{3.63}$$

For large z we have

$$\mathrm{Di}\Gamma(z) \sim \log(z) - 1/(2z) + O(z^{-2}) \tag{3.64}$$

$$\mathrm{Re}[\mathrm{Di}\Gamma(iz)] \sim \log(z) + 1/(12z^2) + O(z^{-3}), \tag{3.65}$$

and the anomalous diffusion coefficient is proportional to

$$D_p \sim \frac{m\gamma\Omega}{\pi}\log\left(\frac{\hbar\Lambda}{2\pi k_{\rm B}T}\right). \tag{3.66}$$

In this limit, we have moreover

$$D_x/C_p = \coth\left(\hbar\Omega/2k_{\rm B}T\right). \tag{3.67}$$

Equation (3.63), with the anomalous diffusion coefficient given in Eq. (3.53), constitutes one of the main results of this section.

3.3.3 Ultra-low temperature limit

We finally consider the limit

$$\Lambda \gg \Omega \gg k_{\rm B}T/\hbar. \tag{3.68}$$

Since both DiΓ functions in Eq. (3.53) diverge logarithmically, the temperature drops completely out of the QME, which reads now

$$\begin{aligned}\dot{\rho}(t) = &-\frac{i}{\hbar}\left[H_{\rm sys},\rho(t)\right] - \frac{i\gamma}{2\hbar}[x,\{p,\rho(t)\}] \\ &- \frac{m\gamma\Omega}{2\hbar}[x,[x,\rho(t)]] - \frac{\gamma}{\hbar\pi}\log\left(\frac{\Lambda}{\Omega}\right)[x,[p,\rho(t)]].\end{aligned} \tag{3.69}$$

It is impossible to remark that the ultra-low temperature limit, as well as that discussed above, have to be considered very carefully. In these regime in fact the Markov approximation could not be properly fulfilled because of the low value of the temperature, as shown in Eq. (3.46).

3.4 Wigner function approach and stationary solutions

The master equation for the density matrix ρ can be particularly well analyzed in terms of the Wigner function W. The Wigner function is a quasi-probability distribution providing a representation of the density matrix in the phase-space. In order to express Eq. (3.36) in terms of the Wigner function it is useful to introduce the differential operators

$$x_\pm = x \pm \frac{i\hbar}{2}\frac{\partial}{\partial p}, \quad p_\pm = p \pm \frac{i\hbar}{2}\frac{\partial}{\partial x}, \tag{3.70}$$

that satisfy the commutation rules

$$\begin{aligned}&[x_+,x_-] = [p_+,p_-] = 0, \\ &[x_+,p_-] = -[x_-,p_+] = i\hbar.\end{aligned} \tag{3.71}$$

The formal substitutions [see Eqs. (4.5.11) of Gardiner and Zoller, 2004] are of great use in the following:

$$\begin{aligned}x\rho \to x_+W, \quad p\rho \to p_-W, \\ \rho x \to x_-W, \quad p \to p_+W.\end{aligned} \tag{3.72}$$

We note here that, while in the previous Sections x and p stood for the usual non-commuting operators, from now on the same symbols will be used to represent the commuting variables of the Wigner function

$W(x,p)$. It turns, for general Ω, Λ and T , the following functional differential equation[6]

$$\dot{W}=\left[m\Omega^2\partial_p x-\frac{\partial_x p}{m}+\frac{2C_p}{m\Omega}\partial_p p+\hbar D_x\partial_p^2-\frac{\hbar D_p}{m\Omega}\partial_x\partial_p\right]W. \tag{3.73}$$

This is the equivalent of the Einstein's equation (2.2): the Wigner function plays here the role of the density probability used by Einstein. The fact that the Hamiltonian introduced in the beginning of the chapter permits to recover an equation showing the same form of the classical one derived by Einstein justifies the use of the name "Brownian motion" to indicate the current quantum model. This shall be even clearer in chapter 6.

The analogy with Einstein's equation allows to better understand the physical meaning of the coefficients (and so their name). For instance it is possible to note that the coefficient D_x multiplies a term yielding a diffusion with respect of the momentum. Similarly, D_p is proportional to mixed diffusion term. For this goal is named *anomalous diffusion term*. The physical meaning of the coefficient will be even clearer when we derive motions equations.

The stationary solution of this equation may be found by inserting a generic Gaussian ansatz

$$W_{\rm st}\propto\exp\left[-\left(\sigma_p\frac{p^2}{2m}+\sigma_x\frac{m\Omega^2x^2}{2}\right)/(k_{\rm B}\tilde{T})\right] \tag{3.74}$$

with real parameters σ_p and σ_x, and equating independently the coefficients of x^2 and p^2 to zero in the resulting equation.

In the oversimplified Caldeira-Leggett limit defined by the constraint in Eq. (3.54), one would set

$$D_x=m\gamma k_{\rm B}T/\hbar,\quad D_p=0, \tag{3.75}$$

and find in this way

$$\sigma_p=\sigma_x=1,\quad \tilde{T}=T. \tag{3.76}$$

By retaining instead the complete expression of all terms in the equation (and, in particular, a non-zero D_p), we find that the stationary Wigner

[6]Note that $[p,\rho]\hat{x}=[(p_-p_+)\rho]\hat{x}=x_-(p_--p_+)W$.

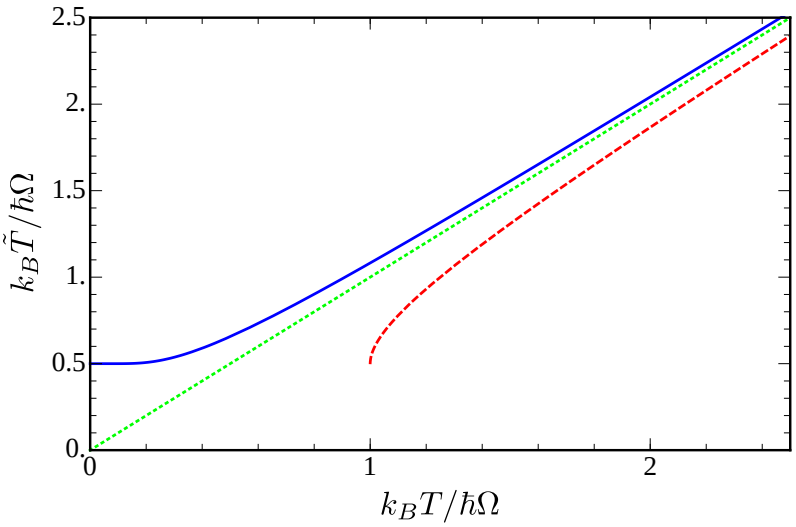

FIGURE 3.2: Effective temperatures as obtained through the complete quantum treatment, Eq. (3.78) (blue), and by means of an oversimplified approximation discussed in App. A, Eq. (A.7) (red). The green line is the high-T result, $\tilde{T} = T$.

function is obtained by choosing $\sigma_p = 1$ and

$$\sigma_x = \frac{1}{1 - 2D_p/(m\Omega^2 \coth[\hbar\Omega/2k_{\rm B}T])}, \tag{3.77}$$

yielding an effective temperature

$$\tilde{T} = \frac{\hbar\Omega}{2k_{\rm B}} \coth\left(\frac{\hbar\Omega}{2k_{\rm B}T}\right). \tag{3.78}$$

This result is shown in Fig. 3.2. A number of interesting conclusions may now be drawn. First of all, a careful treatment of the equation at low-T yields an effective temperature which saturates to the zero-point motion energy. When $\sigma_p = \sigma_x = 1$, the Gaussian stationary solution with an effective temperature $\tilde{T}$ as given by the quantum result in Eq. (3.78) corresponds to the exact quantum thermal Gibbs-Boltzmann density matrix of an harmonic oscillator (the system) at the temperature T. In this case, the

contours of the stationary distributions are circles of radius $\sqrt{2k_{\rm B}\tilde{T}/\hbar\Omega}$ for arbitrary T (*i.e.* of radius 1 at $T=0$).

More generally, in units of the normalized standard deviations

$$\delta_x = 2\sqrt{\frac{m\Omega^2\langle x^2\rangle_{\rm st}}{2\hbar\Omega}} = \sqrt{\frac{2k_{\rm B}\tilde{T}}{\hbar\Omega\sigma_x}} \tag{3.79}$$

$$\delta_p = 2\sqrt{\frac{\langle p^2\rangle_{\rm st}}{2m\hbar\Omega}} = \sqrt{\frac{2k_{\rm B}\tilde{T}}{\hbar\Omega\sigma_p}}, \tag{3.80}$$

the Heisenberg uncertainty relation requires that

$$\delta_x\delta_p \geq 1, \tag{3.81}$$

i.e. that the contour of the distribution encircles an area not smaller than π. An important effect of D_p is that it allows for a contraction of the distribution in x vs. p. The Heisenberg uncertainty principle then puts an important constraint on our theory, forcing us to exclude the region where the inequality is violated. In Fig. 3.3 we illustrate this region of validity, as obtained by inserting Eq. (3.77) in Eq. (3.81): for any $\Lambda > \Omega$, we find that there exists a critical temperature below which the Heisenberg uncertainty principle is violated. Similar squeezing effects have been discussed in the literature, for instance by Haake and Reibold, 1984, in the context of the so called Ullersma model (Ullersma, 1966). At $T=0$, the Heisenberg principle requires $\Lambda < \Omega$.

Interestingly, there are no log-corrections to $\tilde{T}$ coming from the log-divergent term D_p. Such coefficient grows with the cut-off, and at very large values σ_x diverges (*i.e.* δ_x^2 approaches zero) and becomes negative, yielding a non-normalizable solution. However, this bound always lies beyond the one set by the Heisenberg principle, which requires $\delta_x\delta_p \geq 1$. We may say that the quantum particle immersed in the bath experiences an effective "heating" if the phase-space area encircled by the normalized standard deviations is larger than the one a quantum Gibbs-Boltzmann (GB) distribution would occupy at the same temperature. Since

$$\langle E_k\rangle_{\rm GB}\langle E_p\rangle_{\rm GB} = (k_{\rm B}\tilde{T}/2)^2, \tag{3.82}$$

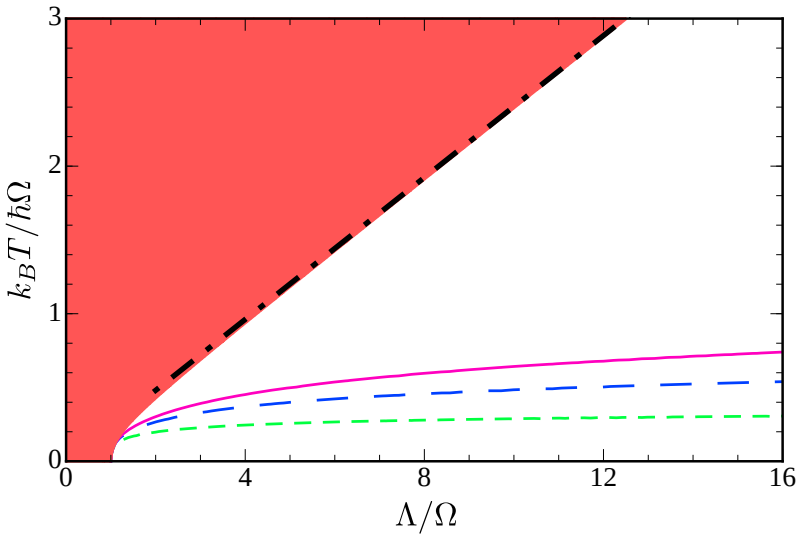

FIGURE 3.3: Minimal temperature for the fulfillment of the Heisenberg uncertainty principle for an Ohmic spectral function with Lorentz-Drude cut-off, for $\gamma/\Omega = 0.1,\ 0.5,\ 1$ (from bottom to top). In the red region, the gas displays effective "heating" and a quenched aspect ratio in p relative to x (*i.e.* $\delta_x/\delta_p > 1$). The black, dot-dashed line is the asymptotic approximation to the boundary of unit aspect ratio, $T = \alpha_{(1)}\Lambda$.

the system is effectively heated if

$$\delta_x \delta_p > \coth\left(\frac{\hbar\Omega}{2k_{\mathrm{B}}T}\right), \tag{3.83}$$

or equivalently $\sigma_x \sigma_p < 1$. Since $\sigma_p = 1$, this amounts to requiring $D_p < 0$, which remarkably does not depend on γ. Asymptotically, we have

$$k_{\mathrm{B}}T/\hbar > \alpha_{(1)}\Lambda + O(\Omega/T), \tag{3.84}$$

with $\alpha_{(1)} \approx 0.24$ solution of the implicit equation

$$\pi\alpha_{(1)} + \mathrm{Di}\Gamma(1/2\pi\alpha_{(1)}) + \tilde{\gamma} = 0. \tag{3.85}$$

Finally, we consider the aspect ratio of the phase-space contour described by the standard deviations. Since σ_p always equals unity, it is easy to see that we have a quenched aspect ratio in x, relative to p (*i.e.* $\delta_x/\delta_p < 1$) in the "cooling" region, and the opposite situation ($\delta_x/\delta_p > 1$) in the "heating" region. In fact the line separating "heating" region from the "cooling" region corresponds to the regime where $D_p = 0$. In this case the Wigner function is exactly given by a Gaussian with effective temperature $\tilde{T}$, and circular shape of the distribution ($\delta_p = \delta_x$); it corresponds precisely to the quantum thermal Gibbs-Boltzmann density matrix.

It should be noted that, when deriving the stationary solutions from a perturbative treatment of the master equation to order $2n$ in the bath-system coupling constant κ_k, one gets a reduced equilibrium state which is exact to order $2n-2$, and contains some (but not all) terms of the order $2n$ solutions. The overall error is therefore of order $(\kappa_k)^{2n}$ itself, as pointed out by Fleming and Cummings, 2011 (for discussion of the nature of exact reduced equilibrium states see also Subaşi et al., 2012). Indeed, the violation of the Heisenberg uncertainty principle we observe within our Born-Markov master equation, which is of second-order in κ_k, is driven by the unphysical logarithmic divergence of D_p, which is itself proportional to γ, *i.e.* to κ_k^2. Obviously, if the exact master equation is used, then Heisenberg uncertainty violation cannot occur in any parameter regime, ergo this violation is not physical, but is rather a result of applied approximations. On the other hand, it is to be expected that both the degree of cooling and squeezing in the considered quantum stochastic process should be bounded from below, and the Heisenberg uncertainty violation gives a reasonable estimate of this bound.

3.5 Near-equilibrium dynamics

We look now into the dynamics of the model in order to get some insight about the motion of the central Brownian particle. For this goal we derive the equations for the first and second moments of the Wigner distribution, that can be easily obtained starting by Eq. (3.73). These moments characterize the Gaussian state fully, and form two closed systems of linear equations:

$$\dot{\langle x\rangle} = \langle p\rangle/m, \tag{3.86}$$

$$\dot{\langle p\rangle} = -m\Omega^2\langle x\rangle - \frac{2C_p}{m\Omega}\langle p\rangle, \tag{3.87}$$

and

$$\dot{\langle x^2\rangle} = 2\langle xp\rangle/m, \tag{3.88}$$

$$\dot{\langle xp\rangle} = \frac{\langle p^2\rangle}{m} - m\Omega^2\langle x^2\rangle - \frac{2C_p}{m\Omega}\langle xp\rangle - \frac{\hbar D_p}{m\Omega}, \tag{3.89}$$

$$\dot{\langle p^2\rangle} = -2m\Omega^2\langle xp\rangle - \frac{4C_p}{m\Omega}\langle p^2\rangle + 2\hbar D_x. \tag{3.90}$$

The solutions of the equations above describe a damped oscillation around their stable stationary values:

$$\langle x\rangle_{\rm st} = \langle p\rangle_{\rm st} = \langle xp\rangle_{\rm st} = 0, \tag{3.91}$$

and

$$\langle p^2\rangle_{\rm st} = \hbar m\Omega D_x/2C_p, \tag{3.92}$$

$$(m^2\Omega^2)\langle x^2\rangle_{\rm st} = \hbar(m\Omega D_x/2C_p - D_p/\Omega). \tag{3.93}$$

The only constraint is imposed by the Heisenberg principle

$$\frac{m\Omega^2\langle x^2\rangle}{2}\frac{\langle p^2\rangle}{2m} \geq \left(\frac{\hbar\Omega}{4}\right)^2. \tag{3.94}$$

The equations for $\langle x^2\rangle_{\rm st}$ and $\langle p^2\rangle_{\rm st}$ and the resulting Heisenberg bound coincides with the one found for σ_x, σ_p, and $\delta_x\delta_p$ in Sec. 3.4, a fact which should not surprise, as we have seen that a Gaussian Ansatz was providing an exact solution of the problem.

The equations for the first and second moments highlight once more the physical meaning of the coefficients of Eq. (3.36). For instance, Eq. (3.87) shows an exponential decreasing of the average value of the momentum induced by the interaction with environment. Here the coefficient C_p provides an information about the timescale ruling such a process. We see that it depends only on the spectral density, and so its parameters such as cut-off and damping constant, but not on the temperature.

We already discussed in Sec. 3.4 the relation between coefficient D_p and decoherence in the position basis which the particle undergoes. Now, Eq. (3.90) sheds light on its role in the momentum diffusion. Focusing on the time-dependence of $\langle p^2 \rangle$ due only to D_x we obtain

$$\langle p^2 \rangle \propto D_x t, \tag{3.95}$$

manifesting a normal diffusion in the momentum-space. Recall that such normal diffusion is a signature of Brownian motion. In fact, it easy to obtain by Eq. (3.88) that D_x also leads to normal diffusion on the position variance, namely the width of the ensemble in the position space asymptotically grows linearly in time.

3.6 Summary

We studied the quantum version of the Brownian motion. Here there is a resume of the main contents of the chapter.

- Quantum Brownian motion model may be described by means of a Hamiltonian [Eq. (3.1)], resulting by the sum of three terms: one related to the central Brownian particle, usually considered as a quantum harmonic oscillator, that related to the environment, modeled as a sum of uncoupled harmonic oscillators, and an interaction term showing a linear dependence in both the positions of central system and the constituents of the environment [Eq. (3.4)].

- The Hamiltonian permits to write the master equation in the Born-Markov regime [Eq. (3.36)], which is the main tool to characterize the dynamics of the Brownian particle under the influence of the environment, *i.e.* evaluate decoherence and dissipation processes and compute the average values of the observables [see Sec. 3.5].

- We focus on the stationary solution of the master equation. We represent it in the phase-space by means of a Wigner function distribution, and we study its geometrical configuration as the system parameters vary. Fig. 3.3 is the main result of the chapter, and highlights the areas where the quantum Brownian particle experiences squeezing and cooling. We note the presence of forbidden zones associated to the violations of Heisenberg principle, due to the non-exact character of Eq. (3.36).

Chapter 4

Non-linear quantum Brownian motion

The previous chapter was devoted to the discussion of the QBM model. We treated such a model by means of a Born-Markov master equation and we studied its stationary solution. All the theory we developed in chapter 3 refers to a Hamiltonian model where the interaction depends linearly on the position of the central particle. This is the conventional case, and we will refer to it in the following also as *linear case*. Now we aim to extend our analysis to an interaction term that manifests a non-linear dependence on the variables of the Brownian particle

$$H_{\mathrm{I}} = -\sum_k \kappa_k X_k f(x). \tag{4.1}$$

The non-linear character of the coupling term above is related to state-dependent damping and diffusion, arising for instance when the quantum Brownian particle is embedded in an inhomogeneous medium, *i.e.* a medium with a space-dependent density. To keep notation as close as possible to the usual case of linear coupling, we take $f(x)$ to have dimension of length, *i.e.* we write it as $f(x) = a\tilde{f}(x/a)$, with $\tilde{f}(x)$ being dimensionless, and a denoting a typical length scale on which f varies. In this case the counter-term in Eq. (3.5) writes as

$$V_c(x) = \sum_k \frac{\kappa_k^2}{2m_k\omega_k^2} f(x)^2. \tag{4.2}$$

In the first part of the chapter we focus on the most simple case provided by an interaction term in the form

$$H_{\rm I} = -\sum_k \kappa_k X_k \frac{x^2}{a}, \tag{4.3}$$

which we will call *quadratic interaction term*. We derive the Born-Markov master equation which corresponds to the dynamics induced by this Hamiltonian, focusing on the analysis of the stationary solution in the phase-space. Here the Gaussian ansatz just constitutes an approximation. Still, we present a quantitative analysis of the geometrical configuration of the Gaussian Wigner function associated to the stationary state, highlighting the forbidden areas and the range of the values of the system parameters where the quantum Brownian particle experiences squeezing and cooling. In the end, we will characterize the structure of the Born-Markov master equation of the most generic function f in the interaction Hamiltonian in Eq. (4.1). The results we are about to present have been published in the work of Massignan et al., 2015.

4.1 Born-Markov master equation with quadratic coupling

In this section we derive the Born-Markov master equation associated to the interaction Hamiltonian term in Eq. (4.3). We note that it differs from the linear case only with respect of the variables related to the central Brownian particle, namely the part associated to the bath operators does not change. Accordingly, the self-correlation function of the environment remains the same, and thus the noise and dissipation kernels, too. Finally, in order to write the Born-Markov master equation we have just to evaluate the time-dependence of the particle position in the interaction picture. It turns:

$$\begin{aligned} x^2(-\tau) &= \left[x\cos(\Omega\tau) - \frac{p}{m\Omega}\sin(\Omega\tau)\right]^2 \\ &= x^2\cos^2(\Omega\tau) - \frac{\{x,p\}}{m\Omega}\sin(\Omega\tau)\cos(\Omega\tau) + \frac{p^2}{m^2\Omega^2}\sin^2(\Omega\tau), \end{aligned} \tag{4.4}$$

so that (using the linearity of commutators and anti-commutators) one finds

$$\begin{aligned}\dot{\rho}(t) = &-\frac{i}{\hbar}\left[H_S, \rho(t)\right] - \frac{iC_{xx}}{\hbar a^2}[x^2, \{x^2, \rho(t)\}] - \frac{iC_{xp}}{\hbar a^2}\left[x^2, \left\{\frac{\{x,p\}}{m\Omega}, \rho(t)\right\}\right] \\ &- \frac{iC_{pp}}{\hbar a^2}\left[x^2, \left\{\frac{p^2}{m^2\Omega^2}, \rho(t)\right\}\right] - \frac{D_{xx}}{\hbar a^2}[x^2, [x^2, \rho(t)]] \\ &- \frac{D_{xp}}{\hbar a^2}\left[x^2, \left[\frac{\{x,p\}}{m\Omega}, \rho(t)\right]\right] - \frac{D_{pp}}{\hbar a^2}\left[x^2, \left[\frac{p^2}{m^2\Omega^2}, \rho(t)\right]\right], \end{aligned} \tag{4.5}$$

with the coefficients $C_{...}$ given by

$$C_{xx} = -\int_0^\infty \mathrm{d}\tau\, \eta(\tau)\cos^2(\Omega\tau), \tag{4.6}$$

$$C_{xp} = \int_0^\infty \mathrm{d}\tau\, \eta(\tau)\sin(\Omega\tau)\cos(\Omega\tau), \tag{4.7}$$

$$C_{pp} = -\int_0^\infty \mathrm{d}\tau\, \eta(\tau)\sin^2(\Omega\tau), \tag{4.8}$$

and the $D_{...}$ by

$$D_{xx} = \int_0^\infty \mathrm{d}\tau\, \nu(\tau)\cos^2(\Omega\tau), \tag{4.9}$$

$$D_{xp} = -\int_0^\infty \mathrm{d}\tau\, \nu(\tau)\sin(\Omega\tau)\cos(\Omega\tau), \tag{4.10}$$

$$D_{pp} = \int_0^\infty \mathrm{d}\tau\, \nu(\tau)\sin^2(\Omega\tau). \tag{4.11}$$

Using

$$\sin(x)\cos(x) = \sin(2x)/2, \tag{4.12}$$

and introducing the shorthand notation

$$c(\Lambda) = \Lambda^2/(4\Omega^2 + \Lambda^2), \tag{4.13}$$

for the cut-off function evaluated at frequency 2Ω, we may exploit the results for C_p and D_p of the previous chapter to find

$$C_{xp} = \frac{1}{2}\int_0^\infty \mathrm{d}\tau\, \eta(\tau)\sin(2\Omega\tau) = \frac{C_p(2\Omega)}{2} = \frac{m\gamma\Omega}{2}c(\Lambda), \tag{4.14}$$

$$D_{xp} = \frac{D_p(2\Omega)}{2} = \frac{m\gamma\Omega}{\pi} c(\Lambda)\{\frac{\pi k_{\rm B}T}{\hbar\Lambda} + {\rm Di}\Gamma\left(\frac{\hbar\Lambda/2}{\pi k_{\rm B}T}\right)\} - \frac{m\gamma\Omega}{\pi} c(\Lambda){\rm Re}\left[{\rm Di}\Gamma\left(\frac{i\hbar\Omega}{\pi k_{\rm B}T}\right)\right]. \tag{4.15}$$

Similarly, noting that

$$\cos^2(x) = [1+\cos(2x)]/2, \tag{4.16}$$

$$I_\nu \equiv \int_0^\infty {\rm d}\tau\, \nu(\tau) = m k_{\rm B} T\gamma/\hbar, \tag{4.17}$$

and D_x for the linear case, it turns

$$D_{xx} = \frac{I_\nu + D_x(2\Omega)}{2} = \frac{m\gamma\Omega}{2}\left[\frac{k_{\rm B}T}{\hbar\Omega} + c(\Lambda)\coth\left(\frac{\hbar\Omega}{k_{\rm B}T}\right)\right], \tag{4.18}$$

$$D_{pp} = I_\nu - D_{xx} = \frac{m\gamma\Omega}{2}\left[\frac{k_{\rm B}T}{\hbar\Omega} - c(\Lambda)\coth\left(\frac{\hbar\Omega}{k_{\rm B}T}\right)\right]. \tag{4.19}$$

Finally, recalling

$$I_\eta \equiv \int_0^\infty {\rm d}\tau\, \eta(\tau) = m\gamma\Lambda/2, \tag{4.20}$$

and the derivation for C_x in chapter 3, one also obtains

$$C_{xx} = -\frac{I_\eta}{2} + \frac{C_x(2\Omega)}{2} = -\frac{m\gamma\Lambda(2\Omega^2+\Lambda^2)}{2(4\Omega^2+\Lambda^2)}, \tag{4.21}$$

$$C_{pp} = -I_\eta - C_{xx} = -\frac{m\gamma\Omega^2}{\Lambda} c(\Lambda). \tag{4.22}$$

In analogy with the linear case, the coefficient C_{xx} diverges with the cut-off Λ, but this poses no problems as

$$[x^2, \{x^2, \rho\}] = [x^4, \rho], \tag{4.23}$$

so this term may always be canceled exactly by an appropriate counter-term

$$V_c(x) = -C_{xx}x^4/a^2, \tag{4.24}$$

representing this time a Lamb-shift of the coefficient of the quartic term in the confinement. All other coefficients remain bounded in the limit of $\hbar\Lambda/k_{\rm B}T \to \infty$, exception made for D_{xp} which exhibits a mild logarithmic

divergence, in complete analogy with D_p in the linear case. The generalized master equation (4.5), together with the explicit forms of its coefficients, represents a central result of the present chapter: it is the main tool to study the dynamics of the central Brownian particle induced by the interaction Hamiltonian (4.3). Here below, we analyze the behavior of the various coefficients in three different limits.

4.1.1 Caldeira-Leggett limit

In the Caldeira-Leggett regime defined in Eq. (3.54), we have

$$\begin{aligned} D_{xx} \approx & m\gamma k_{\mathrm{B}}T/\hbar, \\ D_{xp} \approx & -m\gamma(k_{\mathrm{B}}T/\hbar)(\Omega/\Lambda) \longrightarrow 0, \\ D_{pp} \approx & -m\gamma\hbar\Omega^2/(6k_{\mathrm{B}}T) \longrightarrow 0, \end{aligned} \tag{4.25}$$

and therefore it results

$$\begin{aligned} \dot{\rho}(t) = & -\frac{i}{\hbar}\left[H_{\mathrm{sys}}, \rho(t)\right] - \frac{im\gamma}{2\hbar}\left[\frac{x^2}{a}, \left\{\frac{\{x,p\}}{ma}, \rho(t)\right\}\right] \\ & - \frac{m\gamma k_{\mathrm{B}}T}{\hbar^2}\left[\frac{x^2}{a}, \left[\frac{x^2}{a}, \rho(t)\right]\right]. \end{aligned} \tag{4.26}$$

In this limit, it is easy to identify C_{xp} as being proportional to the momentum damping coefficient, and D_{xx} to the normal momentum diffusion coefficient. In analogy with the traditional QBM model, this latter term may also be seen as the one responsible for decoherence in the position basis. The off-diagonal components of ρ are in this way found to decohere at a rate

$$\gamma^{(2)}_{x_1,x_2} = D_{xx}(x_1^2 - x_2^2)^2/\hbar a^2, \tag{4.27}$$

This is an important result, providing a typical timescale for decoherence of states entangled in position space in presence of a bath coupling of the form $f(x) \propto x^2$. In the end of the chapter we will provide a general formula which yields the position-space decoherence rate $\gamma^{(n)}_{x_1,x_2}$ associated to a coupling with an arbitrary power of the system's coordinate, $f(x) \propto x^n$. Remarkably, and at odds with what found in Ref. Hu, Paz, and Zhang, 1993, we find that superposition states which are symmetric around the origin (e.g., sharply localized around both $+x_0$ and $-x_0$) will

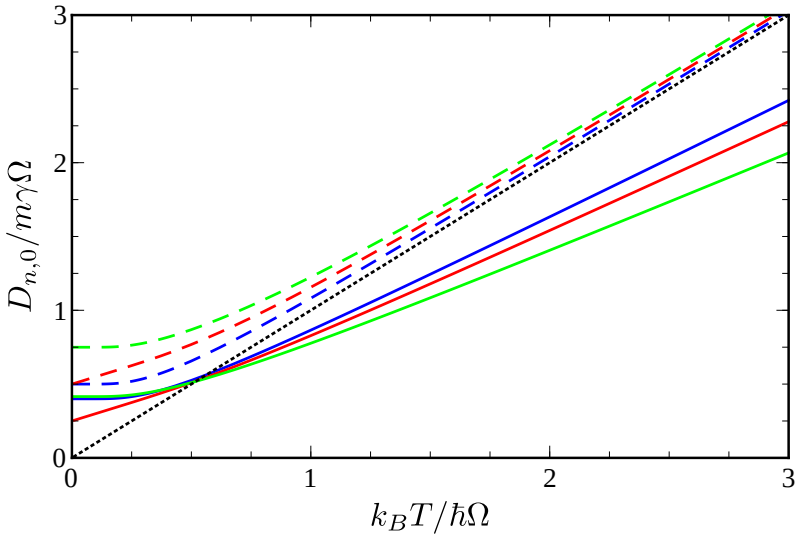

FIGURE 4.1: Plot of the coefficients $D_{n,0}$, which control the decoherence rate of the off-diagonal elements of the density matrix $\rho(x_1, x_2)$ in the position basis. The lines represent respectively $D_{1,0} = D_x$ (blue), $D_{2,0} = D_{xx}$ (red), and $D_{3,0}$ (green). Continuous lines are for $\Lambda = 2\Omega$, dashed lines for $\Lambda = 100\Omega$. In the Caldeira-Leggett limit $k_{\rm B}T/\hbar \gg \Lambda \gg \Omega$, we find $D_{n,0} \to m\gamma k_{\rm B}T/\hbar$ (dotted line), independent of n.

be protected by decoherence in presence of couplings containing only even powers of n.

Note also that in this limit we recover again the classical Gibbs-Boltzmann stationary states, and the dynamics satisfies the fluctuation-dissipation relation. Namely, in the case of a harmonic potential, or more generally upon neglecting quantum effects induced by an anharmonic potential, the time dependent equation for the Wigner function has the interpretation of a Fokker–Plank equation for the probability distribution in the phase space of a classical Brownian particle undergoing damped motion with an x–dependent damping $\gamma(x/a)^2$ under the influence of a multiplicative Langevin stochastic noise–force $F(t)(x(t)/a)$. The noise is Gaussian and white, and it fulfills the fluctuation–dissipation relation, *i.e.* the

average of the noise correlation yields

$$\langle F(t+\tau)x(t+\tau)F(t)x(t)\rangle = 2\gamma k_{\rm B}T\langle x^2\rangle. \tag{4.28}$$

This relation assures that the stable stationary state of the dynamics is the classical Gibbs-Boltzmann state. In terms of the coefficients entering the master equation the fluctuation–dissipation relation implies that

$$D_{xx}/C_{xp} = 2k_{\rm B}T/\hbar\Omega. \tag{4.29}$$

4.1.2 Large cut-off limit

Taking the limit

$$\Lambda \gg \Omega, \frac{k_{\rm B}T}{\hbar}, \tag{4.30}$$

the quantity simply amounts to setting $c(\Lambda) = 1$ in the expression for the various coefficients. Such a regime shows the following features i) the coefficient C_{pp} (a term contributing to a Lamb-shift of the trap frequency Ω) is suppressed as Ω/Λ; ii) the normal momentum diffusion (or position-basis decoherence) coefficient D_{xx}, which is analogous to the D_x of the previous chapter, develops a non-trivial quantum dependence on $\hbar\Omega/k_{\rm B}T$; iii) the coefficient D_{xp} (which contributes to both the Lamb-shift and the anomalous diffusion) becomes log-divergent in Λ, analogously to D_p for the traditional QBM model; iv) there appears a new coefficient, D_{pp}, which depends on $\hbar\Omega/k_{\rm B}T$, and vanishes for $k_{\rm B}T \gg \hbar\Omega$.

We note here that, in this limit, the coefficients of the master equation satisfy the generalized fluctuation-dissipation relations

$$(D_{xx} + D_{pp})/C_{xp} = 2k_{\rm B}T/\hbar\Omega \tag{4.31}$$

$$(D_{xx} - D_{pp})/C_{xp} = 2\coth(\hbar\Omega/k_{\rm B}T). \tag{4.32}$$

Finally, we note that the Caldeira-Leggett limit, should be taken with precaution in the case of non-linear coupling. Indeed, as we will see in the following (cf. Fig. 4.2), for strong damping the system in a purely harmonic trap may become dynamically unstable at sufficiently large temperatures.

4.1.3 Ultra-low temperature

The master equation for

$$k_{\mathrm{B}}T/\hbar \ll \Omega \ll \Lambda \tag{4.33}$$

reads:

$$\begin{aligned}\dot{\rho}(t) = &-\frac{i}{\hbar}\left[H_{\mathrm{sys}}, \rho(t)\right] - \frac{im\gamma}{2\hbar}\left[\frac{x^2}{a}, \left\{\frac{\{x,p\}}{ma}, \rho(t)\right\}\right] \\ &- \frac{m\gamma\Omega}{2\hbar}\left[\frac{x^2}{a}, \left[\frac{x^2}{a} - \frac{p^2}{m^2\Omega^2 a}, \rho(t)\right]\right] \\ &- \frac{m\gamma}{\hbar\pi}\log\left(\frac{\Lambda}{2\Omega}\right)\left[\frac{x^2}{a}, \left[\frac{\{x,p\}}{ma}, \rho(t)\right]\right].\end{aligned} \tag{4.34}$$

As expected the temperature drops out of the equation, and the D_{xp} term is log-divergent in the cut-off Λ. The fact that the self-correlation function writes in the same way for both quadratic and linear QBM implies that the formal condition in Eq. (3.46) associated to the Markov hypothesis shows the same form. According, also in this context the low-temperature limit has to be studied carefully because it could affect the approximations underling the derivation of the Born-Markov treatment, on which discussion relies.

4.2 Stationary solution

The equation of motion for the Wigner function of a harmonically confined particle reads

$$\begin{aligned}\dot{W} =& -\frac{i}{\hbar}\left[\frac{p_-^2-p_+^2}{2m}+V(x_+)-V(x_-)\right]W \\ &-(x_+^2-x_-^2)\left[\frac{iC_{xp}\Big(\{x_+,p_-\}+\{x_-,p_+\}\Big)}{\hbar m\Omega a^2}+\frac{iC_{pp}(p_-^2+p_+^2)}{\hbar m^2\Omega^2 a^2}\right. \\ &\left.+\frac{D_{xx}(x_+^2-x_-^2)}{\hbar a^2}+\frac{D_{xp}\Big(\{x_+,p_-\}-\{x_-,p_+\}\Big)}{\hbar m\Omega a^2}+\frac{D_{pp}\Big(p_-^2-p_+^2\Big)}{m^2\Omega^2\hbar a^2}\right]W \qquad (4.35)\\ =&\left[-\frac{\partial_x p}{m}+m\Omega^2\partial_p x+\frac{8C_{xp}}{m\Omega a^2}\left(\partial_p p x^2+\frac{\hbar^2}{4}\partial_p^2(\partial_x x-1)\right)\right. \\ &+\frac{C_{pp}}{(m\Omega a)^2}\Big(4\partial_p x p^2-\hbar^2\partial_p\partial_x^2 x+2\hbar^2\partial_p\partial_x\Big) \\ &\left.+\frac{4\hbar D_{xx}\partial_p^2 x^2}{a^2}+\frac{4\hbar D_{xp}(\partial_p^2 x p-\partial_p\partial_x x^2+\partial_p x)}{m\Omega a^2}-\frac{4\hbar D_{pp}(\partial_x x-1)\partial_p p}{m^2\Omega^2 a^2}\right]W\end{aligned}$$

Interestingly, the Gaussian ansatz (3.74) would provide a stationary solution to the equation above if we neglected the terms proportional to C_{pp} and D_{xp}. Remembering that

$$D_{xx}-D_{pp}=2C_{xp}\coth\left(\hbar\Omega/k_{\mathrm{B}}T\right), \qquad (4.36)$$

the stationary solution is found when

$$\sigma_p=\sigma_x=1 \qquad (4.37)$$

and

$$k_{\mathrm{B}}\tilde{T}\overset{(C_{pp}=D_{xp}=0)}{=}\frac{\hbar\Omega}{2}\coth\left(\frac{\hbar\Omega}{2k_{\mathrm{B}}T}\right), \qquad (4.38)$$

which coincides with the result found in chapter 3. Unfortunately however D_{xp} is generally not negligible, as for example it diverges logarithmically with the cut-off Λ. In order to incorporate the neglected terms, one may try to generalize the ansatz by including in the exponent terms

proportional to higher polynomials in x^2 and p^2 (*i.e.* terms such as x^4, x^2p^2, or p^4), but no closed solution can be be found in this way, as moments of a given order always couple with higher ones.

The contributions higher than quadratic can, however, be reasonably taken into account by means of the so-called *self-consistent Gaussian (or pairing) approximation* (Gardiner, 2009; Risken, 2012). The D_{xp} term is proportional to

$$\begin{aligned}&\partial_p^2 xp - \partial_p\partial_x x^2 + \partial_p x \simeq \partial_p^2\langle xp\rangle_{\rm st} - \partial_p\partial_x\langle x^2\rangle_{\rm st} + \partial_p x\\ =& -\partial_p\partial_x\frac{k_{\rm B}\tilde{T}}{\sigma_x m\Omega^2} + \partial_p x.\end{aligned} \tag{4.39}$$

As a general rule, averages of odd functions or partial derivatives vanish when performed with respect to the Gaussian distribution (3.74). Similarly, the C_{pp} term contributes

$$4\partial_p xp^2 - \hbar^2\partial_p\partial_x^2 x + 2\hbar^2\partial_p\partial_x \approx \frac{4mk_{\rm B}\tilde{T}}{\sigma_p}\partial_p x + 2\hbar^2\partial_p\partial_x, \tag{4.40}$$

as (mixed) derivatives of order higher than two vanish in this approximation. In this way, we get the two equations

$$\delta_p^2 = \frac{\delta_x^2}{\zeta} + \Gamma c_{pp}\left(\frac{\delta_x^2\delta_p^2}{2} - 1\right) \tag{4.41}$$

$$\delta_x^2\delta_p^2 = \frac{\delta_x^2 d_{xx} - \delta_p^2 d_{pp}}{c_{xp}} - 1. \tag{4.42}$$

To simplify notation, we have introduced the normalized damping $\Gamma \equiv 2\hbar\gamma/(m\Omega^2a^2)$, the adimensional variables $c_{xp} = 2C_{xp}/(m\gamma\Omega)$ (and similarly for c_{pp}, d_{xp}, ...), and the quantity $\zeta = 1/(1 + 2\Gamma d_{xp})$.

The two coupled equations (4.41) and (4.42) may be combined to obtain a single quadratic equation determining, e.g., δ_x^2, from which we may then extract δ_p^2. The quadratic equation has two solutions, and the correct one may selected by looking at its behaviour in the regime $\Omega \ll k_{\rm B}T/\hbar \ll \Lambda$. The (-) solution unphysically tends towards zero there. On the other hand, the (+) solution correctly yields $\delta_x^2 \sim 2k_{\rm B}T/\hbar\Omega$, *i.e.* an effective temperature $\tilde{T} \sim T$. At odds with the linear case, however, $\tilde{T}$ strongly deviates from T when $T \sim O(\Lambda/\Omega)$.

A detailed phase diagram for the present case of quadratic coupling

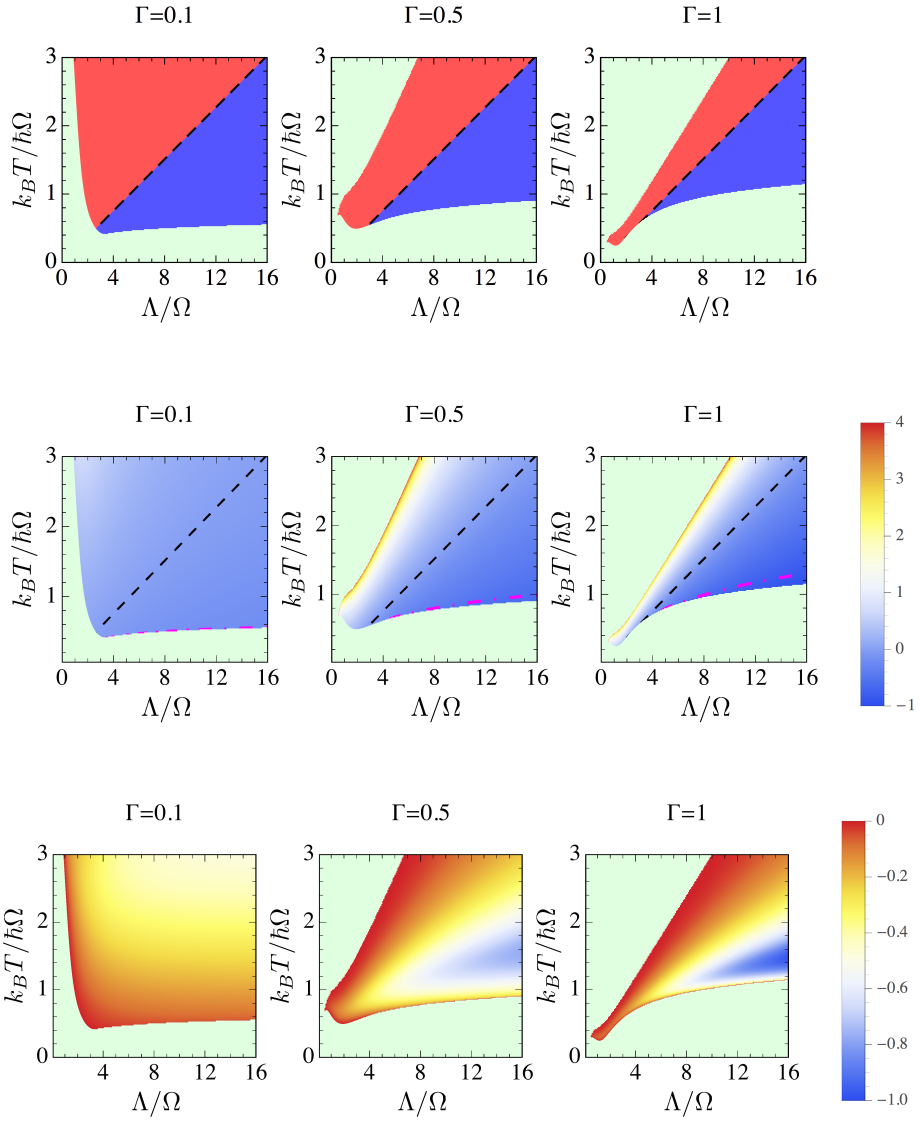

FIGURE 4.2: Phase diagram of our equation for a quadratic coupling, under the self-consistent Gaussian approximation. From left to right, plots are for $\Gamma = 0.1, 0.5, 1$. Top **(a)**: the gas experiences an effective "cooling" in the blue regions, and an effective "heating" in the red regions. Center **(b)**: density plot of the logarithm of the aspect ratio $\log(\delta_x^2/\delta_p^2)$. Bottom **(c)**: maximum of the real part of the eigenvalues of the matrix of coefficients of the linear system defined in Eq. (4.54).

is presented in Fig. 4.2. The Heisenberg principle requires $\delta_x\delta_p \geq 1$, a condition which gives rise to a minimal acceptable temperature which grows as $T_{min} \sim \log(\Lambda)$ for large Λ/Ω, in close analogy to the linear case. The Heisenberg bound is shown in Fig. 4.2a, together with the region where the gas experiences an effective heating, or cooling, with respect to its Gibbs-Boltzmann counterpart.

The corresponding degree of deformation of the phase-space distribution, as measured by the logarithm of the aspect ratio $\log(\delta_x^2/\delta_p^2) = \log(\sigma_p/\sigma_x)$, is shown in Fig. 4.2b. At small temperatures, we observe the emergence of a region (below the magenta, dot-dashed lines) where $\delta_x^2 < 1$, *i.e.* of *genuine quantum squeezing*. Notice that, for damping $\Gamma \gtrsim 0.1$, at large temperatures the aspect ratio of the distribution displays a very sharp increase; beyond a certain point, the solution of Eqs. (4.41) and (4.42) yields a value for the fluctuations δ_x^2 which diverges and turns negative, a clearly unphysical feature signaling the breakdown of the Gaussian Ansatz in that region.

It may be noticed by comparing Figs. 4.2a and 4.2b that, as in previous chapter, the Gibbs-Boltzmann boundary coincides with the one of unit aspect ratio, a condition which again is independent of Γ. This may be explicitly checked by employing the trial GB solution $\delta_x^2 = \delta_p^2 = \coth(\hbar\Omega/2k_{\rm B}T)$, which is an identical solution of Eq. (4.42) for every $\{\Lambda, \Omega, T\}$, and a solution of Eq. (4.41) for every Γ provided that $k_{\rm B}T/\hbar = \alpha_{(2)}\Lambda + O(\Omega/T)$, with $\alpha_{(2)} \approx 0.189$ satisfying the implicit equation

$$\pi\alpha_{(2)} + 2[\mathrm{Di}\Gamma(1/2\pi\alpha_{(2)}) + \tilde{\gamma}] = 0. \tag{4.43}$$

At odds with the linear case seen in the previous chapter, the equations for a quadratic coupling determine the two ratios $\delta_x^2 \propto \tilde{T}/\sigma_x$ and $\delta_p^2 \propto \tilde{T}/\sigma_p$, but do not provide an explicit expression for $\tilde{T}$, σ_x and σ_p separately, leaving therefore open various possible applications of this theory.

As an example, we may fix $\tilde{T}$ in accordance to the standard formula for the quantum mechanical harmonic oscillator, Eq. (3.78), and then interpret σ_p and σ_x as quantum corrections to the inverse mass $1/m$ and the spring constant $m\Omega^2$. Such "renormalization" should be used if we considered the starting model as a fundamental quantum field theoretic construct.

Alternatively, one may set, say, $\sigma_p = 1$, and consider quantum modification of the effective temperature, and the spring constant. From Eq.

(4.41) one finds in this way

$$k_{\mathrm{B}}\tilde{T} = \frac{\hbar\Omega}{2}\frac{\delta_x^2/\zeta - \Gamma c_{pp}}{1 - \Gamma c_{pp}\delta_x^2/2}. \tag{4.44}$$

In the green regions, one of the validity conditions is violated, *i.e.* either the Heisenberg principle is not satisfied, or one of the eigenvalues of the stability equations becomes positive, or fluctuations δ_x^2 and δ_p^2 are complex numbers. The black dashed lines are the boundaries of unity aspect ratio, where $\delta_x^2 = \delta_p^2$. One needs to examine the nature of Heisenberg uncertainty pathologies in the present quadratic case. Obviously, the exact stationary state should not violate the Heisenberg uncertainty inequality. In the quadratic case, however, the exact solution is not known, and the results of Fleming and Cummings, 2011 cannot be applied directly. The pathologies may result from solutions being of mixed order as in Fleming and Cummings, 2011, or from the non-Gaussian form of the unknown exact solution. In any case the pathologies signal the invalidity of applied approximations and offer a reasonable bound for the degree of cooling and squeezing in the considered quantum stochastic process.

4.3 Near-equilibrium dynamics in self-consistent Gaussian approximation

In this case, the Gaussian Ansatz provides only an approximate solution. Again, the first and second moments of the Wigner distribution characterize the Gaussian state fully, but this time they couple to higher moments, so that Wick (Gaussian) de-correlation techniques have to be used. We obtain for the first moments

$$\begin{aligned}\dot{\langle x\rangle} =& \langle p\rangle/m, \\ \dot{\langle p\rangle} =& -m\Omega^2\langle x\rangle - \frac{8C_{xp}}{m\Omega a^2}\langle x^2p\rangle - \frac{4C_{pp}}{(m\Omega a)^2}\langle xp^2\rangle \\ & - \frac{4\hbar D_{xp}}{m\Omega a^2}\langle x\rangle - \frac{4\hbar D_{pp}}{m^2\Omega^2 a^2}\langle p\rangle.\end{aligned} \tag{4.45}$$

The Wick's theorem allows to replace

$$\langle x^2p\rangle = \langle x\rangle^2\langle p\rangle + 2\langle\Delta_x\Delta_p\rangle\langle x\rangle + \langle\Delta_x^2\rangle\langle p\rangle, \tag{4.46}$$

and similarly for $\langle xp^2\rangle$, where we represent the Gaussian random variables

$$x = \langle x\rangle + \Delta_x, \quad p = \langle p\rangle + \Delta_p. \tag{4.47}$$

We obtain thus

$$\begin{aligned}\dot{\langle p\rangle} =& - m\Omega^2\langle x\rangle - \frac{8C_{xp}(\langle x\rangle^2 + \langle\Delta_x^2\rangle)}{m\Omega a^2}\langle p\rangle \\ &- \frac{4C_{pp}(\langle p\rangle^2 + \langle\Delta_p^2\rangle)}{m^2\Omega^2a^2}\langle x\rangle - \frac{4\hbar D_{xp}}{m\Omega a^2}\langle x\rangle \\ &- \frac{4\hbar D_{pp}}{m^2\Omega^2a^2}\langle p\rangle - \frac{8\langle\Delta_x\Delta_p\rangle}{m^2\Omega^2a^2}(C_{pp}\langle p\rangle + 2m\Omega C_{xp}\langle x\rangle).\end{aligned} \tag{4.48}$$

These equations have a stable stationary solution $\langle x\rangle_{\rm st} = \langle p\rangle_{\rm st} = 0$, provided that they describe a damped harmonic oscillator. If such a solution exists, in its vicinity we may identify

$$\langle\Delta_x^2\rangle_{\rm st} = \langle x^2\rangle_{\rm st} = \delta_x^2\hbar/(2m\Omega), \tag{4.49}$$

and

$$\langle\Delta_p^2\rangle_{\rm st} = \langle p^2\rangle_{\rm st} = \hbar m\Omega\delta_p^2/2, \tag{4.50}$$

since by hypothesis the first moments are zero, and we may neglect the quadratic terms $\langle x\rangle^2$, $\langle p\rangle^2$ and the crossed fluctuation term $\langle\Delta_x\Delta_p\rangle$, to get the two simultaneous conditions

$$1 + \Gamma d_{xp} + \Gamma c_{pp}\delta_p^2/2 \geq 0, \qquad c_{xp}\delta_x^2 + d_{pp} \geq 0 \tag{4.51}$$

These, in turn, depend self-consistently on the equations for the second moments,

$$\dot{\langle x^2\rangle} = \frac{2}{m}\langle xp\rangle, \tag{4.52}$$

$$\begin{aligned}\dot{\langle xp\rangle} =& \frac{\langle p^2\rangle}{m} - m\Omega^2\langle x^2\rangle - \frac{8}{m\Omega a^2}\left[C_{xp}\langle x^3p\rangle + \hbar D_{xp}\langle x^2\rangle\right] \\ &- \frac{1}{m^2\Omega^2a^2}\Big[C_{pp}\Big(4\langle x^2p^2\rangle - 2\hbar^2\Big) + 8\hbar D_{pp}\langle xp\rangle\Big], \\ \dot{\langle p^2\rangle} =& - 2m\Omega^2\langle xp\rangle - \frac{4C_{xp}}{m\Omega a^2}\Big(4\langle x^2p^2\rangle + \hbar^2\Big) \\ &- \frac{8C_{pp}}{m\Omega a^2}\langle xp^3\rangle + \frac{8\hbar D_{xx}}{a^2}\langle x^2\rangle - \frac{8\hbar D_{pp}}{m^2\Omega^2a^2}\langle p^2\rangle.\end{aligned}$$

From the first equation, we see that if a stable stationary solution exists then $\langle xp\rangle_{\rm st} = 0$. The quartic terms may be decomposed as above, using the Wick's method, and in this way one may compute the stationary solution. A straightforward calculation then shows that in the stationary state described by the momenta $\langle x^2\rangle_{\rm st}$ and $\langle p^2\rangle_{\rm st}$ satisfy Eqs. (4.41) and (4.42). To check the stability of the steady-state, we write

$$\langle x^2\rangle = \langle x^2\rangle_{\rm st} + \Delta_{x^2}, \quad \langle p^2\rangle = \langle p^2\rangle_{\rm st} + \Delta_{p^2}, \quad \langle xp\rangle = \Delta_{xp}, \tag{4.53}$$

and perform linear stability analysis in Δ's,

$$\begin{aligned}
\partial_t(\Delta_{x^2}) =& \frac{2}{m}\Delta_{xp} \\
\partial_t(\Delta_{xp}) =& \frac{\Delta_{p^2}}{m} - m\Omega^2\Delta_{x^2} - \frac{24C_{xp}\langle x^2\rangle_{\rm st}\Delta_{xp} + 8\hbar D_{xp}\Delta_{x^2}}{m\Omega a^2} \\
&- \frac{4C_{pp}(\langle x^2\rangle_{\rm st}\Delta_{p^2} + \langle p^2\rangle_{\rm st}\Delta_{x^2}) + 8\hbar D_{pp}\Delta_{xp}}{m^2\Omega^2 a^2} \\
\partial_t(\Delta_{p^2}) =& -2m\Omega^2\Delta_{xp} - \frac{16C_{xp}}{m\Omega a^2}[\langle p^2\rangle_{\rm st}\Delta_{x^2} + \langle x^2\rangle_{\rm st}\Delta_{p^2}] \\
&- \frac{24C_{pp}}{m^2\Omega^2 a^2}\langle p^2\rangle_{\rm st}\Delta_{xp} + \frac{8\hbar D_{xx}}{a^2}\Delta_{x^2} - \frac{8\hbar D_{pp}}{m^2\Omega^2 a^2}\Delta_{p^2}.
\end{aligned} \tag{4.54}$$

The stability requires that the real parts of all eigenvalues of the matrix governing the above linear evolution have to be negative, *i.e.* have to describe damping. Numerical analysis of the eigenvalues of this matrix is presented in Fig. 4.2c. The plot indicates that all eigenvalues are negative in most of the region of existence of the physically Gaussian stationary solution, but at the same time the region of validity rapidly shrinks with increasing damping Γ. To summarize, regions colored in green are not accessible by the system because either the normalized standard deviations δ_x^2 and δ_p^2 have an unphysical imaginary part, or they do not satisfy the Heisenberg bound $\delta_x^2\delta_p^2 \geq 1$, or the equations for the first moments do not describe a damped harmonic oscillator (*i.e.* inequalities in (4.51) are not satisfied), or at least one of the eigenvalues of the linear stability matrix of the second moments (4.54) becomes positive.

Note that on top of the stability question, Eqs. (4.52) and (4.54) incorporate quantum dynamical effects: they describe dynamics clearly different from their high T classical analogues, due to the quantum form/origin of the diffusion coefficients D_{xx}, D_{xp} and D_{pp}.

Finally, let us comment about the large prohibited region we find in

the quadratic case at large T. This region is generally dynamically unstable, and arises because of the diverging fluctuations in x caused by a large Lamb-shift of the effective trap frequency, which turns the attractive harmonic potential into an effectively repulsive one. It is reasonable to expect that this region would become allowed if we added a quartic term to the confinement, on top of the usual quadratic one. Indeed, Hu, Paz, and Zhang, 1993 considered only this case, for non-linear couplings. However, traps for ultracold atoms are generally to a very high approximation purely quadratic in the region where the atoms are confined, so that the presence of a quartic component may be unjustified in a real experiment.

4.4 General non-linear coupling

We consider here the interaction term with a completely general coupling in the position of the particle in Eq. (4.1). If $f \in \mathcal{C}^\infty(I)$ and thus may be expanded in Taylor series, the master equation can be written in the form:

$$\dot{\rho} = -\frac{i}{\hbar}[H_S, \rho] - \sum_{j,n=0}^{\infty} \sum_{k=0}^{n} \frac{\tilde{f}^{(j)} \tilde{f}^{(n)}}{a^{j+n-2} j! n! (m\Omega)^k} \mathcal{L}_{n,k,j}[x, p, \rho] \tag{4.55}$$

with

$$\mathcal{L}_{n,k,j}[x, p, \rho] = \left[x^j, \frac{iC_{n,k}}{\hbar}\{\sigma(x^{n-k}p^k), \rho\} + \frac{D_{n,k}}{\hbar}\left[\sigma(x^{n-k}p^k), \rho\right]\right] \tag{4.56}$$

where $\sigma(x^m p^k)$ is the sum of the $\frac{(m+k)!}{m!k!}$ distinguishable permutations of the $m+k$ operators in the polynomial $x^m p^k$ [e.g., $\sigma(x^2 p) = x^2 p + xpx + px^2$]. We have introduced here

$$\begin{aligned} C_{n,k}(\Omega) =& (-1)^{k+1} \int_0^\infty \mathrm{d}\tau\, \eta(\tau) \cos^{n-k}(\xi) \sin^k(\xi) \\ D_{n,k}(\Omega) =& (-1)^k \int_0^\infty \mathrm{d}\tau\, \nu(\tau) \cos^{n-k}(\xi) \sin^k(\xi) \end{aligned} \tag{4.57}$$

where $\xi = \Omega\tau$. These integrals may be calculated by Laplace transformation, as detailed in Appendix B. Alternatively, we will outline in the

same Appendix a simpler method which employs standard trigonometric identities to straightforwardly reduce every $C_{n,k}$ to a linear combination of C_x and C_p (the ones computed in the linear case), and similarly every $D_{n,k}$ in terms of D_x and D_p. As an example, since

$$\cos^3(\xi)\sin(\xi) = [2\sin(2\xi) + \sin(4\xi)]/8, \tag{4.58}$$

it is obvious that

$$D_{4,1}(\Omega) = [2D_p(2\Omega) + D_p(4\Omega)]/8, \tag{4.59}$$

In complete analogy with the linear and quadratic cases, for a power law coupling with $f(x) = a(x/a)^n$ the coefficient $D_{n,0}$ determines the decoherence in the position basis, which for a quantum superposition of two states centered respectively at x and x' happens with a characteristic rate

$$\gamma^{(n)}_{x_1,x_2} = D_{n,0}(x_1^n - x_2^n)^2/\hbar a^{2n-2}. \tag{4.60}$$

As a consequence, for an even more general coupling containing various powers of (x/a), the total decay rate in position space reads

$$\gamma_{x_1,x_2} = \sum_{j,n=0}^{\infty} \frac{\tilde{f}^{(j)}\tilde{f}^{(n)}D_{n,0}(x_1^n - x_2^n)^2}{\hbar j!n!a^{j+n-2}}. \tag{4.61}$$

In contrast with the work of Hu, Paz, and Zhang, 1993, we find here that quantum superpositions which are sharply localized at positions symmetric with respect to the origin (e.g., in the vicinity of, say, x_0 and $-x_0$) will be characterized by a vanishing decoherence rate (*i.e.* a diverging lifetime) in presence of couplings which contain only even powers of n. The decoherence rates in Eq. 4.61 are plotted in Fig. 4.1.

Large cut-off limit

In the limit $\Lambda \gg k_{\rm B}T/\hbar, \Omega$, we find:

- $C_{n,k} \propto \Lambda^{1-k}$, such that at every order n the only divergent term is linear, and it is the one which may be re-absorbed in the Hamiltonian; indeed, $C_{n,0}$ is the coefficient in front of the term $i[x^n, \{x^n, \rho\}] = i[x^{2n}, \rho]$, so that the divergent term is canceled by taking $H_{\rm sys} = H_{\rm S} - C_{n,0}f(x)^2$. Moreover, for every n we have $C_{n,1} = m\gamma\Omega/2$.

- between the coefficients $D_{n,k}$, only the term with $k = 1$ diverges, logarithmically as $D_{n,1} \sim \frac{m\gamma\Omega}{\pi} \log\left(\frac{\hbar\Lambda}{2\pi k_{\mathrm{B}} T}\right) + \ldots$. All terms with $k \neq 1$ are instead finite.

High-temperature limit

In the high-temperature limit $\frac{k_{\mathrm{B}}T}{\hbar} \gg \Lambda \gg \Omega$, the coefficients C are as in the large-cut-off limit, as they do not depend on T. In the set of D coefficients, only $D_{n,0} \sim m\gamma k_{\mathrm{B}} T/\hbar$ remains finite, while all others go to zero. Using the identity $\sigma(x^{n-1}p) = n\{x^{n-1}, p\}/2$, it is easy to show that the master equation (4.55) reduces at high temperatures to

$$\dot{\rho} = -\frac{i}{\hbar}[H_{\mathrm{sys}}, \rho] - \frac{i\gamma m}{2\hbar}[f(x), \{\dot{f}(x), \rho\}] - \frac{m\gamma k_{\mathrm{B}} T}{\hbar^2}[f(x), [f(x), \rho]], \quad (4.62)$$

where

$$\begin{aligned}\dot{\rho} = &-\frac{i}{\hbar}[H_{\mathrm{sys}}, \rho] - \frac{i\gamma m}{2\hbar}[f(x), \{\dot{f}(x), \rho\}] \\ &- \frac{m\gamma k_B T}{\hbar^2}[f(x), [f(x), \rho]].\end{aligned} \quad (4.63)$$

In this *classical* limit, we see that in presence of a non-linear coupling the coefficients of the QME satisfy a generalized fluctuation-dissipation theorem, since for any n we have $D_{n,0}/C_{n,1} \approx 2k_{\mathrm{B}}T/\hbar\Omega$.

4.5 Summary

We presented an analysis of QBM model with inhomogeneous damping and diffusion, relying on the material published by Massignan et al., 2015. Here we resume the main contents of the chapter.

- The physics of a quantum Brownian particle in an inhomogeneous medium may be treated switching from the linear dependence on the particle position in the interaction Hamiltonian (3.4) to a non-linear one. This situation is modeled by the coupling term in Eq. (4.1).

- We pay particular attention to the quadratic coupling in Eq. (4.3), studying the dynamics described by the corresponding Hamiltonian by means of the resulting Born-Markov master equation in Eq. (4.5).

- We look into the stationary solutions of this equation and we represent it in the phase space. In this case the Gaussian ansatz proposed in the previous chapter only provides an approximation. We discuss how the geometrical configuration of this approximated Gaussian Wigner function changes, as the system parameters are tuned. The main result of this analysis is presented in Fig. 4.2, showing the regime where the particle experiences cooling and squeezing.

- We also characterize the structure of the Born-Master equation for the most general coupling (4.1). Its form is presented in Eq. (4.55). We use it to evaluate the rates associated to the decoherence process it induces. They are plotted in Fig. 4.1.

Chapter 5

A Lindblad model for quantum Brownian motion

In chapters 3 and 4 we investigated the QBM model and its extensions by means of Born-Markov master equations. This approach leads to violations of the Heisenberg principle as the temperature decreases and interaction strength grows. Such a pathology avoids the possibility to study the low-temperature regime, as well as that associated to certain values of the system-bath coupling. Overcoming this problem is a fundamental step towards a correct description of the dynamics of the quantum Brownian particle.

There are several possible manners to deal with the violations of the Heisenberg uncertainty principle. First of all, one has to note that, obviously, if the exact master equation is used, violation of Heisenberg principle cannot occur in any parameter regime. Conversely, the master equation (3.36) (as well as that in Eq. (4.5)) is the result of a perturbative expansion to the second order in the bath-particle coupling constant (actually, expanding to second order requires weaker assumptions than the Born and Markov ones; the resulting equation may still take into account some non-Markovian effects which vanish in the limit of large times, as shown in the book of Breuer and Petruccione, 2007). In the work of Fleming and Cummings, 2011 it has been shown that Heisenberg principle violations in the stationary state disappear if one performs a perturbative expansion beyond the second order in the coupling constant.

In the present chapter we aim to cure the forbidden areas detected in the Born-Markov approach by recalling a Lindblad master equation. Such master equations preserve the positivity of the density operator at all times (Lindblad, 1976a; Schlosshauer, 2007; Breuer and Petruccione,

2007), and this in turn guarantees that the Heisenberg uncertainty principle is always satisfied. A brief, self-contained demonstration of the latter is given in Appendix C. Various ways of addressing this difficulty have been put forward by Lindblad, 1976b; Diósi, 1993; Isar et al., 1994; Săndulescu and Scutaru, 1987; Gao, 1997; Wiseman and Munro, 1998; Gao, 1998; Ford and O'Connell, 1999; Gao, 1999; Vacchini, 2000. We first consider, in Sec. 5.1, the master equation (3.36), associated to the Hamiltonian with the linear interaction in Eq. (3.4). We shall refer in the following to this situation as *linear case*. We add a term to the Eq. (3.36), that vanishes in the classical limit, bringing the equation to the Lindblad form and, in particular, ensuring that the Heisenberg principle is always satisfied (Lindblad, 1976a). We then rewrite it in the Wigner function representation, deriving the time-dependent equations for the moments of this distribution, showing that they have an exact Gaussian solution, and study in detail its long-time behavior. Up to this point, the results we present belong to well-known papers, such as that of Gao, 1997. The original part of the chapter lies in the study of the stationary Gaussian solution in the phase space, and has been published in the paper of Lampo et al., 2016. In particular, we analyze the correlations induced by the environment, which cause a rotation and distortion of the distribution, as well as squeezing effects expressed by the widths and the area of the distribution's effective support.

In the second part of the chapter we move our analysis to the QBM with a quadratic coupling in Eq. (4.3). We again modify the related master equation to obtain a Lindblad one and we study its stationary solutions in the phase space (Wigner) representation. For the quadratic QBM, the exact stationary state is no longer Gaussian, but a Gaussian approximation can be used in certain regimes. However, when the damping is strong, the Gaussian ansatz does not converge for large times, showing that it is not a good approximation to a stationary state.

5.1 Linear case

A Lindblad master equation has the form

$$\frac{\partial \rho}{\partial t} = -\frac{i}{\hbar}\left[H_{\mathrm{S}}, \rho\right] + \sum_{i,j} \kappa_{ij}\left[A_i \rho A_j^{\dagger} - \frac{1}{2}\{A_i^{\dagger} A_j, \rho\}\right], \tag{5.1}$$

where A_i are called Lindblad operators and (κ_{ij}) is a positive-definite matrix. The derivation of Eq. (5.1) goes widely beyond the goal of this thesis, and it may be found anyway in Sec. 3.2.1 of the book of Breuer and Petruccione, 2007 or in that of Rivas and Huelga, 2012.

Following the approach proposed by Gao, 1997 we will replace the Born-Markov master equation (3.36), which cannot be brought to a Lindblad form, by an equation of the form Eq. (5.1) with a single Lindblad operator of the form

$$A_1 = \alpha x + \beta p, \qquad \text{with } \kappa_{11} = 1. \tag{5.2}$$

Substituting this operator into Eq. (5.1) we obtain

$$\begin{aligned}\frac{\partial \rho}{\partial t} =& -\frac{i}{\hbar}\left[H'_{\mathrm{S}}, \rho\right] - i\frac{C_{XP}}{\hbar}\left[x, \{p, \rho\}\right] - \frac{D_{XX}}{2\hbar^2}\left[x, [x, \rho]\right] \\ & - \frac{D_{XP}}{\hbar^2}\left[x, [p, \rho]\right] - \frac{D_{PP}}{2\hbar^2}\left[p, [p, \rho]\right],\end{aligned} \tag{5.3}$$

with

$$H'_{\mathrm{S}} = H_{\mathrm{S}} - \frac{C_{XP}}{2}\{x, p\} \equiv H_{\mathrm{S}} + \Delta H \tag{5.4}$$

and

$$\begin{aligned} D_{XX} =& \hbar^2|\alpha|^2, & D_{XP} =& \hbar^2 \mathrm{Re}\left(\alpha^*\beta\right), \\ D_{PP} =& \hbar^2|\beta|^2, & C_{XP} =& \hbar \mathrm{Im}\left(\alpha^*\beta\right). \end{aligned} \tag{5.5}$$

One could obtain the same result employing two Lindblad operators, proportional to x and p respectively. Without loss of generality, we may take α to be a positive real number since multiplying A_1 by a phase factor does not change Eq. (5.1), and we will restrict ourselves to $\mathrm{Im}\beta > 0$, because, as seen from Eq. (5.5), $\alpha \mathrm{Im}(\beta)$ is the damping coefficient C_{XP}, which must be positive.

Equation (5.3) differs from Eq. (3.36) just by two extra terms, involving D_{PP} and ΔH. Equating the coefficients of the remaining terms with those of the analogous terms appearing in Eq. (3.36), one finds

$$\begin{aligned} D_{XX} &= 2\hbar D_x, & D_{XP} &= \frac{\hbar D_p}{m\Omega}, \\ C_{XP} &= \frac{C_p}{m\Omega}, & D_{PP} &= \frac{(\hbar C_{XP})^2 + D_{XP}^2}{D_{XX}}. \end{aligned} \tag{5.6}$$

In the Caldeira-Leggett limit defined in Eq. (3.54), these reduce to

$$\begin{aligned} C_{XP} &\approx \gamma/2, \\ D_{XX} &\approx 2m\gamma k_{\mathrm{B}}T, \\ D_{XP} &\approx -\gamma\frac{k_{\mathrm{B}}T}{\Lambda}, \\ D_{PP} &\approx \frac{\gamma k_{\mathrm{B}}T}{2m\Lambda^2}. \end{aligned} \tag{5.7}$$

Following Schlosshauer, 2007, since the quantities represented by P and $m\Omega X$ have generally the same order of magnitude, one can argue, as in Eq. (5.56) of the book of Schlosshauer, 2007, that the terms proportional to D_{XP} and D_{PP} are negligible in the Caldeira-Legget limit, recovering the structure of the usual master equation. We may state so that the Caldeira-Leggett equation (3.59) approximate the Lindblad master equation (5.3). This is in agreement with the fact that at large values of the cut-off and at high-temperature (the Caldeira-Leggett limit) no violations of the Heisenberg principle arise.

The operator ΔH can be absorbed into the unitary part of the dynamics defined by Eq. (5.3), so it can be eliminated by introducing a counter term into the system's Hamiltonian. More generally, we will add to H_{S} a counter term

$$H_{\mathrm{C}} = (r-1)\Delta H, \tag{5.8}$$

which depends on a parameter $r \in \mathbb{R}$, leading to the modified Hamiltonian

$$\begin{aligned} H'_{\mathrm{S}} =& H_{\mathrm{S}} - (rC_{XP}/2)\{x,p\} \\ =& \frac{(p - mrC_{XP}x)^2}{2m} + \frac{m(\Omega^2 - r^2C_{XP}^2)x^2}{2}. \end{aligned} \tag{5.9}$$

The effect of r is twofold: it introduces a gauge transformation which shifts the canonical momentum p, and it renormalizes the frequency of the harmonic potential. In the rest of the section we shall study the dynamics defined by Eq. (5.3), first for general values of r and then, for the discussion of the stationary state, focusing on the case $r = 0$. We stress that the introduction of a counter term in the Hamiltonian does not affect the Lindblad character of Eq. (5.3), since it just enters in its unitary part.

5.1.1 Solution of the Lindblad equation

We are interested in the study of the long-time dynamics of the Brownian particle. In particular, we consider its configuration in the phase space, employing the Wigner function representation. In terms of the Wigner function, Eq. (5.3) becomes $\dot{W} = \mathcal{L}W$, with

$$\begin{aligned}\mathcal{L}W = &- \frac{p}{m}\frac{\partial W}{\partial x} + m\Omega^2 x\frac{\partial W}{\partial p} \\ &+ C_{XP}\left[r\frac{\partial}{\partial x}(xW) + (2-r)\frac{\partial}{\partial p}(pW)\right] \\ &+ \frac{1}{2}\left[D_{XX}\frac{\partial^2 W}{\partial P^2} + D_{PP}\frac{\partial^2 W}{\partial x^2}\right] - D_{XP}\frac{\partial^2 W}{\partial x \partial p}.\end{aligned} \tag{5.10}$$

Equivalently, one can look at the equations for its moments

$$\begin{aligned}\frac{\partial\langle x\rangle_t}{\partial t} &= \frac{\langle p\rangle_t}{m} - rC_{XP}\langle x\rangle_t \\ \frac{\partial\langle p\rangle_t}{\partial t} &= -m\Omega^2\langle x\rangle_t - (2-r)C_{XP}\langle p\rangle_t \\ \frac{\partial\langle x^2\rangle_t}{\partial t} &= -2rC_{XP}\langle x^2\rangle_t + \frac{2\langle xp\rangle_t}{m} + D_{PP} \\ \frac{\partial\langle xp\rangle_t}{\partial t} &= -m\Omega^2\langle x^2\rangle_t - 2C_{XP}\langle XP\rangle_t + \frac{\langle p^2\rangle_t}{m} - D_{XP} \\ \frac{\partial\langle p^2\rangle_t}{\partial t} &= -2m\Omega^2\langle xp\rangle_t - (4-2r)C_{XP}\langle p^2\rangle_t + D_{XX},\end{aligned} \tag{5.11}$$

where the moments of the Wigner function are calculated as

$$\langle f(x,p)\rangle_t = \int_{-\infty}^{\infty} dx \int_{-\infty}^{\infty} dp\; f(x,p)W(x,p,t). \tag{5.12}$$

These moments correspond to symmetric ordering of the quantum mechanical operators x and p (Schleich, 2001). In particular, note that the time-dependence is solely contained in the Wigner function, in agreement with the fact that we work in the Schrödinger picture.

The solutions for the first moments are

$$\langle x\rangle_t = e^{-C_{XP}t}\left[x_0\cos(\beta_r t) + x_r^0\sin(\beta_r t)\right], \tag{5.13}$$

$$\langle p\rangle_t = e^{-C_{XP}t}\left[p_0\cos(\beta_r t) - p_r^0\sin(\beta_r t)\right], \tag{5.14}$$

where

$$x_r^0 = \frac{mC_{XP}x_0(1-r)+p_0}{m\beta_r}, \tag{5.15}$$

$$p_r^0 = \frac{C_{XP}p_0(1-r)+mx_0\Omega^2}{\beta_r}, \tag{5.16}$$

with

$$x_0 \equiv \langle x\rangle_0, \quad p_0 \equiv \langle p\rangle_0, \tag{5.17}$$

and

$$\beta_r \equiv \sqrt{\Omega^2 - C_{XP}^2(r-1)^2}. \tag{5.18}$$

Similar solutions have been presented in the works of Kumar, Sinha, and Sreeram, 2009; Săndulescu and Scutaru, 1987; Isar et al., 1994. Eqs. (5.11) may alternatively be written in terms of the kinetic momentum

$$\langle\tilde{p}\rangle_t = \langle p\rangle_t - mrC_{XP}\langle x\rangle_t. \tag{5.19}$$

It follows

$$\begin{aligned}\frac{\partial\langle x\rangle_t}{\partial t} &= \frac{\langle\tilde{p}\rangle_t}{m},\\ \frac{\partial\langle\tilde{p}\rangle_t}{\partial t} &= -m\left[\Omega^2 - r(r-2)C_{XP}^2\right]\langle x\rangle_t - 2C_{XP}\langle\tilde{p}\rangle_t,\end{aligned} \tag{5.20}$$

or equivalently gathered in the compact form

$$\frac{\partial^2\langle x\rangle_t}{\partial t^2} + 2C_{XP}\frac{\partial\langle x\rangle_t}{\partial t} + \left[\Omega^2 - r(r-2)C_{XP}^2\right]\langle x\rangle_t = 0. \tag{5.21}$$

which, of course, can be derived directly from the equations Eq. (5.11). For both $r = 0$ and $r = 2$ one obtains a damped oscillator with the original frequency of the harmonic trap, Ω. For other values of r the frequency is renormalized, with the maximal renormalization corresponding to $r = 1$.

In Eqs. (5.11) we see that r introduces apparent damping in the position, as already noted by Wiseman and Munro, 1998. Because of this, in the following we will set $r = 0$. The extra term proportional to D_{PP}, not present in the starting Born-Markov master equation, appears only in the equation for $\langle\dot{x}^2\rangle$, without affecting the other equations, and in particular those for the first moments, so that it may be interpreted as a *position*

diffusion coefficient.

We focus now on the stationary solution of Eq. (5.10). The latter may be found by means of the following Gaussian ansatz

$$W_{ST} = \zeta \exp\left[\frac{1}{2(\rho^2-1)}\left(\frac{x^2}{\sigma_x^2} + \frac{p^2}{\sigma_p^2} + \frac{2\rho x p}{\sigma_x \sigma_p}\right)\right], \tag{5.22}$$

which is normalized to one taking

$$\zeta \equiv \frac{1}{2\pi\sigma_x\sigma_p\sqrt{1-\rho^2}}, \quad |\rho| \leq 1, \tag{5.23}$$

with

$$\sigma_x = \sqrt{\langle x^2\rangle}, \quad \sigma_p = \sqrt{\langle p^2\rangle}, \quad \rho = -\frac{\langle xp\rangle}{\sigma_x\sigma_p}, \tag{5.24}$$

and, in the remainder of this Section, the variances are computed using the time-independent Gaussian Ansatz in Eq. (5.22) of Weedbrook et al., 2012. Inserting the Gaussian ansatz in Eq. (5.22) into Eq. (5.10) we find:

$$\begin{aligned}
\sigma_x^2 &= \frac{D_{XX} - 4mC_{XP}D_{XP} + m^2(4C_{XP}^2 + \Omega^2)D_{PP}}{4m^2C_{XP}\Omega^2} \\
\sigma_p^2 &= \frac{D_{XX} + m^2\Omega^2 D_{PP}}{4C_{XP}} \\
\sigma_p\sigma_p\rho &= mD_{PP}/2.
\end{aligned} \tag{5.25}$$

Again, we introduce the dimensionless variables

$$\delta_x = \sqrt{\frac{2m\Omega\sigma_x^2}{\hbar}}, \quad \delta_p = \sqrt{\frac{2\sigma_p^2}{m\Omega\hbar}}. \tag{5.26}$$

With this parametrization, the Heisenberg inequality $\sigma_x\sigma_p \geq \hbar/2$ reads $\delta_x\delta_p \geq 1$.

The Lindbladian character of Eq. (5.10) guarantees that the second moments will satisfy the Heisenberg relation at all times. We furthermore note that the term with coefficient D_{PP}, *i.e.* the extra term induced by the Lindblad form of the ME, leads to a correlation between the two canonical variables.

Geometrically, this correlation can be interpreted as a rotation of the stationary solution in the phase space, see the black sketches in Fig. 5.1.

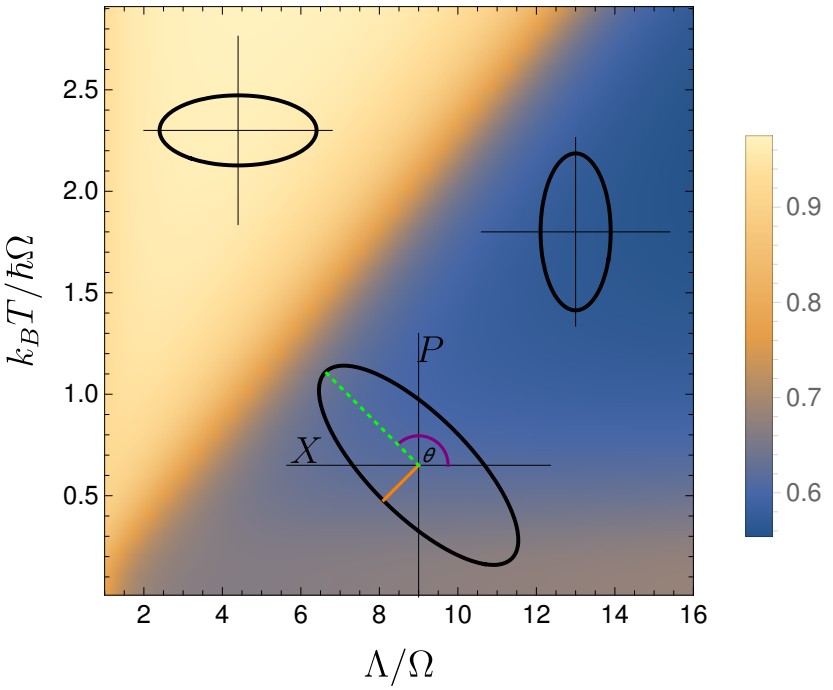

FIGURE 5.1: Plot of the angle θ/π at $\gamma/\Omega = 0.8$. This angle is represented in the ellipse at the bottom of the picture. Here, the orange-solid (green-dashed) line represents the minor (major) axis of the Wigner function, *i.e.* that related to δ_l (δ_L). The axes X and P are those of the phase space.

In the CL limit, the term with the coefficient D_{PP} is negligible, and the solution is an ellipse with its axes parallel to the canonical ones, reproducing the well-known results.

To analyze the properties of the stationary state in the phase space, we consider the variances of the major and minor axes of the Wigner function. These axes are defined as the eigenvectors of the covariance matrix

$$\mathrm{cov}(X,P) = \begin{pmatrix} \delta_x^2 & -\rho\delta_x\delta_p \\ -\rho\delta_x\delta_p & \delta_p^2 \end{pmatrix} \tag{5.27}$$

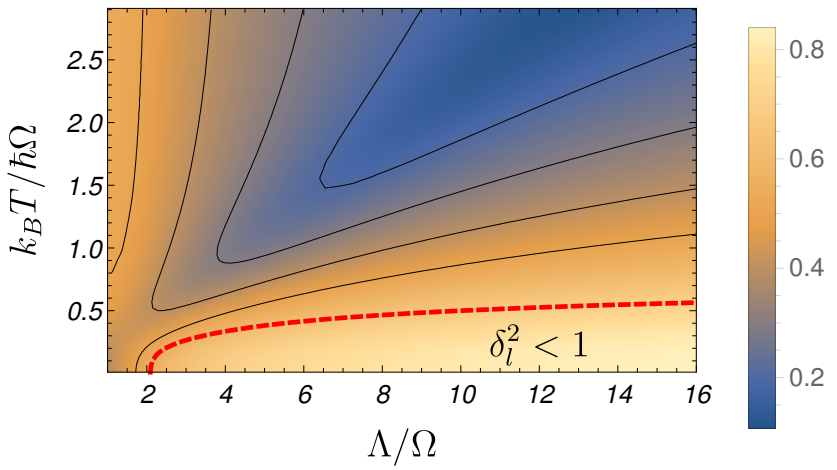

FIGURE 5.2: Eccentricity of the Wigner function introduced in Eq. (5.22), at $\gamma/\Omega = 0.8$. The red dashed line represents the values of T and Λ yielding $\delta_l^2 = 1$, and we have genuine squeezing below it.

The smaller and larger eigenvalues of this matrix, δ_l and δ_L, are given respectively by:

$$\delta_{l,L}^2 = \frac{1}{2}\left(\delta_x^2 + \delta_p^2 \mp \sqrt{\left(\delta_x^2 - \delta_p^2\right)^2 + 4\delta_x^2\delta_p^2\rho^2}\right). \tag{5.28}$$

We now aim to quantify such a rotation, calculating the angle θ between the major axis of the Wigner function (*i.e.* the eigenvector corresponding to δ_L), and the x-axis of the phase space. In Fig. 5.1 we present the behavior of θ as function of T and Λ, at fixed γ. At high Λ the major axis aligns approximately with the p-axis of the phase space ($\theta = \pi/2$), while at low Λ, it is close to the x-axis ($\theta = \pi$), in agreement with the behavior of the Born-Markov master equation discussed by Massignan et al., 2015, where $\langle xp \rangle$ was identically zero. On the other hand, at low temperatures the Wigner function associated to the stationary solution of the Lindblad equation may be significantly rotated with respect to the axes of the phase space.

In the previous chapters it has been shown that, in the low temperature regime, the position of the Brownian particle governed by the Born-Markov master equation experiences *genuine squeezing* along x in the

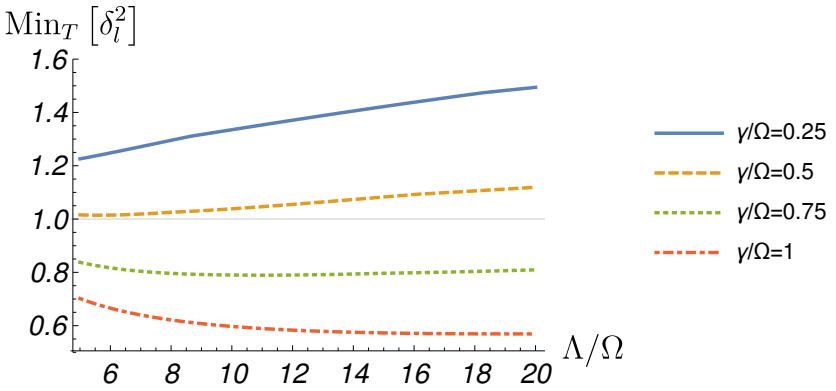

FIGURE 5.3: Minimum value of δ_l^2 over all temperatures, as a function of the cut-off frequency, at several values of the damping constant.

Wigner function representation, *i.e.* $\delta_x < 1$. Similar squeezing effects are pointed out by Maniscalco et al., 2004, by studying the numerical solution of the exact master equation. In the case of the Lindblad equation, it was checked numerically that δ_x introduced in Eq. (5.25) is always bigger than one. However, the minor axis of the ellipse describing the Wigner function can display genuine squeezing. To quantify the degree of squeezing of the Wigner function, Fig. 5.2 shows the values of eccentricity defined as

$$\eta = \sqrt{1 - (\delta_l/\delta_L)^2}, \tag{5.29}$$

computed for different values of temperature T and UV-cut-off Λ. The eccentricity is larger at low temperatures. In particular, below the red dashed line, we find an area where $\delta_l < 1$, corresponding to genuine squeezing along the minor axis of the Wigner Function, while in the Caldeira-Leggett limit the eccentricity η approaches zero, and we obtain a Wigner function with circular symmetry. In Fig. 5.3 we present the minimal value of δ_l^2 obtained by choosing the appropriate (low) temperature. This picture highlights the range of values of Λ and γ where genuine squeezing occurs. We find that the eccentricity is an increasing function of the damping constant, *i.e.* squeezing becomes more pronounced as γ grows. In particular, at least $\gamma/\Omega > 0.5$ is needed to obtain $\delta_l < 1$.

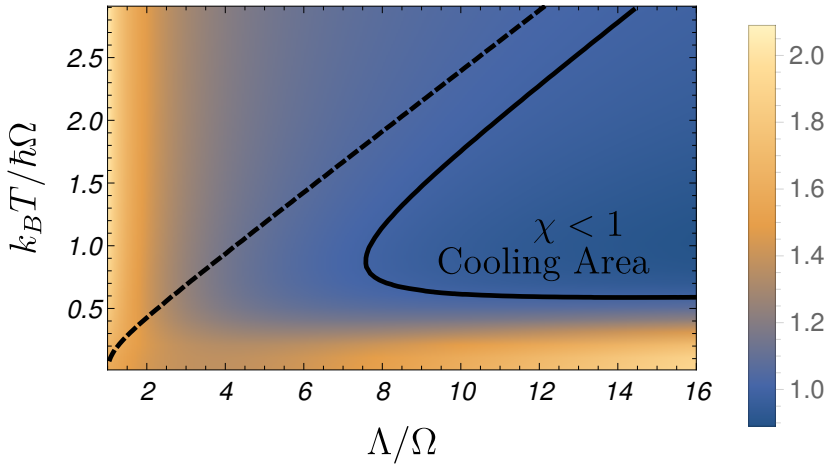

FIGURE 5.4: Cooling parameter χ introduced in Eq. (5.30), plotted for $\gamma/\Omega = 0.8$. The system exhibits cooling to the right of the solid line, and heating to its left. For comparison, the dashed line represents the cooling/heating boundary obtained with the Born-Markov master equation (3.36), which is independent of γ.

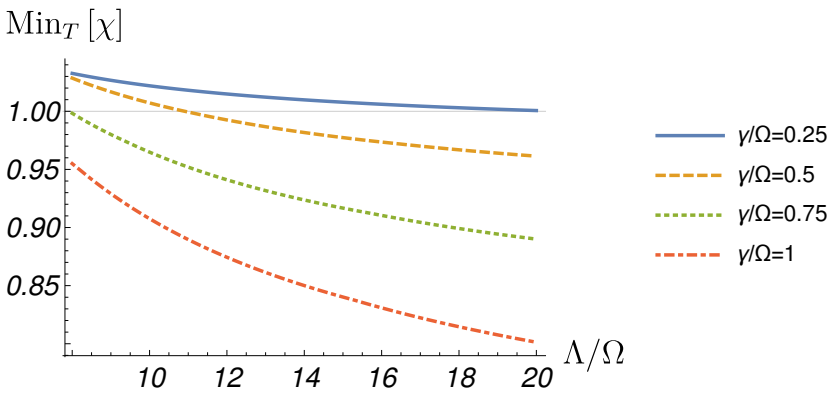

FIGURE 5.5: Minimum value of the cooling parameter χ over all temperatures, as a function of the cut-off frequency, at several values of the damping constant.

We look now into the cooling effect introduced in chapter 3. Recalling Eq. (3.83), we thus define the system to be cooled if[1]

$$\chi = \frac{\delta_l \delta_L}{\coth\left(\frac{\hbar\Omega}{2k_{\rm B}T}\right)} < 1, \tag{5.30}$$

and heated otherwise. The degree of heating/cooling χ is shown in Fig. 5.4. In Fig. 5.5 we present the minimal value achieved by χ as the temperature is varied. We note that to obtain small values of χ one needs to choose large values of both Λ and γ.

There is a difference between the configuration of the cooling areas arising in the Lindblad dynamics studied here, and the ones produced by Eq. (3.36) studied in chapter 3. In the latter, the cooling/heating boundary coincides with the line defined by $\delta_x = \delta_p$, and this condition does not depend on γ, while in the present Lindblad model, the location of the boundary varies with γ. However, the boundary calculated within the Lindblad approach converges to that predicted in the Born-Markov one in the $\gamma \to 0$ limit. Moreover, the Lindblad equation discussed here displays heating at very low temperatures.

[1]For the Gibbs-Boltzmann distribution we have $\langle X^2\rangle_{GB}\langle P^2\rangle_{GB} \sim \coth^2(\hbar\Omega/2k_{\rm B}T)$. So the denominator of Eq. (5.30) provides information regarding the area of the Gibbs-Boltzmann distribution.

In Figs. 5.3 and 5.5 we have not extended the range of values of the damping constant beyond $\gamma = 1$. In fact, the expressions for the coefficients of Eq. (5.3) have been obtained by comparing it with the Eq. (3.36). The latter is perturbative to second order in the strength of the coupling between the Brownian particle and the environment. The square of the coupling constant is proportional to the damping coefficient, so the validity of the perturbative expansion fails for γ large. In particular, in the case of QBM this perturbative expansion holds for $\gamma \lesssim \Omega$ (Breuer and Petruccione, 2007; Haake and Reibold, 1985).

Low temperature regime

We consider here in detail the stationary state in the low temperature regime $k_{\mathrm{B}}T < \hbar\Omega$. Such a study was impossible in chapter 3 because solutions violated the Heisenberg principle there. Here, the Lindblad form of Eq. (5.3) ensures the positivity of the density matrix at all times, so no violations of the Heisenberg principle occur.

In the discussion above, we noticed that the time-dependent equations of motion of the Lindblad equation admit as an exact solution a Gaussian with non-zero correlations between the two canonical variables x and p. In the stationary state, in particular, one finds $\langle xp \rangle = -mD_{PP}/2 \neq 0$. This is a novelty in comparison with the stationary solution of Eq. (3.36), which shows no correlations between x and p. In the range of Λ explored in Fig. 5.1, the correlation between x and p becomes noticeable for $k_{\mathrm{B}}T \lesssim 0.5\hbar\Omega$. So, an important feature of the stationary solution of the Lindblad equation at low temperature is that its major axis is rotated with respect to those of the phase space.

In Fig. 5.2 we analyze the eccentricity of the stationary state. We point out that as the temperature decreases, the distribution becomes increasingly more squeezed. In particular, at low temperature we find a region displaying genuine squeezing of the probability distribution in the direction of l. In Fig. 5.4 we also note the presence of a cooling area in the low temperature regime. Nevertheless, in the zero-temperature limit the stationary state shows again heating.

The zero-temperature limit of the Lindblad model deserves special attention, as the two limits $T \to 0$ and $\gamma \to 0$ do not commute. Taking first the zero-coupling and then the zero-temperature limit, one simply finds $\delta_x = \delta_p$ (in agreement with the general result for a free harmonic oscillator), but no further information on their specific value. If instead

one takes first $T \to 0$ and then $\gamma \to 0$, one finds $\delta_x = \delta_p$ and the additional condition

$$\delta_x \delta_p = \delta_l \delta_L = \frac{5}{4} + \frac{\left[\log(\Lambda/\Omega)\right]^2}{\pi^2} > 1, \tag{5.31}$$

indicating that for the Lindblad model the Heisenberg inequality is not saturated in the limit when the particle becomes free. This is in contrast with the behavior of the non-Lindblad equation (3.36), for which, in this limit, we have $\delta_x \delta_p = 1$. Summarizing, the effect of D_{PP} is to introduce extra heating at low temperatures and couplings, manifested by a small constant, and a weak logarithmic dependence on the ultraviolet cut-off Λ.

5.2 Quadratic case

5.2.1 The Hamiltonian and the Lindblad equation

In this section we consider the quadratic QBM, whose coupling is still linear in the positions of the oscillators of the bath, but is quadratic in the position of the Brownian particle

$$H_{\rm I} = \sum_k \frac{g_k}{a} X_k x^2. \tag{5.32}$$

Here a is a characteristic length related to the motion of the Brownian particle and we set it to be $a = \sqrt{\hbar/m\Omega}$. The interaction term in Eq. (5.32) describes an interaction of the particle with an inhomogeneous environment, giving rise to position-dependent damping and diffusion.

The dynamics induced by the interaction term in Eq. (5.32) has already been discussed in detail in chapter 4. There, the master equation for the Brownian particle has been derived in the Born-Markov approximations, for a Lorentz-Drude spectral density. Nevertheless, this master equation is not in a Lindblad form, nor is exact. Accordingly, the stationary solution is not defined for some values of the model parameters because of violations of the Heisenberg uncertainty principle at low temperatures.

In this Section, we aim to find a Lindblad equation as similar as possible to that derived in (4). Just like in the case of linear QBM, we expect it to differ from the Born-Markov by some extra terms. To achieve this

goal, we consider a single Lindblad operator

$$A_1 = \mu x^2 + \nu\{x,p\} + \epsilon p^2, \tag{5.33}$$

where μ, ν and ϵ are non-zero complex numbers. Substituting it into Eq. (5.1) we obtain:

$$\begin{aligned}\frac{\partial\rho}{\partial t} =& -\frac{i}{\hbar}\left[H_{\rm S}+\Delta H_2,\rho\right] \\ &-\frac{D_{\mu\nu}}{\hbar^2}\left[x^2,[\{x,p\},\rho]\right]-\frac{D_{\mu\epsilon}}{\hbar^2}\left[x^2,\left[p^2,\rho\right]\right]-\frac{D_{\epsilon\nu}}{\hbar^2}\left[p^2,[\{x,p\},\rho]\right] \\ &-i\frac{C_{\mu\nu}}{\hbar}\left[x^2,\{\{x,p\},\rho\}\right]-i\frac{C_{\mu\epsilon}}{\hbar}\left[x^2,\{p^2,\rho\}\right]-i\frac{C_{\epsilon\nu}}{\hbar}\left[p^2,\{\{x,p\},\rho\}\right] \\ &-\frac{D_{\mu}}{2\hbar^2}\left[x^2,\left[x^2,\rho\right]\right]-\frac{D_{\nu}}{2\hbar^2}\left[\{x,p\},[\{x,p\},\rho]\right]-\frac{D_{\epsilon}}{2\hbar^2}\left[p^2,\left[p^2,\rho\right]\right]\end{aligned} \tag{5.34}$$

where

$$\frac{D_\mu}{\hbar^2}\equiv|\mu^2|,\quad \frac{D_{\mu\nu}}{\hbar^2}\equiv{\rm Re}(\mu^*\nu),\quad \frac{C_{\mu\nu}}{\hbar}\equiv{\rm Im}(\mu^*\nu), \tag{5.35}$$

and similarly for the other combinations of indices. We could have obtained the same result by means of three Lindblad operators (rather than a single one), each proportional to one of the terms appearing on the right-hand side of Eq. (5.33). Similarly to the linear case, there is a term which appears in the unitary part of the master equation

$$\begin{aligned}H_2 =& \,2D_{\mu\nu}x^2-2D_{\epsilon\nu}p^2+2D_{\mu\epsilon}\{x,p\} \\ &-\frac{1}{2}C_{\mu\nu}\{\{x,p\},x^2\}-\frac{1}{2}C_{\mu\epsilon}\{p^2,x^2\} \\ &+\frac{1}{2}C_{\epsilon\nu}\{\{x,p\},p^2\}.\end{aligned} \tag{5.36}$$

We eliminate it by introducing appropriate counter terms in the Hamiltonian.

Equation (5.34) is in a Lindblad form. Proceeding as in Sec. 5.1, equating the coefficients on the right hand side of Eq. (5.34) to the corresponding ones in the Born-Markov master equation for quadratic QBM derived

in chapter 3, we obtain:

$$D_{\mu\epsilon} = \frac{D_{pp}}{m\Omega}, \quad D_{\mu\nu} = D_{xp}, \tag{5.37}$$
$$C_{\mu\epsilon} = \frac{C_{pp}}{\hbar m\Omega}, \quad C_{\mu\nu} = \frac{C_{xp}}{\hbar},$$

and $D_\mu = 2m\Omega D_{xx}$. The remaining coefficients are then uniquely determined as

$$D_{\epsilon\nu} = \frac{1}{D_\mu}\left[D_{\mu\nu}D_{\mu\epsilon} + \hbar^2 C_{\mu\nu}C_{\mu\epsilon}\right], \tag{5.38}$$
$$C_{\epsilon\nu} = \frac{1}{D_\mu}\left[C_{\mu\nu}D_{\mu\epsilon} - D_{\mu\nu}C_{\mu\epsilon}\right],$$
$$D_\epsilon = \frac{1}{D_\mu}\left[D_{\mu\epsilon}^2 + (\hbar C_{\mu\epsilon})^2\right],$$
$$D_\nu = \frac{1}{D_\mu}\left[D_{\mu\nu}^2 + (\hbar C_{\mu\nu})^2\right].$$

It is easy to check that in the limit $k_{\mathrm{B}}T \gg \hbar\Lambda \gg \hbar\Omega$, the coefficients of all extra terms vanish, and Eq. (5.34) recovers the structure of Eq. (4.5).

5.2.2 Stationary state of the quadratic quantum Brownian motion

We turn now to the study of the stationary state of the Brownian particle in the case of quadratic coupling. To this end we express the Lindblad master in Eq. (5.34) in terms of the Wigner function W, and obtain an equation of the form $\dot{W} = \mathcal{L}W$, with:

$$\begin{aligned}\mathcal{L} = &-\frac{\partial_x p}{m} + m\Omega^2\partial_p x + 2D_\mu\partial_p^2 X^2 + 2D_\nu\left(\partial_p p - \partial_x x\right)^2 + 2D_\epsilon\partial_x^2 p^2 \\ &+ 4D_{\mu\nu}(\partial_p^2 xp - \partial_p\partial_x x^2 + \partial_p x) - 4D_{\epsilon\nu}p\partial_x\left(\partial_p p - \partial_x x\right) \\ &+ 8C_{\mu\nu}\left[\partial_p p x^2 + \frac{\hbar^2}{4}\partial_P^2(\partial_x x - 1)\right] + C_{\mu\epsilon}\left[4\partial_p x p^2 - \hbar^2\partial_P\partial_x^2 x + 2\hbar^2\partial_p\partial_x\right] \\ &- 2C_{\epsilon\nu}p\partial_x\left(4xp + \hbar^2\partial_p\partial_x\right) - 4D_{\mu\epsilon}(\partial_x x - 1)\partial_p p.\end{aligned} \tag{5.39}$$

We now find the stationary solution of the above equation. In this

case the Gaussian ansatz in Eq. (5.22) may at best provide an approximate solution, in contrast with the case of the linear QBM, since the system of equations for the second moments is not closed. We approximate higher-order moments by their Wick expressions in terms of second moments (which would be exact in a Gaussian case), obtaining the following closed, non-linear system of equations in the variables δ_x, δ_p and ρ

$$\begin{aligned}\frac{1}{2}\frac{\partial\delta_x^2}{\partial t} &= 4m\hbar\Omega C_{\epsilon\nu}[1+\delta_x^2\delta_p^2(1+2\rho^2)] + 2m^2\Omega^2 D_\epsilon\delta_p^2 \\ &\quad + 4D_\nu\delta_x^2 - \Omega\delta_x\delta_p\rho,\end{aligned} \tag{5.40}$$

$$\frac{1}{2}\frac{\partial\delta_p^2}{\partial t} = \frac{2D_\mu}{m^2\Omega^2}\delta_x^2 - \frac{4\hbar}{m\Omega}C_{\mu\nu} + 6\hbar C_{\mu\epsilon}\delta_x\delta_p^3\rho + \Omega\delta_x\delta_p\rho \tag{5.41}$$

$$+4\delta_p^2\left[D_\nu - D_{\mu\epsilon} - \frac{\hbar C_{\mu\nu}}{m\Omega}\left(1+2\rho^2\right)\delta_x^2\right], \tag{5.42}$$

and

$$\begin{aligned}-\frac{1}{2}\frac{\partial(\delta_x\delta_p\rho)}{\partial t} &= 4\hbar C_{\mu\epsilon} + \Omega\delta_p^2 - 8m\Omega D_{\epsilon\nu}\delta_p^2 + \frac{12\hbar}{m\Omega}C_{\mu\nu}\delta_p\delta_x^3\rho \\ + \left(8D_{\mu\epsilon} - 12m\hbar\Omega C_{\epsilon\nu}\delta_p^2\right)\delta_x\delta_p\rho &- \left[\Omega + 8\frac{D_{\mu\nu}}{m\Omega} + 2\hbar\left(1+2\rho^2\right)C_{\mu\epsilon}\delta_p^2\right]\delta_x^2.\end{aligned} \tag{5.43}$$

This system of equations could admit more than one stationary solution, so we have to study the proper one. We choose the solution that coincides with that obtained with the non-Lindblad dynamics in the Caldeira-Leggett limit, since in this limit the coefficients of the extra terms of Eq. (5.34) vanish. In chapter 4 the stationary state in the case of the non-Lindblad dynamics has been studied in detail, and the variances have been calculated analytically.

Similarly to the linear QBM studied in the previous section, we characterize the stationary state in terms of the variances of the Wigner function, and define the eccentricity, the cooling parameter, and the angle between the major axis and the position axis of the phase space as before. These quantities are shown in Figs. 5.6, 5.7, and 5.8, as functions of Λ and T, when $\gamma/\Omega = 0.1$. In Fig. 5.6 we point out that the eccentricity tends to zero in the Caldeira-Leggett limit, while it increases away from it. This behavior is similar to that found for the linear QBM. We found that for

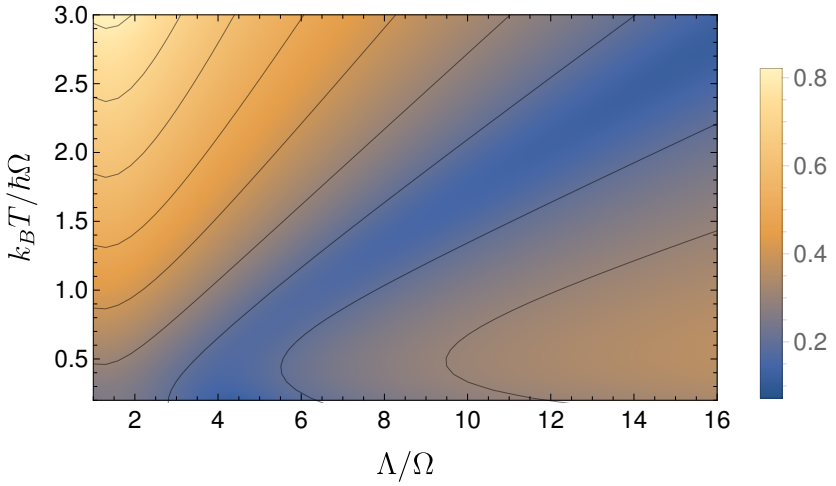

FIGURE 5.6: Eccentricity η of the Wigner function at $\gamma/\Omega = 0.1$, for quadratic coupling.

$\gamma/\Omega \leq 0.1$ the Brownian particle experiences neither cooling nor genuine squeezing.

In contrast to the linear case, we do not find a noticeable rotation at low temperature in the quadratic one. We would expect to observe this at larger values of γ, as in the case of linear coupling. However, for larger values of the damping constant the many stationary solutions of the system of Eqs. (5.40-5.43) cross, and therefore it is not straightforward to determine the stationary solution of (5.39) that coincides with the one obtained in the Caldeira-Leggett limit. Moreover, for larger values of γ the Gaussian ansatz given in Eq. (5.22) may fail to approximate any stationary states. To show this point, in Fig. 5.9 we plotted the time dependence of δ_x^2 for several values of γ, at fixed values of T and Λ. Above a certain value of γ, the position variance does not converge to a stationary value. This suggests that in these cases the Gaussian solution of Eq. (5.39) is not stationary. Figure 5.9 is plotted for the initial conditions $\delta_x^2 = \delta_p^2 = 1$, corresponding to the case when the harmonic oscillator is in its ground state. The choice of the initial conditions is not crucial, as we observe a very similar behavior with quite different initial conditions.

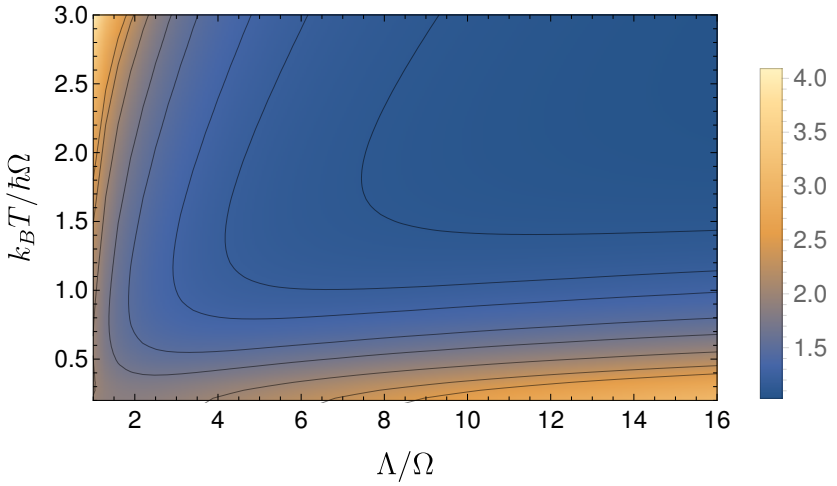

FIGURE 5.7: Cooling parameter χ for quadratic coupling, at $\gamma/\Omega = 0.1$.

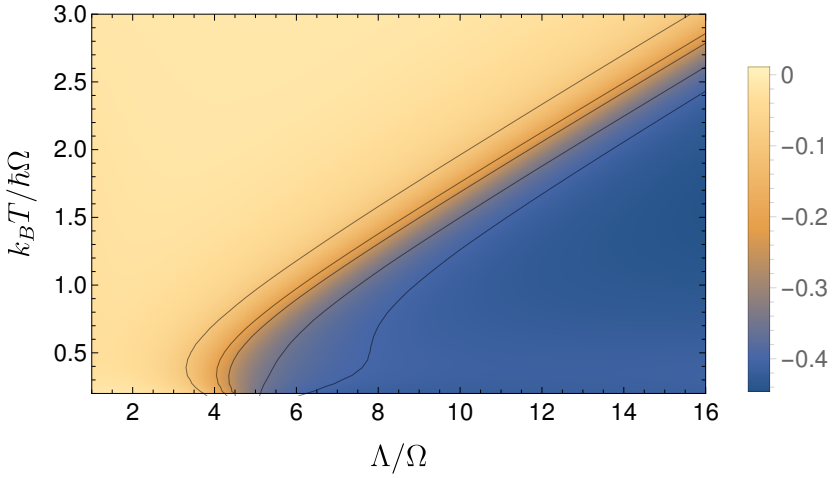

FIGURE 5.8: Angle θ/π between the major axis of the Wigner function, and the X axis of the phase space at $\gamma/\Omega = 0.1$, for quadratic coupling.

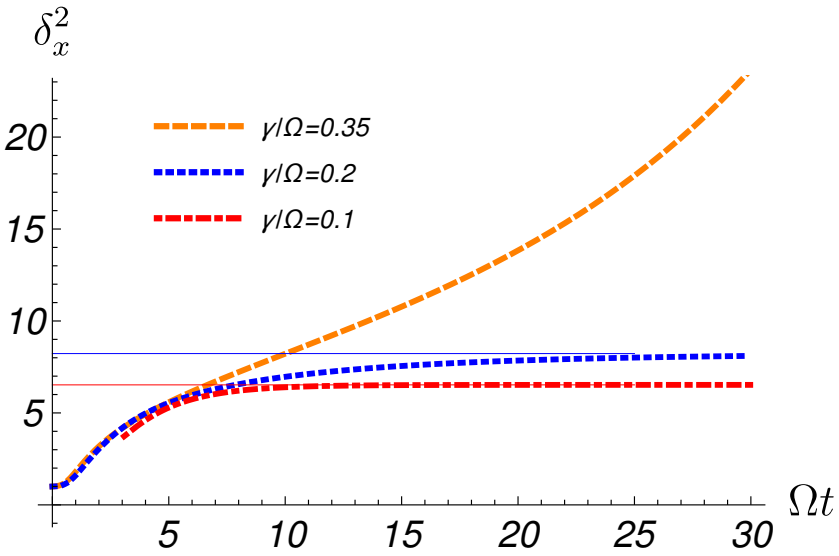

FIGURE 5.9: Time dependence of δ_x^2 for several values of γ, at $\Lambda/\Omega = 16$ and $k_{\rm B}T/\hbar\Omega = 4$. The thin solid lines represent the stationary value of δ_x^2 in the state, namely the stationary solution of Eqs. (5.40-5.43) for such a quantity.

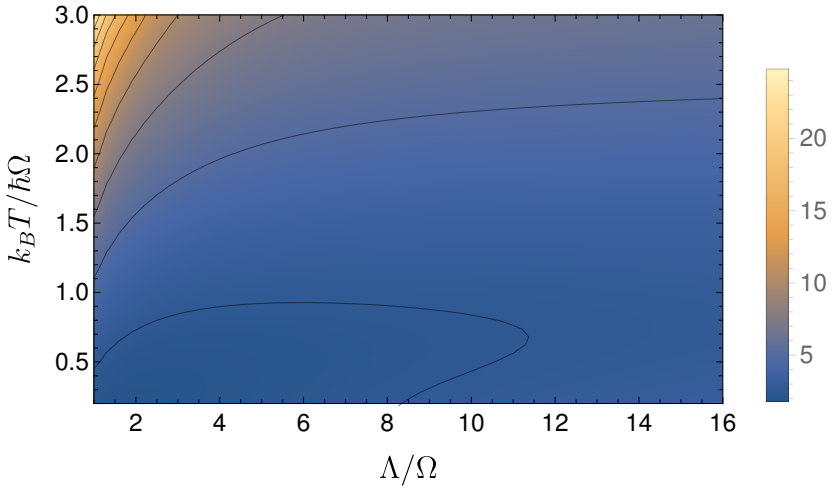

FIGURE 5.10: Plot of the product $\delta_x \delta_p$ at $\gamma/\Omega = 0.1$, for quadratic coupling. This quantity is always larger than 1, in accordance with the Heisenberg principle.

We conclude this Section pointing out that, although in Eqs. (5.40-5.43) we performed the Gaussian approximation at the level of the equations for the moments, it is possible to obtain exactly the same result applying the approximation directly on the original equation in Eq. (5.34), or on that Lindblad equation expressed in terms of the Wigner function, Eq. (5.39). In Appendix D we show, by a very general analytical demonstration, that the Gaussian approximation applied to the original Lindblad equation yields again a master equation of the Lindblad form, guaranteeing therefore that the approximated solutions will preserve the Heisenberg principle at all times. We provide further numerical evidence of this fact in Fig. 5.10, where we plot the product of the two uncertainties δ_x and δ_p resulting by Eqs. (5.40-5.43), on which the Gaussian approximation has been carried out. As may be noticed in the figure, the approximated equations do not produce any violation of the Heisenberg principle.

5.3 Summary

We present the main results obtained in the Lindblad approach to QBM. This analysis relies on the material published in the work of Lampo et al., 2016.

- Starting by the general form of a Lindblad equation and considering a particular expression for the Lindblad operator, we obtain equation (5.3), which exhibits a Lindblad form and differs from that of Born-Markov just for one extra-term.

- This term leads to a rotation in the phase space of the Gaussian Wigner function associated to the stationary solution of the Lindblad equation (Fig. 5.1). We also detect the regime of the parameters where the Brownian particle experiences cooling (Fig. 5.4) and squeezing (Fig. 5.2).

- We repeat the analysis for the quadratic case. Also in this case it is possible to derive a Lindblad equation [see Eq. (5.34)] differing by the original Born-Markov one just by a few extra-terms. We study the effects of such terms on the stationary state, focusing on the angle (Fig. 5.8), the degree of cooling (Fig. 5.7), and the eccentricity (Fig. 5.6). Here, up a certain value of the coupling the stationary solution of the Lindblad equation does not approach a Gaussian stationary state (Fig. 5.9).

Chapter 6

Heisenberg equations approach

In the previous chapter we have proposed a Lindblad model for QBM, exploring both the cases of linear and non-linear coupling. Lindblad equations differ from the original Born-Markov ones just for a few extra-terms (only one term in the linear case), curing the forbidden area detected in chapters 3 and 4. In this way, it is possible to evaluate the correlation functions of both position and momentum at each temperature and for each value of the bath-system coupling strength. The problem of the Lindblad approach to QBM is that the corresponding equations cannot be obtained microscopically by a Hamiltonian model. For instance, in the context of Polaron physics, where will apply the model in the next chapter, the physical Hamiltonian of the system does not lead to a master equation in the Lindblad form.

We go through another approach to investigate the dynamics of QBM model: Heisenberg equations formalism. We derive equations for the observables of the quantum Brownian particle, as well as those for the bath's operators, describing the behavior of the system in the Heisenberg picture. It is possible to note that they may be opportunely combined in order to obtain an equation ruling the temporal evolution of the particle position, where the influence of the bath appears in the form of noise and damping: it is a quantum stochastic equation. In particular, considering an ohmic Lorentz-Drude spectral density in the infinite cut-off limit, such an equation takes the form of the Langevin one in Eq. (2.18), for the classical Brownian motion: it shows a white noise and a local in time damping. The main goal of the chapter is to present in detail the procedure to solve this quantum Langevin equation, aiming to calculate the position variance. Here, we distinguish two cases: the situation in which the particle

is in a harmonic potential and that where it is untrapped. In the latter, the particle runs away from the initial position. Such a behavior may be described by means of the mean square displacement discussed in chapter 2, providing a signature of Brownian motion. We recover the traditional diffusive behavior, constituting here a consequence of the local in time form of the quantum Langevin equation, *i.e.* of the absence of memory effect in the dynamical behavior of the Brownian particle. If the particle is trapped in a harmonic potential, instead, it approaches an equilibrium state localized in average in the middle of the trap. We evaluate position and momentum variances related to such a long-time state, proving that the Heisenberg principle is always fulfilled and a proper analysis of the zero-temperature limit is finally possible.

This topic belongs to standard textbook material (Weiss, 2008; Breuer and Petruccione, 2007), and has been recently considered by Boyanovsky and Jasnow, 2017. We shall follow the revisited treatment published by Lampo et al., 2017, discussing in detail the techniques we use. In the end of the chapter, we will extend the Heisenberg equation formalism to nonlinear QBM, proceeding as in the work of Barik and Ray, 2005. In this situation, to provide an analytical expression for the position variance is not an easy task so we limit to present the form of the equation without to solve it.

6.1 Derivation of the Heisenberg equations in the linear case

In this section we consider the QBM Hamiltonian in the linear case, *i.e.* that with interaction term in Eq. (3.4). Such a model leads to the following exact Heisenberg equations of motion for the central particle and the environmental oscillators

$$\dot{x}(t) = \frac{i}{\hbar}\left[H, x(t)\right] = p(t)/m, \tag{6.1}$$

$$\dot{x}_n(t) = \frac{i}{\hbar}\left[H, x_n(t)\right] = p_n/m_n, \tag{6.2}$$

$$\dot{p}(t) = \frac{i}{\hbar}\left[H, p(t)\right] = -H_c'(x(t)) + \sum_n \kappa_n x_n(t), \tag{6.3}$$

$$\dot{p}_n(t) = \frac{i}{\hbar}\left[H, p_n(t)\right] = -m_n\omega_n^2 x_n(t) + \kappa_n x(t), \tag{6.4}$$

with

$$H_c(x) = V_c(x) + U(x), \tag{6.5}$$

where V_c is the counter-term introduced in Eq. (3.5) and $U(x)$ is the bare impurity potential. For sake of clearness we underline that, differently by the previous chapters, the operators of the system are no longer in the Schrödinger picture, but in the Heisenberg one. It is easy to find that the equation for the coordinate of the Brownian particles is

$$m\ddot{x}(t) + H_c'(x(t)) - \sum_n \kappa_n x_n(t) = 0, \tag{6.6}$$

while the equations for the coordinates of the bath oscillators take the form

$$m\ddot{x}_n(t) + m_n\omega_n^2 x_n^2(t) - \kappa_n x(t) = 0. \tag{6.7}$$

The last equation shows that the n^{th} bath oscillator is driven by the force $\kappa_n x(t)$ which depends linearly on the coordinate of the Brownian particle. In order to get a closed equation of motion for $x(t)$ the first step is to solve Eq. (6.7) in terms of $x(t)$ and of the initial conditions for the bath modes. The solution of this equation is the sum of that of the related homogeneous equation plus the particular one, that may be expressed as convolution product of Green function and the particle position. This calculation is very well known, but we specify it in Appendix E, where the procedure is presented in detail for the concrete case of the polaron. It results

$$x_n(t) = \sqrt{\frac{\hbar}{2m_n\omega_n}}\left(e^{-i\omega_n t}b_n + e^{i\omega_n t}b_n^\dagger\right) + \frac{\kappa_n}{m_n\omega_n}\int_0^t ds\,\sin\left[\omega_n(t-s)\right]x(s). \tag{6.8}$$

where we have introduced again the bath creation and annhilation operators

$$x_n(t) = \sqrt{\frac{\hbar}{2m_n\omega_n}}\left(b_n + b_n^\dagger\right), \quad p_n(t) = -i\sqrt{\frac{m_n\omega_n\hbar}{2}}\left(b_n - b_n^\dagger\right). \tag{6.9}$$

Replacing Eq. (6.8) in Eq. (6.6) we obtain

$$m\ddot{x}(t) + H_c'(x(t)) - \sum_n \frac{\kappa_n^2}{m_n\omega_n}\int_0^t ds\,\sin\left[\omega_n(t-s)\right]x(s) = B(t), \tag{6.10}$$

where we recall that the operator $B(t)$ appearing here on the right-hand side is

$$B(t) = \sum_n \kappa_n \sqrt{\frac{\hbar}{2m_n\omega_n}} \left(e^{-i\omega_n t} b_n + e^{i\omega_n t} b_n^\dagger \right), \tag{6.11}$$

representing the temporal evolution of the Schrödinger operator $B = \sum_n \kappa_n x_n(0)$. With the help of the dissipation kernel (3.30) in Eq. (6.10) may be cast in the form

$$\ddot{x}(t) + \frac{1}{m} H_c'(x(t)) - \frac{1}{\hbar m} \int_0^t ds \eta(t-s) x(s) = \frac{1}{m} B(t). \tag{6.12}$$

In the theory of QBM it is useful to express the dissipation kernel in terms of another quantity which is known as the damping kernel

$$\Gamma(t-s) = \frac{1}{m} \int_0^\infty d\omega J(\omega) \cos[\omega(t-s)], \tag{6.13}$$

fulfilling

$$\frac{\partial \Gamma}{\partial t} = -\frac{1}{\hbar m} \eta(t-s), \tag{6.14}$$

and

$$\Gamma(0) = \frac{1}{m} \int_0^\infty d\omega \frac{J(\omega)}{\omega} = \sum_n \frac{\kappa_n^2}{m m_n \omega_n^2}, \tag{6.15}$$

where $J(\omega)$ is the spectral density introduced in chapter 3 in Eq. (3.31). With the help of the damping kernel we may write the dissipative term in Eq. (6.12) as follows

$$-\frac{1}{\hbar m} \int_0^t ds \eta(t-s) x(s) = \int_0^t ds \frac{\partial}{\partial t} \Gamma(t-s) x(s) = \tag{6.16}$$

$$= \frac{\partial}{\partial t} \int_0^t ds \Gamma(t-s) x(s) - \Gamma(0) x(t). \tag{6.17}$$

In view of Eq. (6.14) the last term $-\Gamma(0)x(t)$ is seen to cancel the contribution from the counter-term contained in the potential H_c. Thus we finally arrive at the following exact Heisenberg equation of motion,

$$\ddot{x}(t) + \frac{1}{m} U'(x(t)) + \frac{\partial}{\partial t} \int_0^t ds \Gamma(t-s) x(s) = \frac{1}{m} B(t). \tag{6.18}$$

Equation (6.18) is the equation of motion for the coordinate of the Brownian particle. It may be viewed as the quantum analogue of a classical stochastic differential equation, involving a damping kernel $\Gamma(t-s)$ and a stochastic force $B(t)$, whose statistical properties depend on the initial distribution at $t=0$. If we consider now the ohmic spectral density with a Lorentz-Drude cut-off (3.41) we have

$$\Gamma(t-s) = \gamma\Lambda \exp(-\Lambda t). \tag{6.19}$$

In the limit $\Lambda \to \infty$ it takes the following form

$$\Gamma(t-s) = 2\gamma\delta(t-s). \tag{6.20}$$

We recognize so the physical meaning of the constants introduced in Eq. (3.41). The damping kernel in Eq. (6.19) induces a dependence of the particle dynamics on its past history, decaying according a timescale given by $1/\Lambda$. We may say thus that it is the characteristic time ruling the lost of memory effects, *i.e.* over which the behavior of the quantum particle may be considered Markovian. The constant γ is the responsible for the damping process, *i.e.* the lost of energy, we interpret therefore $1/\gamma$ as the relaxation timescale associated to dissipation.

Replacing Eq. (6.20) into (6.18), the latter writes as

$$\ddot{x}(t) + \frac{1}{m}U'(x(t)) + \gamma\dot{x}(t) = \frac{1}{m}B(t). \tag{6.21}$$

We recover so the equation derived by Langevin in the classical context, presented in Eq. (2.18). This result justifies the name of the Hamiltonian model we are dealing with: quantum Brownian motion. In fact, when in chapter 3 we proposed a Hamiltonian to study the quantum version of the phenomenon we looked for an operator yielding to dynamical equations manifesting the same form of the phenomenological ones discussed in chapter 2. The fact that the operator in Eq. (3.1) with the bilinear interaction (3.4) leads to a Langevin-type equation endorses the appropriateness of such a Hamiltonian to study the Brownian motion in the quantum regime. Of course, to justify the Hamiltonian model we use, it is not necessary to switch to the quantum regime. One could indeed work in a classical framework with canonical equations, obtaining a functional equation with the form in Eq. (2.18). This was actually the historical procedure: to write a functional classical Hamiltonian such that Brownian

motion equations arise, and then, switching from canonical variables to operator ones, one gets Hamiltonian (3.1).

Equation (6.21) is local in time, so it is free of memory effects, *i.e.* it corresponds to a pure Markovian dynamics. This is not only consequence of the ohmic character of the spectral density, because one has also to consider the large cut-off limit. From the physical point of view such a limit corresponds to focus on the long-time behavior of the particle, thus we may state that the in the long-time the dynamics of the quantum particle does not carry memory effects.

6.2 Solution of the Heisenberg equations in the linear case

The purpose of the present section is to solve Eq. (6.21). For this goal, we distinguish between the cases in which the Brownian particle is trapped in a harmonic potential and that where it is free of any trap.

6.2.1 Brownian particle trapped in a harmonic potential

We start by considering the situation where the particle is trapped in a quadratic potential

$$U(x) = \frac{1}{2} m\Omega^2 x^2. \tag{6.22}$$

Accordingly equation (6.21) takes the following form

$$\ddot{x}(t) + \Omega^2 x(t) + \gamma \dot{x}(t) = \frac{1}{m} B(t). \tag{6.23}$$

This equation may be treated switching to the Laplace transform domain. Here, its solution follows directly[1]:

$$x(t) = G_1(t)x(0) + G_2(t)\dot{x}(0) + \frac{1}{m}\int_0^t G_2(t-s)B(s), \tag{6.24}$$

where G_1 and G_2 are defined by means of their Laplace transforms:

$$\mathcal{L}_z[G_1(t)] = \frac{z+\gamma}{z^2+\Omega^2+\gamma z}, \quad \mathcal{L}_z[G_2(t)] = \frac{1}{z^2+\Omega^2+\gamma z}, \tag{6.25}$$

[1]This calculation is explained in detail in Appendix E.

fulfilling the initial conditions

$$G_1(0) = 1, \quad G_2(0) = 0, \tag{6.26}$$

$$\dot{G}_1(0) = 0, \quad \dot{G}_2(0) = 1. \tag{6.27}$$

The Laplace transforms in Eq. (6.25) maybe easily inverted, by calculating the roots of the denominators and expressing the functions as sum of the inverse of first degree polynomials. We obtain

$$G_1(t) = e^{-\gamma t}\left[\tilde{\Omega}\sinh\left(\gamma\tilde{\Omega}t\right) + \cosh\left(\gamma\tilde{\Omega}t\right)\right], \tag{6.28}$$

$$G_2(t) = \frac{e^{-\gamma t}}{\gamma\tilde{\Omega}}\sinh\left(\gamma\tilde{\Omega}t\right), \tag{6.29}$$

where we introduced the dimensionless parameter

$$\tilde{\Omega} = \sqrt{1-(\Omega/\gamma)^2}, \tag{6.30}$$

ruling the qualitative behavior of the motion. In fact, if $\Omega > \gamma$, the quantity in Eq. (6.30) becomes imaginary and the particle performs oscillations. This does not occur if $\Omega \leq \gamma$. However, the presence of the exponential $e^{-\gamma t}$ in both expressions implies that, in any case, the contribution of the initial conditions exponentially vanishes in a range equals to the relaxation timescale: in general, oscillating or not, we have an exponentially damped motion. The long-time state is characterized by the third term in the left hand-side in Eq. (6.24). It may be employed to calculate the position and momentum variances related to the asymptotic stationary state. For this goal one has to evaluate

$$\langle x^2(t)\rangle = \int_0^t ds \int_0^t d\sigma G_2(t-s)G_2(t-\sigma)\langle\{B(s),B(\sigma)\}\rangle. \tag{6.31}$$

We recall that

$$\langle\{B(s),B(\sigma)\}\rangle = \nu(s-\sigma) = \frac{m\gamma\hbar}{\pi}\int_0^\Lambda d\omega\omega\coth\left(\hbar\omega/2k_{\mathrm{B}}T\right)\cos\left[\omega(t-t')\right], \tag{6.32}$$

where ν is the noise kernel introduced in Eq. (3.29) evaluated for an ohmic spectral density. Replacing this expression in Eq. (6.31), and expanding the cosine function in complex exponential one may relate, in

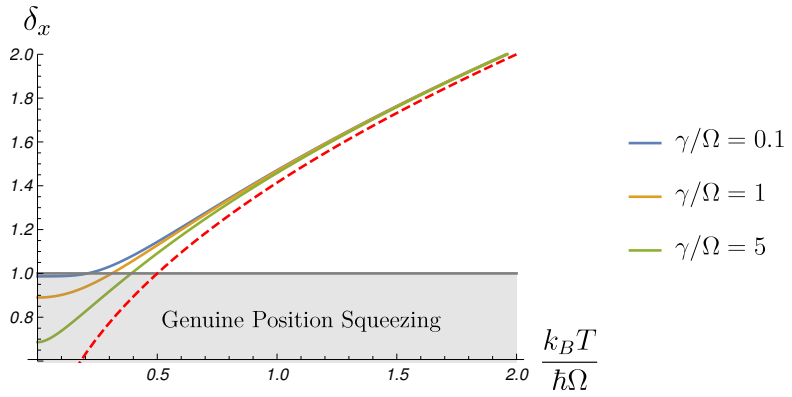

FIGURE 6.1: Position variance in Eq. (6.35) for the ohmic spectral density in Eq. (3.41) in the large cut-off limit. The red dashed line represents the behavior predicted by the Equipartition theorem.

the long time limit, the integral defining $\langle x^2 \rangle$ to the Laplace transform of G_2. It turns

$$\langle x^2 \rangle = \int_{-\Lambda}^{\Lambda} d\omega \frac{\hbar}{2\pi m} \frac{\gamma\omega}{1 + (\gamma - 2)\omega^2 + \omega^4} \coth\left(\frac{\hbar\omega}{2k_{\rm B}T}\right). \tag{6.33}$$

Similarly it is possible to find that

$$\langle p^2 \rangle = \int_{-\Lambda}^{\Lambda} d\omega \frac{m\hbar}{2\pi} \frac{\gamma\omega^3}{1 + (\gamma - 2)\omega^2 + \omega^4} \coth\left(\frac{\hbar\omega}{2k_{\rm B}T}\right). \tag{6.34}$$

Position and momentum variances can be calculated by solving numerically the integrals above, or analytically recalling the Jordan's Lemma. Still, we recover the dimensionless quantities we introduced in Eqs. (3.79) and (3.80):

$$\delta_x = \sqrt{\frac{2m_{\rm I}\Omega\langle x^2 \rangle}{\hbar}}, \quad \delta_p = \sqrt{\frac{2\langle p^2 \rangle}{m_{\rm I}\hbar\Omega}}, \tag{6.35}$$

in terms of which the Heisenberg principle writes as

$$\delta_x \delta_p \geq 1. \tag{6.36}$$

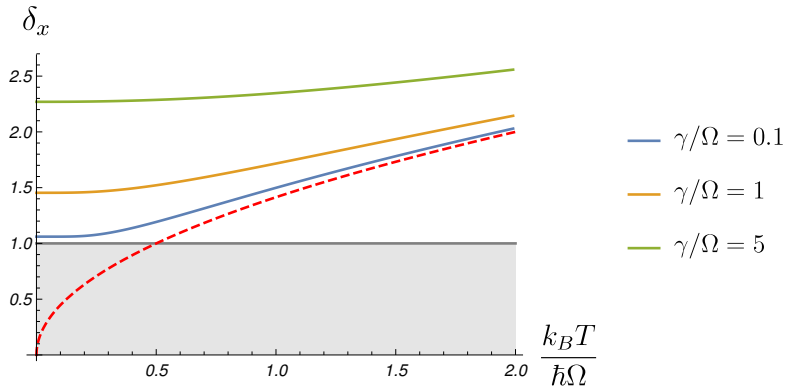

FIGURE 6.2: Momentum variance in Eq. (6.35) for the ohmic spectral density in Eq. (3.41) in the large cut-off limit The red dashed line represents the behavior predicted by the Equipartition theorem.

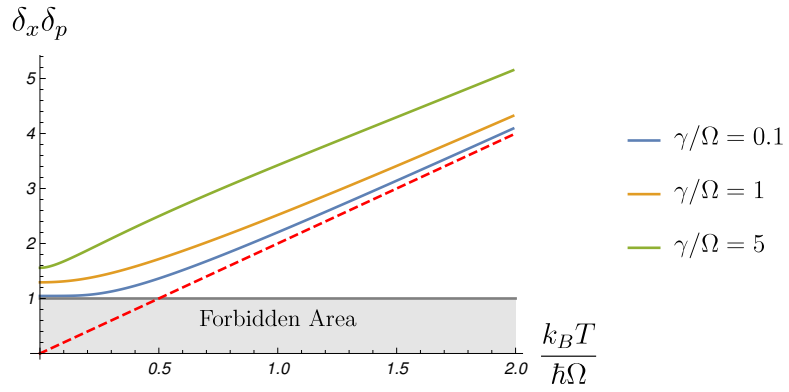

FIGURE 6.3: Product of position and momentum variance in the left hand-side of Eq. (6.36) for the ohmic spectral density in Eq. (3.41) in the large cut-off limit The red dashed line represents the behavior predicted by the Equipartition theorem.

These quantities are plotted in Figs. 6.1 and 6.2. Both variances show an agreement with the equipartition theorem as the temperature grows. At low temperature, instead, the position variance becomes smaller than the value associated to the Heisenberg threshold, *i.e.* it exhibits genuine

position squeezing. Such an effect, corresponding to high spatial localization of the particle is enhanced increasing the value of the system-bath coupling. In this approach, differently by those adopted in the previous chapters, the low-temperature limit does not alter the Heisenberg principle. This is clear in Fig. 6.3, where we plotted the product of position and momentum variance. The fact that Heisenberg principle is preserved at any temperature is one of the most important result of this chapter and shows the vantage of the Heisenberg equations formalism to explore concrete systems, for instance the polaron, as we shall do in chapter 7. We finally mention that the analytical expressions we found for the correlation functions of position and momentum could be derived also by means of the fluctuation-dissipation theorem. A proof of this statement is presented in Appendix G.

6.2.2 Untrapped Brownian particle

We move now to the situation where the central particle is untrapped, *i.e.* we have $\Omega = 0$. In this case the kernels G_1 and G_2 may found by inverting the Laplace transforms in Eq. (6.25) by putting $\Omega = 0$. The calculation can be done immediately: it follows that for an ohmic spectral density and for a very large large cut-off the quantities in Eq. (6.25) take the following form

$$G_1(t) = 1, \quad G_2(t) = \frac{1}{\gamma}\left(1 - e^{-\gamma t}\right), \tag{6.37}$$

yielding to

$$x(t) = x(0) + \frac{1}{\gamma}\left(1 - e^{-\gamma t}\right)\dot{x}(0) + \int_0^t ds \frac{1}{\gamma m}\left[1 - e^{-\gamma(t-s)}\right] B(s). \tag{6.38}$$

Remembering Eq. (6.1) one easily obtains the expression for the momentum:

$$p(t) = e^{-\gamma t}p(0) + \int_0^t ds e^{-\gamma(t-s)} B(s). \tag{6.39}$$

We aim to evaluate the mean square displacement, defined as

$$\mathrm{MSD}(t, t') = \langle \left[x(t) - x(t')\right]^2 \rangle. \tag{6.40}$$

We replace in this expression that in Eq. (6.38) obtaining

$$\mathrm{MSD}(t,t') = \frac{1}{m\gamma^2}\left(e^{-\gamma t} - e^{-\gamma t'}\right)\langle p^2(0)\rangle \tag{6.41}$$

$$+\frac{\gamma\hbar}{m\pi}\int_0^\Lambda \frac{\omega}{\omega^2+\gamma^2}\coth\left(\frac{\hbar\omega}{2k_\mathrm{B}T}\right)\left|\frac{e^{i\omega t}-e^{i\omega t'}}{i\omega}+\frac{e^{-\gamma t}+e^{-\gamma t'}}{\gamma}\right|. \tag{6.42}$$

The second term within the squared modulus may be suppressed by looking into the limit in which t and t' go to infinity, but their difference $\tau = t - t'$ is kept fixed. It deserves to be noted that such a term leads to an integral that diverges in the limit of an infinite cut-off, as discussed by Breuer and Petruccione, 2007. From the physical point of view it means that the central particle can absorb an arbitrary amount of energy and can travel an arbitrary distance within a finite time interval. This singular behavior, known as initial jolts, is clearly a result of the artificial assumption of an uncorrelated initial state. We treat it considering the long-time limit as stated above, where the initial conditions do not affect the motion anymore. It results in

$$\mathrm{MSD}(\tau) = \frac{\gamma\hbar}{m\pi}\int_0^\infty d\omega \frac{\omega}{\omega^2+\gamma^2}\coth\left(\frac{\hbar\omega}{2k_\mathrm{B}T}\right)\frac{4\sin^2(\omega\tau/2)}{\omega^2}. \tag{6.43}$$

For any finite temperature, considering large values of τ one may use the relation

$$\lim_{\tau\to\infty}\frac{\sin(\omega\tau)}{\pi\omega} = \delta(\omega), \tag{6.44}$$

we finally get

$$\mathrm{MSD}(\tau) = 2\frac{k_\mathrm{B}T}{m\gamma}t. \tag{6.45}$$

We recover so also in this case the result obtained in chapter 2 for classical Brownian motion. The approach presented in this chapter permits to highlight the relation existing between the diffusive behavior in Eq. (6.40) and the form of the spectral density: normal diffusion arises for an ohmic spectral density. As we will see in the next chapter this is not the case for the polaron problem. Here, in fact, starting by a the realistic Hamiltonian we derive in an exact manner the analytical structure of the spectral density, finding a non-ohmic behavior. This induces us to generalize the procedure to solve Heisenberg equations, and in particular its result, such

as the expression for position and momentum variance in Eqs. (6.33) and (6.34).

6.3 Heisenberg equations for non-linear coupling

For sake of completeness we pay a little bit of attention to the form of the equations arising if we consider the non-linear coupling. This problem has already been treated by Barik and Ray, 2005. Starting by the Hamiltonian in Eq. (3.1) with the non-linear interaction (4.1), and following the same procedure in section 6.1 one obtains:

$$\dot{x}(t) = p(t), \tag{6.46}$$

and

$$\begin{aligned}\dot{p}(t) = &-U'(x) - f'(x(t)) \int_0^t f'(x(t))\Gamma(t-t')p(t')dt' \\ &+ f'(x(t))\eta(t).\end{aligned} \tag{6.47}$$

where $f'(x) = 2x/a$. The quantity

$$\begin{aligned}\eta(t) = &\sum_n \left(\frac{\omega_n}{\left(g_n^{(0)}\right)^2} x_n(0) - f(x(0)) \right) \frac{\left(g_n^{(0)}\right)^2}{\omega_n^2} \cos(\omega_n t) \\ &+ \sum_n \frac{g_\nu}{\omega_n} p_n(0) \sin(\omega_n t),\end{aligned} \tag{6.48}$$

is the noise kernel, where $\omega_n \equiv \omega\epsilon_n$, while

$$\Gamma(t) = \sum_n \left(\frac{g_n}{\omega_n} \right)^2 \cos(\omega_n t), \tag{6.49}$$

is the damping kernel.

In conclusion, the dynamics of the impurity is ruled by the equations (7.54) and (7.55). Their main feature is the position dependence of the damping and the multiplicative noise. This is a consequence of the non-linear coupling in the Hamiltonian, induced by the inhomogeneous character of the gas.

6.4 Summary

We briefly summarize the main contents of the chapter:

- Starting by the Hamiltonian with the linear coupling and considering an ohmic spectral density one obtains in the large cut-off limit an equation for the position of the Brownian particle in the Heisenberg picture representing the quantum counterpart of that derived by Langevin (see Eq. (6.21)).
- Such equation shows white noise and local in time damping. These features are consequences of the ohmic character of the spectral density.
- One may solve this equation applying the Laplace transform operator. It is possible so to calculate position and momentum variance related to the long-time stationary state. The most important result is that now Heisenberg principle is always satisfied (see Fig. 6.3).
- If the particle is free of any trap the position variance exhibits a diffusive behavior [Eq. (6.40)], as in the classical case: this is a consequence of the ohmic spectral density.
- In conclusion (see Sec. 6.3) we present the form of the equation resulting for non-linear coupling. This non-linearity induces a position-dependent damping and a multiplicative noise.

Chapter 7

Bose Polaron as an instance of Brownian motion

In the previous chapter we presented a study of the QBM dynamics based on Heisenberg equations. This formalism represents a suitable method to evaluate the correlation functions of the central particle, providing an information about its motion. Moreover, differently from the master equation approach discussed in chapters 3-5 no violations of the Heisenberg principle occur and a correct analysis of the low-temperature limit is finally possible.

We employ thus such a theoretical framework to deal with a concrete real system: the Bose polaron. It consists of an impurity embedded in a Bose-Einstein condensate. This system is usually realized in experiments by considering a mixture of two different species, with a very low density of one of the species. In this way, the interactions among the atoms of the very diluted species are negligible and we may treat them as impurities in a sea of a different species. In the current chapter we shall focus on a homogeneous gas, *i.e.* a gas with a constant density, while the extension to the trapped inhomogeneous one is discussed in the next chapter.

From the point of view of open quantum systems, the impurity may be considered as a Brownian particle coupled to an environment made up by the degrees of freedom of the gas. This approach was recently introduced in the work of Lampo et al., 2017. Actually, the open quantum systems approach has been used recently in the context of ultracold quantum gases, although with different techniques and for different systems. For instance, it deserves to mention the work of Efimkin, Hofmann, and Galitski, 2016, focused on a bright soliton in a superfluid in one dimension, and that of Hilary M. Hurst, 2016 looking into the system of a dark soliton in a one-dimensional BEC coupled to a non-interacting Fermi gas.

Then, Keser and Galitski, 2016 dealt with the system of the component of a moving superfluid, and the system of an impurity in a Luttinger liquid has been treated by Bonart and Cugliandolo, 2012; Bonart and Cugliandolo, 2013.

The possibility to employ the QBM model to investigate the Bose polaron relies on the fact that the physical Hamiltonian of the latter may be cast in the form of the former once one performs a Bogoliubov transformation. This procedure is described in Sec. 7.1. The result is the so-called *Frölich Hamiltonian*, describing the physics of the impurity under the influence of the Bogoliubov excitations. Importantly, in the open quantum systems framework, the constituents of the environment are now represented by the Bogoliubov modes, rather than the atoms of the gas. So the present approach permits one to study the effects induced on the impurity by the surrounding Bogoliubov cloud.

It is important to note that in the Frölich Hamiltonian the coupling term depends in a non-linear manner on the impurity position. One could so recall the non-linear Heisenberg equations (6.46) and (6.47) derived in the previous chapter, valid for the most general dependence on the impurity position. The problem is that, in the case of the polaron, this dependence changes for each oscillator of the environment and so the coupling term may be not correctly factorized. Therefore we perform a linear approximation that allows to approach the standard QBM Hamiltonian, with a bilinear interaction term. In Sec. 7.6 we discuss the validity of such an approximation, finding that it is reasonable for realistic values of the system parameters.

Once we express the physical Hamiltonian of the system in the form of that of the QBM, we may use it to derive the spectral density. This task is performed in Sec. 7.2 where we calculate such an object in d dimensions. In all the cases it results in a super-ohmic behavior, responsible of a certain amount of memory effects in the dynamics of the impurity. In fact, a super-ohmic spectral density leads to a damping kernel which is not reducible to a Dirac Delta, and therefore the equation for the impurity position is not local in time. Note that it still shows the form of a Langevin one because it comes from the same Hamiltonian. Therefore the procedure to solve Heisenberg equations we presented in the previous chapter has to be generalized to a generic spectral density: this is the main aim of the work behind such a chapter, and contained in the paper of Lampo et al., 2017.

Again, in order to solve the equation of motion of the impurity, we

distinguish the situation where it is untrapped and that in which is confined in a harmonic potential. In the former case, the position operator in the Heisenberg picture exhibits, in the long-time limit, a ballistic dependence on time. This is in agreement with the fact that, if there is not any trap, the particle runs-away. Such a behavior may be characterized in a quantitative manner by means of the mean square displacement introduced in Eq. (7.75), providing a signature of the motion of the impurity. We find that, differently from the case of an ohmic spectral density, the mean square displacement is proportional to the square of time, *i.e.* the particle experiences a super-diffusive behavior. This is a consequence of the super-ohmic form of the spectral density associated to presence of memory effects. The super-diffusive behavior we detected constitutes so an important result because it represents a witness of memory effects on a measurable quantity.

When we put the impurity in a harmonic potential, instead, it reaches an equilibrium state localized on average in the middle of the trap. In the long-time limit so the position variance does not depend on time anymore. We thus study how it varies by tuning the system parameters, such as temperature and interaction strength. We find that, as the temperature decreases and the interaction gets stronger, the impurity experiences genuine position squeezing. Such an effect is very important because it corresponds to high spatial localization of the impurity. Even more it may be detected in experiments.

In order to optimize genuine position squeezing we have to consider the bath-impurity interaction strength as strong as possible. In this context it is important to notice that the Frölich Hamiltonian on which our treatment relies, is not valid for each value of the coupling. We will show anyway that the results we find lie in the regime of the validity of the model we deal with.

7.1 Hamiltonian

We consider a single impurity atom with mass m_{I} immersed in a $d-$dimension gas of N bosons with mass m_{B}. The interactions among the bosons are described by a potential $V_{\mathrm{B}}(\mathbf{x})$. Let $\Psi(\mathbf{x})$, $\Psi^{\dagger}(\mathbf{x})$ denote the annihilation and creation operators of atoms at the position $\mathbf{x}$. They fulfill the canonical bosonic commutation relation, $[\Psi(\mathbf{x}), \Psi^{\dagger}(\mathbf{x'})] = \delta(\mathbf{x} - \mathbf{x'})$. Bosonic

density thus reads $n_{\mathrm{B}}(\mathbf{x}) = \Psi^{\dagger}(\mathbf{x})\Psi(\mathbf{x})$. The Hamiltonian of the system is

$$H = H_{\mathrm{I}} + H_{\mathrm{B}} + H_{\mathrm{BB}} + H_{\mathrm{IB}}, \tag{7.1}$$

where:

$$H_{\mathrm{I}} = \frac{\mathbf{p}^2}{2m_{\mathrm{I}}} + U(\mathbf{x}), \tag{7.2}$$

$$H_{\mathrm{B}} = \int d^d\mathbf{x}\, \Psi^{\dagger}(\mathbf{x}) \left(\frac{\mathbf{p}_{\mathrm{B}}^2}{2m_{\mathrm{B}}} + V(\mathbf{x}) \right) \Psi(\mathbf{x}) \tag{7.3}$$

$$= \sum_{\mathbf{k}} \epsilon_{\mathbf{k}} a_{\mathbf{k}}^{\dagger} a_{\mathbf{k}}, \tag{7.4}$$

$$H_{\mathrm{BB}} = g_{\mathrm{B}} \int d^d\mathbf{x}\, \Psi^{\dagger}(\mathbf{x})\Psi^{\dagger}(\mathbf{x})\Psi(\mathbf{x})\Psi(\mathbf{x}) \tag{7.5}$$

$$= \frac{1}{2V} \sum_{\mathbf{k},\mathbf{k'},\mathbf{q}} V_{\mathrm{B}}(\mathbf{q}) a_{\mathbf{k'}-\mathbf{q}}^{\dagger} a_{\mathbf{k}+\mathbf{q}}^{\dagger} a_{\mathbf{k'}} a_{\mathbf{k}}, \tag{7.6}$$

$$H_{\mathrm{IB}} = g_{\mathrm{IB}} n_{\mathrm{B}}(\mathbf{x}) \tag{7.7}$$

$$= \frac{1}{V} \sum_{\mathbf{k},\mathbf{q}} V_{\mathrm{IB}}(\mathbf{k}) \rho_{\mathrm{I}}(\mathbf{q}) a_{\mathbf{k}-\mathbf{q}}^{\dagger} a_{\mathbf{k}}, \tag{7.8}$$

in which the operator $a_{\mathbf{k}}$ ($a_{\mathbf{k}}^{\dagger}$) destroys (creates) a boson of mass m_{B}, wave vector $\mathbf{k}$, and energy $\epsilon_{\mathbf{k}} = (\hbar k)^2/(2m_{\mathrm{B}}) - \mu$, measured from its chemical potential, μ. Equation (7.2) is the Hamiltonian for the free impurity. Equation (7.4) is the Hamiltonian of non-interacting bosons in a potential $V(\mathbf{x})$. We consider in the following that the potential is homogeneous and the system is enclosed in a box of volume V. The last two terms in Eqs. (7.6) and (7.8) are the interaction among the atoms of the gas and between them and the impurity, respectively. The quantities

$$V_{\mathrm{B}}(\mathbf{q}) = \mathcal{F}_{\mathbf{q}}\left[g_{\mathrm{B}}\delta(\mathbf{x}-\mathbf{x'})\right], \quad V_{\mathrm{IB}}(\mathbf{q}) = \mathcal{F}_{\mathbf{q}}\left[g_{\mathrm{IB}}\delta(\mathbf{x}-\mathbf{x'})\right], \tag{7.9}$$

represent respectively the Fourier transforms of the boson-boson and impurity-boson interaction, with

$$g_{\mathrm{B}} = 4\pi\hbar^2 a_{\mathrm{B}}/m_{\mathrm{B}}, \quad g_{\mathrm{IB}} = 2\pi\hbar^2 a_{\mathrm{IB}}/m_{\mathrm{R}}. \tag{7.10}$$

Here a_{B} is the scattering length between two identical bosons and a_{IB} represents that between the impurity and the BEC bosons. The reduced

mass is $m_{\mathrm{R}} = m_{\mathrm{B}} m_{\mathrm{I}}/(m_{\mathrm{B}} + m_{\mathrm{I}})$ and the (dimensionless) density of the impurity in the momentum domain is

$$\rho_{\mathrm{I}}(\mathbf{q}) = \int_{-\infty}^{+\infty} e^{-i\mathbf{q}\cdot\tilde{\mathbf{x}}} \delta\left(\tilde{\mathbf{x}} - \mathbf{x}\right) d^3\tilde{\mathbf{x}}. \tag{7.11}$$

In experiments, we usually have more than one impurity in the gas, so one can include a term modeling the interaction between several impurities in Eq. (7.1). Here we consider that the impurities concentration is low enough as to neglect such an additional interacting term. This is expressed by the following condition

$$\frac{1}{N_{\mathrm{I}}} \sum_{i \neq j} (\mathbf{x}_i - \mathbf{x}_j) \gg n_0^{-\frac{1}{3}}, \tag{7.12}$$

where N_{I}.

It is important to realize that the Hamiltonian is positively defined, and as such cannot lead to instabilities – this is clearly seen from the form of the various parts of the Hamiltonian in the position representation.

To obtain the QBM form of the Hamiltonian we first replace the creation/annihilation operator in the fundamental state by its average value $\sqrt{N_0}$. For bosons below the critical temperature the atoms mainly occupy the ground mode, with negligible fluctuations to other modes, thus forming a BEC. Consequently, we neglect the terms proportional to $N_{\mathbf{k}}$ ($\mathbf{k} \neq \mathbf{0}$), *i.e.* the number of particles out of the ground state. Then, we apply the Bogoliubov transformation

$$a_{\mathbf{k}} = u_{\mathbf{k}} b_{\mathbf{k}} - v_{\mathbf{k}} b^{\dagger}_{-\mathbf{k}}, \quad a_{-\mathbf{k}} = u_{\mathbf{k}} b_{-\mathbf{k}} - v_{\mathbf{k}} b^{\dagger}_{\mathbf{k}}, \tag{7.13}$$

with

$$u^2_{\mathbf{k}} = \frac{1}{2}\left(\frac{\epsilon_{\mathbf{k}} + n_0 V_{\mathrm{B}}}{E_{\mathbf{k}}} + 1\right), \quad v^2_{\mathbf{k}} = \frac{1}{2}\left(\frac{\epsilon_{\mathbf{k}} + n_0 V_{\mathrm{B}}}{E_{\mathbf{k}}} - 1\right), \tag{7.14}$$

in which

$$E_{\mathbf{k}} = \hbar c |\mathbf{k}| \sqrt{1 + \frac{1}{2}\left(\xi \mathbf{k}\right)^2} \equiv \hbar \omega_{\mathbf{k}} \tag{7.15}$$

is the Bogoliubov spectrum and n_0 is the density of particles in the ground state. Since we consider a homogeneous gas, the density n_0 is constant.

In Eq. (7.15) the quantities

$$\xi = \frac{\hbar}{\sqrt{2 g_{\mathrm{B}} m_{\mathrm{B}} n_0}}, \quad c = \sqrt{\frac{g_{\mathrm{B}} n_0}{m_{\mathrm{B}}}} = \frac{\hbar}{\sqrt{2} m_{\mathrm{B}} \xi} \tag{7.16}$$

represent respectively the coherence length and the speed of sound. The transformations (7.13) diagonalize the terms describing the condensed atoms [see e.g. Pitaevskii and Stringari, 2003]

$$H_{\mathrm{B}} + H_{\mathrm{BB}} = \sum_{\mathbf{k} \neq \mathbf{0}} E_{\mathbf{k}} b^{\dagger}_{\mathbf{k}} b_{\mathbf{k}}, \tag{7.17}$$

apart of a few non-operator terms, simply providing a shift of the energy levels of the atoms of the BEC.

We treat in the same manner the bosons-impurity interaction. We are going now to keep only the terms proportional to $\sqrt{N_0}$ – this is in principle a well motivated approximation, since the condensate is macroscopically occupied and $N_{i \neq 0} \ll N_0$. Unfortunately, this approximation is dangerous. Our model generically has an ultraviolet divergence, like most of models of the non-relativistic quantum field theory. We do all the calculations with a physical cut-off, so that the ultraviolet divergences do not really affect our theory. Still, at large values of the cut-off we might expect large negative shifts of the impurity energy, that might cause unphysical instability. After dropping out the terms bilinear in $N_{i \neq 0}$ we obtain

$$H_{\mathrm{IB}} = n_0 V_{\mathrm{IB}} + \sqrt{\frac{n_0}{V}} \sum_{\mathbf{k} \neq \mathbf{0}} \rho_{\mathrm{I}}(\mathbf{k}) V_{\mathrm{IB}} \left(a_{\mathbf{k}} + a^{\dagger}_{-\mathbf{k}} \right). \tag{7.18}$$

The first term on the right hand-side represents the mean field energy. It is a constant just providing a shift of the energy of the polaron, so we will neglect it in what follows. Inserting Eq. (7.13) into Eq. (7.18), one gets

$$\begin{aligned} H_{\mathrm{IB}} =& \sqrt{\frac{n_0}{V}} \sum_{\mathbf{k} \neq \mathbf{0}} \rho_{\mathrm{I}}(\mathbf{k}) V_{\mathrm{IB}} \left(u_{\mathbf{k}} - v_{\mathbf{k}} \right) \left(b_{\mathbf{k}} + b^{\dagger}_{-\mathbf{k}} \right) \\ =& \sqrt{\frac{n_0}{V}} \sum_{\mathbf{k} \neq \mathbf{0}} \rho_{\mathrm{I}}(\mathbf{k}) V_{\mathrm{IB}} \sqrt{\frac{\epsilon_{\mathbf{k}}}{E_{\mathbf{k}}}} \left(b_{\mathbf{k}} + b^{\dagger}_{-\mathbf{k}} \right), \end{aligned} \tag{7.19}$$

where we again neglected the non-operator terms.
By some algebra, the expression in Eq. (7.19) reads

$$H_{\mathrm{IB}} = \sum_{\mathbf{k}\neq\mathbf{0}} V_{\mathbf{k}} e^{i\mathbf{k}\cdot\mathbf{x}} \left(b_{\mathbf{k}} + b^{\dagger}_{-\mathbf{k}}\right), \tag{7.20}$$

in which

$$V_{\mathbf{k}} = g_{\mathrm{IB}} \sqrt{\frac{n_0}{V}} \left[\frac{(\xi k)^2}{(\xi k)^2 + 2}\right]^{\frac{1}{4}}. \tag{7.21}$$

The expression in Eq. (7.20) is known in the literature as the interaction term of the Fröhlich Hamiltonian. We restrict to the limit

$$\mathbf{k}\cdot\mathbf{x} \ll 1. \tag{7.22}$$

Accordingly Eq. (7.20) assumes the form:

$$H_{\mathrm{IB}} = \sum_{\mathbf{k}\neq\mathbf{0}} V_{\mathbf{k}} \left(\mathbb{I} + i\mathbf{k}\cdot\mathbf{x}\right) \left(b_{\mathbf{k}} + b^{\dagger}_{-\mathbf{k}}\right). \tag{7.23}$$

Equation (7.22) is a crucial assumption of this paper. It allows for a linear coupling between the impurities and the bosons, which will play the role of an environment. This is crucial when considering this system from an open quantum systems perspective. In Sec. 7.6 we justify when this assumption is valid as a function of the relevant physical parameters in the problem. A similar assumption is considered in the works of Efimkin, Hofmann, and Galitski, 2016 to study the physics of a bright soliton in a superfluid, and in that of Bonart and Cugliandolo, 2012 where QBM has been employed to treat the dynamics of an impurity in a Luttinger Liquid.

The resulting Hamiltonian of the impurity in a BEC is

$$H = H_{\mathrm{I}} + \sum_{\mathbf{k}\neq\mathbf{0}} E_{\mathbf{k}} b^{\dagger}_{\mathbf{k}} b_{\mathbf{k}} + \sum_{\mathbf{k}\neq\mathbf{0}} \hbar g_{\mathbf{k}} \pi_{\mathbf{k}} \mathbf{x}, \tag{7.24}$$

with

$$g_{\mathbf{k}} = \mathbf{k} V_{\mathbf{k}}/\hbar, \quad \pi_{\mathbf{k}} = i\left(b_{\mathbf{k}} - b^{\dagger}_{\mathbf{k}}\right). \tag{7.25}$$

To get Eq. (7.24) we redefined the Bogoliubov modes operators as $b_{\mathbf{k}} \to b_{\mathbf{k}} - V_{\mathbf{k}}/E_{\mathbf{k}}\mathbb{I}$, in order to get rid of the term in Eq. (7.20) proportional to the identity operator. This operation yields a non-operator term which

has been neglected in agreement with the procedure above.

The Hamiltonian in Eq. (7.24) describes an impurity coupled to a bath of Bogoliubov modes through an interaction term linearly dependent on the impurity position. This is exactly the same situation of the QBM. Here the impurity plays the role of the Brownian particle, while the Bogoliubov modes represent the environment. The Hamiltonian in Eq. (7.24) is in fact almost the same of that of the QBM model. The only difference lies in the dependence of the interaction term on the Bogoliubov modes operator: while in the QBM model it depends on their positions, for the present system it depends on their (dimensionless) momenta, $\pi_{\mathbf{k}}$. We will see in the following that the two situations are equivalent, and the theory of the QBM can be exploited to investigate the impurity problem.

Unfortunately, the Hamiltonian in Eq. (7.24) is not positively defined (note that at this point we match the situation described by Canizares and Sols, 1994, where translational symmetry is broken). We could repair this by taking into account bilinear terms in $a_{\mathbf{k}}$ and $a_{\mathbf{k}}^\dagger$ in Eq. (7.18), or equivalently $b_{\mathbf{k}}$ and $b_{\mathbf{k}}^\dagger$, as in the works of Bruderer et al., 2007; Rath and Schmidt, 2013; Christensen, Levinsen, and Bruun, 2015b; Shchadilova et al., 2016b; Shchadilova et al., 2016a. One way of curing it is to include these terms in the theory in an exact manner, which is possible, but technically complex. It is much easier to use the same trick as Caldeira and Leggett used in their seminal paper – *i.e.* complete the Hamiltonian to a positively defined one by writing

$$H = H_{\mathrm{I}} + \sum_{\mathbf{k}\neq\mathbf{0}} E_{\mathbf{k}} \left(b_{\mathbf{k}}^\dagger + i\hbar g_{\mathbf{k}} \mathbf{x}/E_{\mathbf{k}} \right) \left(b_{\mathbf{k}} - i\hbar g_{\mathbf{k}} \mathbf{x}/E_{\mathbf{k}} \right). \tag{7.26}$$

Clearly, Caldeira-Leggett remedy leads directly to the trapping harmonic potential for the impurity that cancels the negative harmonic frequency shift that appears in the absence of the compensation term. In Appendix E it is shown how this negative contribution arises by evaluating its effect directly in the equations of motion derived from Hamiltonian (7.24). The equations of motion are presented in Sec. 7.3.

The Hamiltonian in Eq. (7.24) is the first step to put the Bose polaron problem in the framework of quantum Brownian motion. This result has been obtained by considering the Hamiltonian in Eq. (7.1), which is a conventional choice in the context of polaron physics and it is largely used in the literature, for example by Tempere et al., 2009; Shashi et al., 2014; Casteels and Wouters, 2014. Nevertheless, this Hamiltonian is not fully

appropriate if we push our analysis towards the strong coupling regime. Here, the interaction term in Eq. (7.8) needs to be generalized by including a quadratic dependence on the operators of the impurity. Accordingly, when one introduces Bogoliubov operators, the interaction term in Eq. (7.20) includes additional terms manifesting a quadratic, rather than linear, dependence on these operators. In this way one goes beyond the Fröhlich paradigm. Such a generalization is widely studied nowadays, for instance by Bruderer et al., 2007; Rath and Schmidt, 2013; Christensen, Levinsen, and Bruun, 2015b; Shchadilova et al., 2016b; Shchadilova et al., 2016a. In particular there is still an open debate concerning the validity regime of the Fröhlich Hamiltonian, *i.e.* for which values of the system parameters the quadratic Bogoliubov operators terms can be dropped out. We neglect these terms, looking to the traditional Fröhlich interaction term in Eq. (7.20). Of course this choice does not allow us to explore the strong coupling regime, but we shall explain in the following that it is appropriate for the values of the system parameters we consider.

7.2 Spectral density

The last term of Hamiltonian (7.24) is a coupling between the impurity position and the momenta of the bath oscillators, $\pi_{\mathbf{k}}$. This plays the role of the interaction Hamiltonian between the system and the bath oscillators, when compared with the QBM Hamiltonian. The difference is that the coupling occurs with the momenta of the oscillators rather than on their positions. In the following, we show that both situations are equivalent. In fact, the interaction with the Bogoliubov modes enters in the dynamics of the system only through the self-correlation function of the environment, defined as

$$\mathcal{C}(\tau) = \sum_{\mathbf{k}\neq\mathbf{0}} \hbar g_{\mathbf{k}}^2 \langle \pi_{\mathbf{k}}(\tau)\pi_{\mathbf{k}}(0)\rangle. \tag{7.27}$$

Replacing the expression for the dimensionless momenta $\pi_{\mathbf{k}}$ in Eq. (7.25) and recalling that the environment is made up by bosons,

$$\langle b_{\mathbf{k}}^\dagger b_{\mathbf{k}}\rangle = \frac{1}{\exp\left(\hbar\omega_{\mathbf{k}}/k_{\mathrm{B}}T\right)-1}, \tag{7.28}$$

we find

$$\mathcal{C}(\tau) = \sum_{\mathbf{k}\neq\mathbf{0}} \hbar g_{\mathbf{k}}^2 \left[\coth\left(\frac{\hbar\omega_{\mathbf{k}}}{2k_{\mathrm{B}}T}\right) \cos\left(\omega_{\mathbf{k}}\tau\right) - i \sin\left(\omega_{\mathbf{k}}\tau\right) \right] \tag{7.29}$$

$$\equiv \nu(\tau) - i\lambda(\tau), \tag{7.30}$$

where

$$\nu(\tau) = \int_0^\infty J(\omega) \coth\left(\frac{\hbar\omega}{2k_{\mathrm{B}}T}\right) \cos\left(\omega\tau\right) d\omega, \tag{7.31}$$

$$\lambda(\tau) = \int_0^\infty J(\omega) \sin\left(\omega\tau\right) d\omega = -m_{\mathrm{I}}\dot{\Gamma}(t), \tag{7.32}$$

are respectively the noise and dissipation kernel, representing the real and imaginary part of the self-correlation function. The latter is related to the damping kernel introduced in Eq. (6.13), which is defined as

$$\Gamma(\tau) = \frac{1}{m_{\mathrm{I}}} \int_0^\infty \frac{J(\omega)}{\omega} \cos(\omega\tau) d\omega, \tag{7.33}$$

where

$$J(\omega) = \sum_{\mathbf{k}\neq\mathbf{0}} \hbar g_{\mathbf{k}}^2 \delta\left(\omega - \omega_{\mathbf{k}}\right) \tag{7.34}$$

is the spectral density already introduced in Eq. (3.31). Note that this quantity depends on the square of the coupling constant. This is the reason why, as we will see in the following, our theory does not depend on the sign of the interaction.

The rest of this section is devoted to the derivation of the spectral density. We first assume that the environment is large, that is, the large number of oscillators within it allows to switch from a discrete to a continuous distribution of Bogoliubov modes in the frequency domain. Then, in the definition of the spectral density, Eq. (7.34), we turn the discrete sum into an integral,

$$\sum_{\mathbf{k}} \to \int \frac{V}{(2\pi)^{\mathrm{d}}} d^{\mathrm{d}}k. \tag{7.35}$$

Using the relation

$$\delta\left(\omega - \omega_{\mathbf{k}}\right) = \frac{1}{\partial_{\mathbf{k}}\omega_{\mathbf{k}}|_{\mathbf{k}=\mathbf{k}_\omega}} \delta\left(\mathbf{k} - \mathbf{k}_\omega\right), \tag{7.36}$$

one finds

$$J(\omega)=\frac{n_0 g_{\mathrm{IB}}^2}{\hbar}\frac{S_{\mathrm{d}}}{(2\pi)^{\mathrm{d}}}\int dk k^{d+1}\sqrt{\frac{(\xi\mathbf{k})^2}{(\xi\mathbf{k})^2+2}}\frac{\delta\left(\mathbf{k}-\mathbf{k}_\omega\right)}{\partial_{\mathbf{k}}\omega_{\mathbf{k}}|_{\mathbf{k}=\mathbf{k}_\omega}}, \tag{7.37}$$

where

$$k_\omega=\xi^{-1}\sqrt{\sqrt{1+2\left(\xi\omega/c\right)^2}-1}, \tag{7.38}$$

is the inverse of the Bogoliubov spectrum in Eq. (7.15). The quantity S_{d} is the surface of the hypersphere in the momentum space with radius k in $\mathrm{d}-$dimensions. For $\mathrm{d}=1,2,3$ it reads

$$S_1=2,\quad S_2=2\pi,\quad S_3=4\pi^2. \tag{7.39}$$

Hereafter, we focus on $\mathrm{d}=1$, but the generalization to higher dimensions is conceptually immediate. Thus, in one dimension the spectral density is

$$J_{1\mathrm{d}}(\omega)=m_{\mathrm{I}}\tilde{\tau}\omega^3\chi_{1\mathrm{d}}(\omega), \tag{7.40}$$

$$\tilde{\tau}=\frac{\eta^2}{2\pi m_{\mathrm{I}}}\left(\frac{m_{\mathrm{B}}}{n_0 g_{\mathrm{B}}^{\frac{1}{3}}}\right)^{\frac{3}{2}}, \tag{7.41}$$

$$\chi_{1\mathrm{d}}(\omega)=2\sqrt{2}\left(\frac{\Lambda}{\omega}\right)^3\frac{\left[\sqrt{1+\frac{\omega^2}{\Lambda^2}}-1\right]^{\frac{3}{2}}}{\sqrt{1+\frac{\omega^2}{\Lambda^2}}}, \tag{7.42}$$

where $\tilde{\tau}$ represents a relaxation time scale. We introduced the interaction strength

$$\eta=g_{\mathrm{IB}}/g_{\mathrm{B}}, \tag{7.43}$$

which expresses the strength of the impurity-bosons interaction in units of the bosons-bosons one. The majority of our results are expressed as a function of such a parameter because in experiments with ultracold gases, such as that of Catani et al., 2012, it can be tuned. This parameter is the crucial one to define the regime of validity of our theory. In fact, in Sec. 7.1 we precised that the form of the Hamiltonian we use, showing a linear, rather than quadratic, dependence on the Bose operators, does not work for strong coupling. The parameter in Eq. (7.43) allows to quantify

to which extent the coupling has to be weak. In particular, in the works of Grusdt and Demler, 2016, and Grusdt, Astrakharchik, and Demler, 2017 have been shown that the standard Fröhlich Hamiltonian in Eq. (7.20) without quadratic terms in the Bose operators holds if

$$\eta \lesssim \eta_c \equiv \pi\sqrt{n_0\,|a_{\mathrm{B}}|} = \pi\sqrt{\frac{2n_0}{m_{\mathrm{B}}g_{\mathrm{B}}}}. \tag{7.44}$$

This equation has been derived for a gas in one dimension, but Grusdt and Demler, 2016 also presented the corresponding 3D generalization. We consider the same situation of Catani et al., 2012, *i.e.* a gas of Rb atoms with

$$n_0 = 7\,(\mu\mathrm{m})^{-1}\,, \quad g_{\mathrm{B}} = 2.36\cdot 10^{-37}\mathrm{J}\cdot\mathrm{m}. \tag{7.45}$$

Accordingly we obtain

$$\eta_c \approx 7, \tag{7.46}$$

providing an upper bound for the acceptable values for the coupling strength.

The quantity

$$\Lambda = n_0 g_{\mathrm{B}}/\hbar \tag{7.47}$$

is a characteristic frequency distinguishing the high-frequency domain from the low-frequency one. The spectral density is ohmic when it depends linearly on the frequency of the oscillators of the environment. This is not the case of the physical system we are dealing with. For $\omega \ll \Lambda$ we find

$$J_{1\mathrm{d}} \sim \omega^3, \tag{7.48}$$

namely the spectral density is proportional to the third power of the frequency of the Bogoliubov modes: it is super-ohmic. Note that it is so also in higher dimensions, as in general

$$J_{\mathrm{d}} \sim \omega^{2+\mathrm{d}}. \tag{7.49}$$

The super-ohmic dependence in Eq. (7.48) has been found by Bonart and Cugliandolo, 2012; Peotta et al., 2013 for an impurity immersed in a Luttinger liquid, and by Efimkin, Hofmann, and Galitski, 2016 for a bright soliton in a superfluid. This behavior is associated to the linear part of the Bogoliubov spectrum. Hereafter we shall focus on the former considering

$$J(\omega) = m_{\mathrm{I}}\tilde{\tau}\omega^3\theta(\omega-\Lambda), \tag{7.50}$$

namely we introduce a sharp ultraviolet cut-off to regularize the spectral density at high-frequency. We emphasize that the results we will present are independent on this ultraviolet regularization. Indeed, we reproduced the calculation by introducing an exponential, rather than a sharp cut-off, and we obtained the same results [see Appendix F].

However, apart of its analytical form, the cut-off plays a crucial role. The results we shall present in the following depend on its presence, because it allows us to focus on the low frequency portion of the spectral density, forgetting about the high frequency one. Such a way to proceed is absolutely fitting if one is interested in the long-time dynamics. In this context the cut-off frequency in Eq. (7.47) is not an artificial quantity, but it arises in a natural manner: it is the characteristic frequency distinguishing the phononic linear part of the Bogoliubov spectrum from the quadratic one. This is more clear if we express it in terms of the traditional parameters of the Bogoliubov spectrum:

$$\Lambda = c/\left(\sqrt{2}\xi\right). \tag{7.51}$$

Precisely by considering $\omega/\Lambda \ll 1$, the inverse of the Bogoliubov spectrum in Eq. (7.38) takes the following form:

$$k_\omega \sim \omega, \tag{7.52}$$

namely the Bogoliubov dispersion relation gets linear. Replacing it in Eq. (7.37) we obtain the cubic behavior in Eq. (7.40).

Finally, the negligibility of the high frequency part of the spectral density, *i.e.* the ultraviolet cut-off, arises naturally if one looks to the phonon linear part of the Bogoliubov spectrum, which is reasonable if we want to study to long-time dynamics. It is important to highlight that in such a regime our results do not depend on whether the cut-off is present or not, as we proved in the end of Appendix F. The spectral density takes thus the polynomial cubic structure in Eq. (7.40). Developing the theory of QBM for such a cubic spectral density is a central part of the current work. In the following section we shall show that such a super-ohmic behavior is related to memory effects.

7.3 Heisenberg equations

In this section we derive the Heisenberg equations of motion. For the sake of simplicity, we focus on the case where the BEC is confined in one dimension. We consider that the impurity is trapped in a harmonic potential, *i.e.*

$$U(x) = m_{\mathrm{I}}\Omega^2 x^2/2, \tag{7.53}$$

which is a common set-up in ultracold atom systems. The Heisenberg equations are

$$\dot{x}(t) = \frac{i}{\hbar}\left[H, x(t)\right] = \frac{p(t)}{m_{\mathrm{I}}}, \tag{7.54}$$

$$\dot{p}(t) = \frac{i}{\hbar}\left[H, p(t)\right] = -m_{\mathrm{I}}\Omega^2 x(t) - \hbar\sum_k g_k \pi_k(t), \tag{7.55}$$

$$\dot{b}_k(t) = \frac{i}{\hbar}\left[H, b_k(t)\right] = -i\omega_k b_k(t) - g_k x(t), \tag{7.56}$$

$$\dot{b}_k^\dagger(t) = \frac{i}{\hbar}\left[H, b_k^\dagger(t)\right] = +i\omega_k b_k^\dagger(t) - g_k x(t), \tag{7.57}$$

where the Hamiltonian is given in Eq.(7.24). Equations (7.54)-(7.57) can be combined to obtain

$$\ddot{x}(t) + \Omega^2 x(t) + \frac{\partial}{\partial t}\int_0^t \Gamma(t-s)x(s)ds = \frac{B(t)}{m_{\mathrm{I}}}, \tag{7.58}$$

as detailed in Appendix E. This is the equation of motion for the impurity position. It may be viewed as the quantum analogue of a classical stochastic differential equation, where

$$B(t) = \sum_k i\hbar g_k (b_k^\dagger e^{i\omega_k t} - b_k e^{-i\omega_k t}) \tag{7.59}$$

plays the role of a stochastic force, and $\Gamma(t)$ is the damping kernel introduced in chapter 6 and recalled in Eq. (7.33), which expression may be obtained through an integration by parts:

$$\Gamma(t) = \frac{\tilde{\tau}}{t^3}\left[2\Lambda t\cos(\Lambda t) - (2-\Lambda^2 t^2)\sin(\Lambda t)\right]. \tag{7.60}$$

An important feature of such an equation is that it is non-local in time, namely the temporal evolution of x at time t depends on its past history,

i.e. $x(s)$ with $s < t$. We can state that in general the dynamics of an impurity in a homogeneous BEC in one dimension, described by Eq. (7.58), carries a certain amount of *memory effects*. Actually, there is one special situation where this equation reduces to a local one, and in particular to a traditional damped harmonic oscillator with a stochastic force. This is the case constituted by a damping kernel proportional to a Dirac delta. In chapter 6 we proved that this expression of the damping kernel results by an *ohmic* spectral density, *i.e.* a spectral density depending linearly on the frequency. As we showed in Sec. 7.2 this is not the case of the present system, where the spectral density is super-ohmic. In conclusion we can state that the dynamics of an impurity in a BEC always carries a certain amount of memory effects.

Equation (7.58) is a second-order linear non-homogeneous differential equation. Its solution is the sum of a particular one and that of the related homogeneous equation. For the latter we can proceed by applying the Laplace transform operator, in order to obtain the solution in terms of the initial position and velocity. The particular solution, instead, is the convolution product of the Green function and the position operator. Therefore, the solution for the impurity position in the Heisenberg picture takes the following form

$$x(t) = G_1(t)x(0) + G_2(t)\dot{x}(0) + \frac{1}{m_{\mathrm{I}}}\int_0^t G_2(t-s)B(s)ds, \tag{7.61}$$

where the functions G_1 and G_2 are defined through their Laplace transforms

$$\mathcal{L}_z[G_1(t)] = \frac{z + \mathcal{L}_z[\Gamma(t)]}{z^2 + \Omega^2 + z\mathcal{L}_z[\Gamma(t)]}, \tag{7.62}$$

$$\mathcal{L}_z[G_2(t)] = \frac{1}{z^2 + \Omega^2 + z\mathcal{L}_z[\Gamma(t)]}, \tag{7.63}$$

and satisfy

$$G_1(0) = 1, \quad \dot{G}_1(0) = 0, \tag{7.64}$$

$$G_2(0) = 0, \quad \dot{G}_2(0) = 1. \tag{7.65}$$

Equations (7.62) and (7.63) generalize the expressions in Eq. (6.25) to a situation associated to a damping kernel induced by a generic spectral density. They depend on the Laplace transform of the damping kernel

which is calculated in Appendix F. Here we present only the final result

$$\mathcal{L}_z\left[\Gamma(t)\right] = z\tilde{\tau}\left[\Lambda - z\arctan\left(\Lambda/z\right)\right]. \tag{7.66}$$

In order to find the expression of the position impurity as a function of the time, and so to characterize its motion, we have to invert the Laplace transforms in Eqs. (7.62) and (7.63). In the following two sections, we will invert this transformations to obtain the complete solution both analytically and numerically, for the case of untrapped (Sec. 7.4) and trapped impurity (Sec. 7.5).

7.4 Untrapped impurity

Here we consider an untrapped impurity, that is $\Omega = 0$ in Eq. (7.53). In this case the impurity position in the Heisenberg picture is described by Eq. (7.61) with

$$\mathcal{L}_z[G_1(t)] = \frac{z + \mathcal{L}_z[\Gamma(t)]}{z^2 + z\mathcal{L}_z[\Gamma(t)]} = 1/z, \tag{7.67}$$

$$\mathcal{L}_z[G_2(t)] = \frac{1}{z^2 + z\mathcal{L}_z[\Gamma(t)]}. \tag{7.68}$$

To completely characterize the motion of the impurity one has to invert these Laplace transforms. For Eq. (7.67) this calculation can be performed straightforwardly to get

$$G_1(t) = 1. \tag{7.69}$$

Thus the contribution of the initial position in Eq. (7.61) is constant in time. We highlight that such a result may be found even without knowledge of the form of the damping kernel, and therefore about the form of the spectral density. Thus, Eq. (7.69) holds for any untrapped impurity, regardless of the details of the coupling.

It is more difficult to handle with the Laplace transform in Eq. (7.68), due to the arctangent in the Laplace transform of the damping kernel in Eq. (7.66). We are interested in the long-time regime, which corresponds to $z \ll \Lambda$. The asymptotic expansion of Eq. (7.66) in this limit reads

$$\mathcal{L}_z\left[\Gamma(t)\right] = z\tilde{\tau}\Lambda + o(z^2), \tag{7.70}$$

and therefore

$$\mathcal{L}_z[G_2(t)] = \frac{1}{(1+\Lambda\tilde{\tau})z^2} \equiv \frac{1}{\alpha z^2}, \tag{7.71}$$

which can be inverted providing

$$G_2(t) = t/\alpha. \tag{7.72}$$

We note that such an expression does not fulfill the boundary conditions in Eq. (7.65), in particular $\dot{G}_2(0) \neq 1$, but this is justified by the fact that Eq. (7.72) refers to a long-time behavior.

Equation (7.72) has been obtained by expanding the Laplace transform of the damping kernel at the first order in z/Λ. In general one may perform such an expansion to the n^{th} order, and the Laplace transform in Eq. (7.68) takes the form of the inverse of a polynomial of $(n+1)^{\text{th}}$ degree. The Laplace transform can be henceforth inverted by computing the roots of such a polynomial, say $\bar{z}_k$, with $k = 1, ..., n+1$, and finally one gets

$$G_2(t) = \sum_{k=1}^{n+1} a_k e^{\bar{z}_k t}, \tag{7.73}$$

where the a_k are constants depending on the roots $\bar{z}_k$. However, one has to notice that some roots have a positive real part, corresponding to divergent run-away solutions (Ford and O'Connell, 1991). These divergent roots have to be dropped out. In fact it is possible to see that they do not satisfy the condition $z \ll \Lambda$ that we assumed in the beginning of the calculation. Then, they are negligible in the long-time limit. One may invert the Laplace transform in Eq. (7.68) through the general approach of the Bromwich integral. Here the run-away roots remain out of the integration contour, and therefore the related residuous do not contribute. We conclude that Eq. (7.72) represents the complete expression for the Laplace transform in Eq. (7.68) in the long-time limit.

In order to go beyond any asymptotic expansion of Eq. (7.66), we have to perform numerically the inversion of the Laplace transform in Eq. (7.68). There exist several algorithms aimed to deal with this problem, as carefully discussed by Wang and Zhan, 2015. Here, we consider

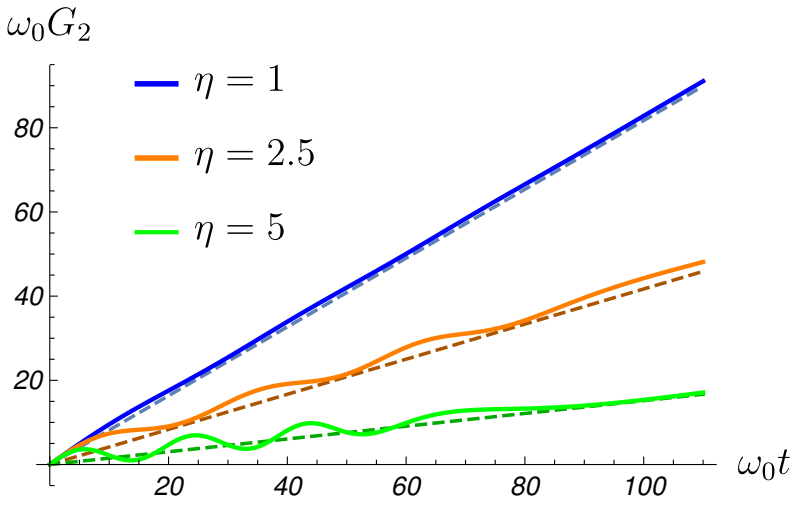

FIGURE 7.1: Inverse Laplace transform of Eq. (7.68). The plot refers to a K impurity embedded in a gas of Rb atoms with a density $n_0 = 7 \cdot 10^6 \mathrm{m}^{-1}$ and a coupling constant $g_B = 2.36 \cdot 10^{-37} \mathrm{J} \cdot \mathrm{m}$. Here $\omega_0 = \hbar n_0^2 / m_I$ represents the characteristic frequency. Solid lines refer to result of the approximation in Eq. (7.74) for $N = 5$, while dashed ones represent analytic long-time predictions from Eq. (7.72).

the Zakian method, where the inverse Laplace transform $f(t)$ of a function $F(z)$ is approximated as

$$\tilde{f}(t) = \frac{2}{t} \sum_{j=1}^{N} \mathrm{Re}\left[k_j F\left(\alpha_j / t\right)\right], \tag{7.74}$$

with α_j and k_j constants that can be either complex or reals. In the limit $N \to \infty$ it turns that $\tilde{f}(t) \to f(t)$. Many studies show that the error in the approximation is negligible in several situations already for $N = 5$, and the parameters α_j and k_j are listed in Table 1 of the paper of Wang and Zhan, 2015. Applying this method to our problem we invert the Laplace transform in Eq. (7.68) without performing any asymptotic approximation. The result is presented in Fig. 7.1. We note that in the long-time limit the numerical solution matches the analytic one presented in

Eq. (7.72). This linear divergence is approached through damped oscillations, which characterize the short- and middle-time regimes. The same behavior is detected by reproducing the calculation by means of other algorithms in (Wang and Zhan, 2015), such as the Fourier and Week ones.

In conclusion, the position operator in the Heisenberg picture for an untrapped impurity is described by the expression in Eq. (7.61), where G_1 is given by Eq. (7.69), while G_2 is represented in Fig. 7.1. Only in the long-time limit it is possible to exhibit an analytic expression for the second function, Eq. (7.72). Such a term shows a ballistic form, namely it is proportional to time. It means that, as time flows the position impurity becomes larger and larger. The untrapped impurity does not approach the equilibrium, but runs away from its initial position. This is a reasonable behavior when we remove trapping. It is natural to characterize quantitatively the motion of the untrapped impurity with the mean square displacement (MSD) already introduced in Eq. (6.40):

$$\mathrm{MSD}(t) = \langle [x(t) - x(0)]^2 \rangle, \tag{7.75}$$

which provides the deviation between the position at time t and the initial one. In experiments dealing with ultracold gases such a quantity can be measured (Catani et al., 2012). In the long-time limit it is possible write

$$\begin{aligned} \mathrm{MSD}(t) &= \left(\frac{t}{\alpha}\right)^2 \langle \dot{x}(0)^2 \rangle \\ &+ \frac{1}{2\left(\alpha m_{\mathrm{I}}\right)^2} \int_0^t ds \int_0^t d\sigma (t-s)(t-\sigma) \langle \{B(s), B(\sigma)\} \rangle, \end{aligned} \tag{7.76}$$

where we considered a factorizing initial state $\rho(t) = \rho_S(0) \otimes \rho_B$. The initial conditions of the impurity and bath oscillators are then uncorrelated. Then, averages of the form $\langle \dot{x}(0) B(s) \rangle$ vanish. The second term on the right-hand side of Eq. (7.76) can be treated noting that

$$\langle \{B(s), B(\sigma)\} \rangle = 2\hbar\nu(s-\sigma), \tag{7.77}$$

and remembering the definition of the noise kernel in Eq. (7.31) it turns:

$$\nu(s-\sigma) = m_{\mathrm{I}} \tilde{\tau} \int_0^{\Lambda} d\omega \cos\left[(s-\sigma)\omega\right] \omega^3, \tag{7.78}$$

where the hyperbolic cotangent in the noise kernel in Eq. (7.31) has been

approximated to one assuming low-temperature. This is an important assumption. It is possible to check that for realistic values of the physical quantities such an approximation for the hyperbolic cotangent is reasonable. Replacing Eq. (7.78) in the second term of the right-hand side of Eq. (7.76), and integrating with respect of time and frequency, it turns

$$\mathrm{MSD}(t) = \left[\langle \dot{x}(0)^2\rangle + \frac{\hbar\tilde{\tau}\Lambda^2}{2m_{\mathrm{I}}}\right]\left(\frac{t}{\alpha}\right)^2. \tag{7.79}$$

When this quantity shows a linear dependence on time, the impurity experiences normal diffusion as shown in Eq. (6.45). Conversely, the MSD is proportional to the square of time in Eq. (7.79). Such a behavior is termed super-diffusion and provides a key signature of the motion of the impurity.

In this context super-diffusion is a consequence of the presence of memory effects. In chapter 6 a similar calculation is performed considering an ohmic spectral density, associated to the absence of memory effects, and leads to a diffusive behavior. Super-diffusion in Eq. (7.79) arises due to the super-ohmic character of the spectral density. Therefore, it represents a witness of memory effects for a measurable observable.

Apart from the position, the result we presented above permits to obtain an expression for the momentum of the impurity in the Heisenberg picture. In fact, by inserting within Eq. (7.54) the expression in Eq. (7.61) with the G_2 function in Eq. (7.72), one infers

$$p(t) = \frac{1}{\alpha}\left[p(0) + \int_0^t B(s)ds\right]. \tag{7.80}$$

Equation (7.80) can be used to compute the average energy of an untrapped impurity

$$E(t) = \frac{\langle p^2(t)\rangle}{2m_{\mathrm{I}}}. \tag{7.81}$$

Proceeding as in the derivation of the MSD we find in the low temperature limit

$$\begin{aligned} E^{LT}(t) =& \eta g_{\mathrm{B}} n_0 + \frac{E(0)}{\alpha^2} + \frac{\hbar\tilde{\tau}}{2\alpha^2}\Lambda^2 \\ &- \frac{\hbar\tilde{\tau}}{(\alpha t)^2}\left[\cos(\Lambda t) + \Lambda t \sin(\Lambda t) - 1\right], \end{aligned} \tag{7.82}$$

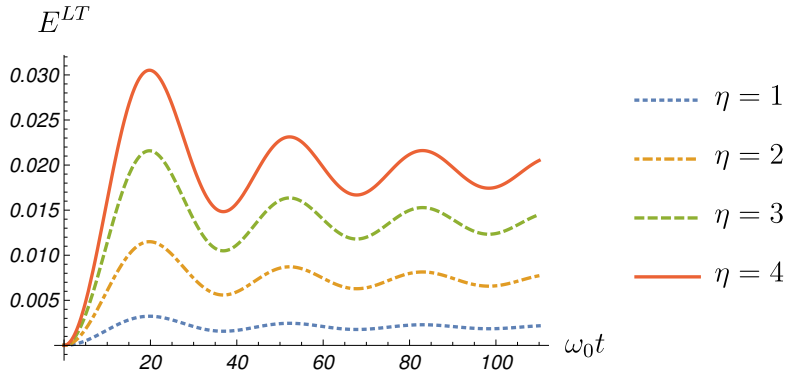

FIGURE 7.2: Average of the energy in the low temperature limit in Eq. (7.82) as a function of the time for different values of the coupling strength. The plot refers to the situation where the initial average energy E(0), as well as the mean-field term, have been set to zero.

where we recover the mean-field energy term, represented now by the first term on the right hand side. Such a quantity is plotted in Fig. 7.2, where it is shown that the average of the energy oscillates initially and after a long time approaches a constant value. These oscillations represent a non-monotonic behavior of the energy. Importantly, the increasing parts correspond to a flow of energy directed from the environment towards the impurity. In the work of Guarnieri, Uchiyama, and Vacchini, 2016 such a backflow energy has been studied for QBM and indicated as a witness of memory effects.

We note that after a long time, in the weak coupling limit, the only term surviving in Eq. (7.82) is the mean-field one. In fact the terms in the second line vanish after a long time. The second term on the right hand-side vanish in the weak coupling limit, since it is proportional to η^2. In the end, in the weak coupling limit, the asymptotic value of the energy approaches the mean-field one.

In the high-temperature limit super-diffusion equally emerges, though with a different coefficient. Also the energy shows qualitatively the same behavior as in the low-temperature limit. Nevertheless, the linear approximation in Eq. (7.22) fails, as discussed in Appendix 7.6.

7.5 Trapped impurity

In this section we restore the presence of a harmonic trap, *i.e.* we look to the situation where $\Omega > 0$ in Eq. (7.53). To investigate the dynamics of the impurity we proceed as in the previous section, namely we invert the Laplace transforms in Eqs. (7.62) and (7.63), in order to characterize the expression of the position operator in the Heisenberg picture, given in Eq. (7.61). Here, an important difference with Sec. 7.4 is that the expression for $G_1(t)$ cannot be obtained regardless of any information about the analytic structure of the damping kernel. Conversely, for a trapped impurity the calculation of G_1 requires the same attention of G_2.

We approach the problem from a numerical point of view, with the Zakian method presented by Wang and Zhan, 2015, briefly described in Sec. 7.4. The results are presented in Fig. 7.3. Both functions exhibit oscillations which get damped in the long-time regime. In particular, in the long-time limit one gets

$$\lim_{t\to\infty} G_1(t) = 0, \quad \lim_{t\to\infty} G_2(t) = 0. \tag{7.83}$$

The boundary conditions in Eqs. (7.64) and (7.65) are satisfied. Employing alternative numerical methods described by Wang and Zhan, 2015 to invert the Laplace transforms we obtain the same result. From the physical point of view it means that, after a long-time, the contributions of the initial position and velocity vanish.

For a trapped impurity we are also interested in the long-time behavior of the particle. We characterize it by means of the position variance, which is a measurable quantity. Taking into account the behavior of G_1 and G_2 functions showed in Fig. 7.3, the expression for the position variance can be easily found starting from Eq. (7.61)

$$\langle x^2(t)\rangle = \int_0^t ds \int_0^t d\sigma G_2(t-s)G_2(t-\sigma)\frac{\nu(s-\sigma)}{m_{\mathrm{I}}^2\hbar^{-1}}, \tag{7.84}$$

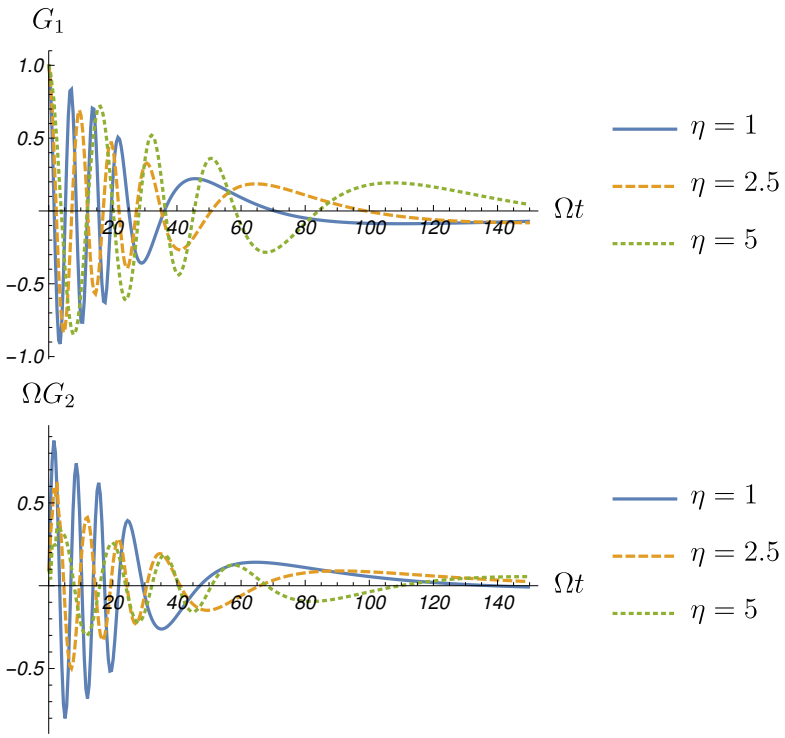

FIGURE 7.3: Inverse Laplace transforms of Eqs. (7.62) (Up) and (7.63) (Down) obtained through the Zakian method. The figures refer to an impurity of K with $\Omega = 2\pi \cdot 500$ Hz in a gas made up by Rb with a density of $n_0 = 7(\mu\text{m})^{-1}$ and a coupling strength $g_B = 2.36 \cdot 10^{-37}$J·m.

where we used the first line in Eq. (7.78). Replacing the expression for the noise kernel one gets

$$\begin{aligned}\langle x^2(t)\rangle =& \frac{\hbar}{m_{\rm I}^2}\int_0^{\Lambda} J(\omega)\coth\left(\hbar\omega/2k_{\rm B}T\right)d\omega \\ &\times\int_0^t ds\int_0^t d\sigma G_2(t-s)G_2(t-\sigma)\cos[\omega(s-\sigma)] \\ \equiv& \frac{\hbar}{m_{\rm I}^2}\int_0^{\Lambda} J(\omega)\coth\left(\hbar\omega/2k_{\rm B}T\right)\phi(t,\omega)d\omega. \end{aligned} \tag{7.85}$$

We stress that once the long-time conditions in Eq. (7.83) are fulfilled, it is not necessary to suppose that the state of the global system is initially non-correlated, as we did in Sec. 7.4. Equation (7.85) turns into

$$\begin{aligned}\phi(t,\omega) =& \frac{1}{2}\int_0^t ds\int_0^t d\sigma G_2(t-s)G_2(t-\sigma)\left[e^{i\omega s}e^{-i\omega\sigma}+c.c.\right] \\ =& \frac{1}{2}\int_0^t d\tilde{s}e^{-i\omega\tilde{s}}G_2(\tilde{s})\int_0^t d\tilde{\sigma}e^{i\omega\tilde{\sigma}}G_2(\tilde{\sigma})+c.c., \end{aligned} \tag{7.86}$$

where we introduced

$$\tilde{s}=t-s,\quad \tilde{\sigma}=t-\sigma. \tag{7.87}$$

We are interested in the long-time limit, $t\to\infty$. In this limit, one gets

$$\phi(t,\omega)=\mathcal{L}_{-i\omega}\left[G_2(t)\right]\mathcal{L}_{+i\omega}\left[G_2(t)\right]. \tag{7.88}$$

Replacing Eq. (7.63) into Eq. (7.88), we obtain the final expression for the position variance:

$$\langle x^2\rangle = \frac{\hbar}{2\pi}\int_{-\Lambda}^{+\Lambda} d\omega\coth\left(\hbar\omega/2k_{\rm B}T\right)\tilde{\chi}''(\omega), \tag{7.89}$$

where

$$\tilde{\chi}''(\omega)=\frac{1}{m_{\rm I}}\frac{\zeta(\omega)\omega}{\left[\omega\zeta(\omega)\right]^2+\left[\Omega^2-\omega^2+\omega\theta(\omega)\right]^2}, \tag{7.90}$$

and

$$\zeta(\omega) = \mathrm{Re}\{\mathcal{L}_{\tilde{z}}[\Gamma(t)]\} = \frac{\pi\tilde{\tau}}{2}\omega^2 + o\left(\frac{\omega}{\Lambda}\right)^5, \tag{7.91}$$

$$\theta(\omega) = \mathrm{Im}\{\mathcal{L}_{\tilde{z}}[\Gamma(t)]\} = -\tilde{\tau}\Lambda\omega + \frac{\tilde{\tau}}{\Lambda}\omega^3 + o\left(\frac{\omega}{\Lambda}\right)^5. \tag{7.92}$$

with $\tilde{z} = -i\omega + 0^+$. The expression in Eq. (7.89), endowed by Eqs. (7.90) and (7.91), completely determines the position variance for an impurity trapped in a harmonic potential. It generalizes that we presented in Eq. (6.31) to generic spectral densities. We emphasize that such an expression has been obtained just by considering the long-time limit of the solution of the Heisenberg equations in Eq. (7.61). It is possible to note, however, that it corresponds to that achieved in the context of the linear response theory by means of the fluctuation-dissipation theorem (Breuer and Petruccione, 2007), as discussed in detail in Appendix G. Indeed, $\tilde{\chi}''$ can be seen as the imaginary part of the Fourier transform of the linear response to an external force applied to the system, at the equilibrium.

In conclusion, in presence of a harmonic trap the impurity approaches the equilibrium in the long-time limit. We describe such a state through position and momentum variance (a similar expression to Eq. (7.89) is also found for the momentum). In particular we recall

$$\delta_x = \sqrt{\frac{2m_{\mathrm{I}}\Omega\langle x^2\rangle}{\hbar}}, \quad \delta_p = \sqrt{\frac{2\langle p^2\rangle}{m_{\mathrm{I}}\hbar\Omega}}, \tag{7.93}$$

which represents the position and momentum variances regularized in order to be dimensionless. In these units the Heisenberg principle reads as $\delta_x\delta_p \geq 1$, so the Heisenberg threshold is set to be equal to one. These quantities do not depend on time, because they refer to an equilibrium stationary state. We study the dependence of δ_x on the system parameters, such as temperature and interaction strength, that can be tuned in experiments.

In Fig. 7.4 we show the position variance for a trapped impurity as a function of the temperature, for several values of the coupling strength. Such a result follows from both a numerical and analytic integration. In the second case, one may proceed by noting that the integrand function rapidly vanishes as ω increases, so we approximate Eq. (7.89) with an integral over the whole real axis (also note that the integrand is an even function). Therefore it is possible to apply the Residue theorem. We also

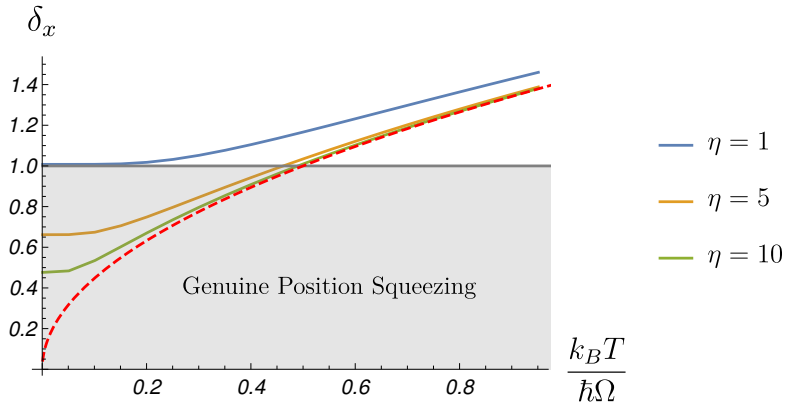

FIGURE 7.4: Dimensionless position variance in Eq. (7.93) as a function of the temperature, for several values of the interaction strength. The red dashed line represents the function $\sqrt{2T}$, associated to the equipartition theorem. The figure refers to an impurity: of K with $\Omega = 2\pi \cdot 500$ Hz in a gas made up by Rb with a density of $n_0 = 7(\mu\text{m})^{-1}$ and a coupling strength $g_{\text{B}} = 2.36 \cdot 10^{-37}\text{J}\cdot\text{m}$.

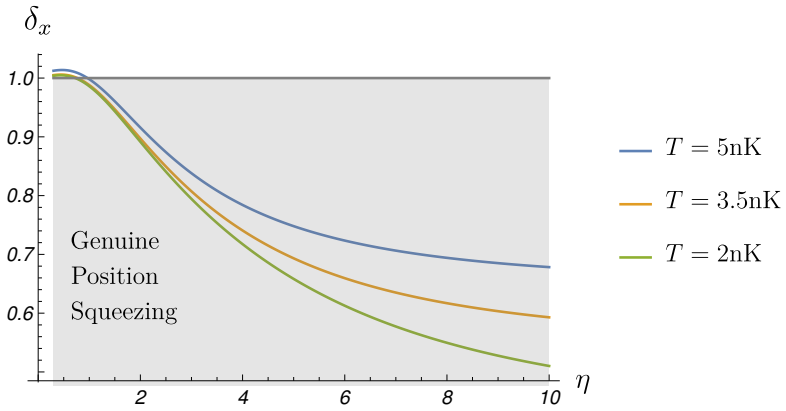

FIGURE 7.5: Dimensionless position variance in Eq. (7.93) as a the interaction strength, for several values of the temperature, satisfying $k_{\rm B}T/\hbar\Omega \ll 0.5$. The figure refers to an impurity: of K with $\Omega = 2\pi \cdot 500$ Hz in a gas made up by Rb with a density of $n_0 = 7(\mu\text{m})^{-1}$ and a coupling strength $g_{\rm B} = 2.36 \cdot 10^{-37}\text{J}\cdot\text{m}$.

stress that Eq. (7.89) refers to the asymptotic expansion in Eq. (7.91), justified in the long-time limit. Such an expansion has been performed till the fifth order in ω/Λ, but even going to higher orders we recover the same result as in Fig. 7.4.

In physical grounds we note from Fig. 7.4 that for $k_{\rm B}T/\hbar\Omega \gtrsim 0.5$, the position variance grows as the square root of the temperature. Indeed, we detect the behavior provided by $\delta_x \sim \sqrt{2T}$ (red dashed line), in agreement with the equipartition theorem. We note that as the temperature increases the value of the position variance turns to be less dependent of the interaction strength.

In the other limit, that is when one approaches the zero-temperature limit (for $k_{\rm B}T/\hbar\Omega \lesssim 0.5$), we find that $\delta_x < 1$. This means that the position variance is smaller than the value related to the Heisenberg threshold in these units. This important effect is named genuine position squeezing, and corresponds to high spatial localization of the impurity. This is an important resource in quantum technologies, and therefore we would like to find under which parameters such an effect is enhanced. In Fig. 7.5 we plot the value of the dimensionless position variance in Eq. (7.93) as a function of the interaction strength, obtained by exploring values of

the temperature as low as possible. We point out that genuine squeezing is maximized, *i.e.* δ_x gets smaller, if the temperature tends to zero, and the interaction becomes stronger. For instance, tuning $\eta \approx 5$ and setting $T = 2$nk it is possible to reach $\delta_x \approx 0.7$. This degree of squeezing may be enhanced by increasing the value of η. In this case, our results would lie at the border of the validity regime of our Hamiltonian model. Note that in experiments the value of η may be pushed towards very high values, for instance Catani et al., 2012 reach $\eta = 30$. Of course, the present theory cannot be employed to investigate such a regime. However, we remark that for $\eta \lesssim 7$, where the theory is well defined, we already find a good degree of genuine position squeezing. We underline, anyway, that even for $\eta \lesssim 7$, the investigation of such a limit would be not possible through the tools developed in the work of Massignan et al., 2015, basically due to the violations of the Heisenberg principle at low temperature. Here, instead, Heisenberg principle is fulfilled.

It is important to note that in the present treatment we considered only one 1D BEC, but in real experiments such as that of Catani et al., 2012 the set-up includes a large number of tubes. The gases confined in these tubes present values of the physical quantities, for instance the density, that in general are different for each tube. This has to be taken into account in the analysis of the theoretical results in the attempt to approach the experimental outcomes. In fact, one should in principle perform a convolution of a particular result over the whole set of tubes, *i.e.* to calculate the average of a result over the parameters associated to each tube. This way to proceed is described for instance in the work of Pagano et al., 2014.

Finally, we would like to underline that the genuine position squeezing appears both for attractive and repulsive interactions. This is in agreement with the results presented by Catani et al., 2012 [see Fig. 4], where it has been shown that the position variance of the impurity does not depend on the sign of the interaction. To understand this, let us first note that in the presence of a trap confining the BEC, the density of the condensate, will be spatially changing and peaked in the center of the trap. If impurity-boson interactions are repulsive, one should expect that the impurity will be pushed away from the center and localized around the distance D resulting from an interplay between the force trapping the impurity and the force resulting from the mean field interactions. While due to the parity symmetry $\langle x \rangle = 0$, one should expect that $\langle x^2 \rangle \simeq D^2$ and, unless D is very small, there will be no squeezing of the position. In

contrast, for attractive interactions the impurity will be localized in the center of the trap and squeezing will be possible. In the work of Lim et al., 2018 it is considered the model when the bath is coupled to the square of the position of the impurity. This is the first step towards the study of the full problem, in which impurity couples to a confined condensate with spatially dependent density and complicated spatially dependent Bogoliubov-de Gennes modes.

In contrast, in the present case we consider a spatially homogeneous condensate with constant density and Bogoliubov-de Gennes modes, which are plane waves. Moreover, we linearize the spatial dependence of modes, assuming self-consistently that the impurity is localized in the region of x allowing for such a linearization. The above arguments do not apply in this case, and our results: i) do not depend on the sign of impurity-bath interaction; ii) squeezing is thus possible for both repulsive and attractive interactions.

7.6 Validity of the linear approximation

In Sec. 7.1 we proved that the Hamiltonian of an impurity in a gas may be expressed in the form of that of the QBM. A crucial step to perform this task consists of a linear expansion of the exponential appearing in Eq. (7.20). The present Appendix is devoted to discuss the validity of such an approximation, namely we wonder for which values of the system parameters the condition

$$kx \ll 1, \tag{7.94}$$

holds, allowing the expansion in Eq. (7.23). Here, k represents the wave number of the Bogoliubov modes, depending on their frequency as showed in Eq. (7.38). This function increases monotonically as

$$k \approx \omega/c \quad \text{for} \quad \omega \ll \Lambda, \tag{7.95}$$
$$k \sim \sqrt{\omega} \quad \text{for} \quad \omega \gg \Lambda, \tag{7.96}$$

hence we can minimize the left-hand side of Eq. (7.94) by looking to the small frequency regime in Eq. (7.95). Note that this is in agreement with our treatment, because all the results presented here refer to the phonon linear part of the Bogoliubov dispersion relation. In fact such a portion of the Bogoliubov spectrum is embodied in the super-ohmic form of the

spectral density we have considered [see Sec. 7.2]. Moreover, the ultraviolet sharp cut-off, Λ, permits to get rid of the contribution due to the non-linear part in Eq. (7.96). The condition in Eq. (7.94) is then

$$\frac{\omega}{c}x \ll 1, \tag{7.97}$$

and recalling the expression

$$c = \sqrt{2}\xi\Lambda, \tag{7.98}$$

it turns into

$$\frac{\omega}{\Lambda}\frac{x}{\xi} \ll \sqrt{2}. \tag{7.99}$$

We point out that, in order to fulfill the condition, the position of the impurity may acquire large values, provided we consider a frequency much smaller than Λ.

The value of the frequency depends in general on the temperature. For a system of bosons the energy at a given temperature T is

$$E(\omega) = \frac{\hbar\omega}{e^{\frac{\hbar\omega}{k_{\mathrm{B}}T}} - 1} \leq k_{\mathrm{B}}T, \tag{7.100}$$

accordingly one can evaluate Eq. (7.99) as

$$\frac{k_{\mathrm{B}}T}{\hbar c}x \ll 1. \tag{7.101}$$

Note that, because of the inequality in Eq. (7.100), the condition in Eq. (7.101) provides an upper bound for Eq. (7.94).

We have to evaluate now the position of the impurity. The quantity appearing in Eq. (7.94) is an operator. The impurity is modeled as a harmonic oscillator, so its state is Gaussian. Therefore it ensues

$$x = \langle x \rangle + \Delta_x = \Delta_x, \tag{7.102}$$

where we considered that, for a harmonic oscillator, the average value of the position is zero. Finally, we can state that the linear approximation underlying our analysis is fulfilled if it is satisfied that

$$\frac{k_{\mathrm{B}}T}{\hbar c}\Delta_x \ll 1. \tag{7.103}$$

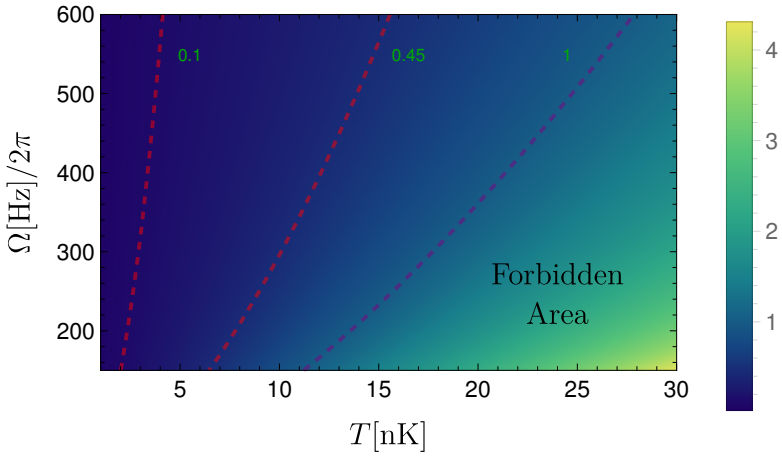

FIGURE 7.6: Behavior of $\chi^{(\mathrm{Tr})}$ [see Eq. (7.104)] as a function of the temperature and of the frequency of the trap. For $\chi^{(\mathrm{Tr})} < 1$ the linear approximation, Eq. (7.22), is appropriate for the trapped impurity. The figure refers to an impurity of K in a gas made up by Rb with a density of $n_0 = 7(\mu\mathrm{m})^{-1}$ and a coupling strength $g_{\mathrm{B}} = 2.36 \cdot 10^{-37}\mathrm{J{\cdot}m}$. The interaction strength is $\eta = 1$.

To evaluate Δ_x, and thus Eq. (7.103), we have to distinguish again the case of trapped and untrapped impurity.

For the trapped case we consider in Eq. (7.103) the fluctuation Δ_x as that given by δ_x in Eq. (7.93),

$$\chi^{(\mathrm{Tr})} \equiv \frac{k_{\mathrm{B}} T}{\hbar c} \delta_x(T, \Omega). \tag{7.104}$$

If $\chi^{(\mathrm{Tr})} < 1$ it is possible to state that the linear approximation, Eq. (7.22), is fulfilled. We plot in Fig. 7.6 the quantity in Eq. (7.104) as a function of the temperature and the trap frequency. Note that δ_x depends also on the interaction strength, but we focus on the case where $\eta = 1$. In general, as the temperature grows the position variance approaches the value predicted by the equipartition theorem, so it gets coupling-independent. At low temperature, instead, the value of the position variance approaches one at weak coupling, *i.e.* $\eta \approx 1$, while in general it is smaller (the impurity experiences genuine position squeezing). Therefore, the value of the

position variance at $\eta = 1$ represents an upper bound. Therefore, if the linear approximation is fulfilled for $\eta = 1$, it also holds for other, smaller or larger, values of η.

Figure 7.6 shows that the linear approximation for a trapped impurity is fulfilled at low temperature. Moreover, it is very well satisfied as the trap potential gets more and more steep, as pointed out also by Bonart and Cugliandolo, 2012. In particular, we see that for the value we selected to detect genuine position squeezing, *i.e.* $\Omega = 2\pi \cdot 500$ and $T \geq 2$nm the threshold in Eq. (7.104) takes a value smaller than 0.1, suggesting that the condition allowing the linear approximation is very well satisfied.

Next we consider the untrapped impurity. In this case Δ_x may be evaluated by means of the MSD in Eq. (7.79). Considering the case in which $\langle \dot{x}^2(0) \rangle = 0$, the left-hand side in Eq. (7.101) is

$$\chi^{(\mathrm{Un})} \equiv \frac{k_{\mathrm{B}} T}{\hbar c} \sqrt{\frac{\hbar \tilde{\tau}}{2 m_{\mathrm{I}}}} \frac{t \Lambda}{\alpha(\eta)}. \tag{7.105}$$

Again, in order to state that our linear approximation is satisfied the quantity in Eq. (7.105) has to be smaller than one.

In Fig. 7.7 we plotted the value of the quantity $\chi^{(\mathrm{Un})}$ introduced in Eq. (7.105). Even in this case we find that the linear approximation underlying our treatment is very well fulfilled at low-temperature. For an untrapped impurity the validity of such an approximation holds until a certain value of the time

$$t^{(\mathrm{cr})} = \frac{\hbar c}{k_{\mathrm{B}} T} \sqrt{\frac{2 m_{\mathrm{I}}}{\hbar \tilde{\tau}}} \frac{\alpha(\eta)}{\Lambda}, \tag{7.106}$$

corresponding to the instant in which the quantity in Eq. (7.6) is equal to one, *i.e.* we have

$$\chi^{(\mathrm{Un})}(t^{(\mathrm{cr})}) = 1. \tag{7.107}$$

The critical time in Eq. (7.106) is plotted in Fig. 7.8 as a function of the temperature, for different values of the interaction strength. Each line corresponds to a different value of η. Once one fixes η, the corresponding line determines the value of time and temperature for which the threshold in Eq. (7.105) is equal to one. Accordingly, above the line we have a forbidden area. Again, we find that this forbidden area is enlarged as the temperature grows, suggesting that our approximation works at low

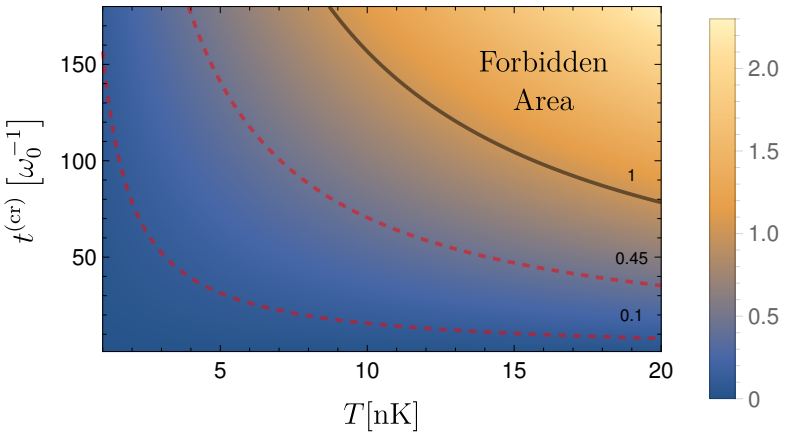

FIGURE 7.7: Behavior of $\chi^{(\mathrm{Un})}$ [see Eq. (7.105)] as a function of the temperature and of the time. For $\chi^{(\mathrm{Un})} < 1$ the linear approximation, Eq. (7.22), is appropriate for the untrapped case. The figure refers to an impurity of K in a gas made up by Rb with a density of $n_0 = 7(\mu\mathrm{m})^{-1}$ and a coupling strength $g_{\mathrm{B}} = 2.36 \cdot 10^{-37}$J·m. The interaction strength is $\eta = 1$.

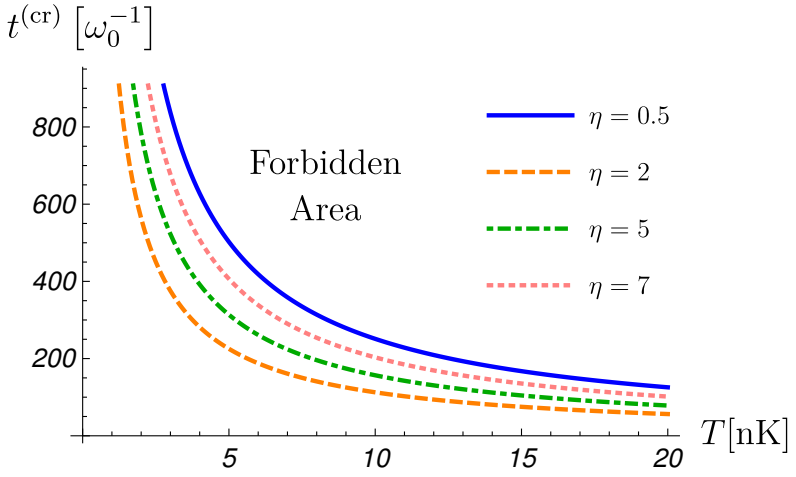

FIGURE 7.8: Critical time in Eq. (7.106) as a function of the temperature for different values of the interaction strength. Below the curves the linear approximation, Eq. (7.22), is fulfilled. The figure refers to an impurity of K in a gas made up by Rb with a density of $n_0 = 7(\mu\mathrm{m})^{-1}$ and a coupling strength $g_{\mathrm{B}} = 2.36 \cdot 10^{-37}\mathrm{J{\cdot}m}$.

temperature.

7.7 Summary

The present chapter covers a very important part of the thesis. We have applied the techniques developed in the previous chapters to a concrete physical system, evaluating quantities that have been measured in experiments. This treatment has been published by Lampo et al., 2017. Our main results are:

- The physical Hamiltonian associated to an impurity in a homogeneous gas may be expressed in the form of that of the QBM model: the impurity plays the role of the Brownian particle while the environment is represented by the surrounding Bogoliubov cloud. In general the coupling between them depends non-linearly on the impurity position, but we linearize it approaching the interaction term of the standard QBM model [Eq. (7.24)]. Very importantly we prove that this approximation is reasonable for the physical values we consider. To this end we find and evaluate that a set of validity relations (Sec. 7.6).

- Once we have the Hamiltonian, it is possible to derive the spectral density of the system [see Sec. 7.2]. We calculate such an object finding a super-ohmic behavior [Eq. (7.49)]. This form corresponds to the presence of memory effects in the dynamics of the impurity. In fact, the position particle is described by an equation of the Langevin-type, but with a dependence on its past history [Eq. (7.58)].

- We solve the equation of motion with both numerical and analytical methods by distinguishing the case where the impurity is trapped in a harmonic potential and that in which is free of any trap. In the latter we calculate the mean square displacement [Eq. (7.79)] which now is proportional to the square of time (super-diffusion). Such an effect represents a witness of memory effect on a measurable quantity.

- If the impurity is confined in a quadratic potential we detect genuine position squeezing at low temperature (Fig. 7.4). This effect

corresponds to high spatial localization of the impurity and maybe detected in experiments.

Chapter 8

Bose Polaron in an inhomogeneous trapped gas

In the current chapter we extend the analysis of the previous one to the case in which the gas is trapped by an external potential. The results we are about to present are contained in the work of Lampo et al., 2018. Here, the presence of the trap makes the gas inhomogeneous, i.e. its density exhibits a spatial dependence. In particular, by considering a harmonic trap we have a Thomas-Fermi (TF) density profile. In this context the spectrum of the Bogoliubov excitations differs from that of a homogeneous BEC, as showed by Öhberg et al., 1997; Stringari, 1996 for a BEC confined in three dimension, and by D.S. Petrov, D.M. Gangardt, and G.V. Shlyapnikov, 2004 in the particular situation of a gas in 1D, *i.e.* with the shape of tube.

Regardless of the form of the spectrum, also in this case Bogoliubov transformations permit to cast the Hamiltonian of the system in the form of that of the QBM model: still, the impurity plays the role of the Brownian particle while the environment is represented by the Bogoliubov modes. In general, the interaction term shows a non-linear dependence on the position impurity, that would lead to a dynamics characterized by a multiplicative noise and a state-dependent damping. However, if we look into the behaviour of the impurity in the middle of the BEC trap, the interaction Hamiltonian can be expressed as a linear function of the position impurity, approaching the form of traditional QBM model.

We may thus follow the procedure of the previous chapter because the behavior of the impurity in this particular regime is ruled by a quantum stochastic differential equation of the Langevin type. Again such an equation is non-local in time, *i.e.* it depends on its past history, and this may be also inferred looking into the spectral density, manifesting

a super-ohmic form. The difference with the homogeneous case is that now the spectral density exhibits a higher degree of super-ohmicity: four rather than three. This does not affect the qualitative long-time behavior of the MSD when the impurity is untrapped. In fact, if the super-ohmic character of the spectral density leads to super-diffusive behavior, the higher degree of ohmicity would suggest that the MSD is proportional to a power of the time higher than two (what emerges in the previous). Still, we find the MSD is proportional to the square of time, as in the homogeneous case.

When the impurity is trapped in a harmonic potential it oscillates collapsing in the middle of the trap. The long-time position variance is time-independent and we may repeat the analysis of the previous chapter by tuning the external parameters. We find again that the particle experiences genuine position squeezing if we explore low-temperatures by increasing the coupling.

It is important to underline that regardless of whether the impurity is trapped or not, in all the chapter we consider the situation in which the BEC is trapped. This leads to the presence of a new variable constituted by the frequency gas trap that affects the physics of the system. The study of the impurity dynamics as such a parameter varies represents the main advance of the current chapter. In particular we describe the behavior of the super-diffusion coefficients associated to an untrapped impurity when the gas trap is made more (or less) tight. Mostly, we study how the emergence of squeezing is related to the value of the gas trap frequency. We find that such en effect result to be improved by making tighter the gas trap.

8.1 Hamiltonian

We consider an impurity with mass m_{I} embedded in a Bose-Einstein condensate with N atoms of mass m_{B}. The system is described by the following Hamiltonian

$$H = H_{\mathrm{I}} + H_{\mathrm{B}} + H_{\mathrm{BB}} + H_{\mathrm{IB}}, \tag{8.1}$$

with

$$H_{\rm I} = \frac{\mathbf{p}^2}{2m_{\rm I}} + U(\mathbf{r}), \tag{8.2a}$$

$$H_{\rm B} = \int d^3\mathbf{r}\, \Psi^\dagger(\mathbf{r}) \left(\frac{\mathbf{p}_{\rm B}^2}{2m_{\rm B}} + V(\mathbf{r}) \right) \Psi(\mathbf{r}), \tag{8.2b}$$

$$H_{\rm BB} = g_{\rm B} \int d^3\mathbf{r}\, \Psi^\dagger(\mathbf{r}) \Psi^\dagger(\mathbf{r}) \Psi(\mathbf{r}) \Psi(\mathbf{r}), \tag{8.2c}$$

$$\begin{aligned} H_{\rm IB} &= g_{\rm IB} \int d\mathbf{r}_{\rm B} \Psi^\dagger(\mathbf{r}_{\rm B}) \Psi(\mathbf{r}_{\rm B}) \delta(\mathbf{r} - \mathbf{r}_{\rm B}) \\ &= g_{\rm IB} \Psi^\dagger(\mathbf{r}) \Psi(\mathbf{r}), \end{aligned} \tag{8.2d}$$

where $\mathbf{r}$ and $\mathbf{r}_{\rm B}$ denote the position coordinate of the impurity and the bosons, respectively. We assume contact interactions among the bosons and between the impurity and the bosons, with strength given by the coupling constants $g_{\rm B}$ and $g_{\rm IB}$, respectively [see Eqs. (8.2c) and (8.2d)]. The impurity is trapped in a potential $U(\mathbf{r}) = \frac{m_{\rm I}\Omega^2\mathbf{r}^2}{2}$. In this paper we discuss both the untrapped ($\Omega = 0$) and trapped cases ($\Omega > 0$). The bosons are trapped in a harmonic potential, namely the potential in Eq. (8.2c) takes the form

$$V(\mathbf{r}) = \sum_{i=1}^{3} \frac{m_{\rm B}\omega_{\rm i}^2 r_{\rm i}^2}{2}. \tag{8.3}$$

This is the crucial difference with the analysis of the previous chapter. The fact that the BEC is trapped gives rise to important consequences, both in the analytical derivation and in the results, as we will discuss throughout the rest of the paper.

In this section we express the Hamiltonian (8.1) in the form of the QBM model. We first write the field operator as the sum of the condensate state and the above-condensate part

$$\Psi = \Psi_0 + \Psi', \quad \Psi_0 \equiv \langle \Psi \rangle. \tag{8.4}$$

We replace Eq. (8.4) in the Hamiltonian (8.1) and make the BEC assumption, *i.e.* that the condensate density greatly exceeds that of the above-condensate particles. In particular this amounts to omitting the terms proportional to $(\Psi')^3$, and $(\Psi')^4$ in the resulting expressions. As showed

by Öhberg et al., 1997, one obtains

$$H_{\mathrm{BB}} + H_{\mathrm{B}} = H_0 + \int d^3\mathbf{r}\Psi'^{\dagger}(\mathbf{r})H_{\mathrm{B}}^{\mathrm{sp}}\Psi'(\mathbf{r}) \tag{8.5}$$
$$+\frac{g_{\mathrm{B}}}{2}\left[4\left|\Psi_0\left(\mathbf{r}\right)\right|^2\Psi'^{\dagger}\left(\mathbf{r}\right)\Psi'\left(\mathbf{r}\right)+\Psi_0^2\Psi'^{\dagger}(\mathbf{r})\Psi'^{\dagger}(\mathbf{r})\right]$$
$$+\frac{g_{\mathrm{B}}}{2}\left(\Psi^*\right)_0^2\Psi'(\mathbf{r})\Psi'(\mathbf{r}),$$

where

$$H_0=\int d^3\mathbf{r}\Psi_0^{\dagger}(\mathbf{r})\left[-\frac{\hbar^2}{2m_{\mathrm{B}}}\Delta+V(\mathbf{r})+\frac{g_{\mathrm{B}}}{2}\left|\Psi_0(\mathbf{r})\right|^2\right]\Psi_0, \tag{8.6}$$

and where

$$H_{\mathrm{B}}^{\mathrm{sp}}\equiv\frac{\mathbf{p}_{\mathrm{B}}^2}{2m_{\mathrm{B}}}+V(\mathbf{r}), \tag{8.7}$$

is the single-particle gas Hamiltonian [see Eq. (8.2b)]. Proceeding in a similar manner with the impurity-gas interaction, Eq. (8.2d), one gets

$$\begin{aligned}H_{\mathrm{IB}}=&g_{\mathrm{IB}}\left[\Psi_0^{\dagger}(\mathbf{r})+\Psi'^{\dagger}(\mathbf{r})\right]\left[\Psi_0(\mathbf{r})+\Psi(\mathbf{r})\right]\\ =&g_{\mathrm{IB}}\left[\left|\Psi_0(\mathbf{r})\right|^2+\Psi'^{\dagger}(\mathbf{r})\Psi_0(\mathbf{r})+\Psi'(\mathbf{r})\Psi_0^{\dagger}(\mathbf{r})\right],\end{aligned} \tag{8.8}$$

where the term proportional to the square power of the above-condensate state has been neglected.

In the QBM Hamiltonian, the environment is modeled as a set of *uncoupled* oscillators. To establish the analogy between the QBM Hamiltonian and that of the impurity immersed in a BEC, we diagonalize the part of the gas Hamiltonian, Eq. (8.5), to express it as a set of uncoupled modes. With the Bogoliubov transformation

$$\Psi'(\mathbf{r})=\sum_{\nu}\left[u_\nu(\mathbf{r})b_\nu-v_\nu^*(\mathbf{r})b_\nu^{\dagger}\right], \tag{8.9}$$

one gets to the diagonalized Hamiltonian

$$H_{\mathrm{B}}+H_{\mathrm{BB}}=H_0+\sum_{\nu}E_\nu b_\nu^{\dagger}b_\nu, \tag{8.10}$$

where E_ν is the energy of the Bogoliubov excitations, which constitute the oscillating modes of the environment dressing the impurity, and $b^{\dagger}$ (b) the related creation (destruction) operators of these modes. Under

the Bogoliubov transformations in Eq. (8.9) the interaction Hamiltonian, Eq. (8.2d), reads

$$\begin{aligned} H_{\mathrm{IB}} =& g_{\mathrm{IB}} \left[\sqrt{n_0(\mathbf{r})} \sum_{\nu} \left(u_{\nu}^{*}(\mathbf{r}) - v_{\nu}^{*}(\mathbf{r}) \right) b_{\nu}^{\dagger} + \text{c.c.} \right] \\ \equiv& g_{\mathrm{IB}} \left[\sqrt{n_0(\mathbf{r})} \sum_{\nu} f_{(\nu,-)} b_{\nu}^{\dagger} + \text{c.c.} \right] \end{aligned} \tag{8.11}$$

where we put $\Psi_0 \approx \sqrt{n_0}$.

To obtain the complete form of the Hamiltonian we need the expressions of the functions u_ν and v_ν introduced in Eq. (8.9), as well as of the energy modes in Eq. (8.10). An important difference with the homogeneous case is that, for the trapped BEC, they have to be obtained as the eigenvectors and eigenvalues of the matrix associated to the Bogoliubov-de-Gennes (BdG) equations

$$H_{\mathrm{B}}^{(sp)} u_\nu + g_{\mathrm{B}} n_0(\mathbf{r}) \left(2u_\nu - v_\nu \right) = \left(\mu + E_\nu \right) u_\nu, \tag{8.12a}$$

$$H_{\mathrm{B}}^{(sp)} u_\nu + g_{\mathrm{B}} n_0(\mathbf{r}) \left(2u_\nu - v_\nu \right) = \left(\mu - E_\nu \right) u_\nu. \tag{8.12b}$$

The solutions of the BdG equations satisfy the orthogonality condition

$$\int d\mathbf{r} \left(u_\nu u_{\nu'}^{*} - v_\nu v_{\nu}^{*} \right) = \delta_{\nu\nu'}. \tag{8.13}$$

In general, the solution of the BdG equations (8.12) does not constitute a simple problem, and often requires the employment of numerical methods. For a BEC confined in one dimension and in the TF limit, one can solve them analytically as showed in D.S. Petrov, D.M. Gangardt, and G.V. Shlyapnikov, 2004. In the current work we focus exactly on the aforementioned situation, namely a gas confined in one dimension with a TF density profile

$$n_0(x) = \frac{\mu}{g_{\mathrm{B}}} \left(1 - \frac{x^2}{R^2} \right), \quad R = \sqrt{2\mu / m_{\mathrm{B}} \omega_{\mathrm{B}}^2}, \tag{8.14}$$

where $\omega_{\rm B}$ is the trapping frequency in the direction x [see Eq. (8.3)]. Here, R is the TF radius and the chemical potential is

$$\mu = \left(\frac{3}{4\sqrt{2}} g_{\rm B} N \omega_{\rm B} \sqrt{m_{\rm B}}\right)^{2/3}. \tag{8.15}$$

Then, the solution of the BdG equations (8.12) gives the following spectrum

$$E_j = \hbar\omega_{\rm B}\sqrt{j(j+1)} \equiv \hbar\omega_j, \tag{8.16}$$

with corresponding Bogoliubov modes

$$f_{(\mathrm{j},-)} = \sqrt{\frac{j+1/2}{R}}\sqrt{\frac{2\mu}{E_j}\left[1-\left(\frac{x}{R}\right)^2\right]} L_j\left(x/R\right). \tag{8.17}$$

where $L_j(z)$ represent the Legendre polynomials and j is the integer quantum number labeling the spectrum.

Finally, we replace the expressions of the Bogoliubov modes, Eq. (8.17) in Eq. (8.11) to get the Hamiltonian of an impurity embedded in a BEC in 1D with a TF density profile,

$$H = H_{\rm I} + H_{\rm E} + H_{\rm int}, \tag{8.18}$$

with

$$H_{\rm E} = \sum_j E_j b_j^\dagger b_j, \tag{8.19}$$

and

$$\begin{aligned} H_{\rm int} &= \sum_j g_{\rm IB}\sqrt{n_0(x)} f_{(\mathrm{j},-)}(x)\left(b_j + b_j^\dagger\right) \\ &\equiv \sum_j F_j(x)\left(b_j + b_j^\dagger\right), \end{aligned} \tag{8.20}$$

Hamiltonian (8.18) is analogous to QBM Hamiltonian, where one identifies the system Hamiltonian as $H_{\rm I}$, the environment set of oscillators as $H_{\rm E}$, and the interaction between system and environment as $H_{\rm int}$. Importantly, the latter presents a non-linear dependence on the position impurity. There exist different techniques aimed to deal with the QBM model with this kind of non-linearity. For instance, one could recall the master equation treatment in the Born-Markov regime in Massignan et al., 2015,

or in the Lindblad framework Lampo et al., 2016. Beyond these approximations, it is possible to look into the non-linear Heisenberg equations derivation carried out in Barik and Ray, 2005, where a Langevin equation with a state-dependent damping and a multiplicative noise has been obtained. Moreover, there is the procedure developed by Lim et al., 2018 relying on quantum stochastic calculation, valid for the small impurity mass limit.

The problem in applying all these methods lies in the fact that the interaction Hamiltonian (8.20) presents a dependence on the position strictly constrained to the index j, *i.e.* we have a different analytical dependence on x for each value of j. To overcome this difficulty, we restrict to the regime defined by the condition $x/R \ll 1$, that is we study the dynamics of the impurity in the middle of the trap. Here, it is possible to expand the interaction term in Eq. (8.20) at the first order in x/R

$$H_{\mathrm{I}} = \sum_j \hbar g_j x \left(b_j + b_j^\dagger\right), \tag{8.21}$$

in which

$$g_j = \frac{g_{\mathrm{IB}}\mu}{\hbar\pi^{3/2}}\left[\frac{1+2j}{\hbar\omega_{\mathrm{B}}g_{\mathrm{B}}R^3}\right]^{\frac{1}{2}} \frac{\Gamma\left[\frac{1}{2}(1-j)\right]\Gamma\left[\frac{1}{2}(1+j)\right]\sin(\pi j)}{[j(j+1)]^{1/4}}. \tag{8.22}$$

This linear approximation is discussed in Sec. 8.4, where we show that such an approximation is appropriate for realistic values of the system parameters. The interaction Hamiltonian above shows a linear dependence on the positions of both the impurity and the oscillators of the bath. This is exactly the situation of the QBM model. A difference with the homogeneous gas discussed in Lampo et al., 2017 is that here the environmental variables appearing in the interaction term are the positions of the oscillators, while in the homogeneous case the variables appearing in the analogous interaction term are the momenta of the oscillators. We note here that this does not imply a qualitative change with respect to the homogeneous case, because the bath variables only play a role in the environmental self-correlation functions, which remain the same as those presented in Lampo et al., 2017.

8.2 Quantum Langevin equation

After expressing the Hamiltonian of an impurity in an inhomogeneous BEC in the form of the QBM one, we are now in the position to provide a careful quantitative description of the motion of the impurity using an open quantum systems approach. First, we write the Heisenberg equations

$$\dot{x}(t) = \frac{i}{\hbar}\left[H, x(t)\right], \quad \dot{p}(t) = \frac{i}{\hbar}\left[H, p(t)\right], \tag{8.23}$$

$$\dot{b}_k(t) = \frac{i}{\hbar}\left[H, b_k(t)\right], \quad \dot{b}_k^\dagger(t) = \frac{i}{\hbar}\left[H, b_k^\dagger(t)\right]. \tag{8.24}$$

These equations may be combined according the procedure presented by Breuer and Petruccione, 2007; Lampo et al., 2017 to derive an equation for the position impurity in the Heisenberg picture,

$$\ddot{x}(t) + \Omega^2 x(t) + \frac{\partial}{\partial t}\int_0^t \Gamma(t-s)x(s)ds = \frac{B(t)}{m_{\mathrm{I}}}. \tag{8.25}$$

Such an equation is formally identical to the Langevin one derived in the context of classical Brownian motion, and completely rules the temporal evolution of the impurity motion. At this level, the influence of the environment is contained in the term in the right hand-side

$$B(t) = \sum_j \hbar g_j (b_j^\dagger e^{-i\omega_j t} + b_j e^{+i\omega_j t}), \tag{8.26}$$

which plays the role of the stochastic noise, and in the damping kernel. Both of them depend on the spectral density. In particular the noise term fulfills the relation

$$\langle\{B(s), B(\sigma)\}\rangle = 2\hbar\nu(s-\sigma), \tag{8.27}$$

in which

$$\nu(\tau) = \int_0^\infty J(\omega)\coth\left(\frac{\hbar\omega}{2k_{\mathrm{B}}T}\right)\cos(\omega\tau)\,d\omega \tag{8.28}$$

is the noise kernel.

Therefore, the influence of the environment on the impurity motion is completely known once we exhibit an expression for the SD. This can be done analytically according the same procedure showed in the previous

chapter. In particular, one has to replace the expression of the coupling constant in Eq. (8.22) into the definition (7.34). Then, we turn the discrete sum in j into an integral in a continuous variable to get

$$J(\omega) = \frac{2g_{\mathrm{IB}}^2\mu^2}{g_{\mathrm{B}}R^3(\hbar\omega_{\mathrm{B}})^2}\left(\frac{\omega}{\omega_{\mathrm{B}}}\right)^4\theta\left(\omega-\omega_{\mathrm{B}}\right) \equiv m_{\mathrm{I}}\gamma\frac{\omega^4}{\omega_{\mathrm{B}}^3}\theta\left(\omega-\omega_{\mathrm{B}}\right), \tag{8.29}$$

with

$$\gamma = \frac{2g_{\mathrm{B}}}{m_{\mathrm{I}}\omega_{\mathrm{B}}R^3}\left(\frac{\eta\mu}{\hbar\omega_{\mathrm{B}}}\right)^2, \quad \eta = \frac{g_{\mathrm{IB}}}{g_{\mathrm{IB}}}. \tag{8.30}$$

In Eq. (8.29), $\theta\left(\omega-\omega_{\mathrm{B}}\right)$ is the Heaviside step function, representing an ultraviolet cut-off, that has been put *ad-hoc* in order to regularize the divergent character of the spectral density at high-frequency. This, however, does not play any role in the dynamics of the system at long-times, as nor the presence, neither the form, of the cut-off affects the dynamics of the impurity at long times. This can be shown by recalling the Tauberian theorem (Nixon, 1965; Feller, 1971).

Therefore, in the middle of the trap ($x \ll R$) and at long times ($\omega \ll \omega_{\mathrm{B}}$) we obtain a super-Ohmic SD. Such a particular form implies the presence of memory effects in the dynamics of the system. In fact, only if the damping kernel reduces to Dirac Delta, Eq. (8.25) acquires a local in time structure, making the evolution of the impurity position independent on its past history. Indeed, by replacing the SD, Eq. (8.29), in the definition of the damping kernel, Eq. (7.33), one gets

$$\Gamma(t) = \frac{\gamma\left[6+3\left(\omega_{\mathrm{B}}^2t^2-2\right)\cos\left(\omega_{\mathrm{B}}t\right)\right]}{t^4\omega_{\mathrm{B}}^3} \tag{8.31}$$

$$+\frac{\gamma\omega_{\mathrm{B}}t\left[\left(\omega_{\mathrm{B}}t\right)^2-6\right]\sin\left(\omega_{\mathrm{B}}t\right)}{t^4\omega_{\mathrm{B}}^3}. \tag{8.32}$$

The form of the damping kernel presented above shows that Eq. (8.25) is non-local in time and the dynamics of the impurity carries a certain amount of memory effects. We underline here an important difference with the case in which the BEC is untrapped: in that situation the spectral density is proportional to the third power of the frequency, while now it goes as the fourth one. We conclude that the presence of the trap for the

gas increases the super-Ohmic degree. This changes the details of the derivation to be developed below, in comparison with the homogeneous case.

The solution of Eq. (8.25) is

$$x(t)=G_1(t)x(0)+G_2(t)\dot{x}(0)+\frac{1}{m_{\rm I}}\int_0^t G_2(t-s)B(s)ds, \tag{8.33}$$

where the functions G_1 and G_2 are defined through their Laplace transforms

$$\mathcal{L}_z[G_1(t)] = \frac{z+\mathcal{L}_z[\Gamma(t)]}{z^2+\Omega^2+z\mathcal{L}_z[\Gamma(t)]}, \tag{8.34}$$

$$\mathcal{L}_z[G_2(t)] = \frac{1}{z^2+\Omega^2+z\mathcal{L}_z[\Gamma(t)]}, \tag{8.35}$$

and satisfy

$$G_1(0)=1, \quad \dot{G}_1(0)=0, \tag{8.36}$$

$$G_2(0)=0, \quad \dot{G}_2(0)=1. \tag{8.37}$$

The Laplace transform of the damping kernel is what carries out the properties of the environment in the solution of the position impurity equation. Recalling the definition of the damping kernel we find

$$\begin{aligned}\mathcal{L}_z[\Gamma(t)] &= \frac{1}{m_{\rm I}}\int_0^\infty dt e^{-zt}\cos(\omega t)\int_0^\infty d\omega J(\omega)/\omega \\ &= \frac{z\gamma}{\omega_{\rm B}^3}\int_0^{\omega_{\rm B}} d\omega \frac{\omega^3}{\omega^2+z^2},\end{aligned} \tag{8.38}$$

where we used the expression of the spectral density in Eq. (8.29) and the formula for the Laplace transform of the cosine

$$\int_0^\infty e^{-zt}\cos(\omega t)dt = \frac{z}{\omega^2+z^2}. \tag{8.39}$$

The integral (8.38) may be calculated straightforwardly noting that

$$\begin{aligned}\int_0^{\omega_{\rm B}} \frac{\omega^3}{\omega^2+z^2} d\omega &= \int_0^{\omega_{\rm B}} \omega \left(1 - \frac{z^2}{\omega^2+z^2}\right) d\omega \\ =&\frac{1}{2}\left[\omega_{\rm B}^2 + z^2 \log\left(\frac{z^2}{z^2+\omega^2}\right)\right]. \end{aligned} \tag{8.40}$$

In the end, replacing Eq. (8.40) into Eq. (8.38) we obtain

$$\mathcal{L}_z[\Gamma(t)] = \frac{z\gamma}{2\omega_{\rm B}^3}\left(\omega_{\rm B}^2 + z^2 \log\left[\frac{z^2}{z^2+\omega_{\rm B}^2}\right]\right). \tag{8.41}$$

Such a quantity completely fixes the kernels in Eqs. (8.34) and (8.35) and thus the temporal evolution of the impurity position in the Heisenberg picture. The problem of deriving an explicit expression for it reduces now to the inversion of the Laplace transform in Eqs. (8.34) and (8.35).

8.3 Position variance

The motion of the impurity is described by the second-order stochastic equation of the Langevin type (8.25). We proceed now to solve this equation in order to evaluate the position variance, which constitutes a measurable quantity (Catani et al., 2012). For this goal we distinguish two situations: the case where there is no trap for the impurity [$\Omega = 0$ in Eq. (8.2a)], and that in which there is a harmonic trap ($\Omega > 0$).

8.3.1 Untrapped impurity

In Sec. 8.2 we showed that the problem of solving Eq. (8.25) reduces to that of inverting the Laplace transforms (8.34) and (8.35). The former may be inverted immediately since, when $\Omega = 0$, it takes the form

$$\mathcal{L}_z[G_1(t)] = 1/z, \tag{8.42}$$

and so

$$G_1(t) = 1. \tag{8.43}$$

This result holds regardless of the properties of the environment, namely for any SD, and in fact corresponds to that derived in the homogeneous gas.

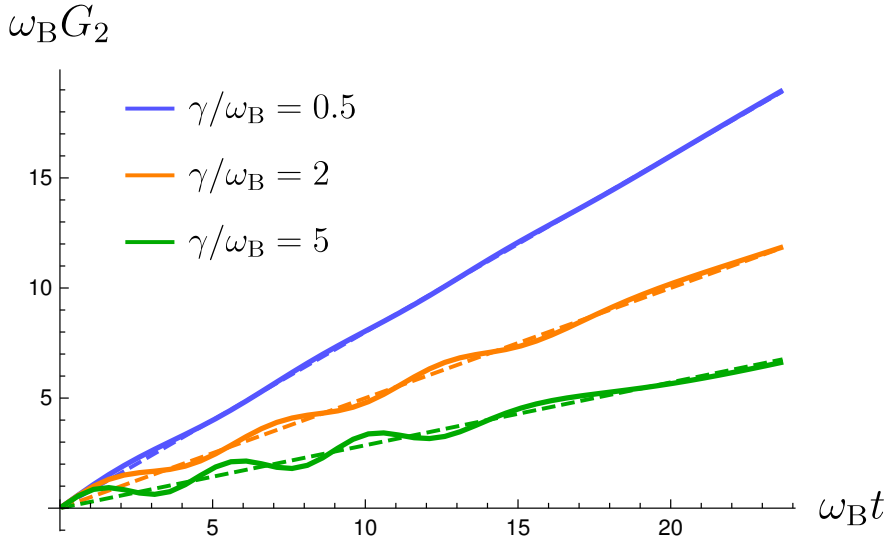

FIGURE 8.1: Time-dependence of the function G_2, defined through its Laplace transform in Eq. (8.35). The solid lines represent the numerical calculation with the Zakian algorithm. The dashed lines refer to the expression in Eq. (8.46), valid in the long-time limit.

The situation is different for Eq. (8.35), where the properties of the environment play a crucial role since they enter through the damping kernel. Here, one cannot perform the inversion of the Laplace transform analytically due the presence of the logarithm [see Eq. (8.41)]. Therefore, we recall the Zakian numerical method, discussed in Wang and Zhan, 2015. Such a method relies on the fact that the inverse Laplace transform $f(t)$ of a function $F(z)$ is approximated as

$$\tilde{f}(t) = \frac{2}{t}\sum_{j=1}^{N} \mathrm{Re}\left[k_{\mathrm{j}} F\left(\alpha_{\mathrm{j}}/t\right)\right], \tag{8.44}$$

with α_{j} and k_{j} constants that can be either complex or reals.

The expression of G_2 as a function of time is presented in Fig. 8.1. The kernel shows an oscillating behavior that diverges linearly in the long-time regime. Such a long-time limit corresponds to $\mathrm{Re}[z] \ll \omega_{\mathrm{B}}$, where the logarithm in the Laplace transform of the damping kernel, *i.e.* the second term in the right hand-side of Eq. (8.41), is negligible. If we keep only the linear term in z within such an equation it is possible to find an explicit analytical expression for the Laplace transform of G_2,

$$\mathcal{L}_z[G_2(t)] = \frac{1}{z^2(1+\frac{\gamma}{2\omega_{\mathrm{B}}})}, \tag{8.45}$$

that can be easily inverted

$$G_2 = \frac{t}{1+\frac{\gamma}{2\omega_{\mathrm{B}}}} \equiv \frac{t}{\tilde{\alpha}}. \tag{8.46}$$

This expression represents the long-time behavior of G_2 and is plotted in Fig. 8.1 for different values of the damping (dashed lines). The figure shows the agreement between the numerical solution and the long-time analytical one.

The knowledge of G_1 and G_2 fixes the structure of the impurity position operator, providing a description of the motion of the particle. The expression for G_2 in Eq. (8.46) induces a ballistic term in the time-evolution of the impurity position. This means that the impurity runs-away from its initial position. Such a behavior can be characterized in a quantitative manner by means of the mean square displacement (MSD),

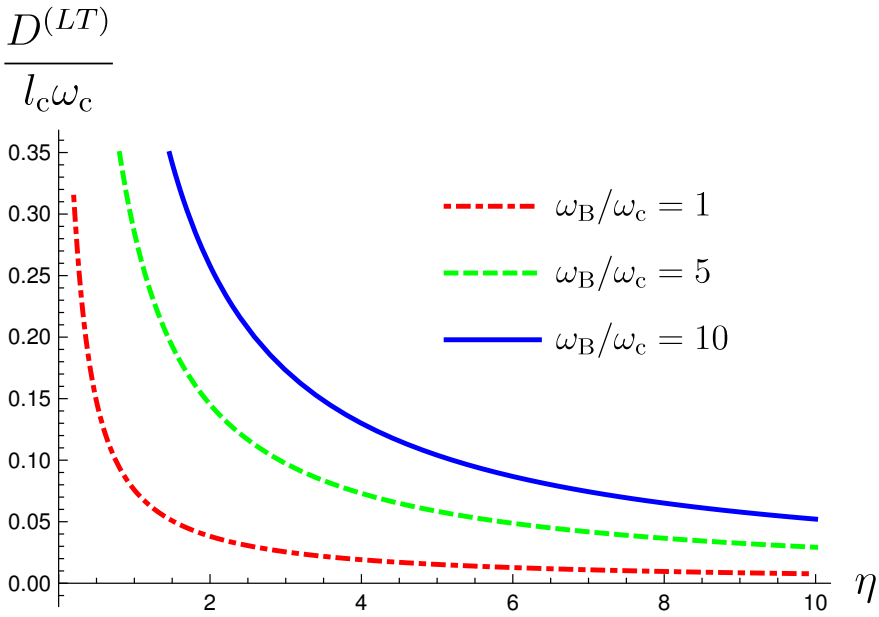

FIGURE 8.2: Super-diffusion coefficient in Eq. (8.51) as a function of the interaction strength for different values of the gas trap frequency. We present the results for an impurity of Yb embedded in a Rb gas of $N = 50000$ atoms with coupling strength $g_B = 10^{-38}\text{J} \cdot \text{m}$. In this context the units of frequency are $\omega_c = \frac{m_1 g_B^2}{\hbar^3}$, while the units of the length are $l_c = \frac{\hbar^2}{m_1 g_B}$.

defined as

$$\mathrm{MSD}(t) = \langle [x(t) - x(0)]^2 \rangle. \tag{8.47}$$

In the long-time limit it is possible write

$$\begin{aligned}\mathrm{MSD}(t) = &\left(\frac{t}{\tilde{\alpha}}\right)^2 \langle \dot{x}(0)^2 \rangle \\ &+ \frac{1}{2\left(\tilde{\alpha} m_{\mathrm{I}}\right)^2} \int_0^t ds \int_0^t d\sigma (t-s)(t-\sigma) \langle \{B(s), B(\sigma)\} \rangle,\end{aligned} \tag{8.48}$$

where we considered a factorizing initial state $\rho(t) = \rho_S(0) \otimes \rho_B$. The initial conditions of the impurity and bath oscillators are then uncorrelated. Then, averages of the form $\langle \dot{x}(0) B(s) \rangle$ vanish. The integral in the second line of Eq. (8.48) can be solved recalling the expression for the two-time correlation function of the noise term (8.27) and that for the noise kernel (8.28). Here, the hyperbolic cotangent can be approximated in two limits: (i) in the zero-temperature limit, where it can be approximated to one; and (ii) in the high-temperature limit, where it can be approximated to the inverse of its argument. In these two limits we have, respectively,

$$\mathrm{MSD}^{(LT)}(t) = \left[\langle \dot{x}(0)^2 \rangle + \frac{\hbar \gamma}{3 m_{\mathrm{I}}} \right] (t/\tilde{\alpha})^2 , \tag{8.49}$$

$$\mathrm{MSD}^{(HT)}(t) = \left[\langle \dot{x}(0)^2 \rangle + \frac{k_{\mathrm{B}} T \gamma}{m_{\mathrm{I}} \omega_{\mathrm{B}}} \right] (t/\tilde{\alpha})^2 . \tag{8.50}$$

In both cases, the MSD is proportional to the square of time. This is a consequence of the super-Ohmic form of the SD, and can be considered as a witness of memory effects. The dependence on time is the same as for the homogeneous case. This is due to the fact that, in the long-time limit, the damping kernel and hence G_2 approaches the same function. Importantly, for a trapped BEC the diffusion coefficients exhibit a different dependence on the system parameters. This is very relevant for the experimental validation of the current theory. In Fig. 8.2 we plot the super-diffusion coefficient

$$D^{(LT)} = \frac{\hbar \gamma}{3 m_{\mathrm{I}} \tilde{\alpha}}, \tag{8.51}$$

related to the MSD in the low-temperature limit. Such a coefficient can be interpreted as the average of the square of the speed with which the

impurity runs away. The picture shows that the quantity in Eq. (8.51) decreases as the interaction strength grows. This implies that the gas acts as a damper on the motion of the impurity. Surprisingly, the value of the super-diffusion coefficients takes larger values as the gas trap frequency grows. One has to note that, as $\omega_{\rm B}$ grows, the density of the gas increases as well, and therefore the number of collisions yielding the Brownian motion also grows. The study of the super-diffusion coefficient at high-temperature shows the same behavior.

8.3.2 Harmonically trapped impurity

We now study the dynamics of the impurity when it is externally trapped, *i.e.* we look into the case in which $\Omega > 0$. In this case the inversion of the Laplace transforms constitutes a difficult task and it is not immediate to get an analytical explicit expression even at long-time. We proceed so by employing the numerical Zakian method introduced above. In Fig. 8.3 we show the functions G_1 and G_2, where one can observe an oscillating behavior in both cases, which gets damped for long times. This damping of the oscillation implies that the contribution of the initial condition vanishes in the long-time limit. Also, this damping implies that the impurity reaches an equilibrium state where it sits on average on the center of the trap, and its position and momentum variances are independent of time. Thus, in the long-time limit, the variances can be represented by

$$\langle x^2\rangle = \frac{\hbar}{2\pi}\int_{-\omega_{\rm B}}^{+\omega_{\rm B}} d\omega \coth\left(\hbar\omega/2k_{\rm B}T\right)\tilde{\chi}''(\omega), \tag{8.52}$$

$$\langle p^2\rangle = \frac{\hbar m_{\rm I}^2}{2\pi}\int_{-\omega_{\rm B}}^{+\omega_{\rm B}} \omega^2 d\omega \coth\left(\hbar\omega/2k_{\rm B}T\right)\tilde{\chi}''(\omega), \tag{8.53}$$

where

$$\tilde{\chi}''(\omega) = \frac{1}{m_{\rm I}}\frac{\zeta(\omega)\omega}{\left[\omega\zeta(\omega)\right]^2 + \left[\Omega^2 - \omega^2 + \omega\theta(\omega)\right]^2}, \tag{8.54}$$

is the response function, and

$$\zeta\left(\omega\right) = \mathrm{Re}\{\mathcal{L}_{\tilde{z}}\left[\Gamma(t)\right]\}, \quad \theta\left(\omega\right) = \mathrm{Im}\{\mathcal{L}_{\tilde{z}}\left[\Gamma(t)\right]\}. \tag{8.55}$$

with $\tilde{z} = -i\omega + 0^+$. The expression in Eq. (8.52) can be obtained directly by the solution of the Heisenberg equations in Eq. (8.33), according the

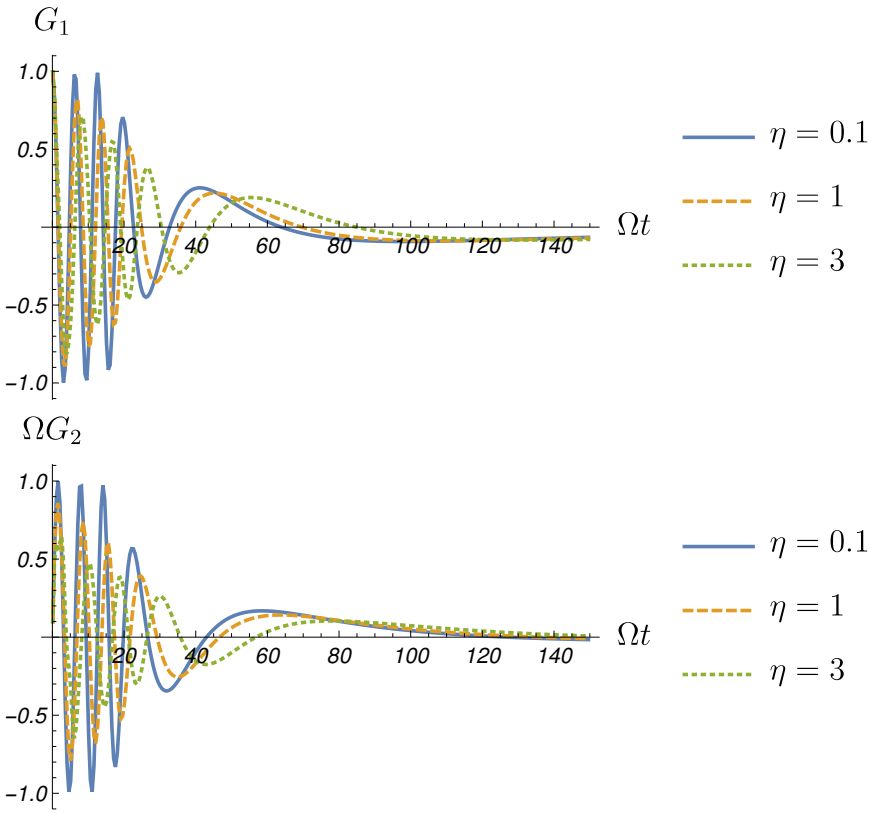

FIGURE 8.3: Time-dependence of the function G_1 (top) and G_2 (bottom), defined through the Laplace transforms in Eqs. (8.34) and (8.35), respectively. The plots refer to an impurity of Yb in a trap with a frequency $\Omega = 2\pi \cdot 200$ Hz, embedded in a Rb gas of $N = 5000$ atoms with trap frequency $\omega_B = 2\pi \cdot 800$ Hz and coupling strength $g_B = 0.5 \cdot 10^{-37}$ J·m.

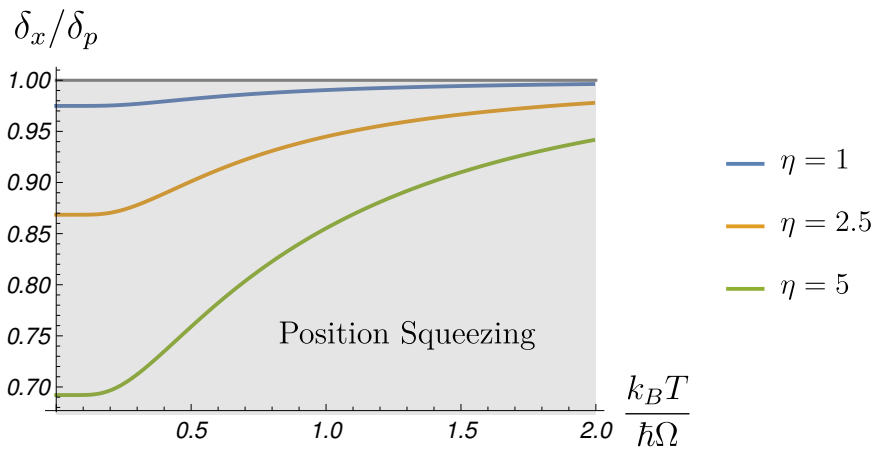

FIGURE 8.4: Temperature dependence of the ratio δ_p/δ_p between the variances introduced in Eq. (8.56). The plot refers to an impurity of Yb in a trap with a frequency $\Omega = 2\pi \cdot 50$ Hz, embedded in a Rb gas of $N = 5000$ atoms with trap frequency $\omega_{\rm B} = 2\pi \cdot 500$ Hz and coupling strength $g_{\rm B} = 0.6 \cdot 10^{-38}$ J·m.

procedure presented for a homogeneous case, and corresponds to the contribution provided by the stochastic noise.

We next study the dependence of the position and momentum variances, Eqs. (8.52) and (8.53), on the system parameters, such as temperature and coupling strength. These parameteres can be tuned in experiments. To this end, we recall the dimensionless variables

$$\delta_x = \sqrt{\frac{2m_{\rm I}\Omega\langle x^2\rangle}{\hbar}}, \quad \delta_p = \sqrt{\frac{2\langle p^2\rangle}{m_{\rm I}\hbar\Omega}}, \tag{8.56}$$

in terms of which the Heisenberg principle reads as $\delta_x\delta_p \geq 1$. In Fig. 8.4 we study the behavior of the ratio δ_x/δ_p as a function of the temperature for different values of the coupling strength. This gives the eccentricity of the uncertainty ellipse. Such an ellipse takes the form of a circle at high-temperature, *i.e.* $\delta_x \approx \delta_p$, for different values of the coupling strength. Precisely, it approaches the circular Gibbs-Boltzmann distribution with $\delta_x = \delta_p \sim \sqrt{T}$. At low temperature, instead, the uncertainties ellipse exhibits position squeezing ($\delta_x < \delta_p$), that is enhanced as the coupling

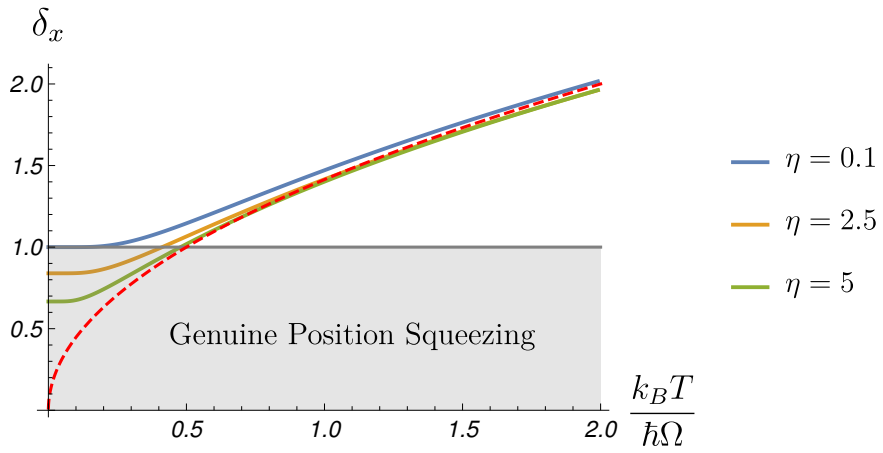

FIGURE 8.5: Temperature dependence of the position variance introduced in Eq. (8.56), for different values of the coupling strength. The plot refers to an impurity of Yb in a trap with a frequency $\Omega = 2\pi \cdot 200$ Hz, embedded in a Rb gas of $N = 5000$ atoms with trap frequency $\omega_B = 2\pi \cdot 800$ Hz and coupling strength $g_B = 0.5 \cdot 10^{-37}$ J·m. The red dashed line represents the function $\sqrt{2T}$, related to the equipartition theorem.

strength increases. In particular, exploring lower values of the temperature the impurity experiences *genuine position squeezing*, *i.e.* we detect $\delta_x < 1$, as shown in Fig. 8.5. The position variance approaches a value smaller than that associated to the Heisenberg principle. This implies that, in this regime, the particle shows less quantum fluctuations in space than in momentum. In plain words, the particle is so localized in space, that its position can be measured with an uncertainty which is smaller than that fixed by the Heisenberg principle. This effect is improved by increasing the value of the coupling strength, and in the regime of very low temperatures. Note that in the opposite limit, namely at high temperature, the position variance follows the behavior predicted by the equipartition theorem, in agreement with the fact that the uncertainties ellipse approaches the Gibbs-Boltzmann distribution. We underline that in all the situations we described Heisenberg uncertainty principle is fulfilled at any time and for each values of the system parameters, even when the particle experiences genuine position squeezing. This may be

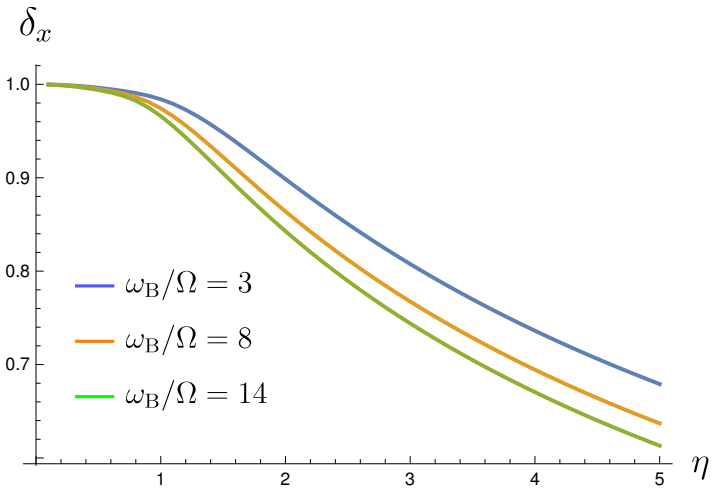

FIGURE 8.6: Position variance introduced in Eq. (8.56) as a function of the coupling strength, for different values of the gas trap frequency, in the low temperature regime. The plot refers to an impurity of Yb in a trap with a frequency $\Omega = 2\pi \cdot 200$ Hz, embedded in a Rb gas of $N = 5000$ atoms with trap frequency $\omega_B = 2\pi \cdot 800$ Hz and coupling strength $g_B = 0.5 \cdot 10^{-37}$ J·m.

checked quickly by evaluating the product between position and momentum variances.

In comparison with the squeezing predicted for the homogeneous gas, for the inhomogeneous case, one has an extra dependence on the additional parameter, the trapping frequency. This sets the possibility of using the BEC trapping frequency to enhance or inhibit the squeezing. In Fig. 8.6 we present the position variance as a function of the coupling for several values of the gas trap frequency, in the low-temperature regime. At weak coupling the gas trap does not play any role and the position variance is approximately equal to one, in agreement with the fact that the impurity approaches the free harmonic oscillator dynamics, collapsing in the ground state ($\delta_x = \delta_p = 1$) in the zero-temperature limit. As the coupling grows the position variance gets sensitive to the trap of the BEC and we see that genuine position squeezing is enhanced as the BEC trap frequency is made tighter. Of course, the dependence on the gas trap frequency is negligible at high-temperature, since in this regime the

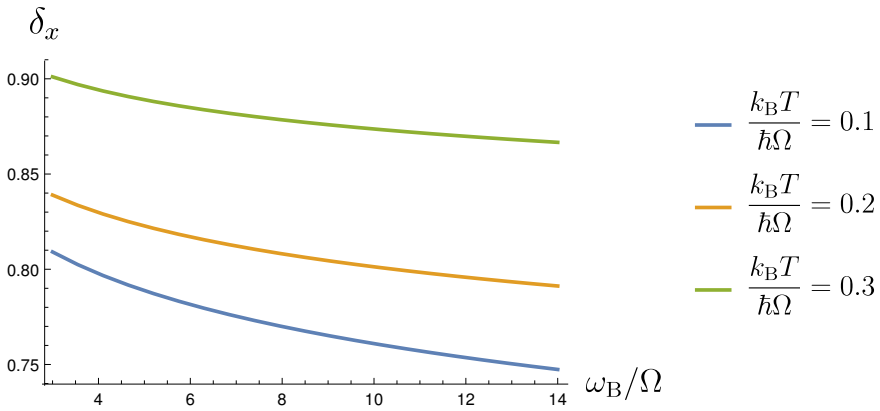

FIGURE 8.7: Position variance in Eq. (8.56) as a function of the gas trap frequency at several different values of the temperature. The plot refers to an impurity of Yb in a trap with a frequency $\Omega = 2\pi \cdot 200$ Hz, embedded in a Rb gas of $N = 5000$ atoms with trap frequency $\omega_B = 2\pi \cdot 800$ Hz and coupling strength $g_B = 0.5 \cdot 10^{-37}$ J·m.

equilibrium correlation functions get independent on the coupling. This may be seen in Fig. 8.7 where we note that, as the temperature grows the position variance approaches a constant value (constant with respect of the frequency) equal to that predicted by the equipartition theorem, in agreement with the behavior presented in Fig. 8.5.

8.4 Validity condition

The results presented for both a trapped and untrapped impurity have been derived by approximating the interaction Hamiltonian in Eq. (8.20) as a linear function of the position impurity. Such a linear expansion is valid in the middle of the trap, *i.e.* when

$$x \ll R \tag{8.57}$$

In this part of the document we study the validity of the condition (8.57) as the parameters of the system vary. For this goal we distinguish the situation where the impurity is trapped ($\Omega > 0$) and that in which it is untrapped ($\Omega = 0$).

For the trapped impurity, in general, the condition in Eq. (8.57) may be expressed as

$$x \approx \langle x \rangle + \delta_x = \Delta_x \ll R, \tag{8.58}$$

where Δ_x is the Gaussian deviation of the position from its average value. At low temperature such a condition is usually fulfilled because the position variance of the impurity achieves very low values, since the particle experiences squeezing. In order to evaluate Eq. (8.58) we recall the values acquired by the dimensionless variance δ_x. For instance, for the system parameters used in Fig. 8.5, it turns

$$\delta_x \ll (R/a_{\mathrm{HO}}) \lesssim 11, \tag{8.59}$$

where $a_{\mathrm{HO}} = \sqrt{\hbar/m_{\mathrm{I}}\Omega}$ is the impurity harmonic oscillator length.

At high-temperature instead, the position variance approaches the behavior predicted by the equipartition theorem, *i.e.*

$$\delta_x \approx \sqrt{\frac{2k_{\mathrm{B}}T}{m_{\mathrm{I}}\Omega^2}}. \tag{8.60}$$

Accordingly, the condition in Eq. (8.58) induces maximum acceptable temperature

$$T_{\mathrm{crit}} = m_{\mathrm{I}}\Omega^2 R^2/k_{\mathrm{B}}. \tag{8.61}$$

In particular, for the values of the physical quantities employed in Fig. 8.5

$$\frac{k_{\mathrm{B}}T_{\mathrm{crit}}}{m_{\mathrm{I}}\Omega^2 a_{\mathrm{HO}}^2} \lesssim 122. \tag{8.62}$$

We now study the validity condition in Eq. (8.58) for an untrapped impurity. In this case it may be expressed as

$$\mathrm{MSD}(t) \ll R^2, \tag{8.63}$$

inducing a constraint on the time and on the interaction strength. Precisely, replacing Eq. (8.49) in Eq. (8.63), we obtain, in the particular case in which $\langle \dot{x}^2(0) \rangle = 0$, that the linear approximation when $\Omega = 0$ is provided

$$\frac{1}{3\tilde{\alpha}^2}\left(\frac{\hbar\gamma(\eta)}{m_{\mathrm{I}}}\right)\left(\frac{t}{R}\right)^2 \ll 1. \tag{8.64}$$

The left hand-side of Eq. (8.64) is plotted in Fig. 8.8 as a function of the interaction strength and the time. The area on the right of the black dashed

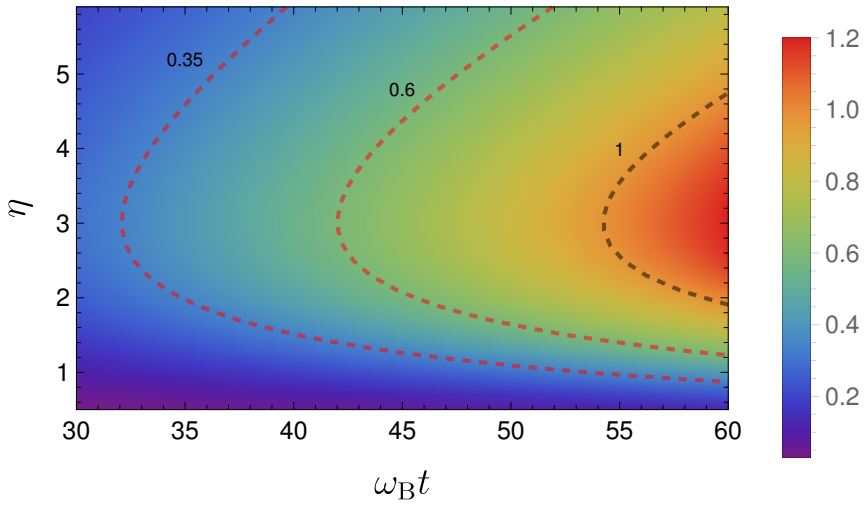

FIGURE 8.8: Validity condition in Eq. (8.64) for an untrapped impurity of Yb in a gas made up by $N = 5000$ atoms of K with a coupling strength $g_{\mathrm{B}} = 0.5 \cdot 10^{-37}$J·m, trapped in a harmonic potential with $\omega_{\mathrm{B}} = 2\pi \cdot 800$ Hz.

line is forbidden because the quantity we plotted gets larger than one. The validity condition in the high-temperature regime is formally equivalent, apart from a factor $k_{\mathrm{B}}T/\hbar\omega_{\mathrm{B}}$ multiplying the left hand-side, inducing a constraint also on the temperature.

8.5 Summary

We investigated the physics of an impurity in a trapped BEC by means of open quantum systems techniques. Here there are the main results

- Also in this case it is possible to express the Hamiltonian of the system in the form of that of QBM. In general the coupling is non-linear but it may be approximated as a linear function [see Eq. (8.21)] of the position if we restrict to the dynamics in the middle of the trap. The validity of such a linear approximation is discussed in Sec. 8.4. In this case the same situation of the QBM model occurs and we can repeat the same analysis of the previous chapter.

- We calculate the spectral density detecting again a super-ohmic behavior. By the way, while for a homogeneous gas such an object is proportional to the third power of the frequency, for a trapped one we have the fourth power [Eq. (8.29)].
- Nevertheless, the MSD still exhibits a dependence on the square of time, as well as in the homogeneous case [Eq. (8.49)]. We find that the super-diffusion coefficient increases as the frequency trap grows (Fig. 8.2).
- Still, the particle exhibits genuine position squeezing at low temperature. In the particular context of an inhomogeneous BEC we find that as its trap frequency grows the impurity squeezing is maximized (Fig. 8.6).

Chapter 9

Conclusions and perspectives

Main Conclusions

In this thesis we presented possible extensions, and consequent applications, of quantum Brownian motion, that represents a paradigmatic model of open quantum system. Mainly, we looked into the possibility to generalize the current model to a situation in which the coupling between the particle and the bath depends in a non-linear manner on the position of the former. In this way we aimed to approach the physics of a system interacting with an inhomgeneous environment, *i.e.* an environment with a space-dependent density, where state-dependent damping and diffusion occur. In particular we focused on the situation in which the interaction Hamiltonian depends quadratically on the particle position.

In both the linear [Eq. (3.4)] and quadratic [Eq. (4.3)] case, the main point of the analysis has been the study of the stationary state of the Brownian particle, performed with different techniques. In chapters 3 and 4, where the dynamics of the system was treated by means of a Born-Markov master equation, we detected the presence of genuine position squeezing, *i.e.* the variance of the particle takes a value smaller than that related to the Heisenberg principle. Such an effect, emerging at low temperature and for large values of the coupling, is very important because it corresponds to high spatial localization of the particle. Accordingly, the subsequent work has been developed in order to improve the analysis of the stationary state and so the squeezing detection, especially in the attempt to look for it in experimentally realistic systems.

This task cannot be performed correctly in the Born-Markov framework. For both linear and non-linear coupling, indeed, we found that, as the temperature decreases and the coupling grows, forbidden areas

emerge with such an approach. These are associated to regimes of parameters where the Heisenberg principle is not fulfilled, or the fluctuations take complex values, or the central particle experiences instability. The presence of forbidden zones makes impossible a correct study of the low-temperature limit and so of genuine position squeezing effect, constituting one of the main goals of the work. We recalled so several alternative techniques to overcame this pathology.

The first method we considered (see chapter 5) was based on a Lindblad master equation, *i.e.* a master equation constructed in order to preserve the positivity of its solution, and so Heisenberg principle, at any time (Appendix C). It is well known that the master equation of quantum Brownian motion cannot be cast in this form. We thus proposed a Lindblad equation as close as possible to the original one studied in chapter 3. In particular in the linear case the difference with the microscopic Born-Markov master equation is constituted just by one extra term.

We analyzed the effect of such a new term on the dynamics of the system, focusing again on the description of its stationary state in the phase-space. Here, this state may be described by means of a Gaussian Wigner function, which now is very well defined for each value of temperature and coupling strength: no forbidden areas occur. We studied how the geometrical configuration of the Gaussian stationary state changes by tuning these parameters. In particular, we found that the extra-term ensuring the Lindblad form of the master equation yields a rotation of its stationary solution in the phase-space. Moreover, we highlighted the parameters regime where the particle experiences genuine position squeezing, with respect to the rotated main axes.

Then, we moved such an analysis to the case in which the interaction term depends quadratically on the particle position. Here, the corresponding Lindblad equation differs from the original Born-Markov one for a few extra terms. In the Wigner representation such a Lindbald master equation takes the form of a functional differential equation, including derivatives of order higher than two. Accordingly, the Gaussian ansatz for its solution just constitutes an approximation. We proceeded by retaining the Gaussian form for the stationary state and treating the high order terms by means of the Wick theorem. For this purpose it is important to state that such an approximation does not alter the Lindblad character of a master equation, and so it does not yield any violation of the Heisenberg principle, regardless of whether it is performed on the

equations for the moments or directly on the Lindblad equation. We developed this demonstration in Appendix D starting from a master equation related to a Lindblad operator which is just quadratic in the creation and annihilation operators, because it is enough to cover the situation analyzed in Sec. 5.2. In general, one could extend the proof to equations associated to Lindblad operators containing n^{th} powers of creation and annihilation operators. This, to the best of our knowledge, has never been shown and constitutes an interesting motivation for future projects. Also, a generalization of this proof to Lindblad equations for fermionic systems (Kraus et al., 2009) is possible and interesting.

However, in contrast to the linear case, we do not find a noticeable rotation at low temperature in the quadratic one, nor a high degree of squeezing. We would expect to observe this at larger values of the interaction strength, as in the case of linear coupling. Nevertheless, for larger values of the damping constant it is not straightforward to determine the stationary solution of the master equation. Moreover, for larger values of the interaction strength the Gaussian ansatz may fail to approximate any stationary state (Fig. 5.9).

Our procedure of adding extra terms to the Born-Markov master equation derived in chapters 3 and 4, so that the resulting equation is in a Lindblad form, is just one of the ways to obtain a Markovian dissipative equation. Other approaches have been presented, e.g., in the works of Taj and Rossi, 2008; Pepe et al., 2012. Moreover, for Gaussian dynamics an exact (non-Markovian) closed master equation with time dependent coefficients can be derived (Diósi and Ferialdi, 2014; Ferialdi, 2016; Carlesso and Bassi, 2016). Another possible perspective is to derive a Lindblad equation describing quantum Brownian motion with a general class of couplings, and study its various limiting behaviors, in particular the small mass limit of the Brownian particle.

The method which we used to treat the Lindblad equation in this manuscript is not the only suitable one. Another possible manner to solve this kind of equations, and in particular to characterize the stationary solution has been presented by Englert, Naraschewski, and Schenzle, 1994. The core of this procedure is turning Lindblad equations into partial first-order differential equations for a phase-space distribution which generalizes well-known ones such as the Wigner function. The main point lies in removing the evolution generated by the free Hamiltonian by including it in the interaction representation. Accordingly,

the time dependence of the distribution originates solely from the interaction term. Although the interaction picture adopted by Englert, Naraschewski, and Schenzle, 1994 could be used in the context we are treating, its usefulness is not guaranteed. In fact, the interaction picture represents a suitable tool when the free part of the Hamiltonian describes a dynamics much faster than that induced by the interaction term. In general this is not the case for the Brownian motion of a trapped particle, where the time scales related to both processes can approach the same order of magnitude. On the other hand, employing this method is a very interesting task, which maybe can allow us to go beyond the Gaussian approximation underlying Sec. (5.2).

Nevertheless, the Lindblad approach we considered has a problem. Lindblad equations we studied cannot be derived from a microscopic Hamiltonian model. This is a problem, especially in the attempt of applying quantum Brownian motion model to concrete real systems. There are other methods to correct the Heisenberg principle violations. The Born-Markov equations derived in chapters 3 and 4 are based on a second order perturbative master equations in the bath-particle coupling constant. Going to higher orders permits one, in principle, to get rid of the violations of the Heisenberg relations. This task can be pursued by means of the time-convolutionless method presented by Breuer and Petruccione, 2007. An advantage of this approach is that the resulting equation incorporates non-Markovian effects. The implementation of these techniques constitutes a future possible perspective. Nevertheless, since the master equation arises from a perturbative expansion, it does not allow to investigate the strong coupling regime $\gamma > \Omega$, where cooling and squeezing effects are expected to be stronger.

We looked so into a treatment of the quantum Brownian motion in terms of Heisenberg equations. This way is particularly convenient to evaluate the correlations functions, especially the position variance, and so to look for genuine position squeezing. One could also consider a path integral treatment, allowing to include the situation in which the initial global state is not separable. However, such method could in general be very laborious, while for a first approach Heisenberg equations constitute an easy and almost complete tool.

This has been the subject of chapter 6 where we proved that such a formalism preserves Heisenberg principle. Then, in chapter 7 we apply such method to the concrete case of an impurity in a Bose-Einstein

condensate (Bose Polaron). This is possible because the physical Hamiltonian of such a system may be cast in the form of that of the quantum Brownian motion model (8.1). In this new framework the impurity plays the role of the Brownian particle while the environment is constituted by the Bogoliubov excitations of the atoms of the gas. In principle the resulting interaction Hamiltonian manifests a non-linear dependence on the impurity position, and this was the motivation for our study of the non-linear quantum Brownian motion pursued in chapters 4 and 5. However, we showed in Sec. 7.6 that for the realistic values of the physical quantity we aim to treat a linear approximation is appropriate. We approach so the same situation of the standard quantum Brownian motion model.

We describe the dynamics of the impurity by means of a stochastic differential equation constituting the quantum counterpart of the Langevin one for classical Brownian motion [Eq. (2.18)]. The main difference with the original Langevin equation is that now, for the concrete case of the Bose polaron, it is non local in time, *i.e.* it depends on its past history. This may be inferred by the form of the spectral density, that has been calculated in Sec. 7.2. In fact, once one knows the Hamiltonian it is possible to calculate the spectral density, embodying the information about the environment. For the Bose polaron, such an object, shows the form a super-ohmic behavior, leading to the presence of memory effects in the dynamics of the impurity.

We solved the Langevin-type equation for the impurity, with both numerical and analytical methods. For this goal we distinguished the situation where the impurity is trapped in a harmonic potential and that where it is free of any trap. In the latter case the impurity runs away from the initial position, and the solution of the equation of motion exhibits a ballistic term. The mean square displacement permits to characterize in a quantitative manner such a behavior. Precisely, at long-time, it is proportional to the square of time (super-diffusive behavior). This is a consequence of the presence of memory effects in the dynamics of the system. In fact, in chapter 6 the same calculation was performed for an ohmic spectral density, which we proved to be associated to absence of memory effects, and this leads to a normal diffusive behavior, as in the classical case. Thus the super-diffusive behavior mentioned above constitutes a witness of memory effects on measurable quantity. The presence of memory effects has also been related by Guarnieri, Uchiyama, and Vacchini, 2016 to a back-flow of energy, directed from the environment to the impurity. We evaluated the average of energy for an untrapped impurity

as a function of the time, and we found a non-monotonic behavior: the impurity does not just release energy to the environment (dissipation), but also acquires energy from it. It is an open question to understand if such a back-flow of energy may be employed as a resource for quantum technologies.

When the impurity is trapped in a harmonic potential, it reaches an equilibrium states localized in average in the middle of the trap. In the long-time limit the contribution on the initial condition vanishes and the position variance gets time-independent. We may study its behavior by tuning the system parameters such as temperature and coupling-strength. We found genuine position squeezing for realistic values of the physical quantity of the system. This effect corresponds to high spatial localization of the impurity, namely to a good knowledge of the position, and now, in the context of polaron may be detected in experiments.

The analysis of the Bose polaron through the quantum Brownian motion model in chapter 7 referred to the situation in which the impurity was embedded in a homogeneous gas, *i.e.* a gas with an uniform density. In chapter 8 we extended the relevant experimental case of a gas confined in a trap. Here the presence of the trap makes the gas inhomogeneous, namely it induces a space-dependence in the density profile. Precisely, we considered a gas confined in a harmonic trap, that leads to a Thomas-Fermi profile. This alters the spectrum of the excitations constituting the environment around the impurity, and so the form of the impurity-bath coupling constants. Therefore, the form of the spectral density changes too. We have still a super-ohmic function, but with a higher degree of super-ohmicity: four, rather than three. However, the calculation for the mean square displacement in absence of trap (we mean the impurity trap) still leads to a quadratic dependence on time. It is important to underline that, although we do not consider any potential for the impurity, this is still subject to trap of the gas. Such a trap affects the behavior of the central particle. In particular we find that the super-diffusion coefficient increases as the frequency associated to trap harmonic potential grows. The study of the context in which the impurity is in a harmonic trap still lead to the emergence of squeezing. In the context of a trapped BEC we find that such an effect result to be optimized if we consider a tighter gas trap.

Main Perspectives

Squeezed soliton

We highlight that the procedure we developed in this work can be exported to others ultracold gases systems. For instance, Efimkin, Hofmann, and Galitski, 2016 proved that the dynamics of a bright soliton in a superfluid in one dimension is described by an equation showing the same form of that in Eq. (7.58). The spectral density for the system is in some circumstances proportional to the third power of the frequency of the Bogoliubov modes, as well as for an impurity in a homogeneous gas. Accordingly one may apply the techniques presented in chapters 7 and 8 and study the stationary state of the bright soliton. In particular one could wonder if also the bright soliton experiences genuine position squeezing at low-temperature.

Polaron thermometer

The detection of genuine position squeezing for a real concrete system, such as an impurity in a Bose-Einstein condensate, represents an important result of the current thesis. Squeezing effect has important applications in quantum metrology and its emergence in a realistic system suggests interesting perspectives for the development of quantum technologies. For instance it is possible to study new protocols for quantum probing, where one aims to extract properties of a quantum system by means of a probe. Here it is possible to employ the impurity as a probe in order to infer characteristics of the surrounding gas. In particular, motivated by the recent advances in quantum thermometry one could look into the temperature of the gas. So, an important consequences of the present thesis is the possibility of creating a minimally-disturbing method to evaluate temperature fluctuations. This issue has been treated in the work of Mehboudi et al., 2018

Two impurities in a BEC

Beyond the squeezing issue, the derivation of a motion equation associated to the dynamics of an impurity may be extended to the so-called bipolaron problem, namely a system compound by two particles in a BEC. Particularly one could look into the very interesting problem of whether the presence of the BEC induces an interaction between the two

impurities. This self-induced interaction results to be a very interesting effects in view of the possibility of generating entanglement. Such a problem has been developed in the work of Charalambous et al., 2018.

Impurity physics in a two species gas

One may also go through the specular point of view, namely to consider an impurity in a two-species gas, which constitutes an experimental feasible system. In the open quantum systems framework such a problem may be treated by extending the quantum Brownian motion model to the situation in which the central particle interacts with two environment. It is possible so to apply the procedure developed in the current thesis to study the physics of the impurity in a double-bath of Bogoliubov modes. Precisely one could still look for squeezing effect and the possibility to construct a thermometer.

Non-Markovianity in ultracold gases

Another important result of the current thesis is the detection of the non-Markovian character of the Bose polaron physics. In our framework, non-Markovianity arises because of the super-ohmic form of the spectral density, leading to a non-local in time motion equation for the impurity. Recently, the control and manipulation of non-Markovian effects attracted a lot of attention in the open quantum systems community, especially because of the analysis of the relation with the thermodynamical properties, in the context of the design of new devices in quantum technologies. We already stated that in some circumstances a non-Markovian dynamics is associated to a back-flow of energy, from the environment to the central system. Moreover, there is a lot of interest in the study of the possibility to extract work form the correlations with the past history. The detection of non-Markovianity in a concrete real system, such as an impurity in a BEC, opens the possibility to propose experiments to treat the above mentioned issues.

Quantum foundations experiments with ultracold gases

In general, the possibility to employ quantum Brownian motion to investigate the physics of an impurity in a BEC opens a wide range of chances for testing in a concrete physical system the multitude of effects detected

for the present model at an abstract level. For instance, Maniscalco, Piilo, and Suominen, 2006 pointed out the emergence of Zeno and anti-Zeno effect for the quantum Brownian motion. We wonder if is it possible to reveal such an effect for an impurity in a (homogeneous and inhomogeneous) gas. Similarly, one could also propose an experiment with ultracold gases to test the emergence of spectrum broadcast structure for the Bose polaron detected by Tuziemski and Korbicz, 2015 and Galve, Zambrini, and Maniscalco, 2016.

Smoluchowski-Kramers limit

Another interesting question concerns the Smoluchowski-Kramers (SK) limit Smoluchowski, 1916; Kramers, 1940, which can be considered as a regime of over-damped quantum Brownian motion, or the case where the mass m of the Brownian particle tends to zero. This limit is already highly non-trivial at the classical level, in the presence of the inhomogeneous damping and diffusion, and it requires a careful application of homogenization theory (cf. Hottovy, Volpe, and Wehr, 2012a; Hottovy, Volpe, and Wehr, 2014; Papanicolaou, 1977; Pavliotis and Stuart, 2008). Of course, the theoretical approach here is based on the separation of time scales, and has been in other contexts studied in the theory of classical and quantum stochastic processes Gardiner, 2009; Risken, 2012. In particular, the theory of adiabatic elimination has been developed to include the short time non-Markovian “initial slip" effects and the effective long time dynamics of the systems and the bath (“adiabatic drag") (cf. Haake, 1982; Haake and Lewenstein, 1983; Haake, Lewenstein, and Reibold, 1985 and references therein).

The Smoluchowski-Kramers limit was also intensively studied in the contexts of Caldeira-Leggett model and quantum Brownian motion (cf. Maier and Ankerhold, 2010; Ankerhold, Pechukas, and Grabert, 2001 and references therein). The problem with this limit is that it corresponds to strong damping, and evidently cannot be described using weak coupling approach that is normally used to derive the master equation from the microscopic model in the Born-Markov approximation. We envisage here two possible and legitimate lines of investigation.

One can forget about the microscopic derivation, and takes the Born-Markov master equation as a starting point. The SK limit corresponds then to setting the spring constant $m\Omega^2$ and friction η to constants, and letting the mass $m \to 0$, so that $\gamma \to \infty$ as $1/m$ and $\Omega \to \infty$ as $1/\sqrt{m}$. The

aim is to eliminate the fast variable (the momentum) and to obtain the resulting equation for the position of the Brownian particle; again, the Wigner function formalism is particularly suited for such a task.

More ambitious and physically more sound is the approach in which the microscopic model is treated seriously, and appropriate scalings are introduced at the microscopic level. One can then start, for instance, from the formally exact path integral expression for the reduced dynamics, as pursued by Ankerhold and collaborators Maier and Ankerhold, 2010; Ankerhold, Pechukas, and Grabert, 2001; Ankerhold and Grabert, 2008. The other possibility is to use a restricted version of the weak coupling assumption, only demanding that the system does not influence the bath, and use the Redfield equation combined with Laplace transform techniques and Zwanzig's approach Zwanzig, 1961. To our knowledge, neither of the two above proposed research tasks has been so far realized for the case of inhomogeneous damping.

Non-linear dynamics extension

We remark once more that, for both a homogeneous and inhomogeneous gas, the polaron Hamiltonian shows an interaction term that depends in a non-linear manner on the impurity position. The results we presented have been obtained by performing a linear approximation of the interaction term, which results to be reasonable for realistic values of the physical quantities. Nevertheless the extension of the mechanism we developed to the general case where the impurity-bath coupling retains its original non-linear form remains an important perspective to extend our analysis beyond the constraint associated to the linearization. Of course, one could pursue this path by means of the techniques discussed in the manuscript (master equations, Heisenberg equations) but we also point out that studied by Lim et al., 2018, that highlights the emergence of a quantum drift due to non-linearity.

Appendix A

High-T limit with leading quantum corrections

A.1 Linear case

Let us now apply the Wigner function formalism to the generalized master equation, Eq. (4.63) valid in the oversimplified high-T limit, and obtain[1]

$$\dot{W} = -\frac{i}{\hbar}\left[\frac{p_-^2 - p_+^2}{2m} + V(x_+) - V(x_-)\right] W - \frac{i\gamma}{4\hbar}[f(x_+) - f(x_-)]\Big(\{p_-, f'(x_+)\} + \{p_+, f'(x_-)\}\Big) W - \frac{\gamma m k T}{\hbar^2}[f^2(x_+) + f^2(x_-) - 2f(x_+)f(x_-)]W, \quad \text{(A.1)}$$

In the case, when the potential $V(x)$ is non-harmonic and/or $f(x)$ is not a linear or quadratic function of x, to proceed further we perform a Taylor expansion in $\hbar$, and keep the leading terms only. In other words we

[1] Note that $\{\dot{f}(\hat{x}), \rho\} f(\hat{x}) = \frac{\{p_-, f'(x_+)\} + \{p_+, f'(x_-)\}}{2m} \rho f(\hat{x}) = f(x_-) \frac{\{p_-, f'(x_+)\} + \{p_+, f'(x_-)\}}{2m} W.$

attempt to include the leading quantum corrections. One finds then

$$\begin{aligned}\dot{W} = &\left[-\partial_x \frac{p}{m} + \partial_p V'(x) - \frac{\hbar^2}{24}\partial_p^3 V'''(x) + \dots\right] W \\ &+ \gamma\left[\partial_p p[f'(x)]^2 + \frac{\hbar^2\partial_p^2}{8}\left(2\partial_x f'(x) f''(x)\right.\right. \\ &\left.\left. - 2[f''(x)]^2 - \frac{4}{3}\partial_p p f'(x) f'''(x)\right) + \dots\right] W \\ &+ m\gamma k_B T\left[\partial_p^2[f'(x)]^2 - \frac{\hbar^2}{12}\partial_p^4 f'(x) f'''(x) + \dots\right] W.\end{aligned} \tag{A.2}$$

The above equation is the main result of this subsection – it combines the (oversimplified) high-T limit with the leading quantum corrections. To zeroth order in $\hbar$, the master equation for the Wigner matrix reads

$$\dot{W} = \mathcal{L}_W, \tag{A.3}$$

$$\mathcal{L}_W = -\frac{p}{m}\partial_x + V'(x)\partial_p + \gamma[f'(x)]^2\partial_p p + m\gamma k_B T[f'(x)]^2\partial_p^2. \tag{A.4}$$

A.2 Quadratic case

As an example we consider the simplest non-linear coupling to the bath, a quadratic one, which we write in the form $f(x) = x^2/a$. We also take the potential to be quadratic, $V(x) = m\Omega^2 x^2/2$. Since $f'''(x) = 0$, from Eq. (A.2) truncated to $O(\hbar^2)$ we have

$$\dot{W} = \mathcal{L}_W^{(2)} W, \tag{A.5}$$

$$\mathcal{L}_W^{(2)} = -\frac{p}{m}\partial_x + m\Omega^2 x\partial_p + \frac{4\gamma x^2}{a^2}\left(\partial_p p + m k_B T\partial_p^2 + \frac{\hbar^2}{4x}\partial_p^2\partial_x\right). \tag{A.6}$$

A stationary solution of this equation is in the form of Eq. (3.74) with $\sigma_p = \sigma_x = 1$ and

$$\tilde{T} = \frac{T}{2}\left[1 \pm \sqrt{1 - \left(\frac{\hbar\Omega}{k_B T}\right)^2}\right]. \tag{A.7}$$

Only the $+$ solution is physically acceptable, as can be seen by looking at large temperature $k_B T \gg \hbar\Omega$, where the $+$ solution becomes

$$\tilde{T} = T\left[1 - \left(\frac{\hbar\Omega}{2kT}\right)^2\right] \tag{A.8}$$

This result is plotted as a red curve in Fig. 3.2, and may be interpreted as an effective cooling, since $\tilde{T} < T$, or as a breakdown of the dissipation-fluctuation relation, or as quantum localization in phase space. However, as we have seen, this result is incorrect. Obviously, it cannot be correct when $k_B T \simeq \hbar\Omega$, but it loses validity already at larger temperatures, when $k_B T \lesssim \hbar\Lambda$, since then neither D_{xp} nor D_{pp} terms can be neglected. Looking from another perspective, this result contains a quantum correction of order $\hbar\Omega/k_B T$, which is simply non-systematic, and moreover it depends on the order of limits: high temperature $T \to \infty$, and stationarity, long time limit $t \to \infty$.

Appendix B

Laplace transforms and trigonometric identities

B.1 Laplace transforms

Here we show how to compute the coefficients of the master equation with a generic coupling by direct Laplace transform. We have

$$C_{n,k}(\Omega) = (-1)^{k+1}\frac{m\gamma\Lambda^2}{2}\mathcal{L}[\cos^{n-k}(\xi)\sin^k(\xi)]_\Lambda \tag{B.1}$$

$$D_{n,k}(\Omega) = \frac{mk_BT\gamma\Lambda^2}{\hbar}\sum_{p=-\infty}^{+\infty}\frac{1}{\Lambda^2-\nu_p^2} \left(\Lambda\mathcal{L}[\cos^{n-k}(\xi)\sin^k(\xi)]_\Lambda - |\nu_p|\mathcal{L}[\cos^{n-k}(\xi)\sin^k(\xi)]_{|\nu_p|}\right), \tag{B.2}$$

where $\mathcal{L}[a(\xi)]_s = \int_0^\infty \mathrm{d}\xi\, a(\xi)e^{-s\xi}$ stands for the Laplace transform of $a(\xi)$ with respect to the variable s. Using the following identity, valid for $s > 0$,

$$\mathcal{L}\left[\cos^{(n-k)}(\xi)\sin^{(k)}(\xi)\right]_s = = \sum_{l=0}^{n-k}\sum_{j=0}^{k}(-1)^{j+k}\frac{i^k}{2^n}\binom{n-k}{l}\binom{k}{j}\mathcal{L}\left[e^{i[n-2(j+l)]\xi}\right]_s = = \sum_{l=0}^{n-k}\sum_{j=0}^{k}(-1)^{j+k}\frac{i^k}{2^n}F_{njl}(s),$$

with

$$F_{njl}(s) \equiv \binom{n-k}{l}\binom{k}{j}\frac{1}{s - i[n-2(j+l)]\Omega}, \tag{B.3}$$

one readily finds

$$C_{n,k} = \frac{m\gamma\Lambda^2}{2}\sum_{l=0}^{n-k}\sum_{j=0}^{k}(-1)^{j+1}\frac{i^k}{2^n}F_{njl}(\Lambda). \tag{B.4}$$

In the expression for $D_{n,k}$, the zero Matsubara-frequency term should must be treated separately, so that one obtains:

$$\begin{aligned} D_{n,k} =& \frac{i^k}{2^n}\frac{mk_BT\gamma}{\hbar}\sum_{l=0}^{n-k}\sum_{j=0}^{k}(-1)^j\Bigg\{\Lambda F_{njl}(\Lambda) \\ &+2\sum_{p=1}^{+\infty}\frac{\Lambda^2}{\Lambda^2-\nu_p^2}\left[\Lambda F_{njl}(\Lambda) - \nu_p F_{njl}(\nu_p)\right]\Bigg\}. \end{aligned} \tag{B.5}$$

B.2 Trigonometric identities

The identities presented here provide a very simple method (alternative to the one described in the previous section) to compute the $2n+2$ coefficients needed to describe the master equation for an arbitrary coupling $f(x) \propto x^n$ in terms of just the two integrals $I_\nu \equiv \int_0^\infty \mathrm{d}\tau\, \nu(\tau)$ and $I_\eta \equiv \int_0^\infty \mathrm{d}\tau\, \eta(\tau)$, and of the four coefficients $\{C_x, C_p, D_x, D_p\}$ we derived for a linear coupling. Take $p+q=n$.

Whenever p is even (or zero), we have

$$\begin{aligned} &\sin^p(x)\cos^q(x) = [1-\cos^2(x)]^{p/2}\cos^q(x) \\ =&c_0 + \sum_{k=0}^{\mathcal{F}[(n-1)/2]}\alpha_k\cos[(n-2k)x], \end{aligned} \tag{B.6}$$

where $\mathcal{F}(x)$ is the "floor" function (giving the greatest integer less than or equal to x), and c_0 and $\{\alpha_k\}$ are constants which may be determined using the power reduction trigonometric formulas (Gradshteyn and Ryzhik,

2000). As an example, we find

$$\sin^2(x)\cos^3(x) = \frac{3\cos(x)+\cos(3x)}{4} - \frac{10\cos(x)+5\cos(3x)+\cos(5x)}{16}. \tag{B.7}$$

This formula reduces high powers of the trigonometric quantity to a sum of cosine-functions of multiples of its argument, thereby reducing the desired integrals to known ones.

Similarly, whenever q is even (or zero), we have

$$\begin{aligned}\sin^p(x)\cos^q(x) &= \sin^p(x)[1-\sin^2(x)]^{q/2} \\ &= c_0 + \sum_{k=0}^{\mathcal{F}[(n-1)/2]} \alpha_k \sin[(n-2k)x].\end{aligned} \tag{B.8}$$

In the case where both p and q are odd integers, we may write

$$\begin{aligned}\sin^p(x)\cos^q(x) &= \sin(x)\cos(x)[1-\cos^2(x)]^{\frac{p-1}{2}}\cos^{q-1}(x) \\ &= \frac{\sin(2x)}{2}\left[c_0 + \sum_{k=0}^{\mathcal{F}[(n-3)/2]} \alpha_k \cos[(n-2k)x]\right],\end{aligned} \tag{B.9}$$

and the resulting integrals may be computed using the simple identity, valid for $n > 0$,

$$\sin(2x)\cos(2nx) = \frac{\sin[(2n+2)x] - \sin[(2n-2)x]}{2}. \tag{B.10}$$

Appendix C

Heisenberg uncertainty principle for density operators

The purpose of this Appendix is to present a self-contained derivation of the Heisenberg uncertainty principle for density operators. We start from the pure state case. Consider an arbitrary state $|\psi\rangle$ and observables A and B. Denoting by $\langle A\rangle$ the mean of the observable A in the state $|\psi\rangle$,

$$\langle A\rangle = \langle\psi|A|\psi\rangle, \tag{C.1}$$

for the variance of A we have

$$\sigma_A^2 = \left\langle \psi \left| (A - \langle A\rangle)^2 \right| \psi \right\rangle, \tag{C.2}$$

and similarly for B. For future reference, let us also note that for any real number a,

$$\left\langle \psi \left| (A - a)^2 \right| \psi \right\rangle \geq \sigma_A^2. \tag{C.3}$$

The claim we want to prove is

$$\sigma_A^2 \sigma_B^2 \geq \frac{1}{4} \left\langle \frac{[A, B]}{i} \right\rangle^2, \tag{C.4}$$

where the right-hand side contains the mean value of the observable $[A, B]/i$ in the state $|\psi\rangle$. Introducing the vectors

$$|f\rangle = |(A - \langle A\rangle)\psi\rangle \quad \text{and} \quad |g\rangle = |(B - \langle B\rangle)\psi\rangle, \tag{C.5}$$

we have

$$\sigma_A^2 \sigma_B^2 = \langle f|f\rangle \langle g|g\rangle \geq |\langle f|g\rangle|^2, \tag{C.6}$$

where we applied the Cauchy-Schwarz inequality. The right-hand side of the last inequality can be rewritten as

$$|\langle f|g\rangle|^2 = \left(\frac{\langle f|g\rangle + \langle g|f\rangle}{2}\right)^2 + \left(\frac{\langle f|g\rangle - \langle g|f\rangle}{2i}\right)^2, \tag{C.7}$$

with both terms on the right-hand side non-negative. Rewriting the second term as the square of the mean of the observable $[A, B]/2i$, and leaving the first term out (keeping it would lead to a stronger inequality, called Robertson-Schrödinger inequality), we obtain the desired bound

$$\sigma_A^2 \sigma_B^2 \geq \frac{1}{4}\left\langle \frac{[A, B]}{i}\right\rangle^2, \tag{C.8}$$

in the pure state case. Now, if $\rho = \sum_j p_j |\phi_j\rangle \langle\phi_j|$ is an arbitrary density operator, with p_j non-negative coefficients summing up to 1, the mean of A in the state ρ equals

$$\langle A\rangle^{(\rho)} = \mathrm{Tr}\,(\hat{\rho}A)\,. \tag{C.9}$$

For the variance of A in the state ρ we have

$$\left(\sigma_A^{(\rho)}\right)^2 = \mathrm{Tr}\left[\hat{\rho}\left(A - \langle A\rangle^{(\rho)}\right)^2\right], \tag{C.10}$$

and similarly for B. We thus have

$$\begin{aligned}\left(\sigma_A^{(\rho)}\right)^2 &= \sum_j p_j \left\langle \phi_j \left| \left(A - \langle A\rangle^{(\rho)}\right)^2 \right| \phi_j \right\rangle \\ &\geq \sum_j p_j \left(\sigma_A^{(\phi_j)}\right)^2,\end{aligned} \tag{C.11}$$

where $\left(\sigma_A^{(\phi_j)}\right)^2$ denotes the variance of A in the state $|\phi_j\rangle$, and in the last step we used inequality Eq. (C.3). Similarly,

$$\left(\sigma_B^{(\rho)}\right)^2 \geq \sum_j p_j \left(\sigma_B^{(\phi_j)}\right)^2, \tag{C.12}$$

By the (discrete version of) the Cauchy-Schwarz inequality (it is crucial that $p_j \geq 0$ here!) we obtain

$$\left(\sigma_A^{(\rho)}\right)^2 \left(\sigma_B^{(\rho)}\right)^2 \geq \left(\sum_j p_j \sigma_A^{(\phi_j)} \sigma_B^{(\phi_j)}\right)^2, \tag{C.13}$$

which, using the pure-state version of the uncertainty principle, is bounded from below by

$$\frac{1}{4}\left(\sum_j p_j \left\langle \phi_j \left| \frac{[A,B]}{i} \right| \phi_j \right\rangle\right)^2 = \frac{1}{4}\left(\left\langle \frac{[A,B]}{i} \right\rangle^{(\rho)}\right)^2. \tag{C.14}$$

This is the desired mixed-state version of the inequality. In the last application of the Cauchy-Schwarz inequality, it is crucial that we are dealing with a density operator, so that the eigenvalues p_j are non-negative.

In the most important case for us, when $A = X$ is the position operator and $B = P$ is the momentum operator, the commutator of A and B is a multiple of identity, $[X, P] = i\hbar I$. The mean value of $\frac{[X,P]}{i}$ in any state is thus equal to $\hbar$ and in particular, for the density operators ρ_t, solving a Lindblad equation we obtain at all times the standard form of the Heisenberg uncertainty principle,

$$\sigma_X^2 \sigma_P^2 \geq \frac{\hbar^2}{4}. \tag{C.15}$$

Appendix D

Gaussian approximation

The purpose of this Appendix is to prove that the Gaussian approximation performed on the Lindblad equation for Quadratic QBM preserves its Lindblad form. The demonstration we are about to present considers a Gaussian approximation carried out directly on the master equation, while in Sec. 5.2.2 it has been done on the equations for the moments. As we will show, the two procedures are completely equivalent.

Theorem For a quadratic Lindblad operator:

$$L = \tilde{\alpha}a^2 + \tilde{\beta}(a^\dagger)^2 + \tilde{\gamma}a^\dagger a + \tilde{\delta}a + \tilde{\epsilon}a^\dagger + \tilde{\eta} \tag{D.1}$$

the self-consistent Gaussian approximation preserves the Lindblad form (and thus the positivity of ρ and Heisenberg principle).

The annihilation and creation operators are represented respectively by a and $a^\dagger$, while $\tilde{\alpha}, \tilde{\beta}, \tilde{\gamma}, \tilde{\delta}, \tilde{\epsilon}, \tilde{\eta}$ are complex parameters. It is immediate to prove that the Lindblad operator introduced in Eq. (5.33) can be expressed in the form showed in Eq. (D.1). Note that it is possible to assume $\langle a \rangle = 0$, since it just shifts the parameters.

Lemma 1 The parameter $\tilde{\eta}$ in Eq. (D.1) can be shifted arbitrarily.

Proof: the core of the proof lies in the fact that any additive constant in the definition of the Lindblad operator can be compensated by a re-definition of the Hamiltonian, namely:

$$\begin{aligned} \frac{\partial \rho}{\partial t} &= -\frac{i}{\hbar}[H, \rho] + \mathcal{D}_{L+\Delta\tilde{\eta}}(\rho) \\ &= -\frac{i}{\hbar}[H + \Delta H_{\Delta\tilde{\eta}}, \rho] + \mathcal{D}_L(\rho), \end{aligned} \tag{D.2}$$

where:

$$\mathcal{D}_L(\rho) = L\rho L^\dagger - L^\dagger L\rho/2 - \rho L^\dagger L/2, \tag{D.3}$$

is the Lindblad dissipator, and:

$$\Delta H_{\Delta\tilde{\eta}} = -\frac{i}{2}[(\Delta\tilde{\eta})L^\dagger - (\Delta\tilde{\eta})^* L], \tag{D.4}$$

with $\Delta\tilde{\eta} \in \mathbb{C}$.

Of course changing of Hamiltonian is allowed, since it just modifies the time dependence of a and $a^\dagger$ in the interaction picture.

Lemma 2 It is possible to perform the factorization:

$$L = d_1 d_2, \tag{D.5}$$

with:

$$\begin{aligned} d_1 &= \tilde{A}a + \tilde{B}a^\dagger + \tilde{C}, \\ d_2 &= a + \tilde{D}a^\dagger + \tilde{E}. \end{aligned} \tag{D.6}$$

Proof: comparing Eqs. (D.5) and (D.1), one obtains:

$$\begin{aligned} &\tilde{A} = \tilde{\alpha}, \quad \tilde{A}\tilde{D} + \tilde{B} = \tilde{\gamma}, \quad \tilde{A}\tilde{D} + \tilde{C}\tilde{E} = \tilde{\eta} \\ &\tilde{B}\tilde{D} = \tilde{\beta}, \quad \tilde{A}\tilde{E} + \tilde{C} = \tilde{\delta}, \quad \tilde{B}\tilde{E} + \tilde{C}\tilde{D} = \tilde{\delta}, \end{aligned} \tag{D.7}$$

so that

$$\tilde{D} = \tilde{\beta}/\tilde{B}, \quad \tilde{\alpha}\tilde{\beta}/\tilde{B} + \tilde{B} = \tilde{\gamma}. \tag{D.8}$$

provide in general two solutions $\tilde{B}_1$ and $\tilde{B}_2$ for $\tilde{B}$, and

$$\tilde{\alpha}\tilde{E} + \tilde{C} = \tilde{\delta}, \quad \tilde{B}\tilde{E} + (\tilde{\beta}/\tilde{B})\tilde{C} = \tilde{\eta}. \tag{D.9}$$

If we can solve these linear equations for $\tilde{E}$ and $\tilde{C}$, we may plug the solution into $\tilde{\alpha}\tilde{D} + \tilde{C}\tilde{E} = \tilde{\eta}$, and adjust η adequately (which we can do according to Lemma 1).

It is easy to check that the two equations for $\tilde{E}$ and $\tilde{C}$ cannot be solved if $\tilde{B}_1 = \tilde{B}_2 = 0$, which implies $\tilde{\gamma} = 0$ and $\tilde{\alpha}\tilde{\beta} = 0$, *i.e.* the non-generic case $L = \tilde{\alpha}a^2 + \tilde{\delta}a + \tilde{\epsilon}a^\dagger + \tilde{\eta}$, and the related one with $\tilde{\alpha} = 0$, $\tilde{\beta} \neq 0$. The case $\tilde{\alpha} = \tilde{\beta} = 0$ is trivial, as it corresponds to linear Lindblad operator: for

such a case, the Gaussian approximation is not needed, since there exists an exact solution of Gaussian form.

Now we prove the Theorem in the generic case:
Proof of the Theorem: We look to the Lindblad dissipator related to the factorized Lindblad operator in Eq. (D.5):

$$\mathcal{D}_L(\rho) = d_1 d_2 \rho d_2^\dagger d_1^\dagger - \frac{1}{2}\{d_2^\dagger d_1^\dagger d_1 d_2, \rho\}. \tag{D.10}$$

In the Gaussian approximation, one replaces pairs of operators by their mean values. "Anomalous" terms generate contributions that may be reabsorbed in the Hamiltonian, such as

$$\langle d_1 d_2\rangle \left[\rho d_2^\dagger d_1^\dagger - \frac{1}{2}\{d_2^\dagger d_1^\dagger, \rho\}\right] = -\frac{1}{2}\langle d_1 d_2\rangle [d_2^\dagger d_1^\dagger, \rho], \tag{D.11}$$

and:

$$\langle d_2^\dagger d_1^\dagger\rangle \left[d_1 d_2 \rho - \frac{1}{2}\{d_1 d_2, \rho\}\right] = \frac{1}{2}\langle d_2^\dagger d_1^\dagger\rangle [d_1 d_2, \rho]. \tag{D.12}$$

The non-trivial terms are:

$$\begin{aligned} &\langle d_2^\dagger d_1\rangle d_2 \rho d_1^\dagger + \langle d_1^\dagger d_1\rangle d_2 \rho d_2^\dagger \\ &+\langle d_2^\dagger d_2\rangle d_1 \rho d_1^\dagger + \langle d_1^\dagger d_2\rangle d_1 \rho d_2^\dagger \\ &- \left\{\left(\langle d_2^\dagger d_1\rangle d_1^\dagger d_2 + \langle d_2^\dagger d_2\rangle d_1^\dagger d_1\right), \frac{\rho}{2}\right\} \\ &- \left\{\left(\langle d_1^\dagger d_1\rangle d_2^\dagger d_2 + \langle d_1^\dagger d_2\rangle d_2^\dagger d_1\right), \frac{\rho}{2}\right\}. \end{aligned} \tag{D.13}$$

The resulting ME has a dissipator of the form:

$$\mathcal{D}_L(\rho) = \sum_{i,j=1,2} \tilde{\Gamma}_{ij}\left(d_i \rho d_j^\dagger - \frac{1}{2}\{d_j^\dagger d_i, \rho\}\right), \tag{D.14}$$

where $\tilde{\Gamma}_{ij} = \langle d_{j'}^\dagger d_{i'}\rangle$, where $1' = 2$ and $2' = 1$. This matrix is evidently positive definite, as follows from the Schwartz inequality, so that the dissipator is again of Lindblad form.

Note that the generalization to many oscillators, many Lindblad operators is straightforward. Note also that the non-generic case is simple to treat. It requires, however, a direct calculation. The quartic Lindblad

term in this case is treated as above, while the quadratic one does not need to be touched, since it already describes a Gaussian quantum process. The third order term on the other hand partially vanishes and partially gives contributions to the Hamiltonian in the Gaussian approximation.

The remaining question is whether the approximation that we perform on the level of the ME is the same as the Gaussian de-correlation we performed according to the Wick's theorem prescription at the level of the equations for the moments in Sec. 5.2.2. To illustrate this, we consider an arbitrary operator 0 and we derive the dynamical equations for its average value starting by the ME induced by the superoperator in Eq. (D.10).

The dynamical equation for the average value of an operator O presents the following form:

$$\frac{\partial\langle O\rangle}{\partial t} = h_O^u + h_O^{(1)} - \frac{1}{2}\left(h_O^{(2)} + h_O^{(3)}\right), \tag{D.15}$$

in which

$$\begin{aligned} h_O^u &= -\frac{i}{\hbar}\mathrm{Tr}\left(O\left[H,\rho\right]\right) \\ h_O^{(1)} &= \mathrm{Tr}(Od_1d_2\rho d_2^\dagger d_1^\dagger) = \langle d_2^\dagger d_1^\dagger O d_1 d_2\rangle \\ h_O^{(2)} &= \mathrm{Tr}(Od_2^\dagger d_1^\dagger d_1 d_2\rho) = \langle O d_2^\dagger d_1^\dagger d_1 d_2\rangle \\ h_O^{(3)} &= \mathrm{Tr}(O\rho d_2^\dagger d_1^\dagger d_1 d_2) = \langle d_2^\dagger d_1^\dagger d_1 d_2 O\rangle. \end{aligned} \tag{D.16}$$

Performing the Gaussian approximation at the level of the equation for the moments means to carry out such an approximation on the average values in Eqs. (D.16),

$$\begin{aligned} h_O^{(1)} &= \mathrm{Tr}(Od_1d_2\rho d_2^\dagger d_1^\dagger) = \langle d_2^\dagger d_1^\dagger O d_1 d_2\rangle, \\ \simeq\ & \langle d_2^\dagger d_1^\dagger\rangle\langle O d_1 d_2\rangle + \langle d_2^\dagger d_1^\dagger O\rangle, \langle d_1 d_2\rangle - \langle d_2^\dagger d_1^\dagger\rangle\langle O\rangle\langle d_1 d_2\rangle, \\ +\ & \langle d_2^\dagger d_1\rangle\langle d_1^\dagger O d_2\rangle + \langle d_2^\dagger O d_1\rangle\langle d_1^\dagger d_2\rangle - \langle d_2^\dagger d_1\rangle\langle O\rangle\langle d_1^\dagger d_2\rangle, \\ +\ & \langle d_2^\dagger d_2\rangle\langle d_1^\dagger O d_1\rangle + \langle d_2^\dagger O d_2\rangle\langle d_1^\dagger d_1\rangle - \langle d_2^\dagger d_2\rangle\langle O\rangle\langle d_1^\dagger d_1\rangle, \end{aligned} \tag{D.17}$$

$$
\begin{aligned}
h_O^{(2)} &= \mathrm{Tr}(O d_2^\dagger d_1^\dagger d_1 d_2 \rho) = \langle O d_2^\dagger d_1^\dagger d_1 d_2 \rangle \qquad \text{(D.18)} \\
\simeq\ & \langle d_2^\dagger d_1^\dagger \rangle \langle O d_1 d_2 \rangle + \langle O d_2^\dagger d_1^\dagger \rangle \langle d_1 d_2 \rangle - \langle d_2^\dagger d_1^\dagger \rangle \langle O \rangle \langle d_1 d_2 \rangle \\
+\ & \langle d_2^\dagger d_1 \rangle \langle O d_1^\dagger d_2 \rangle + \langle O d_2^\dagger d_1 \rangle \langle d_1^\dagger d_2 \rangle - \langle d_2^\dagger d_1 \rangle \langle O \rangle \langle d_1^\dagger d_2 \rangle \\
+\ & \langle d_2^\dagger d_2 \rangle \langle O d_1^\dagger d_1 \rangle + \langle O d_2^\dagger d_2 \rangle \langle d_1^\dagger d_1 \rangle - \langle d_2^\dagger d_2 \rangle \langle O \rangle \langle d_1^\dagger d_1 \rangle,
\end{aligned}
$$

$$
\begin{aligned}
h_O^{(3)} &= \mathrm{Tr}(O \rho d_2^\dagger d_1^\dagger d_1 d_2) = \langle d_2^\dagger d_1^\dagger d_1 d_2 O \rangle \qquad \text{(D.19)} \\
\simeq\ & \langle d_2^\dagger d_1^\dagger \rangle \langle d_1 d_2 O \rangle + \langle d_2^\dagger d_1^\dagger O \rangle \langle d_1 d_2 \rangle - \langle d_2^\dagger d_1^\dagger \rangle \langle O \rangle \langle d_1 d_2 \rangle \\
+\ & \langle d_2^\dagger d_1 \rangle \langle d_1^\dagger d_2 O \rangle + \langle d_2^\dagger d_1 O \rangle \langle d_1^\dagger d_2 \rangle - \langle d_2^\dagger d_1 \rangle \langle O \rangle \langle d_1^\dagger d_2 \rangle \\
+\ & \langle d_2^\dagger d_2 \rangle \langle d_1^\dagger d_1 O \rangle + \langle d_2^\dagger d_2 O \rangle \langle d_1^\dagger d_1 \rangle - \langle d_2^\dagger d_2 \rangle \langle O O \rangle \langle d_1^\dagger d_1 \rangle.
\end{aligned}
$$

It is now tedious but easy to check that replacing the expressions in Eq. (D.17-D.19) in Eq. (D.15) we get the dynamical equations generated by the terms in Eqs. (D.11-D.13), obtained by performing the Gaussian approximation on the master equation related to a dissipator in Eq. (D.10). This proves that performing the Gaussian approximation at the level of the master equation is equivalent to doing it at the level of the equations for the moments of an observable. Note that the equations resulting by this approximation will always admit a Gaussian solution, although it is not guaranteed that the latter is stationary.

The demonstration we developed holds for Lindblad operators which are quadratic in the creation and annihilation operators. This case covers the situation studied in Sec. (5.2), but it is not the most general one. In fact, one could consider also Lindblad equations with Lindblad operators containing higher powers of creation and annihilation operators. Extending the proof we presented to this general case is an interesting perspective that we reserve for future works.

Appendix E

Derivation of the equation for the impurity position

In this Appendix we show in detail the calculation leading to Eq. (7.58). The starting point is constituted by the Eqs. (7.54)-(7.57). The first step is to derive both sides of Eq. (7.54) and to replace the result in Eq. (7.55), thus obtaining an equation just for the position of the impurity

$$\ddot{x}(t) + \Omega^2 x(t) = -i \sum_k \frac{\hbar g_k}{m_{\mathrm{I}}} \left[b_k(t) - b_k^\dagger(t) \right]. \tag{E.1}$$

The time dependence of the Bogoliubov modes can be extracted from Eqs. (7.56) and (7.57). They are linear but non-homogeneous first-order differential equations. Therefore their solution is the sum of that of the related homogeneous one and a particular integral. The former can be easily obtained since it is just that of a harmonic oscillator,

$$b_k(t) = b_k e^{-i\omega_k t} + h_k^-(t), \quad b_k^\dagger(t) = b_k^\dagger e^{+i\omega_k t} + h_k^+(t). \tag{E.2}$$

The quantities h_k^- and h_k^+ represent the particular solutions of Eqs. (7.56) and (7.57), that may be expressed as convolution product of the unknown function $x(t)$ and the Green function

$$h_k^\pm(t) = \int_0^t G_k^\pm(t-s)x(s)ds. \tag{E.3}$$

Then, the problem of solving the Heisenberg equations for the Bogoliubov modes reduces to that of finding the Green function of Eqs. (7.56)

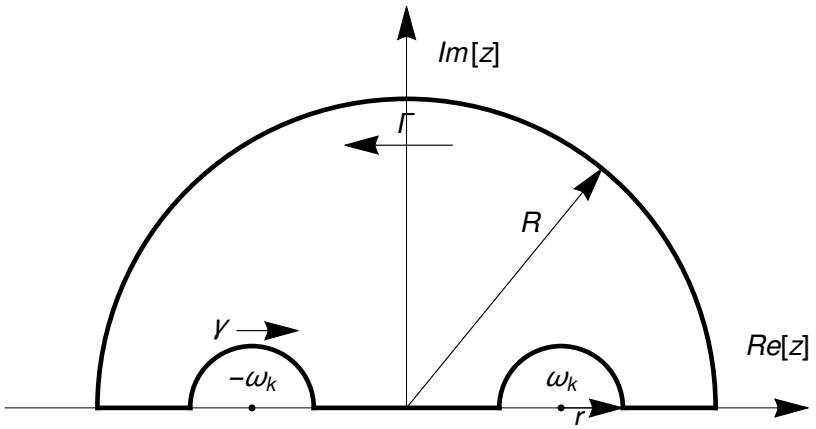

FIGURE E.1: Path in complex plane to solve the integral in Eq. (E.6).

and (7.57). The Green function is defined by the equation

$$\dot{G}_k^{\pm}(t) \mp i\omega_k G_k^{\pm}(t) = -g_k \delta(t), \tag{E.4}$$

which applying Fourier transform turns into

$$\mathcal{F}_{\tilde{\omega}}\left[G_k^{\pm}(t)\right] = -\frac{ig_k}{\tilde{\omega} \pm \omega}. \tag{E.5}$$

Thus, the problem of determining the Green function is solved if one performs the inversion of the Fourier transform in Eq. (E.5). Namely, one has to calculate the following integral

$$G_k^{\pm}(t) = -\frac{ig_k}{2\pi}\mathcal{P}\int_{-\infty}^{+\infty} \frac{e^{i\tilde{\omega}t}}{\tilde{\omega} \pm \omega_k} d\tilde{\omega}, \tag{E.6}$$

where we introduced the principal Cauchy part $\mathcal{P}$ because otherwise the integral is not well-defined in $\tilde{\omega} = \pm\omega_k$. The integral in Eq. (E.6) can be solved recalling the Jordan Lemma, selecting the path in Fig. E.1. It follows

$$G_k^{\pm}(t) = \frac{g_k}{2} \exp\left(\mp i\omega_k t\right). \tag{E.7}$$

In conclusion, Eq. (E.1) takes the form

$$\ddot{x}(t) + \Omega^2 x(t) - \frac{\hbar}{m_{\mathrm{I}}} \sum_k g_k^2 \int_0^t x(s) \sin\left[\omega_k (t-s)\right] ds \tag{E.8}$$
$$= \frac{B(t)}{m_{\mathrm{I}}},$$

where

$$B(t) \equiv -\sum_k \hbar g_k \pi_k(t) = \sum_k i\hbar g_k (b_k^\dagger e^{i\omega_k t} - b_k e^{-i\omega_k t}). \tag{E.9}$$

Equation (E.8) can be expressed in terms of the dissipation kernel, Eq. (7.32)

$$\ddot{x}(t) + \Omega^2 x(t) - \frac{1}{m_{\mathrm{I}}} \int_0^t \lambda(t-s) x(s) ds = \frac{B(t)}{m_{\mathrm{I}}}. \tag{E.10}$$

One can also introduce the damping kernel in Eq. (7.33). The third term in the first hand-side of Eq. (E.8) so writes as

$$-\frac{1}{m_{\mathrm{I}}} \int_0^t \lambda(t-s) x(s) ds = \int_0^t \dot{\Gamma}(t-s) x(s) ds = \tag{E.11}$$
$$= \frac{\partial}{\partial t} \int_0^t \Gamma(t-s) x(s) ds - \Gamma(0) x(t).$$

Accordingly it is possible to express Eq. (E.10) as

$$\ddot{x}(t) + \tilde{\Omega}^2 x(t) + \frac{\partial}{\partial t} \int_0^t \Gamma(t-s) x(s) ds = \frac{B(t)}{m_{\mathrm{I}}}, \tag{E.12}$$

in which we introduced the renormalized frequency

$$\tilde{\Omega}^2 = \Omega^2 - \Gamma(0). \tag{E.13}$$

Hereafter we neglect the contribution to the frequency provided by $\Gamma(0)$. This term grows as the interaction strength increases and could lead to a negative renormalized frequency. In this context the impurity experiences instability. By deriving the equations of motion directly from Hamiltonian Eq. (7.26) one avoids the instability problem, at the cost of introducing and additional counter term *ad hoc*. With the procedure here presented we can identify in the equations of motion the effect of the

absence of such a term.

Appendix F

Laplace tranform of the damping kernel

In this Appendix we derive the expression of the Laplace transform of the damping kernel presented in Eq. (7.66). We perform the calculation for a cubic spectral density with a general ultraviolet regularization

$$J(\omega) = m_{\mathrm{I}}\tilde{\tau}\omega^3\Theta(\omega,\Lambda), \tag{F.1}$$

with $\Theta(\omega,\Lambda) > 0$ specifying the dependence on the cut-off of the spectral density. The spectral density in Eq. (7.66) corresponds to the particular case when

$$\Theta(\omega,\Lambda) = \theta(\omega-\Lambda), \tag{F.2}$$

with $\theta(\cdot)$ the Heaviside step function. We will also compute the Laplace transform considering an exponential cut-off

$$\Theta(\omega,\Lambda) = \exp\left(-\Lambda\omega\right), \tag{F.3}$$

showing that a much complicated expression turns out.

In general, we assume that $\Theta(\omega,\Lambda)$ decays fast enough so that

$$\int_0^\infty e^{-zt}\left(\int_0^\infty |\omega^2\Theta(\omega,\Lambda)\cos(\omega t)|d\omega\right)dt < \infty. \tag{F.4}$$

Note that such a behavior covers both the sharp and the exponential dependence on the cut-off. Therefore, by Fubini-Tonelli theorem one can

interchange the integrals in the following. For $z > 0$, it results in

$$\mathcal{L}\left[\Gamma\left(t\right)\right]_z = \tilde{\tau}\int_0^\infty e^{-zt}\left(\int_0^\infty \omega^2\Theta(\omega,\Lambda)\cos(\omega t)d\omega\right)dt \tag{F.5}$$

$$= \tilde{\tau}z\int_0^\infty \frac{\omega^2}{\omega^2+z^2}\Theta(\omega,\Lambda)d\omega, \tag{F.6}$$

where we used the expression

$$\int_0^\infty \exp\left(-zt\right)\cos(\omega t)dt = \frac{z}{\omega^2+z^2}, \tag{F.7}$$

that is the result of an integration by parts.

Choosing the cut-off function in Eq. (F.2), we obtain

$$\mathcal{L}\left[\Gamma\left(t\right)\right]_z = z\tilde{\tau}\left[\Lambda - z\arctan\left(\Lambda/z\right)\right], \tag{F.8}$$

as we presented in Eq. (7.66). If we consider the cut-off function in Eq. (F.3), the Laplace transform of the damping kernel results to be expressed in terms of the Mejer function. Such a function is not suitable to handle in an analytic calculation. For the environment given by a BEC, the analytical behavior together with the form of the Bogoliubov spectrum justify the consideration of a sharp cut-off.

Let us finally note that, regardless of its analytic form, the presence of the cut-off introduced in Eq. (7.50) does not affect our results. This is because our results refer to the long time limit, which is not influenced by the high-frequency part of the spectral density. To prove this, one should compare the Laplace transform of the damping kernel induced by the spectral density in Eq. (7.50) (shown in Eq. (F.8)) with that induced by the spectral density in Eq. (7.40), where there is not any cut-off. This is enough because such a Laplace transform is the only object carrying information about the spectral density along all the theory.

However, the calculation of the Laplace transform of the damping kernel induced by the "uncutted" spectral density in Eq. (7.40) is not an easy task, due to the very complicated form at high-frequency (see Eq. (7.42)). It is given by:

$$\mathcal{L}\left[\Gamma\left(t\right)\right]_z = \tilde{\tau}z\int_0^\infty \frac{\omega^2}{\omega^2+z^2}\chi_{1d}(\omega,\Lambda)d\omega. \tag{F.9}$$

We may evaluate it at the first-order in z, which is the relevant one at long times,

$$\mathcal{L}\left[\Gamma\left(t\right)\right]_z = \tilde{\tau} z \int_0^\infty \chi_{1d}(\omega, \Lambda) d\omega + o(z/\Lambda)^2. \tag{F.10}$$

Since

$$\int_0^\infty \chi_{1d}(\omega, \Lambda) d\omega = \Lambda, \tag{F.11}$$

we recover the expression in Eq. (F.8), derived with a sharp cut-off.

In the end, we conclude that at the long-times our results do not depend on whether the spectral density is cut or not, *i.e.* on the existence of the cut-off. This could also be inferred by recalling the Tauberian theorem (Nixon, 1965; Feller, 1971) according to which the long time behavior of a function (in the time domain) is determined by the low frequency behavior of its Laplace transform (in the frequency domain). Since the low frequency behavior of the Laplace transform of the damping kernels for both spectral densities coincides, the long time dynamics of the impurity do not depend on whether there is a cutoff or not.

Appendix G

Derivation of the position variance by means of the fluctuation-dissipation theorem

In this Appendix we present an alternative way to derive the position variance for a trapped impurity, employing the linear response theory. For this goal we introduce the response function, $\chi(t) = \frac{i}{\hbar}\theta(t)\langle[x(t), x(0)]\rangle$, describing the linear response of the system to an external force at the equilibrium. Here $\theta(t)$ is the step function, specifying causality. The response function defined here is also known as generalized susceptibility. Taking the commutator with $x(0)$ on both sides of (7.58) and then averaging (note the initial slip term and the stochastic forcing term are absent once a commutator of $x(0)$ is applied to them), we obtain the following c-valued equation for $\chi(t)$

$$\ddot{\chi}(t) + \Omega^2\chi(t) + \int_0^t \Gamma(t-s)\dot{\chi}(s)ds = 0, \tag{G.1}$$

with $\chi(0) = 0$, $\dot{\chi}(0) = 1/m_{\rm I}$.

Next, consider the symmetric position autocorrelation function, defined as

$$S(t) = \frac{1}{2}\langle\{x(t), x(0)\}\rangle. \tag{G.2}$$

We recall the fluctuation-dissipation relation of Callen-Welton (Breuer and Petruccione, 2007), which relates the equilibrium fluctuation to the

response function in the frequency domain as follows:

$$\tilde{S}(\omega) = \hbar \coth\left(\frac{\hbar\omega}{2k_{\mathrm{B}}T}\right)\tilde{\chi}''(\omega), \tag{G.3}$$

where

$$\tilde{S}(\omega) = \int_{-\infty}^{\infty} dt\, \cos(\omega t) S(t), \tag{G.4}$$

and

$$\tilde{\chi}''(\omega) = \mathrm{Im}\{\mathcal{F}_{\omega}\left[\chi(t)\right]\}. \tag{G.5}$$

Using this, we can obtain the symmetric position autocorrelation function

$$S(t) = \int_{-\infty}^{\infty} d\omega \frac{\hbar}{2\pi} \coth\left(\frac{\hbar\omega}{2k_{\mathrm{B}}T}\right)\tilde{\chi}''(\omega)\cos(\omega t). \tag{G.6}$$

from which the position variance at the equilibrium follows

$$\langle x^2\rangle = S(0) = \int_{-\infty}^{\infty} d\omega \frac{\hbar}{2\pi} \coth\left(\frac{\hbar\omega}{2k_{\mathrm{B}}T}\right)\tilde{\chi}''(\omega) \tag{G.7}$$

Note that $\tilde{\chi}''(w) = \mathrm{Im}\{\mathcal{L}_{\bar{z}}[\chi(t)]\}$, in which

$$\mathcal{L}_{\bar{z}}[\chi(t)] = \frac{1}{m_{\mathrm{I}}}\mathcal{L}_{\bar{z}}[G_2(t)] \tag{G.8}$$

$$= \frac{1}{m_{\mathrm{I}}}\frac{1}{(\Omega^2-\omega^2) - i\omega\mathcal{L}_{\bar{z}}[\Gamma(t)]}, \tag{G.9}$$

where we used the expression in Eq. (7.63) for the Laplace transform of G_2, and $\bar{z} = -\omega + 0^+$ as defined in Sec. 7.5. Therefore, we have

$$\tilde{\chi}''(\omega) = \frac{1}{m_{\mathrm{I}}}\frac{\omega\xi(\omega)}{\left[\Omega^2-\omega^2-\omega\theta(\omega)\right]^2 + \left[\omega\xi(\omega)\right]^2}. \tag{G.10}$$

This expression has the same form as Eq. (7.90). Accordingly, the position variance in Eq. (G.7), obtained recalling the fluctuation-dissipation theorem, corresponds to that in Eq. (7.89), calculated by solving Heisenberg equation and adopting the spectral density in Eq. (7.50). Therefore, we prove that the two methods lead to the same result.

One can proceed in a similar way to evaluate the MSD for an untrapped impurity in the context of linear response theory, rather than

solving Heisenberg equation. This method leads however to a very complicated expression for the MSD, that does not provide a more convenient alternative to Eq. (7.76). This topic is discussed in detail in Grabert, Schramm, and Ingold, 1987.

Bibliography

Abbot, Davies, and Pati (2008). *Quantum Aspects of the Life*. Oxford: World Scientific. ISBN: ISBN: 978-1-84816-253-2. URL: http://www.worldscientific.com/worldscibooks/10.1142/p581.

Ackerhalt, J. R. and K. Rzazewski (1975). "Heisenberg-picture operator perturbation theory". In: *Phys. Rev. A* 12 (6), pp. 2549–2567. DOI: 10.1103/PhysRevA.12.2549. URL: https://link.aps.org/doi/10.1103/PhysRevA.12.2549.

Alexandrov, A.S. and J.T. Devreese (2009). *Advances in Polaron Physics*. Springer Series in Solid-State Sciences. Springer. ISBN: 9783642018961. URL: http://books.google.es/books?id=EI0Hql-9oY8C.

Ankerhold, Joachim and Hermann Grabert (2008). "Erratum: Strong Friction Limit in Quantum Mechanics: The Quantum Smoluchowski Equation [Phys. Rev. Lett. 87, 086802 (2001)]". In: *Phys. Rev. Lett.* 101 (11), p. 119903. DOI: 10.1103/PhysRevLett.101.119903. URL: http://link.aps.org/doi/10.1103/PhysRevLett.101.119903.

Ankerhold, Joachim, Philip Pechukas, and Hermann Grabert (2001). "Strong Friction Limit in Quantum Mechanics: The Quantum Smoluchowski Equation". In: *Phys. Rev. Lett.* 87 (8), p. 086802. DOI: 10.1103/PhysRevLett.87.086802. URL: http://link.aps.org/doi/10.1103/PhysRevLett.87.086802.

Ardila, L. A. Pena and S. Giorgini (2015). "Impurity in a Bose-Einstein condensate: Study of the attractive and repulsive branch using quantum Monte Carlo methods". In: *Phys. Rev. A* 92 (3), p. 033612. DOI: 10.1103/PhysRevA.92.033612. URL: https://link.aps.org/doi/10.1103/PhysRevA.92.033612.

— (2016). "Bose polaron problem: Effect of mass imbalance on binding energy". In: *Phys. Rev. A* 94 (6), p. 063640. DOI: 10.1103/PhysRevA.94.063640. URL: https://link.aps.org/doi/10.1103/PhysRevA.94.063640.

Bakker, Gert Jan et al. (2012). "Lateral mobility of individual integrin nanoclusters orchestrates the onset for leukocyte adhesion". In: *Proceedings of the National Academy of Sciences* 109.13, pp. 4869–4874. DOI: 10.1073/pnas.1116425109. URL: http://www.pnas.org/content/109/13/4869.abstract.

Banerjee, Subhashish and R. Ghosh (2003). "General quantum Brownian motion with initially correlated and nonlinearly coupled environment". In: *Phys. Rev. E* 67 (5), p. 056120. DOI: 10.1103/PhysRevE.67.056120. URL: http://link.aps.org/doi/10.1103/PhysRevE.67.056120.

Barik, Debashis and Deb Shankar Ray (2005). "Quantum State-Dependent Diffusion and Multiplicative Noise: A Microscopic Approach". In: *Journal of Statistical Physics* 120.1, pp. 339–365. ISSN: 1572-9613. DOI: 10.1007/s10955-005-5251-y. URL: https://doi.org/10.1007/s10955-005-5251-y.

Benjamin, David and Eugene Demler (2014). "Variational polaron method for Bose-Bose mixtures". In: *Phys. Rev. A* 89 (3), p. 033615. DOI: 10.1103/PhysRevA.89.033615. URL: https://link.aps.org/doi/10.1103/PhysRevA.89.033615.

Bloch, Immanuel, Jean Dalibard, and Wilhelm Zwerger (2008). "Many-body physics with ultracold gases". In: *Rev. Mod. Phys.* 80 (3), pp. 885–964. DOI: 10.1103/RevModPhys.80.885. URL: http://link.aps.org/doi/10.1103/RevModPhys.80.885.

Blume-Kohout, R. and W.H. Zurek (2008). "Quantum Darwinism in Quantum Brownian Motion". In: *Phys. Rev. Lett.* 101 (24), p. 240405. DOI: 10.1103/PhysRevLett.101.240405. URL: http://link.aps.org/doi/10.1103/PhysRevLett.101.240405.

Bonart, J. and L. F. Cugliandolo (2013). "Effective potential and polaronic mass shift in a trapped dynamical impurity Luttinger liquid system". In: *EPL (Europhysics Letters)* 101.1, p. 16003. URL: http://stacks.iop.org/0295-5075/101/i=1/a=16003.

Bonart, Julius and Leticia F. Cugliandolo (2012). "From nonequilibrium quantum Brownian motion to impurity dynamics in one-dimensional quantum liquids". In: *Phys. Rev. A* 86 (2), p. 023636. DOI: 10.1103/PhysRevA.86.023636. URL: http://link.aps.org/doi/10.1103/PhysRevA.86.023636.

Bouchaud, J.-P. and A. Georges (1990). "Anomalous diffusion in disordered media: Statistical mechanisms, models and physical applications". In: *Physics Reports* 195, pp. 127–293. DOI: 10.1016/0370-1573(90)90099-N.

Boyanovsky, Daniel and David Jasnow (2017). "Heisenberg-Langevin versus quantum master equation". In: *Phys. Rev. A* 96 (6), p. 062108. DOI: 10.1103/PhysRevA.96.062108. URL: https://link.aps.org/doi/10.1103/PhysRevA.96.062108.

Brettschneider, T. et al. (2011). "Force measurement in the presence of Brownian noise: Equilibrium-distribution method versus drift method". In: *Phys. Rev. E* 83, p. 041113.

Breuer, H.P. and F. Petruccione (2007). *The Theory of Open Quantum Systems*. Oxford: OUP. ISBN: 9780199213900. URL: http://books.google.es/books?id=DkcJPwAACAAJ.

Brown, Robert (1828). "A brief account of microscopical observations made in the months of June, July and August 1827, on the particles contained in the pollen of plants; and on the general existence of active molecules in organic and inorganic bodies". In: *The Philosophical Magazine* 4.21, pp. 161–173. DOI: 10.1080/14786442808674769. eprint: https://doi.org/10.1080/14786442808674769. URL: https://doi.org/10.1080/14786442808674769.

— (1829). "Additional remarks on active molecules". In: *The Philosophical Magazine* 6.33, pp. 161–166. DOI: 10.1080/14786442908675115. eprint: https://doi.org/10.1080/14786442908675115. URL: https://doi.org/10.1080/14786442908675115.

Bruderer, Martin et al. (2007). "Polaron physics in optical lattices". In: *Phys. Rev. A* 76 (1), p. 011605. DOI: 10.1103/PhysRevA.76.011605. URL: http://link.aps.org/doi/10.1103/PhysRevA.76.011605.

Brun, Todd A. (1993). "Quasiclassical equations of motion for nonlinear Brownian systems". In: *Phys. Rev. D* 47 (8), pp. 3383–3393. DOI: 10.1103/PhysRevD.47.3383. URL: http://link.aps.org/doi/10.1103/PhysRevD.47.3383.

Caldeira, A.O. and A.J. Leggett (1983a). "Path integral approach to quantum Brownian motion". In: *Physica A: Statistical Mechanics and its Applications* 121.3, pp. 587 –616. ISSN: 0378-4371. DOI: 10.1016/0378-4371(83)90013-4. URL: http://www.sciencedirect.com/science/article/pii/0378437183900134.

Caldeira, A.O and A.J Leggett (1983b). "Quantum tunnelling in a dissipative system". In: *Annals of Physics* 149.2, pp. 374 –456. ISSN: 0003-4916. DOI: http://dx.doi.org/10.1016/0003-4916(83)90202-6. URL: http://www.sciencedirect.com/science/article/pii/0003491683902026.

Canizares, J. Sánchez and F. Sols (1994). "Translational symmetry and microscopic preparation in oscillator models of quantum dissipation". In: *Physica A: Statistical Mechanics and its Applications* 212.1–2, pp. 181 –193. ISSN: 0378-4371. DOI: 10.1016/0378-4371(94)90146-5. URL: http://www.sciencedirect.com/science/article/pii/0378437194901465.

Carlesso, M. and A. Bassi (2016). "Quantum Brownian Motion in the Heisenberg picture: derivation of the adjoint master equation and applications". In: *arXiv:1602.05116*. URL: http://arxiv.org/abs/1602.05116.

Casteels, W. and M. Wouters (2014). "Polaron formation in the vicinity of a narrow Feshbach resonance". In: *Phys. Rev. A* 90 (4), p. 043602. DOI: 10.1103/PhysRevA.90.043602. URL: https://link.aps.org/doi/10.1103/PhysRevA.90.043602.

Castelnovo, Claudio, Jean-Sébastien Caux, and Steven H. Simon (2016). "Driven impurity in an ultracold one-dimensional Bose gas with intermediate interaction strength". In: *Phys. Rev. A* 93 (1), p. 013613. DOI: 10.1103/PhysRevA.93.013613. URL: https://link.aps.org/doi/10.1103/PhysRevA.93.013613.

Catani, J. et al. (2012). "Quantum dynamics of impurities in a one-dimensional Bose gas". In: *Phys. Rev. A* 85 (2), p. 023623. DOI: 10.1103/PhysRevA.85.023623. URL: http://link.aps.org/doi/10.1103/PhysRevA.85.023623.

Charalambous, C. et al. (2018). "Two distinguishable impurities in BEC: squeezing and entanglement of two Bose polarons". In: *arXiv:1805.00709*. URL: https://arxiv.org/pdf/1805.00709.pdf.

Cherstvy, Andrey G. and Ralf Metzler (2013). "Population splitting, trapping, and non-ergodicity in heterogeneous diffusion processes". In: *Phys. Chem. Chem. Phys.* 15 (46), pp. 20220–20235. DOI: 10.1039/C3CP53056F. URL: http://dx.doi.org/10.1039/C3CP53056F.

Christensen, Rasmus Søgaard, Jesper Levinsen, and Georg M. Bruun (2015a). "Quasiparticle Properties of a Mobile Impurity in a Bose-Einstein Condensate". In: *Phys. Rev. Lett.* 115 (16), p. 160401. DOI: 10.1103/

PhysRevLett.115.160401. URL: https://link.aps.org/doi/10.1103/PhysRevLett.115.160401.

— (2015b). "Quasiparticle Properties of a Mobile Impurity in a Bose-Einstein Condensate". In: *Phys. Rev. Lett.* 115 (16), p. 160401. DOI: 10.1103/PhysRevLett.115.160401. URL: https://link.aps.org/doi/10.1103/PhysRevLett.115.160401.

Cisse, Ibrahim I. et al. (2013). "Real-Time Dynamics of RNA Polymerase II Clustering in Live Human Cells". In: *Science* 341.6146, pp. 664–667. DOI: 10.1126/science.1239053. URL: http://www.sciencemag.org/content/341/6146/664.abstract.

Côté, R., V. Kharchenko, and M. D. Lukin (2002). "Mesoscopic Molecular Ions in Bose-Einstein Condensates". In: *Phys. Rev. Lett.* 89 (9), p. 093001. DOI: 10.1103/PhysRevLett.89.093001. URL: http://link.aps.org/doi/10.1103/PhysRevLett.89.093001.

Cucchietti, F. M. and E. Timmermans (2006). "Strong-Coupling Polarons in Dilute Gas Bose-Einstein Condensates". In: *Phys. Rev. Lett.* 96 (21), p. 210401. DOI: 10.1103/PhysRevLett.96.210401. URL: http://link.aps.org/doi/10.1103/PhysRevLett.96.210401.

Diósi, L. (1993). "On High-Temperature Markovian Equation for Quantum Brownian Motion". In: *EPL (Europhysics Letters)* 22.1, p. 1. URL: http://stacks.iop.org/0295-5075/22/i=1/a=001.

Diósi, L. and L. Ferialdi (2014). "General Non-Markovian Structure of Gaussian Master and Stochastic Schrödinger Equations". In: *Phys. Rev. Lett.* 113 (20), p. 200403. DOI: 10.1103/PhysRevLett.113.200403. URL: http://link.aps.org/doi/10.1103/PhysRevLett.113.200403.

D.S. Petrov, D.M. Gangardt, and G.V. Shlyapnikov (2004). "Low-dimensional trapped gases". In: *J. Phys. IV France* 116, pp. 5–44. DOI: 10.1051/jp4:2004116001. URL: https://doi.org/10.1051/jp4:2004116001.

Dykman, M. I. and M. A. Krivoglaz (1975). "Spectral distribution of nonlinear oscillators with nonlinear friction due to a medium". In: *Physica Status Solidi (B)* 68.1, pp. 111–123. ISSN: 1521-3951. DOI: 10.1002/pssb.2220680109. URL: http://dx.doi.org/10.1002/pssb.2220680109.

Efimkin, Dmitry K., Johannes Hofmann, and Victor Galitski (2016). "Non-Markovian Quantum Friction of Bright Solitons in Superfluids". In: *Phys. Rev. Lett.* 116 (22), p. 225301. DOI: 10.1103/PhysRevLett.

116.225301. URL: http://link.aps.org/doi/10.1103/PhysRevLett.116.225301.

Einstein, Albert (1905). "Die von der Molekularkinetischen Theorie von Wärme geforderte Bewegung von in ruhenden Flüssigktein suspendierten Teilchen". In: *Ann. Phys.* 17.549.

— (1906a). "Eine neue Bestimmung der Molekuldimensionen". In: *Ann. Phys.* 19.289.

— (1906b). "Zur Theorie der Brownschen Bewegung". In: *Ann. Phys.* 19.371.

— (1907). "Theoretische Bemerkungen über die Brownsche Bewegung". In: *Zeit. f. Electrochem* 13.371.

— (1908). "Elementaire Theorie der Brownsche Bewegung". In: *Zeit. f. Electrochem* 14.235.

Englert, Berthold-Georg, Martin Naraschewski, and Axel Schenzle (1994). "Quantum-optical master equations: An interaction picture". In: *Phys. Rev. A* 50 (3), pp. 2667–2679. DOI: 10.1103/PhysRevA.50.2667. URL: http://link.aps.org/doi/10.1103/PhysRevA.50.2667.

Exner, Felix M. (1900). "Notiz zu Brown's Molecularbewegung". In: *Annalen der Physik* 307.8, pp. 843–847. ISSN: 1521-3889. DOI: 10.1002/andp.19003070813. URL: http://dx.doi.org/10.1002/andp.19003070813.

Feller, William (1971). *An Introduction to Probability Theory and Its Applications*. Wiley. ISBN: 978-0-471-25709-77. URL: http://eu.wiley.com/WileyCDA/WileyTitle/productCd-0471257095.html.

Ferialdi, L. (2016). "Exact Closed Master Equation for Gaussian Non-Markovian Dynamics". In: *Phys. Rev. Lett.* 116.12, 120402, p. 120402. DOI: 10.1103/PhysRevLett.116.120402.

Fleming, C. H. and N. I. Cummings (2011). "Accuracy of perturbative master equations". In: *Phys. Rev. E* 83 (3), p. 031117. DOI: 10.1103/PhysRevE.83.031117. URL: http://link.aps.org/doi/10.1103/PhysRevE.83.031117.

Ford, G. W. and R. F. O'Connell (1991). "Radiation reaction in electrodynamics and the elimination of runaway solutions". In: *Physics Letters A* 157 (4-5), pp. 217–220. DOI: 10.1016/0375-9601(91)90054-C.

— (1999). "Comment on Dissipative Quantum Dynamics with a Lindblad Functional". In: *Phys. Rev. Lett.* 82 (16), pp. 3376–3376. DOI: 10.1103/PhysRevLett.82.3376. URL: http://link.aps.org/doi/10.1103/PhysRevLett.82.3376.

Fröhlich, H. (1954). "Electrons in lattice fields". In: *Advances In Physics* 3(11):325. URL: http://www.tandfonline.com/doi/abs/10.1080/00018735400101213.

Fukuhara, T. et al. (2013). "Quantum dynamics of a mobile spin impurity". In: *Nature Physics* 9, pp. 235–241. DOI: 10.1038/nphys2561.

Galve, Fernando, Roberta Zambrini, and Sabrina Maniscalco (2016). "Non-Markovianity hinders Quantum Darwinism". In: *Scientific Reports* 6. DOI: 10.1038/srep19607. URL: http://www.nature.com/articles/srep19607.

Gao, Shiwu (1997). "Dissipative Quantum Dynamics with a Lindblad Functional". In: *Phys. Rev. Lett.* 79 (17), pp. 3101–3104. DOI: 10.1103/PhysRevLett.79.3101. URL: http://link.aps.org/doi/10.1103/PhysRevLett.79.3101.

— (1998). "Gao Replies". In: *Phys. Rev. Lett.* 80 (25), pp. 5703–5703. DOI: 10.1103/PhysRevLett.80.5703. URL: http://link.aps.org/doi/10.1103/PhysRevLett.80.5703.

— (1999). "Gao Replies". In: *Phys. Rev. Lett.* 82 (16), pp. 3377–3377. DOI: 10.1103/PhysRevLett.82.3377. URL: http://link.aps.org/doi/10.1103/PhysRevLett.82.3377.

Gardiner, C. and P. Zoller (2004). *Quantum Noise: A Handbook of Markovian and Non-Markovian Quantum Stochastic Methods with Applications to Quantum Optics*. Springer Series in Synergetics. Berlin: Springer. ISBN: 9783540223016.

Gardiner, C.W. (2009). *Stochastic Methods: A Handbook for the Natural and Social Sciences*. Vol. 13. Springer Series in Synergetics. Heidelberg: Springer.

Gil, G. Muñoz et al. (2017). "Transient subdiffusion from an Ising environment". In: *Phys. Rev. E* 96 (5), p. 052140. DOI: 10.1103/PhysRevE.96.052140. URL: https://link.aps.org/doi/10.1103/PhysRevE.96.052140.

Golding, Ido and Edward C. Cox (2006). "Physical Nature of Bacterial Cytoplasm". In: *Phys. Rev. Lett.* 96 (9), p. 098102. DOI: 10.1103/PhysRevLett.96.098102. URL: http://link.aps.org/doi/10.1103/PhysRevLett.96.098102.

González-Tudela, A. and J. I. Cirac (2017). "Markovian and non-Markovian dynamics of quantum emitters coupled to two-dimensional structured reservoirs". In: *Phys. Rev. A* 96 (4), p. 043811. DOI: 10.1103/PhysRevA.96.043811. URL: https://link.aps.org/doi/10.1103/PhysRevA.96.043811.

Gorini, V., A. Kossakowski, and E. C. G. Sudarshan (1976). "Completely positive dynamical semigroups of N-level systems". In: *Journal of Mathematical Physics* 17, pp. 821–825. DOI: 10.1063/1.522979.

Grabert, Hermann, Peter Schramm, and Gert-Ludwig Ingold (1987). "Localization and anomalous diffusion of a damped quantum particle". In: *Phys. Rev. Lett.* 58 (13), pp. 1285–1288. DOI: 10.1103/PhysRevLett.58.1285. URL: https://link.aps.org/doi/10.1103/PhysRevLett.58.1285.

— (1988). "Quantum Brownian motion: The functional integral approach". In: *Physics Reports* 168.3, pp. 115 –207. ISSN: 0370-1573. DOI: http://dx.doi.org/10.1016/0370-1573(88)90023-3. URL: http://www.sciencedirect.com/science/article/pii/0370157388900233.

Gradshteyn, I. S. and I. M. Ryzhik (2000). *Table of Integrals, Series, and Products*. Sixth. San Diego: Academic Press. ISBN: 9780080542225.

Gröblacher, S et al. (2015). "Observation of non-Markovian micromechanical Brownian motion". In: *Nature communications* 6, p. 7606. ISSN: 2041-1723. DOI: 10.1038/ncomms8606. URL: http://europepmc.org/articles/PMC4525213.

Grusdt, F. and E. Demler (2016). "New theoretical approaches to Bose polarons". In: *arxiv* 1510.04934. URL: https://arxiv.org/pdf/1510.04934.pdf.

Grusdt, F. et al. (2014a). "Bloch oscillations of bosonic lattice polarons". In: arXiv: 1410.1513.

Grusdt, F. et al. (2014b). "Renormalization group approach to the Fröhlich polaron model: application to impurity-BEC problem". In: arXiv: 1410.2203.

Grusdt, Fabian, Gregory E. Astrakharchik, and Eugene A. Demler (2017). "Bose polarons in ultracold atoms in one dimension: beyond the Fröhlich paradigm". In: *arXiv:1704.02606*. URL: https://arxiv.org/pdf/1704.02606.pdf.

Grusdt, Fabian and Michael Fleischhauer (2016). "Tunable Polarons of Slow-Light Polaritons in a Two-Dimensional Bose-Einstein Condensate". In: *Phys. Rev. Lett.* 116 (5), p. 053602. DOI: 10.1103/PhysRevLett.116.053602. URL: https://link.aps.org/doi/10.1103/PhysRevLett.116.053602.

Guarnieri, G., C. Uchiyama, and B. Vacchini (2016). "Energy backflow and non-Markovian dynamics". In: *Phys. Rev. A* 93 (1), p. 012118. DOI:

10.1103/PhysRevA.93.012118. URL: http://link.aps.org/doi/10.1103/PhysRevA.93.012118.

Haake, F., M. Lewenstein, and R. Reibold (1985). *Adiabatic drag and initial slip for random processes with slow and fast variables*. Ed. by L. Accardi and W. von Waldenfels. Lecture Note in Mathematics: Quantum Probability and Applications II. Heidelberg: Springer.

Haake, Fritz (1982). "Systematic adiabatic elimination for stochastic processes". English. In: *Zeitschrift für Physik B Condensed Matter* 48.1, pp. 31–35. ISSN: 0722-3277. DOI: 10.1007/BF02026425. URL: http://dx.doi.org/10.1007/BF02026425.

Haake, Fritz and Maciej Lewenstein (1983). "Adiabatic drag and initial slip in random processes". In: *Phys. Rev. A* 28 (6), pp. 3606–3612. DOI: 10.1103/PhysRevA.28.3606. URL: http://link.aps.org/doi/10.1103/PhysRevA.28.3606.

Haake, Fritz and Reinhard Reibold (1984). "Strong damping and low-temperature anomalies for the harmonic oscillator". In: *Phys. Rev. A* 29, p. 3208.

— (1985). "Strong damping and low-temperature anomalies for the harmonic oscillator". In: *Phys. Rev. A* 32 (4), pp. 2462–2475. DOI: 10.1103/PhysRevA.32.2462. URL: http://link.aps.org/doi/10.1103/PhysRevA.32.2462.

Haus, J. W. and K. Kehr (1987). "Diffusion in regular and disordered lattices". In: *Phys. Rep.* 150, pp. 263–406.

Havlin, Shlomo and Daniel Ben-Avraham (1987). "Diffusion in disordered media". In: *Advances in Physics* 36.6, pp. 695–798. DOI: 10.1080/00018738700101072. URL: http://www.tandfonline.com/doi/abs/10.1080/00018738700101072.

Hilary M. Hurst Dmitry K. Efimkin, I. B. Spielman Victor Galitski (2016). "Kinetic theory of dark solitons with tunable friction". In: *arxiv*. URL: https://arxiv.org/abs/1703.00809.

Höfling, Felix and Thomas Franosch (2013). "Anomalous transport in the crowded world of biological cells". In: *Reports on Progress in Physics* 76.4, p. 046602. DOI: 10.1088/0034-4885/76/4/046602.

Hottovy, S., G. Volpe, and J. Wehr (2012a). "Noise-induced drift in stochastic differential equations with arbitrary friction and diffusion in the Smoluchowski-Kramers limit". In: *J. Stat. Phys.* 146, p. 762.

— (2012b). "Thermophoresis of Brownian particles driven by coloured noise". In: *EPL* 99, p. 60002.

Hottovy, S., G. Volpe, and J. Wehr (2014). "The Smoluchowski-Kramers limit of stochastic differential equations with arbitrary state-dependent friction". In: *Preprint (Comm. Math. Phys, in press)*, arXiv:1404.2330.

Hu, B. L., Juan Pablo Paz, and Yuhong Zhang (1992). "Quantum Brownian motion in a general environment: Exact master equation with nonlocal dissipation and colored noise". In: *Phys. Rev. D* 45 (8), pp. 2843–2861. DOI: 10.1103/PhysRevD.45.2843. URL: http://link.aps.org/doi/10.1103/PhysRevD.45.2843.

— (1993). "Quantum Brownian motion in a general environment. II. Nonlinear coupling and perturbative approach". In: *Phys. Rev. D* 47 (4), pp. 1576–1594. DOI: 10.1103/PhysRevD.47.1576. URL: http://link.aps.org/doi/10.1103/PhysRevD.47.1576.

Hu, Ming-Guang et al. (2016). "Bose Polarons in the Strongly Interacting Regime". In: *Phys. Rev. Lett.* 117 (5), p. 055301. DOI: 10.1103/PhysRevLett.117.055301. URL: https://link.aps.org/doi/10.1103/PhysRevLett.117.055301.

Isar, A. et al. (1994). "Open quantum systems". In: *International Journal of Modern Physics E* 03.02, pp. 635–714. DOI: 10.1142/S0218301394000164. URL: http://www.worldscientific.com/doi/abs/10.1142/S0218301394000164.

Jeon, Jae-Hyung et al. (2011). "In Vivo Anomalous Diffusion and Weak Ergodicity Breaking of Lipid Granules". In: *Phys. Rev. Lett.* 106 (4), p. 048103. DOI: 10.1103/PhysRevLett.106.048103. URL: http://link.aps.org/doi/10.1103/PhysRevLett.106.048103.

Jørgensen, Nils B. et al. (2016). "Observation of Attractive and Repulsive Polarons in a Bose-Einstein Condensate". In: *Phys. Rev. Lett.* 117 (5), p. 055302. DOI: 10.1103/PhysRevLett.117.055302. URL: https://link.aps.org/doi/10.1103/PhysRevLett.117.055302.

Keser, Aydin Cem and Victor Galitski (2016). "Analogue Stochastic Gravity in Strongly-Interacting Bose-Einstein Condensates". In: *arXiv:1612.08980*. URL: https://arxiv.org/pdf/1612.08980.pdf.

Kirton, P. G. et al. (2012). "Quantum current noise from a Born-Markov master equation". In: *Phys. Rev. B* 86 (8), p. 081305. DOI: 10.1103/PhysRevB.86.081305. URL: https://link.aps.org/doi/10.1103/PhysRevB.86.081305.

Klafter, Joseph and Igor M Sokolov (2011). *First Steps in Random Walks*. Oxford: Oxford University Press.

Kohstall, C. et al. (2012). "Metastability and coherence of repulsive polarons in a strongly interacting Fermi mixture". In: *Nature* 485, pp. 615–618. ISSN: 0028-0836. URL: http://dx.doi.org/10.1038/nature11065.

Koschorreck, M. et al. (2012). "Attractive and repulsive Fermi polarons in two dimensions". In: *Nature* 485, pp. 619–622. DOI: 10.1038/nature11151.

Kramers, H.A. (1940). "Brownian motion in a field of force and the diffusion model of chemical reactions". In: *Physica* 7.4, pp. 284 –304. ISSN: 0031-8914. DOI: http://dx.doi.org/10.1016/S0031-8914(40)90098-2. URL: http://www.sciencedirect.com/science/article/pii/S0031891440900982.

Kraus, Christina V. et al. (2009). "Pairing in fermionic systems: A quantum-information perspective". In: *Phys. Rev. A* 79 (1), p. 012306. DOI: 10.1103/PhysRevA.79.012306. URL: http://link.aps.org/doi/10.1103/PhysRevA.79.012306.

Krinner, S. et al. (2013). "Direct Observation of Fragmentation in a Disordered, Strongly Interacting Fermi Gas". In: arXiv: 1311.5174.

Kumar, Jishad, S. Sinha, and P. A. Sreeram (2009). "Dissipative dynamics of a harmonic oscillator: A nonperturbative approach". In: *Phys. Rev. E* 80 (3), p. 031130. DOI: 10.1103/PhysRevE.80.031130. URL: http://link.aps.org/doi/10.1103/PhysRevE.80.031130.

Kusumi, Akihiro et al. (2012). "Dynamic Organizing Principles of the Plasma Membrane that Regulate Signal Transduction: Commemorating the Fortieth Anniversary of Singer and Nicolson's Fluid-Mosaic Model". In: *Annual Review of Cell and Developmental Biology* 28.1, pp. 215–250. DOI: 10.1146/annurev-cellbio-100809-151736. URL: http://www.annualreviews.org/doi/abs/10.1146/annurev-cellbio-100809-151736.

Lampo, A. et al. (2018). "Open quantum system theory for Bose polarons in a trapped Bose-Einstein condensate". In: *arXiv:1803.08946*. URL: https://arxiv.org/pdf/1803.08946.pdf.

Lampo, Aniello et al. (2016). "Lindblad model of quantum Brownian motion". In: *Phys. Rev. A* 94 (4), p. 042123. DOI: 10.1103/PhysRevA.94.042123. URL: http://link.aps.org/doi/10.1103/PhysRevA.94.042123.

Lampo, Aniello et al. (2017). "Bose polaron as an instance of quantum Brownian motion". In: *Quantum* 1, p. 30. ISSN: 2521-327X. DOI: 10.

22331/q-2017-09-27-30. URL: https://doi.org/10.22331/q-2017-09-27-30.

Lan, Z. and C. Lobo (2014). "A single impurity in an ideal atomic Fermi gas: current understanding and some open problems". In: *J. Indian I. Sci.* 94, p. 179. URL: http://journal.library.iisc.ernet.in/index.php/iisc/search/advancedResults.

Landau, L. D. and S. I. Pekar (1948). "Effective mass of a polaron". In: *Zh. Eksp. Teor. Fiz.* URL: http://www.ujp.bitp.kiev.ua/files/journals/53/si/53SI15p.pdf.

Landauer, R. (1957). "Spatial Variation of Currents and Fields Due to Localized Scatterers in Metallic Conduction". In: *I.B.M. J. Res. Develop.* 149.1, p. 223.

Langevin, Paul (1908). "Sur la theorie de mouvement brownien". In: *C. R. Acad. Sci. Paris.* 146.530.

Leggett, A. J. et al. (1987). "Dynamics of the dissipative two-state system". In: *Rev. Mod. Phys.* 59 (1), pp. 1–85. DOI: 10.1103/RevModPhys.59.1. URL: http://link.aps.org/doi/10.1103/RevModPhys.59.1.

Levinsen, J. and M. M. Parish (2014). "Strongly interacting two-dimensional Fermi gases". In: arXiv: 1408.2737.

Levinsen, Jesper, Meera M. Parish, and Georg M. Bruun (2015). "Impurity in a Bose-Einstein Condensate and the Efimov Effect". In: *Phys. Rev. Lett.* 115 (12), p. 125302. DOI: 10.1103/PhysRevLett.115.125302. URL: https://link.aps.org/doi/10.1103/PhysRevLett.115.125302.

Lewenstein, M. and K. Rzazewski (1980). "Collective radiation and the near-zone field". In: *Journal of Physics A: Mathematical and General* 13.2, p. 743. URL: http://stacks.iop.org/0305-4470/13/i=2/a=035.

Lewenstein, M., A. Sanpera, and V. Ahufinger (2012). *Ultracold atoms in optical lattices: Simulating quantum many-body systems*. Oxford: OUP.

Lim, Soon Hoe et al. (2018). "On the Small Mass Limit of Quantum Brownian Motion with Inhomogeneous Damping and Diffusion". In: *Journal of Statistical Physics* 170.2, pp. 351–377. ISSN: 1572-9613. DOI: 10.1007/s10955-017-1907-7. URL: https://doi.org/10.1007/s10955-017-1907-7.

Lindblad, G. (1976a). "On the generators of quantum dynamical semigroups". In: *Comm. Math. Phys.* 48.2, pp. 119–130. URL: http://projecteuclid.org/euclid.cmp/1103899849.

Lindblad, Göran (1976b). "Brownian motion of a quantum harmonic oscillator". In: *Reports on Mathematical Physics* 10.3, pp. 393 –406. ISSN: 0034-4877. DOI: http://dx.doi.org/10.1016/0034-4877(76)90029-X. URL: http://www.sciencedirect.com/science/article/pii/003448777690029X.

Liu, Bi-Heng et al. (2011). "Experimental control of the transition from Markovian to non-Markovian dynamics of open quantum systems". In: *Nature Physics* 7, 931–934. DOI: http://dx.doi.org/10.1038/nphys2085. URL: https://www.nature.com/articles/nphys2085#supplementary-information.

Maier, Stefan A. and Joachim Ankerhold (2010). "Quantum Smoluchowski equation: A systematic study". In: *Phys. Rev. E* 81 (2), p. 021107. DOI: 10.1103/PhysRevE.81.021107. URL: http://link.aps.org/doi/10.1103/PhysRevE.81.021107.

Maniscalco, S. et al. (2004). "Lindblad and non-Lindblad type dynamics of a quantum Brownian particle". In: *Phys. Rev. A* 70 (3), p. 032113. DOI: 10.1103/PhysRevA.70.032113. URL: http://link.aps.org/doi/10.1103/PhysRevA.70.032113.

Maniscalco, Sabrina, Jyrki Piilo, and Kalle-Antti Suominen (2006). "Zeno and Anti-Zeno Effects for Quantum Brownian Motion". In: *Phys. Rev. Lett.* 97 (13), p. 130402. DOI: 10.1103/PhysRevLett.97.130402. URL: http://link.aps.org/doi/10.1103/PhysRevLett.97.130402.

Manzo, C. et al. (2014). "Weak ergodicity breaking of receptor motion in living cells stemming from random diffusivity". In: arXiv: 1407.2552.

Markov, Andrey Andreyevich (1907). "Investigation of a remarkable case of dependent trials". In: *Izv. Akad. Nauk St. Petersburg* 6, p. 61.

Marshall, William et al. (2003). "Towards Quantum Superpositions of a Mirror". In: *Phys. Rev. Lett.* 91 (13), p. 130401. DOI: 10.1103/PhysRevLett.91.130401. URL: http://link.aps.org/doi/10.1103/PhysRevLett.91.130401.

Massignan, P., C. J. Pethick, and H. Smith (2005). "Static properties of positive ions in atomic Bose-Einstein condensates". In: *Phys. Rev. A* 71 (2), p. 023606. DOI: 10.1103/PhysRevA.71.023606. URL: http://link.aps.org/doi/10.1103/PhysRevA.71.023606.

Massignan, P. et al. (2014). "Nonergodic Subdiffusion from Brownian Motion in an Inhomogeneous Medium". In: *Phys. Rev. Lett.* 112 (15),

p. 150603. DOI: 10.1103/PhysRevLett.112.150603. URL: http://link.aps.org/doi/10.1103/PhysRevLett.112.150603.

Massignan, Pietro, Matteo Zaccanti, and Georg M Bruun (2014). "Polarons, dressed molecules and itinerant ferromagnetism in ultracold Fermi gases". In: *Reports on Progress in Physics* 77.3, p. 034401. URL: http://stacks.iop.org/0034-4885/77/i=3/a=034401.

Massignan, Pietro et al. (2015). "Quantum Brownian motion with inhomogeneous damping and diffusion". In: *Phys. Rev. A* 91 (3), p. 033627. DOI: 10.1103/PhysRevA.91.033627. URL: http://link.aps.org/doi/10.1103/PhysRevA.91.033627.

Mazo, Robert M. (2002). *Brownian Motion: Fluctuations, Dynamics, and Applications*. Clarendon Press. ISBN: 9780198515678. URL: http://eu.wiley.com/WileyCDA/WileyTitle/productCd-0471257095.html.

McDaniel, A. et al. (2014). "An SDE approximation for stochastic differential delay equations with colored state-dependent noise". In: arXiv: 1406.7287.

Mehboudi, M. et al. (2018). "Using polarons for sub-nK quantum nondemolition thermometry in a Bose-Einstein condensate". In: *arXiv:1806.07198*. URL: https://arxiv.org/pdf/1806.07198.pdf.

Metzler, Ralf and Joseph Klafter (2004). "The restaurant at the end of the random walk: recent developments in the description of anomalous transport by fractional dynamics". In: *Journal of Physics A: Mathematical and General* 37.31, R161. URL: http://stacks.iop.org/0305-4470/37/i=31/a=R01.

Metzler, Ralf et al. (2014). "Anomalous diffusion models and their properties: non-stationarity, non-ergodicity, and ageing at the centenary of single particle tracking". In: *Phys. Chem. Chem. Phys.* 16 (44), pp. 24128–24164. DOI: 10.1039/C4CP03465A. URL: http://dx.doi.org/10.1039/C4CP03465A.

Montroll, Elliott W. and George H. Weiss (1965). "Random Walks on Lattices. II". In: *Journal of Mathematical Physics* 6.2, pp. 167–181. DOI: http://dx.doi.org/10.1063/1.1704269. URL: http://scitation.aip.org/content/aip/journal/jmp/6/2/10.1063/1.1704269.

Moy, G. M., J. J. Hope, and C. M. Savage (1999). "Born and Markov approximations for atom lasers". In: *Phys. Rev. A* 59 (1), pp. 667–675. DOI: 10.1103/PhysRevA.59.667. URL: https://link.aps.org/doi/10.1103/PhysRevA.59.667.

Newburgh, Ronald, Joseph Peidle, and Wolfgang Rueckner (2006). "Einstein, Perrin, and the reality of atoms: 1905 revisited". In: *American Journal of Physics* 74, p. 478. DOI: 10.1119/1.2188962. URL: http://dx.doi.org/10.1119/1.2188962.

Nixon, Floyd E. (1965). *Handbook of Laplace transformation: fundamentals, applications, tables, and examples*. Prentice-Hall. ISBN: 0133791807. URL: https://books.google.es/books/about/Handbook_of_Laplace_transformation.html?id=QRsnAAAAMAAJ&redir_esc=y.

Öhberg, P. et al. (1997). "Low-energy elementary excitations of a trapped Bose-condensed gas". In: *Phys. Rev. A* 56 (5), R3346–R3349. DOI: 10.1103/PhysRevA.56.R3346. URL: https://link.aps.org/doi/10.1103/PhysRevA.56.R3346.

Pagano, Guido et al. (2014). "A one-dimensional liquid of fermions with tunable spin". In: *Nature Physics* 10 (198). DOI: http://dx.doi.org/10.1038/nphys2878. URL: https://www.nature.com/articles/nphys2878#supplementary-information.

Palzer, Stefan et al. (2009). "Quantum Transport through a Tonks-Girardeau Gas". In: *Phys. Rev. Lett.* 103 (15), p. 150601. DOI: 10.1103/PhysRevLett.103.150601. URL: http://link.aps.org/doi/10.1103/PhysRevLett.103.150601.

Papanicolaou, G.C. (1977). *Modern modeling of continuum phenomena (Ninth Summer Sem. Appl. Math., Rensselaer Polytech. Inst., Troy, N.Y., 1975)*. Vol. 16. Lect. in Appl. Math. Amer. Math. Soc., pp. 109–147.

Pavliotis, G.A. and A.M. Stuart (2008). *Multiscale methods*. Vol. 53. Texts in Applied Mathematics. New York: Springer.

Peotta, Sebastiano et al. (2013). "Quantum Breathing of an Impurity in a One-Dimensional Bath of Interacting Bosons". In: *Phys. Rev. Lett.* 110 (1), p. 015302. DOI: 10.1103/PhysRevLett.110.015302. URL: http://link.aps.org/doi/10.1103/PhysRevLett.110.015302.

Pepe, Michele et al. (2012). "Microscopic theory of energy dissipation and decoherence in solid-state systems: A reformulation of the conventional Markov limit". In: *Physica Status Solidi (b)* 249.11, pp. 2125–2136. ISSN: 1521-3951. DOI: 10.1002/pssb.201147541. URL: http://dx.doi.org/10.1002/pssb.201147541.

Perrin, Jean Baptiste (1908a). "La loi de Stokes et le mouvment brownien". In: *C. R. Acad. Sci. Paris* 147.475.

Perrin, Jean Baptiste (1908b). "L'origen de mouvement brownien". In: *C. R. Acad. Sci. Paris* 147.530.

— (1909). "Mouvment brownien et realité moleculair". In: *Ann. de Chim. et de Phys.* 18.1.

Pesce, G. et al. (2012). "Dynamical Effects of Multiplicative Feedback on a Noisy System". In: *Preprint*, arXiv:1206.6271.

Pitaevskii, L. and S. Stringari (2003). *Bose-Einstein Condensation*. Oxford: Oxford University Press.

Rath, Steffen Patrick and Richard Schmidt (2013). "Field-theoretical study of the Bose polaron". In: *Phys. Rev. A* 88 (5), p. 053632. DOI: 10.1103/PhysRevA.88.053632. URL: http://link.aps.org/doi/10.1103/PhysRevA.88.053632.

Rentrop, T. et al. (2016). "Observation of the Phononic Lamb Shift with a Synthetic Vacuum". In: *Phys. Rev. X* 6 (4), p. 041041. DOI: 10.1103/PhysRevX.6.041041. URL: https://link.aps.org/doi/10.1103/PhysRevX.6.041041.

Risken, H. (2012). *The Fokker-Planck Equation: Methods of Solution and Applications*. Vol. 18. Springer Series in Synergetics. Heidelberg: Springer. ISBN: 9783642968099. URL: http://books.google.es/books?id=ThNnMQEACAAJ.

Rivas, Á. and S. F. Huelga (2012). *Open Quantum Systems*. DOI: 10.1007/978-3-642-23354-8.

Robinson, Neil J., Jean-Sébastien Caux, and Robert M. Konik (2016). "Motion of a Distinguishable Impurity in the Bose Gas: Arrested Expansion Without a Lattice and Impurity Snaking". In: *Phys. Rev. Lett.* 116 (14), p. 145302. DOI: 10.1103/PhysRevLett.116.145302. URL: https://link.aps.org/doi/10.1103/PhysRevLett.116.145302.

Rzazewski, K. and W. Zakowicz (1971). "On the interaction of harmonic oscillators with the radiation field". In: *Il Nuovo Cimento B (1971-1996)* 1.2, pp. 111–122. ISSN: 1826-9877. DOI: 10.1007/BF02815271. URL: https://doi.org/10.1007/BF02815271.

— (1976). "Initial value problem and causality of radiating oscillator". In: *Journal of Physics A: Mathematical and General* 9.7, p. 1159. URL: http://stacks.iop.org/0305-4470/9/i=7/a=018.

— (1980). "Initial value problem for two oscillators interacting with electromagnetic field". In: *Journal of Mathematical Physics* 21.2, pp. 378–388. DOI: 10.1063/1.524426. eprint: https://doi.org/10.1063/1.524426. URL: https://doi.org/10.1063/1.524426.

Saxton, M J (1993). "Lateral diffusion in an archipelago. Single-particle diffusion." In: *Biophysical journal* 64.6, pp. 1766–80. ISSN: 0006-3495. DOI: 10.1016/S0006-3495(93)81548-0. URL: http://www.pubmedcentral.nih.gov/articlerender.fcgi?artid=1262511\&tool=pmcentrez\&rendertype=abstract.

Scher, Harvey and Elliott W. Montroll (1975). "Anomalous transit-time dispersion in amorphous solids". In: *Phys. Rev. B* 12 (6), pp. 2455–2477. DOI: 10.1103/PhysRevB.12.2455. URL: http://link.aps.org/doi/10.1103/PhysRevB.12.2455.

Schirotzek, André et al. (2009). "Observation of Fermi Polarons in a Tunable Fermi Liquid of Ultracold Atoms". In: *Phys. Rev. Lett.* 102 (23), p. 230402. DOI: 10.1103/PhysRevLett.102.230402.

Schleich, W.P. (2001). *Quantum Optics in Phase Space*. Berlin: Wiley-VCH. ISBN: 978-3527294350. URL: https://books.google.es/books?id=2jUjQPW-WXAC&printsec=frontcover&hl=it&source=gbs_ge_summary_r&cad=0#v=onepage&q&f=false.

Schlosshauer, M.A. (2007). *Decoherence and the Quantum-To-Classical Transition*. The Frontiers Collection. Springer. ISBN: 9783540357759. URL: http://www.springer.com/physics/quantum+physics/book/978-3-540-35773-5.

Schlosshauer, Maximilian (2005). "Decoherence, the measurement problem, and interpretations of quantum mechanics". In: *Rev. Mod. Phys.* 76 (4), pp. 1267–1305. DOI: 10.1103/RevModPhys.76.1267. URL: http://link.aps.org/doi/10.1103/RevModPhys.76.1267.

Schmidt, Richard et al. (2012). "Fermi polarons in two dimensions". In: *Phys. Rev. A* 85 (2), p. 021602. DOI: 10.1103/PhysRevA.85.021602. URL: https://link.aps.org/doi/10.1103/PhysRevA.85.021602.

Shashi, Aditya et al. (2014). "Radio-frequency spectroscopy of polarons in ultracold Bose gases". In: *Phys. Rev. A* 89 (5), p. 053617. DOI: 10.1103/PhysRevA.89.053617. URL: http://link.aps.org/doi/10.1103/PhysRevA.89.053617.

Shchadilova, Yulia E. et al. (2016a). "Polaronic mass renormalization of impurities in Bose-Einstein condensates: Correlated Gaussian-wavefunction approach". In: *Phys. Rev. A* 93 (4), p. 043606. DOI: 10.1103/PhysRevA.93.043606. URL: https://link.aps.org/doi/10.1103/PhysRevA.93.043606.

Shchadilova, Yulia E. et al. (2016b). "Quantum Dynamics of Ultracold Bose Polarons". In: *Phys. Rev. Lett.* 117 (11), p. 113002. DOI: 10.1103/

PhysRevLett.117.113002. URL: https://link.aps.org/doi/10.1103/PhysRevLett.117.113002.

Smoluchowski, M. V. (1916). "Drei Vorträge über Diffusion, Brownsche Bewegung und Koagulation von Kolloidteilchen". In: *Zeitschrift für Physik* 17, pp. 557–585.

Smoluchowski, Marian von (1906). "Kinetische Theorie der Brownsche Bewegung und der Suspensionen". In: *Ann. Phys.* 21.756.

Spethmann, Nicolas et al. (2012). "Dynamics of Single Neutral Impurity Atoms Immersed in an Ultracold Gas". In: *Phys. Rev. Lett.* 109 (23), p. 235301. DOI: 10.1103/PhysRevLett.109.235301. URL: https://link.aps.org/doi/10.1103/PhysRevLett.109.235301.

Stringari, S. (1996). "Collective Excitations of a Trapped Bose-Condensed Gas". In: *Phys. Rev. Lett.* 77 (12), pp. 2360–2363. DOI: 10.1103/PhysRevLett.77.2360. URL: https://link.aps.org/doi/10.1103/PhysRevLett.77.2360.

Subaşi, Y. et al. (2012). "Equilibrium states of open quantum systems in the strong coupling regime". In: *Phys. Rev. E* 86 (6), p. 061132. DOI: 10.1103/PhysRevE.86.061132. URL: http://link.aps.org/doi/10.1103/PhysRevE.86.061132.

Săndulescu, A and H Scutaru (1987). "Open quantum systems and the damping of collective modes in deep inelastic collisions". In: *Annals of Physics* 173.2, pp. 277–317.

Svedberg, Theodor (1906). "Über die Eigenbewegung der Teilchen in Kolloidalen Lösungen. Von The Svedberg". In: *Zeitschrift für Elektrochemie und angewandte physikalische Chemie* 12.47, pp. 853–860. ISSN: 0005-9021. DOI: 10.1002/bbpc.19060124702. URL: http://dx.doi.org/10.1002/bbpc.19060124702.

Taj, David and Fausto Rossi (2008). "Completely positive Markovian quantum dynamics in the weak-coupling limit". In: *Phys. Rev. A* 78 (5), p. 052113. DOI: 10.1103/PhysRevA.78.052113. URL: http://link.aps.org/doi/10.1103/PhysRevA.78.052113.

Tempere, J. et al. (2009). "Feynman path-integral treatment of the BEC-impurity polaron". In: *Phys. Rev. B* 80 (18), p. 184504. DOI: 10.1103/PhysRevB.80.184504. URL: http://link.aps.org/doi/10.1103/PhysRevB.80.184504.

Tolić-Nørrelykke, Iva Marija et al. (2004). "Anomalous Diffusion in Living Yeast Cells". In: *Phys. Rev. Lett.* 93 (7), p. 078102. DOI: 10.1103/

PhysRevLett.93.078102. URL: http://link.aps.org/doi/10.1103/PhysRevLett.93.078102.

Tuziemski, W.H.J. and J.K. Korbicz (2015). "Objectivisation In Simplified Quantum Brownian Motion Models". In: *Photonics*, pp. 228–240. DOI: http://dx.doi.org/10.1016/0370-1573(88)90023-3. URL: http://www.sciencedirect.com/science/article/pii/0370157388900233.

Ullersma, P. (1966). "An exactly solvable model for Brownian motion: I. Derivation of the Langevin equation". In: *Physica* 32, p. 27. DOI: 10.1016/0031-8914(66)90102-9.

Vacchini, Bassano (2000). "Completely Positive Quantum Dissipation". In: *Phys. Rev. Lett.* 84 (7), pp. 1374–1377. DOI: 10.1103/PhysRevLett.84.1374. URL: http://link.aps.org/doi/10.1103/PhysRevLett.84.1374.

Vega, Inés de and Daniel Alonso (2017). "Dynamics of non-Markovian open quantum systems". In: *Rev. Mod. Phys.* 89 (1), p. 015001. DOI: 10.1103/RevModPhys.89.015001. URL: https://link.aps.org/doi/10.1103/RevModPhys.89.015001.

Volosniev, A. G., H.-W. Hammer, and N. T. Zinner (2015). "Real-time dynamics of an impurity in an ideal Bose gas in a trap". In: *Phys. Rev. A* 92 (2), p. 023623. DOI: 10.1103/PhysRevA.92.023623. URL: https://link.aps.org/doi/10.1103/PhysRevA.92.023623.

Volpe, G. et al. (2010). "Influence of Noise on Force Measurements". In: *Phys. Rev. Lett.* 104, p. 170602.

Waldenfels, W. von (2014). *A Measure Theoretical Approach to Quantum Stochastic Processes*. Lecture Notes in Physics. Heidelberg: Springer. ISBN: 9783642450815.

Wang, Q. and H. Zhan (2015). "On different numerical inverse Laplace methods for solute transport problems". In: *Advances in Water Resources* 75, pp. 80–92. DOI: 10.1016/0375-9601(91)90054-C.

Weedbrook, Christian et al. (2012). "Gaussian quantum information". In: *Rev. Mod. Phys.* 84 (2), pp. 621–669. DOI: 10.1103/RevModPhys.84.621. URL: http://link.aps.org/doi/10.1103/RevModPhys.84.621.

Weigel, Aubrey V. et al. (2011). "Ergodic and nonergodic processes coexist in the plasma membrane as observed by single-molecule tracking". In: *Proceedings of the National Academy of Sciences* 108.16, pp. 6438–

6443. DOI: 10.1073/pnas.1016325108. URL: http://www.pnas.org/content/early/2011/03/28/1016325108.abstract.

Weiss, U. (2008). *Quantum Dissipative Systems*. Singapore: World Scientific.

Wiseman, H. M. and W. J. Munro (1998). "Comment on Dissipative Quantum Dynamics with a Lindblad Functional". In: *Phys. Rev. Lett.* 80 (25), pp. 5702–5702. DOI: 10.1103/PhysRevLett.80.5702. URL: http://link.aps.org/doi/10.1103/PhysRevLett.80.5702.

Wodkiewicz, K. and J.H. Eberly. In:

Zakowicz, W. and K. Rzazewski (1974). "Collective radiation by harmonic oscillators". In: *Journal of Physics A: Mathematical, Nuclear and General* 7.7, p. 869. URL: http://stacks.iop.org/0301-0015/7/i=7/a=012.

Zurek, W.H. (2009). "Quantum Darwinism". In: *Nature Physics* 3, pp. 181–188. DOI: http://dx.doi.org/10.1016/0370-1573(88)90023-3. URL: http://www.sciencedirect.com/science/article/pii/0370157388900233.

Zurek, Wojciech Hubert (2003). "Decoherence, einselection, and the quantum origins of the classical". In: *Rev. Mod. Phys.* 75 (3), pp. 715–775. DOI: 10.1103/RevModPhys.75.715. URL: http://link.aps.org/doi/10.1103/RevModPhys.75.715.

Zwanzig, Robert (1961). "Memory Effects in Irreversible Thermodynamics". In: *Phys. Rev.* 124 (4), pp. 983–992. DOI: 10.1103/PhysRev.124.983. URL: http://link.aps.org/doi/10.1103/PhysRev.124.983.